THE UNIVERSITY OF SYDNEY

Characterisation of Echocardiographic Markers of Right Ventricular Function in Non-ischaemic Cardiomyopathy

Dr. Henry Heng Li Chen

A thesis submitted to fulfil the requirements for the degree of

Doctor of Philosophy

Western Sydney Clinical Schools

Faculty of Medicine and Health

December 2025

Table of Contents

(ii) Statement of Originality

This thesis is original and independent work by the author Dr Henry H Chen, who is responsible for all major areas of study design, data collection and analysis, and drafting of this manuscript.

This thesis is submitted in fulfilment of the requirements of the degree of Doctor of Public Health

This is to certify that the content of this thesis is my own work. This thesis has not been submitted for any other degree or purpose.

I certify that intellectual content of this thesis is the product of my own work, and that all assistance received in preparing this thesis and all sources have been acknowledged.

Dr Henry H Chen

17th June 2025

(iii) Acknowledgements

The completion of this dissertation marks the culmination of one of the most demanding yet rewarding chapters of my academic journey. Undertaking this PhD has tested my resilience, expanded my understanding, and shaped me both as a researcher and a clinician. I could not have reached this milestone without the support, encouragement, and contributions of many people, to whom I owe my deepest gratitude.

First and foremost, I would like to express my heartfelt thanks to my principal supervisor, **Professor Timothy Tan**, for his support, mentorship, and belief in this project. His clarity of thought, attention to detail, and commitment to this project have left a lasting impact on me.

I am equally grateful to my co-supervisor, **Professor Kazuaki Negishi**, whose remarkable expertise and broad insight continually inspired me to think critically and deeply. His depth of knowledge in the field of imaging and perspective on statistical analysis added a layer of refinement to this work that I greatly value.

To my friends and co-authors, **Dr Aditya Bhat** and **Dr Gary Gan**, thank you for walking this path with me. Your collaboration, thoughtful contributions, and moral support made the research process more productive and, just as importantly, more enjoyable. I have learned a great deal from our discussions and shared experiences.

I wish to extend my sincere appreciation to **Professor Andrew Sindone**, whose wealth of clinical experience and knowledge of heart failure has been like a living history book. His insights bridged the gap between research and real-world practice to help shape the clinical background relevance of this thesis.

To **Ms Alma Latumahina**, thank you for your dedication, warmth, and tireless support. Your work behind the scenes in the heart failure service and assisting with patient recruitment was instrumental to the progress of this research. Your calm presence and professionalism were a source of reassurance throughout.

To our chief sonographer, **Mr Fernando Fernandez**, I am sincerely grateful. Your leadership and pursuit of excellence have set a benchmark in echocardiographic imaging that made this work possible. The high standards maintained in our department owe much to your expertise and passion for echocardiography.

On a personal note, I am forever indebted to my family. To my parents, **Tong Su Chen** and **Ling Wang**, thank you for instilling in me the values of perseverance and humility. Your love and sacrifices laid the foundation for everything I have achieved. To my sister, **Renee Chen**, thank you for your encouragement and for always being there in moments of doubt.

Most of all, to my wife, **Claire Huang**, thank you for your boundless patience, quiet strength, and unwavering support. You have walked with me through every late night, every moment of frustration, and every small victory. Your presence has been my greatest source of comfort and motivation throughout this journey, and I could not have done this without you.

This thesis is not just a culmination of research, it is a reflection of the many people who believed in me, guided me, and stood by me. For that, I am profoundly thankful.

(iv) Author Attribution Statement

Preliminary data for chapter 3 of this thesis was published in abstract form as "H Chen, A Bhat et al. Prognostic value of right ventricular free wall strain in stable non-ischaemic cardiomyopathy. Heart, Lung Circulation. 2022;31(s3):S98-99" (10.1016/j.hlc.2022.06.121). I designed the study, collected and analysed the data, and wrote the drafts of the manuscript.

Chapter 4 of this thesis has been published as "H Chen, A Bhat et al. The impact of body mass index on cardiac structure and function in a cohort of obese patients without traditional cardiovascular risk factors. International Journal of Cardiology Cardiovascular Risk and Prevention. 2023;19: 2772-4875" (10.1016/j.ijcrp.2023.200211). I designed the study, collected and analysed the data, and wrote the drafts of the manuscript.

Preliminary data for chapter 5 of this thesis was published in abstract form as "H Chen, F Oh et al. The Immediate Impact of Electrical Cardioversion on Right Ventricular Systolic Function in Patients with Non-Valvular Atrial Fibrillation. Heart Lung Circulation. 2020;29(s2):S225-226" (10.1016/j.hlc.2020.09.422). I designed the study, collected and analysed the data, and wrote the drafts of the manuscript.

Preliminary data arising from chapter 6 of this thesis was published in two abstracts: "H Chen, A Bhat et al. Global myocardial work index is an independent predictor of functional capacity on 6-minute walk test in stable non-ischaemic cardiomyopathy. European heart journal. 2024;45:s1(ehae666.851)" (10.1093/eurheartj/ehae666); and "H Chen, A Bhat et al. Impact of atrial fibrillation on functional capacity in heart failure with reduced ejection fraction secondary to non-ischaemic cardiomyopathy. Heart, lung and circulation. 2024;33:s4-629". I designed these studies, collected and analysed the data, and wrote the drafts of the manuscripts.

In addition to the authorship attribution statements above, in cases where I am not the corresponding author of a published item, permission to include the published material has been granted by the corresponding author, who is also my supervisor for this thesis.

Dr Henry H Chen

As supervisor for the candidature upon which this thesis is based, I can confirm that the authorship attribution statements above are correct.

Prof Timothy C Tan

(v) Artificial Intelligence Statement

This thesis did not utilise generative artificial intelligence.

(vi) Australian Government Support

This research was supported by an Australian Government Research Training Program (RTP) scholarship.

(vii) List of Figures

Chapter 1

Chapter 2

No Figures

Chapter 3

Chapter 4

Chapter 5

Chapter 6

Chapter 7

Chapter 8

No Figures

(viii) List of Tables

Chapter 1

No Tables

Chapter 2

Chapter 3

Chapter 4

Chapter 5

Chapter 6

Chapter 7

Chapter 8

No Tables

(ix) Thesis Abstract

Non-ischaemic cardiomyopathy (NICM) is characterised by intrinsic myocardial dysfunction that culminates in heart failure (HF), a syndrome associated with significant symptoms, morbidity and mortality. Contemporary guidelines classify and manage NICM solely based on left ventricular (LV) systolic function, often overlooking the significance of the right ventricle (RV). RV function remains under-represented in risk stratification tools and treatment pathways despite its critical role in maintaining cardiac output.

RV systolic function in NICM can be evaluated using several non-invasive imaging modalities, including radionuclide techniques, cardiac magnetic resonance imaging, cardiac computed tomography, and most commonly, transthoracic echocardiography. This body of work focuses on echocardiographic measures of RV systolic function given their accessibility and widespread use in clinical practice, including conventional parameters as well as advanced techniques such as speckle-tracking echocardiography and three-dimensional imaging.

In this thesis, we hypothesise that structural and functional abnormalities of the RV are present even in early stages of NICM and in associated cardiovascular diseases, and that these abnormalities correlate with reduced exercise capacity and adverse cardiovascular outcomes in stable NICM patients.

To investigate our hypothesises, we conducted a series of studies. Firstly, in retrospective cohorts, we examined the impact of LV systolic dysfunction, obesity and atrial fibrillation on the prevalence and severity of RV systolic dysfunction. We subsequently assessed the prognostic value of a range of conventional and advanced echocardiographic parameters for exercise capacity and adverse cardiovascular outcomes in a prospectively recruited cohort of stable NICM on optimal contemporary guideline directed HF therapy. Stringent exclusion criteria were applied which excluded those with obstructive coronary artery disease, primary valvular disease, congenital heart disease, previous cardiac surgery or significant pulmonary disease.

Our findings confirmed that each progressive grade of LV systolic dysfunction in NICM is associated with a higher prevalence and increasing severity of RV dysfunction. We also demonstrated that

elevated body mass index and atrial fibrillation are both associated with reduced RV systolic function even in the absence of other cardiac pathologies. Finally, in our prospective NICM cohort, impairment in RV longitudinal function as assessed by RV free wall strain was independently associated with reduced exercise capacity on 6-minute walk test. Additionally, a 3D-RVEF reduction to below 44.7% best discriminated for and independently predicted cardiovascular death and HF hospitalisation in compensated NICM patients on optimal contemporary HF therapy.

The findings generated in this body of work emphasises the significant impact of RV function has on HF symptomology and cardiovascular prognosis in patients with NICM. Apart from highlighting the importance of routine and comprehensive assessment of RV size and function, a comprehensive assessment of RV size and function may also improve risk stratification by identifying patients who would benefit from individualised treatment with closer monitoring and more aggressive therapeutic interventions.

CHAPTER ONE

Overview of right ventricular function in heart failure with reduced ejection fraction

1.0 Abbreviations:

2D = Two-dimensional

3D = Three-dimensional

3D-RVEF = Three-dimensional right ventricular ejection fraction

AF = Atrial fibrillation

BMI = Body mass index

CMR = Cardiac magnetic resonance imaging

CRT = Cardiac resynchronisation therapy

CRT-D = Cardiac resynchronisation therapy - defibrillator

FAC = Fractional area change

HF = Heart failure

HFmEF = Heart failure with mildly reduced ejection fraction

HFpEF = Heart failure with preserved ejection fraction

HFrEF = Heart failure with reduced ejection fraction

ICM = Ischaemic cardiomyopathy

LV = Left ventricle / left ventricular

LVEF = Left ventricular ejection fraction

MPI = Myocardial performance index

MW = Myocardial work

NICM = Non-ischaemic cardiomyopathy

PASP = Pulmonary artery systolic pressure

RV = Right ventricle / right ventricular

RV-FWS = Right ventricular free wall strain

RV-GLS = Right ventricular global longitudinal strain

RVS’ = Tissue Doppler derived peak systolic velocity at the tricuspid annulus

STE = Speckle tracking echocardiography

TAPSE = Tricuspid annular plane systolic excursion

TTE = Transthoracic echocardiogram / echocardiography

1.1.0 Heart failure

1.1.1 Heart failure epidemiology

Heart failure (HF) is a heterogenous clinical syndrome, in which the heart cannot supply adequate cardiac output to meet the body's metabolic demands. (1) HF is named a global epidemic, (2-4) affecting approximately 2% of the adult population. (5) In the United States, HF affects around 6 million adults, and its prevalence is projected to increase by a further third in the coming decades due to the aging population. (6) HF hospitalisation is also a major burden for the health system and accounts for approximately 10% of all cardiovascular health expenditure in the United States. (7) Additionally, HF is associated with high mortality prior to the advent of contemporary HF therapy with approximately 50-75% of HF patients dying within five years of their diagnosis in the 2000s. (8, 9)

Similarly, the prevalence of HF in Australia is estimated at between 1.0% and 2.0% with a significant proportion of these being previously undiagnosed. (10) The underlying burden of HF maybe even higher based on analysis of Australian primary care databases with 9.7% of adults attending primary care being diagnosed with "definite HF" based on documented medical history, clinical signs and symptoms. (11)

1.1.2 Heart failure classification

Conventionally, the classification of HF is based on left ventricular (LV) systolic function with left ventricular ejection fraction (LVEF) commonly utilised as its primary measure. (12, 13) Heart failure with preserved ejection fraction (HFpEF) is classified as LVEF ≥50%, heart failure with reduced ejection fraction (HFrEF) is classified as LVEF ≤40%, and heart failure with mildly reduced ejection fraction (HFmEF) is classified as LVEF 41-49%. (12) These classifications are historically based on large randomised controlled trials over the past few decades, which have sought to establish a threshold ejection fraction for ease of recruitment. (12)

Severity of LV systolic impairment can also be subdivided into mild (LVEF 41-49%), moderate (LVEF 30-40%) and severe (LVEF <30%) ranges based on echocardiographic recommendations. (14) Historically, HF patients with LVEF <50% have been collectively termed as systolic HF. (15, 16)

In Australia, HF is traditionally classified into two groups: reduced and preserved ejection fraction, based on a single LVEF cutoff of 50%. (16) A recent Australian consensus statement has provided further rationale to support the use of certain HF therapy in those with LVEF 41-49% based on post-hoc and sub-group analyses of randomised controlled trials. (17)

1.1.3 Heart failure aetiology

HF classification can also be based on the causative aetiology rather than the degree of LV systolic impairment. Non-ischaemic cardiomyopathy (NICM) refers to myocardial disease processes caused by aetiologies other than coronary artery disease, while ischaemic cardiomyopathy (ICM) refers to those caused by coronary artery disease and myocardial infarction. (18-20)

Although ICM and NICM both lead to the systolic HF syndrome, their clinical course and underlying mechanistic pathways differ markedly. (21) The ICM process occurs as the result of an initial large ischaemic injury or via repeated smaller injuries over time. (22) As such, ICM is invariably associated with more extensive LV myocardial scarring. (22, 23) Comparatively, NICM patients tend to have less extensive or even no LV scar burden and a correspondingly higher proportion of viable myocardium on magnetic resonance imaging. (24)

Clinically, NICM patients also tend to be younger, male and have a lower risk of overall mortality. (21, 25) On top of standard HF pharmacotherapeutics, NICM have additional disease-specific therapies available for certain subgroups such as amyloidosis, sarcoidosis, Fabry's disease and hypertrophic obstructive cardiomyopathies. (13, 26, 27) Due to the lower

scar burden, the risk of sudden arrhythmic death is thought to be lower in NICM and the benefit conferred from implantable cardioverter defibrillators may be smaller. (26, 28, 29)

1.2.0 The right ventricle

RV failure often accompanies LV failure, though these disease entities are distinct. Compared to the LV, the right ventricle (RV) has been neglected or at least has not attracted significant attention for most of the twentieth century. This is likely in part due to inherent methodological limitations in evaluating RV function. The RV was thought to be a cardiac chamber which was "not necessary for the maintenance of a normal circulation" in older literature. (30) These ideas were further reinforced by the Fontan cardiac corrective surgery, in which a functioning circulatory system could be reliably created without the need of a native RV. (31) As a result, LV systolic function remains at the center of attention in current HF guidelines. (12, 26)

1.2.1 Right ventricular anatomy and physiology

Located anteriorly just behind the sternum, the RV is anatomically and functionally distinct from the LV. While the RV volume is smaller compared to the LV, it has a more complex three-dimensional geometry, appearing triangular when viewed from the front and crescentic when viewed in cross-section. (32)

The RV chamber is constituted from the RV free wall that forms a triangular pouch around the left ventricular wall and the transverse fibres that encompass the septum. The rigid tricuspid valve and pulmonary valve annulus form the structural base to complete the RV chamber. (32)

The RV cavity can be subdivided into three parts: 1) the apex, situated at the tip of the triangle, is a heavily trabeculated portion of the cavity and is the most compliant segment of the RV wall; 2) the inlet, which provides the rigid structural base of the RV and is comprised of the

tricuspid valve, tricuspid annulus, and the papillary muscles; 3) the outlet, consisting of the pulmonary valve and the RV outflow tact (Figure 1.1). (33)

Compared to the LV, the RV wall is thinner and comprises of only two distinct myocardial layers. The inner or endocardial layer of the RV consists of longitudinally aligned cardiomyocyte fibers, which accounts for approximately 75% of the RV wall thickness. These longitudinal fibers attach the cardiac apex to the RV base. A thinner circumferentially arranged layer form the superficial layer of the RV myocardial wall. These circumferential cardiomyocytes also extend into the LV myocardium to wrap around both ventricles. (32)

Due to the lower right-sided pressures and wall stress, the RV has lower oxygen requirement compared to that of the LV. Under normal circumstances, the RV has lower coronary blood flow and oxygen extraction, which can be augmented with during exercise or in the presence of pulmonary hypertension. (34) Consequently, the RV wall is more resistant to ischaemic injury as it has less myocardial mass and faces lower preload and afterload conditions. (23) Therefore, RV function is usually preserved in the face of ischaemia, even with chronic total occlusion of the right coronary artery. (35, 36)

The primary function of the RV is to receive systemic venous return and to forward it into the pulmonary arteries. RV contraction occurs in a sequential manner. Firstly, the inward movement of the free wall starting with contraction of the apex; followed by basal free wall contraction after a short delay of around 20-50ms; then the longitudinal shortening of the RV cavity occurs; lastly, the circumferential shortening and contraction of the RV. Additionally, the LV also contributes to overall RV contractile function through coordinated contraction of the shared LV septal wall (Figure 1.2). (32)

Figure 1.1. The right ventricle

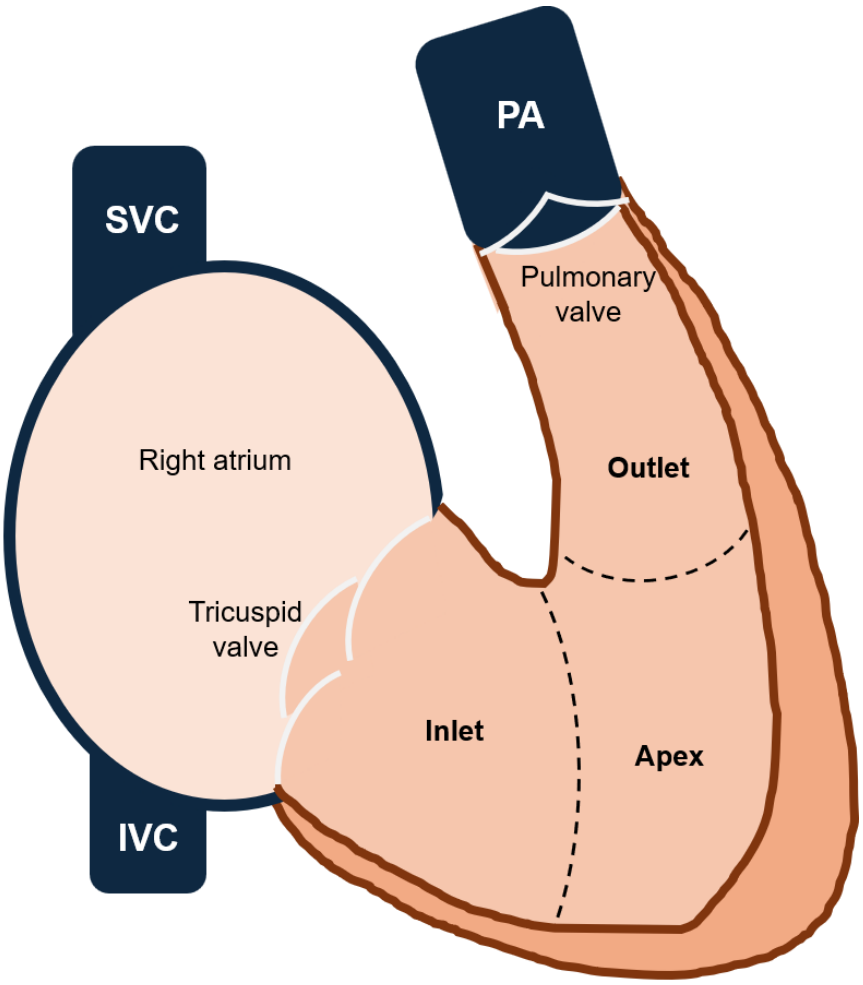

Figure 1.1. The right ventricle consists of three major components: the inlet, the apex (or body) and the outlet (or infundibulum).

Abbreviations. *SVC: superior vena cava, IVC: inferior vena cava, PA: pulmonary artery*

Figure 1.2. Right ventricular myocardial layers

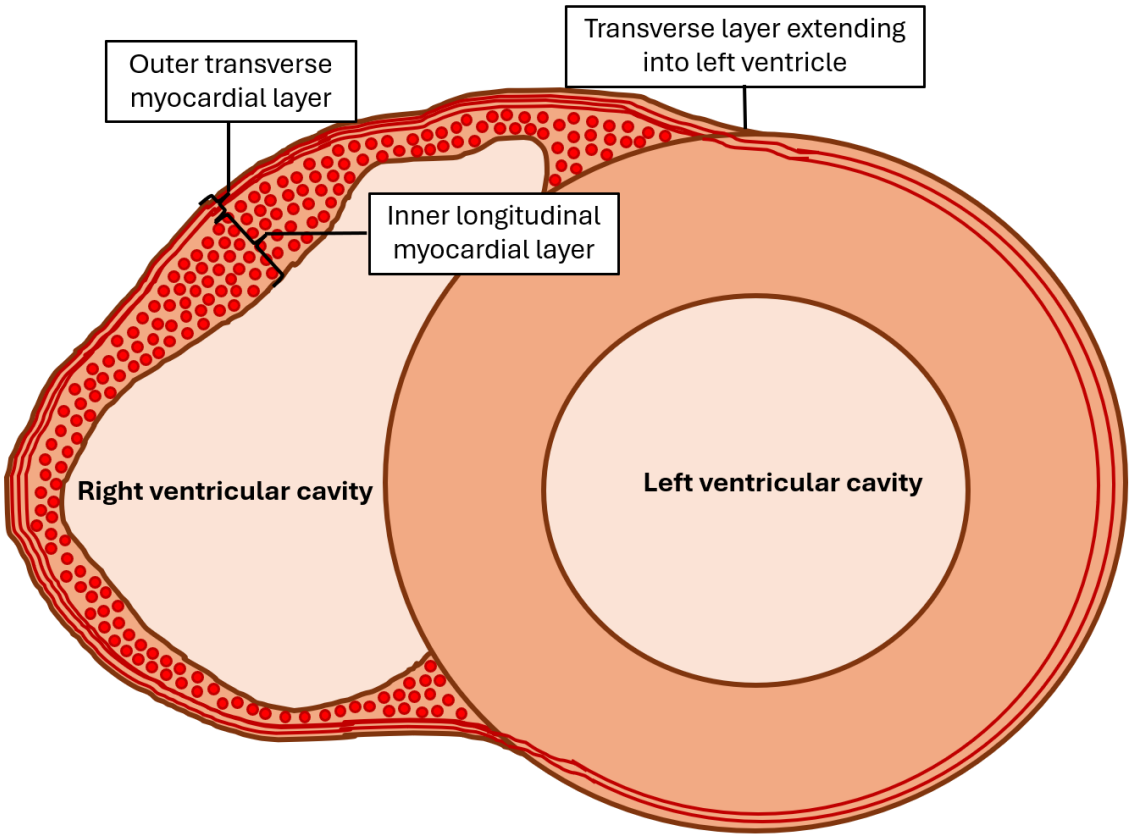

Figure 1.2. The right ventricular wall is thinner than the left ventricle and consists of two myocardial layers. The inner endocardial layer consists of longitudinal fibers which account for over two thirds of the right ventricular wall thickness. The outer layer consists of transverse fibres which continue into the left ventricular wall.

1.2.2 Right ventricular function in heart failure

RV function plays a major role in determining the symptoms and prognosis of patients with HF. (37) The RV is responsible for generating adequate preload for the LV, while regulating systemic venous pressure. This role becomes increasingly important as LV filling pressures become elevated. The RV can be seen as the common final pathway in both the systemic and pulmonary systems and therefore serves as a “barometer” for all the haemodynamic loads accumulated across the preceding cardiac chambers. (37) Compared to patients with isolated LV systolic impairment, those with concomitant RV dysfunction have been shown to have increased mortality and adverse cardiovascular outcomes. (38)

There is a myriad of factors that have been attributed to the pathogenesis of RV dysfunction in systolic HF and other cardiopulmonary conditions. These can be organised into three broad categories: 1) increased preload; 2) increased afterload, and 3) intrinsic dysfunction in RV relaxation and /or contraction. (39, 40)

Increase in RV preload predominantly occurs with volume overload, usually in the presence of tricuspid or pulmonary regurgitation, and less commonly from left to right intra-cardiac shunting. The RV wall is more compliant compared to the LV and can tolerate a higher degree of volume overload without elevation of RV end-diastolic pressure. This can be attributed to the smaller individual RV cardiomyocyte size and a higher density ratio of collagen and connective tissue. Subsequently, RV contractile function often remains preserved in volume overload. (32) However, while the RV is in this volume overloaded state, its adaptive response to additional pressure overload is blunted. (41)

The primary cause of RV pressure overload is elevated pulmonary pressures from either pre- or post-capillary aetiologies, which is due to pulmonary bed vasculature abnormalities or left heart diseases respectively. In contrast to volume overload, the thinner and more compliant RV wall does not tolerate pressure overload well. In the face of elevated pressures, RV cardiomyocytes initially undergo hypertrophy to augment overall contractile force, which

compensates for the afterload increase. This process is termed adaptive remodeling. With sustained exposure to pressure overload, the contractile reserve of the RV becomes exhausted and will then undergo maladaptive remodeling. This occurs when the contractile reserve of the RV can no longer overcome the elevated afterload, which results in elevation of RV end-diastolic pressure, progressive stretching of the RV matrix, and eventually, dilatation of the RV cavity. (42)

The final factor contributing to RV dysfunction is the intrinsic failure of the RV to generate sufficient end systolic pressure either through loss of contractile force or impaired relaxation. The reduced contractile strength of the RV free wall can be attributed to cardiomyopathy, myocardial ischemia, or inadequate coronary perfusion resulting from poor cardiac output. (32, 40) Since the RV is less prone to ischaemic injury, ICM aetiology tends to have limited direct impact on RV function. (23) In contrast, NICM is a primary cardiomyopathic process that leads to myocyte dysfunction in both the left and right ventricles. (37) Unsurprisingly, NICM is associated with a higher prevalence of RV dysfunction, ranging from 20% to 65% depending on the imaging modality and parameter used. (43-46)

Furthermore, the uncoupling of interventricular dependence can also impair intrinsic RV output. This can occur through the loss of coordinated LV septal and RV wall contraction, leading to lowered overall systolic performance of the RV. (32) And additionally, through constriction of the RV cavity by a severely dilated LV within the confines of the shared pericardial sac, which limits RV diastolic filling and reduces overall RV function. (37)

1.3.0 Assessment of right ventricular function

Impairment of RV function was first assessed using thermodilution and radionuclide techniques. Recent interests in physiology and pathogenesis of the RV have led to the development of new modalities and novel imaging parameters. (32)

1.3.1 Invasive haemodynamics

Invasive assessment of RV function is achieved using a high-conductance catheter which can simultaneously measure pressure and volume by constructing end-systolic and end-diastolic pressure volume loops to generate load-independent measures of systolic and diastolic function. (47) Right heart catheterisation is traditionally considered the “gold standard” of right heart assessment, but its use has declined with the advent of more accessible and safer non-invasive modalities. (38)

1.3.2 Nuclear imaging

Nuclear imaging techniques enable assessment of RV morphology, perfusion and metabolism. Gated positron emission tomography can evaluate RV volumes and ejection fraction with simultaneous assessment of glucose metabolism. Gated blood pool single photon-emission computed tomography can bypass geometric assumptions to calculate RV function. (38) Reduction of RV ejection fraction based on nuclear imaging has been found to correlate with adverse clinical outcomes and reduced exercise capacity in systolic HF. (48-50)

1.3.3 Computed tomography

Cardiac computed tomography (CT) quantifies RV function and volume via retrospective electrocardiogram-gated helical acquisition throughout the entire cardiac cycle. While this technique allows rapid acquisition of the entire RV, it is associated with higher radiation exposure. This modality has demonstrated good accuracy and reproducibility compared to magnetic resonance imaging techniques but tends to overestimate both RV volumes and RV ejection fraction. (51-53) Consequently, CT assessment of RV size and function is usually reserved as an alternative modality in cases where echocardiography and magnetic resonance imaging is insufficient, unavailable or contraindicated. (38)

Advancements in multidetector CT technology over the past two decades have significantly enhanced the spatial resolution of cardiac CT, establishing it as a valuable tool in the assessment of arrhythmogenic RV cardiomyopathy and tricuspid regurgitation. Its superior spatial resolution allows for detailed delineation of the RV endocardium and associated structures, to facilitate detection of fibrofatty replacement of the RV wall which is characteristic of arrhythmogenic RV cardiomyopathy. (54) Additionally, cardiac CT provides essential "gold standard" anatomical and structural information required for the planning of percutaneous tricuspid valve intervention. (55)

1.3.4 Magnetic resonance imaging

Cardiac magnetic resonance imaging (CMR) is often heralded as the "gold standard" of non-invasive assessment of RV function due to its high spatial resolution and ability to map the anatomically complex RV. (56-58) However, the use of CMR has remained a "complimentary" modality to echocardiography due to its relative scarcity and higher cost. (26, 57, 58) On CMR assessment, the entire RV is acquired using contiguous steady-state free precession cine images acquired across the short-axis. Evaluation of RV ejection fraction is then performed by calculating the end-diastolic and end-systolic volume based on automated traces of the RV endocardium on short-axis slices. (38) Studies have shown that reduction in CMR-derived RV ejection fraction and RV longitudinal strain independently prognosticate cardiac mortality in HFrEF. (43, 59)

Furthermore, CMR offers the unique capability to characterise myocardial tissue to detect myocardial fibrosis through late gadolinium enhancement (LGE) and oedema through extra cellular volume quantification. (60) The presence of LGE in the RV may indicate fibrofatty replacement, a hallmark of arrhythmogenic RV cardiomyopathy or other infiltrative conditions such as sarcoidosis and amyloidosis. However, accurate interpretation of LGE patterns

remains challenging due to the thinness of the RV free wall and distinguishing between these differential diagnoses can be difficult. (61)

1.3.5 Transthoracic echocardiography

Transthoracic echocardiography (TTE) is the most widely used modality of cardiac imaging in HF and has a core role in the assessment of left heart function. (62) Because of this, TTE has been adapted to become the mainstay of RV functional and structural assessment. (63)

Assessment of RV function by TTE is complicated by the RV's asymmetrical shape, limited acoustic window, and the lack of parameters that can simultaneously assess all three components of its contractile movement. (38) Despite this, TTE remains the initial diagnostic modality of choice for RV function assessment due to its accessibility, cost-effectiveness and non-invasive nature. (38, 64) This reliance on TTE assessment has spurned rapid development in TTE technology, which has allowed the introduction of new techniques and measures such as deformation imaging and three-dimensional echocardiography into the recent echocardiographic guidelines for assessment of the RV. (64, 65) Despite advances in imaging technology, we have yet to form a universally accepted definition of RV dysfunction or a system to grade the severity of RV dysfunction. (39)

1.4.0 Conventional echocardiographic measures of right ventricular function

Echocardiography remains the most common imaging modality for RV assessment and is often the imaging modality of choice. Multiple conventional and novel echocardiographic measures of RV structure and function have subsequently been developed and refined. (38)

1.4.1 Tricuspid annular plane systolic excursion

Tricuspid annular plane systolic excursion (TAPSE) is a one-dimensional measure of RV function. It measures the linear displacement of the anterolateral tricuspid valve annulus towards the RV apex during systole on M-mode imaging. (66) TAPSE only requires the visualisation of the RV annular segment, which is the most easily visualised portion of the RV wall on apical 4-chamber view. Hence it is one of the most convenient and reproducible RV systolic parameters.

A lower TAPSE has been independently associated with cardiac death, all-cause death, and HF hospitalisation in cohorts with LVEF <35% (67-69), LVEF <40% (59, 70-73) and LVEF <45% (74). In these cohorts, TAPSE values of 14mm and 16mm have been identified on receiver operator characteristic (ROC) curve analysis as optimal cutoff points in the prediction of these cardiovascular outcomes. (69, 72) Preservation of TAPSE, defined as ≥16mm, has also been associated with LV recovery (LVEF improvement>10%) (75), and response to cardiac resynchronisation therapy (CRT), defined as LVEF improvement (>5% or >10%). (76, 77)

TAPSE is one of the earliest accepted measures of RV function that has been adopted into routine clinical practice predominantly due to its ease of use. However, TAPSE simplifies RV systolic function to a one-dimensional, longitudinal movement of the anterolateral tricuspid annulus and requires further consideration for angle dependency. Therefore, it fails to adequately account for the lateral expansion of the RV free wall, altered angulation in distorted RV geometry, contribution of the LV septum, or in the context of pericardial constriction. (66)

Contemporary guidelines recommend that in the general population, interpretation of TAPSE should be performed in conjunction with supportive findings. A TAPSE of >17mm is considered normal when supported by other parameters and the patient's clinical context. (65)

Figure 1.3. Tricuspid annular plane systolic excursion

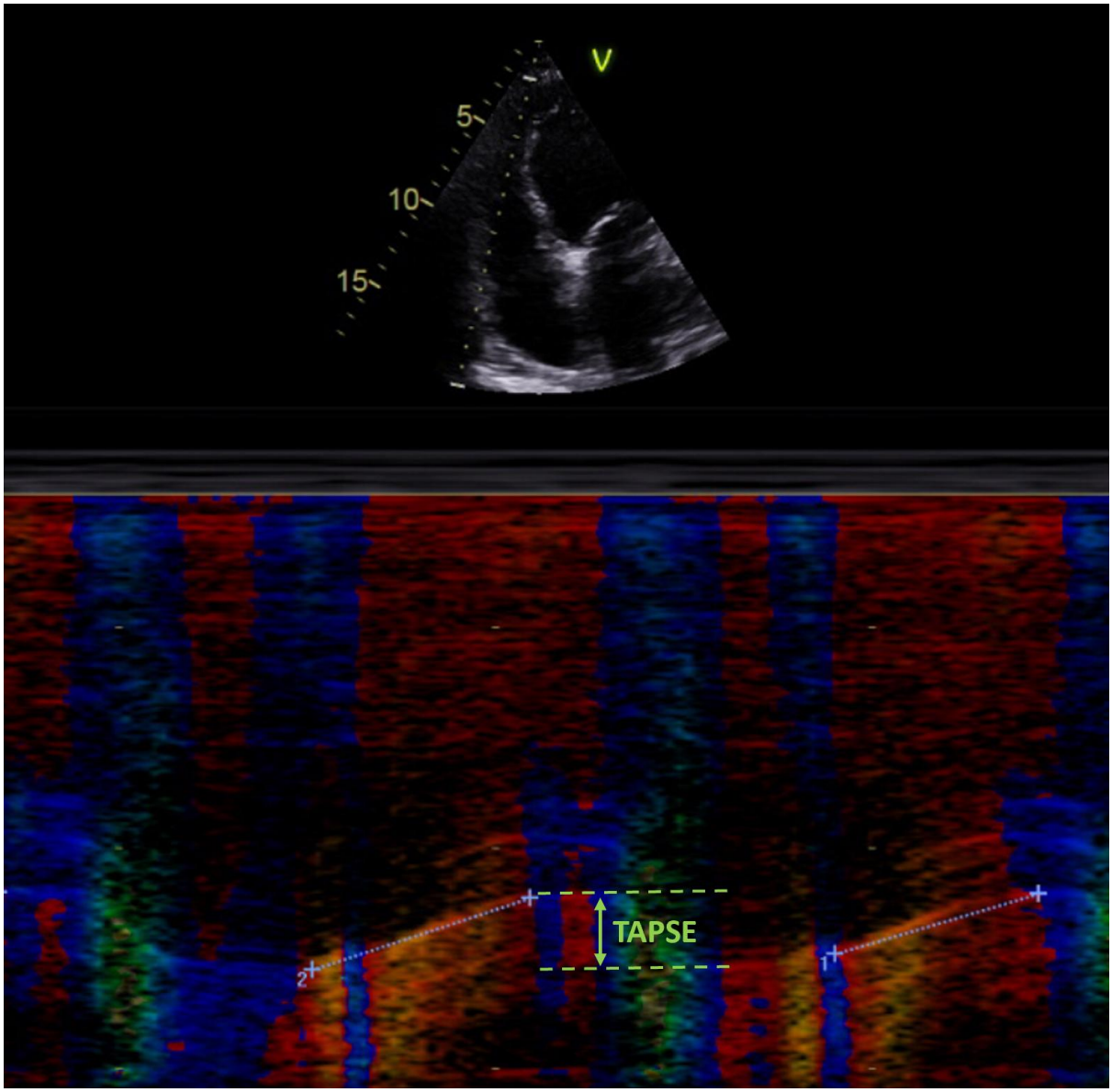

Figure 1.3. TAPSE is measured in the apical 4-chamber view by aligning the M-mode cursor along the tricuspid annulus to track its longitudinal movement. The value of TAPSE is the longitudinal distance travelled by the tricuspid annulus during systole.

Abbreviations. *TAPSE: tricuspid annular plane systolic excursion*

1.4.2 Pulsed Doppler peak velocity at the tricuspid annulus

The longitudinal movement of the anterolateral tricuspid annulus can also be assessed by its peak velocity during systole, which is calculated as its displacement over a unit of time. This measurement is termed RV systolic excursion velocity (RVS') and is usually expressed as centimetres per second. (78) RVS' has shown good correlations with RV ejection fraction on CMR and radionuclide angiography. (79, 80) This measure of RV systolic function is quick, reliable, and reproducible. (64) Like all Doppler techniques, pulsed Doppler peak velocity at the tricuspid annulus is an angle-dependent measure. Therefore, care must be taken by the operator to ensure the correct orientation of the image to prevent underestimation of the measured velocity.

Like TAPSE in systolic HF, RVS' impairment has been shown to be independently associated with cardiac death, all-cause death, and HF hospitalisation. (81-84) RVS' has been shown to be superior to TAPSE in a chronic HFrEF cohort with LVEF <40% by Darahim et al. (83) Additionally, Giannini et al. showed that in an advanced HF population with severe secondary mitral regurgitation planned for transcatheter edge to edge repair procedure, RVS' independently predicted cardiovascular death while TAPSE did not. (85) On the other hand, RVS' was inferior to TAPSE in predicting LV recovery of ≥10% in a chronic HFrEF cohort by Shah et al. (75) Furthermore, TAPSE was associated with RV stroke volume on right heart study but RVS' was not. (67)

Most published studies utilise the traditional 10cm/s RVS' cutoff value. (64) Several studies individually identified their own optimal RVS' cutoff values based on the predictive power on ROC curve analysis. Bistola et al. and Groote et al. found 7.3cm/s and 9.6cm/s to be the ideal cutoff for predicting cardiovascular death respectively. (81, 86) While Melzuni et al. selected 10.8cm/s as the best predictor for combined death and HF hospitalisation. (84) Contemporary guideline recommendation lists a normal RVS' for the general population as >9.5cm/s. (65)

Figure 1.4. Systolic excursion on pulsed Doppler velocity at the tricuspid annulus

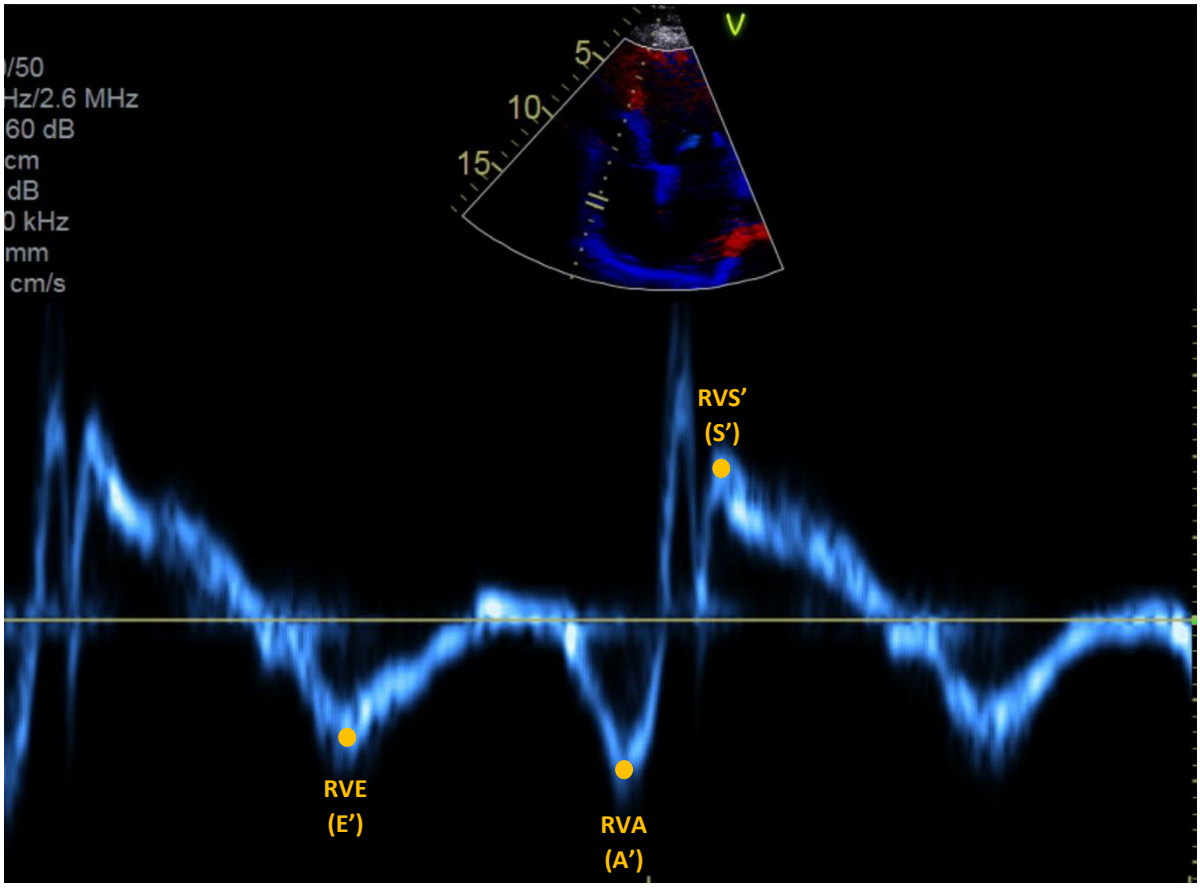

Figure 1.4. The pulsed Doppler velocity at the annulus is measured in the 4-chamber view by focusing the pulse Doppler at the lateral tricuspid annulus or at the base of the RV wall. The systolic excursion marked as RVS', is the highest systolic reading during the ejection time (see above). (64)

1.4.3 Right ventricular pulmonary arterial coupling

One of the short falls of RV longitudinal assessment is its load dependence. Both TAPSE and RVS' do not account for RV afterload, which is dependent on the pulmonary artery systolic pressure (PASP). Subsequently, the concept of right ventricular pulmonary arterial coupling was devised and adopted by several groups to assess the relationship between TAPSE and PASP. (70, 87-89) The TAPSE / PASP ratio is an afterload independent measure with the ability to measure RV contractile reserve in the face of rising afterload. (90)

TAPSE / PASP ratio has been demonstrated to be independently associated with all-cause death (88), and with combined death and HF hospital in systolic HF patients. (70) A TAPSE / PASP ratio of 0.36 mm/mmHg was found to be the optimal cutoff point for discriminating for all cause death in a study of both systolic and diastolic HF patients by Guazzei et al. (91) However, TAPSE alone had a similar statistical yield on c-statistics and multivariate regression compared to TAPSE / PASP ratio in two of these studies. (70, 91) Ishiwata et al., on the other hand, did not find any independent association between TAPSE / PASP ratio and all-cause mortality in an ICM population. (73) Similarly, RVS' / PASP has also been examined for RV pulmonary arterial coupling. However, its performance fell short of the traditional TAPSE / PASP ratio. (92)

In the general population, the normal range of TAPSE / PASP ratio is described as 0.5-0.7mm/mmHg in contemporary guideline recommendations. (65)

1.4.4 Myocardial performance index

Myocardial performance index (MPI) is a Doppler index of combined systolic and diastolic function. This is a ratio calculated from the duration of cardiac phases on tissue Doppler or pulse wave assessment. It was first hypothesised and validated by Tei et al. for the assessment of LV function. (93) This was subsequently adapted for the RV in pulmonary hypertension in the 1990's. (94) MPI, also known as the Tei index, is calculated with the

equation: (RV isovolumetric contraction time + RV isovolumetric relaxation time) / Pulmonary ejection time. (95) As such, MPI attracted attention especially because it provides combined systolic and diastolic function, when there were limited methodologies for RV diastolic assessment at that time. MPI has the added advantage of being a dimensionless measure of RV function and with no geometric assumptions made. (65)

To examine the utility of MPI, Field et al. separated a cohort of patients planned for CRT-defibrillator (CRT-D) implantation into tertiles based on RV MPI. The first and second tertiles were not associated with the primary outcome of death, cardiac transplantation, and LVAD placement. The third tertile had a RV MPI range of 0.84 to 2.21 and was independently associated with the primary outcome (Hazard ratio 3.3, CI: 1.3-8.5). (96)

On the other hand, in two separate cohorts of systolic HF patients examined by Verhaet et al. and Vizzardi et al. did not find an independent association between RV MPI and their endpoint of combined death and HF hospitalisation. Instead, these two groups found that RV-GLS and RV basal strain were independently associated with their endpoints instead. (97, 98)

A normal MPI is listed as <0.40ms based on pulse wave assessment and <0.55ms using tissue Doppler method in current society guideline. (65)

Figure 1.5. Myocardial performance index - tissue Doppler

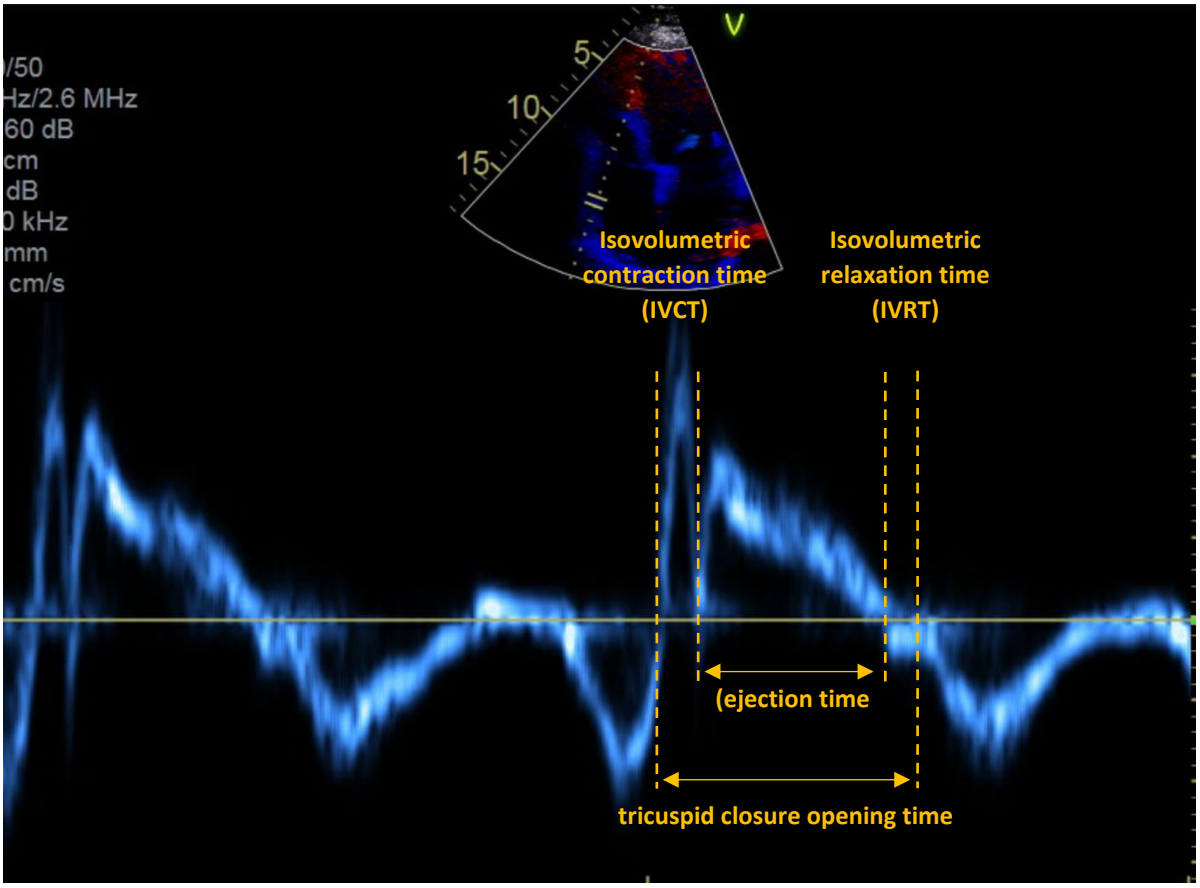

Figure 1.5. Calculation of right ventricular myocardial performance index (MPI) by pulsed tissue Doppler (above). The tricuspid (valve) closure opening time (TCO) encompasses isovolumic contraction time (IVCT), ejection time (ET), and isovolumic relaxation time (IVRT). (96)

Figure 1.6. Myocardial performance index - pulsed Doppler

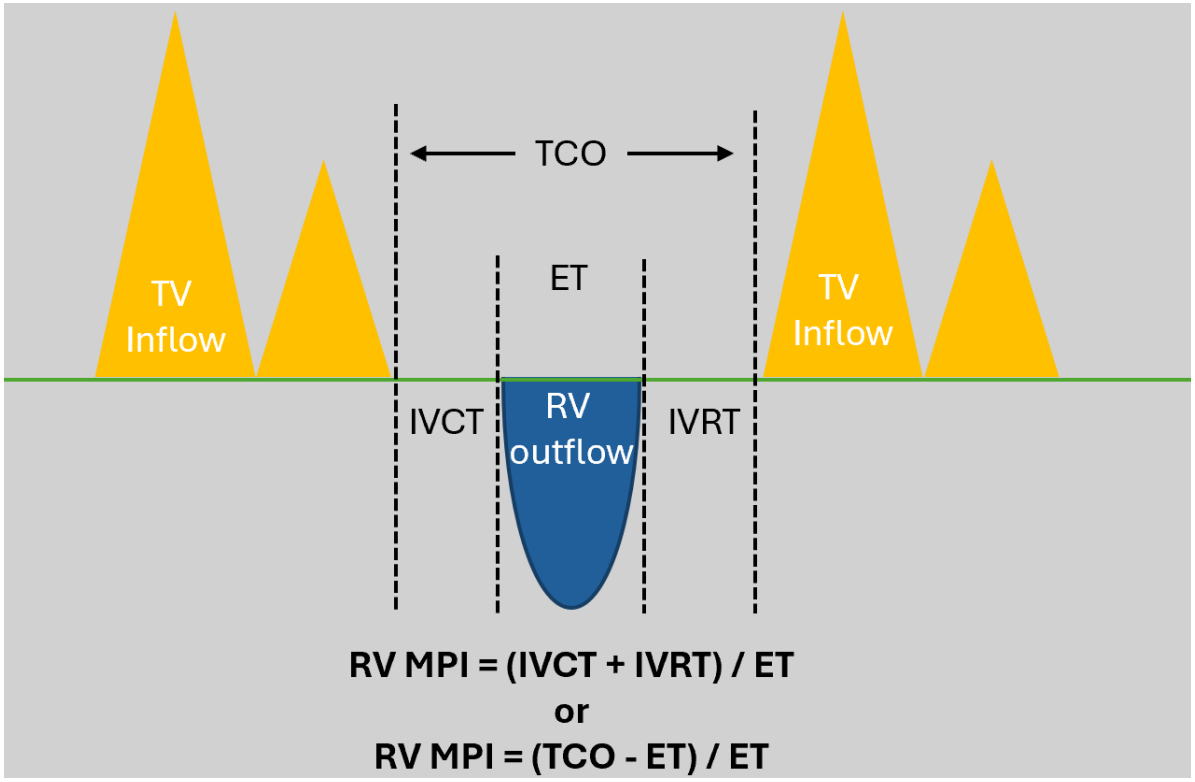

Figure 1.6. Calculation of right ventricular myocardial performance index (MPI) by the pulsed Doppler (above). In the pulsed Doppler method, TCO can also be measured by the duration of the tricuspid regurgitation continuous-wave Doppler signal. MPI = (IVCT+ IVRT)/ET or = (TCO - ET)/ET. (96)

1.4.5 Right ventricular fractional area change

Fractional area change (FAC) is the percentage change of RV area between systole and diastole as seen on TTE in the apical RV focused view. It is defined as: (RV end-diastolic area – RV end-systolic area) / RV end-diastolic area x 100%. This two-dimensional measure of RV systolic function accounts for both the longitudinal contraction of the RV wall and the lateral displacement of the lateral tricuspid annulus from radial contraction and the contribution from the interventricular septum. (64, 99) FAC has been shown to correlate with CMR derived RV ejection fraction in HF and other populations. (100) It is a simple two-dimensional measure that does not require use of any additional software. As such it holds great promise as a measure of RV systolic function. However, it should be remembered that FAC does not account for the work contributed by the RV outflow tract and is a two-dimensional surrogate measure of three-dimensional contraction. (99, 101)

In HFrEF, FAC impairment has been shown to be independently associated with all-cause death. (59, 73, 102) Furthermore, it has independent association with CRT-D response and cellular rejection in cardiac transplantation. (77, 103)

The traditional FAC cutoff value of 35% (64) was used in two studies. (102, 103) ROC curve defined FAC cutoffs of 39% (59) and 27% (73) were used to predict all-cause death by Houard and Ishiwata et al. respectively. While Abdelheim used a FAC cutoff of 32% for predicting CRT-D response. (77)

Contemporary guidelines recommend the use of FAC as a supporting parameter, or in place of conventional TAPSE or RVS' in situations where they are unreliable. (65) The normal reference range for FAC has been set at >35% in the general population. (99)

Figure 1.7. Right ventricular fractional area change

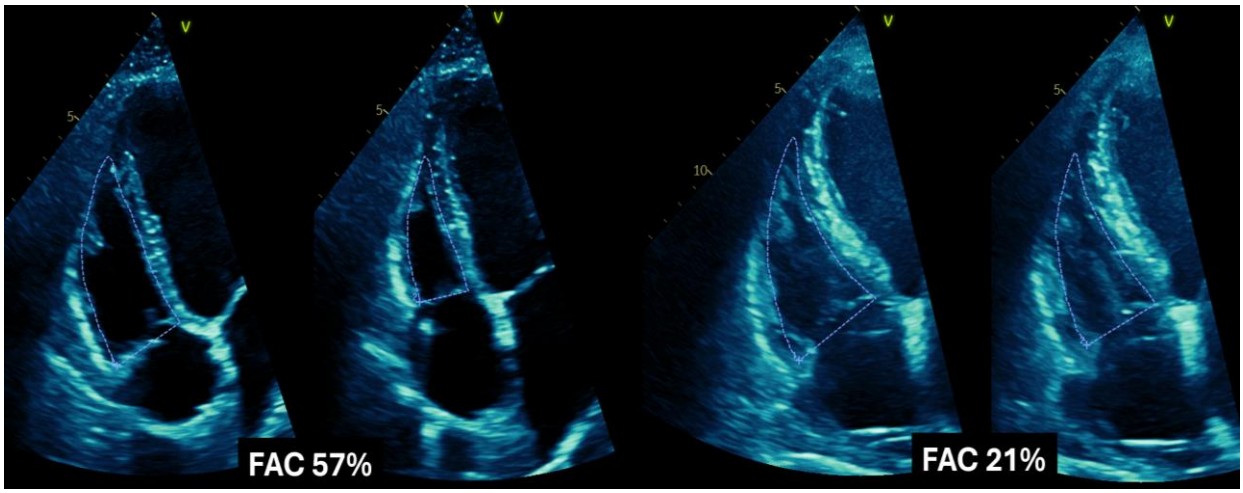

Figure 1.7. The RV area is calculated by tracing the RV endocardial border using the RV-focused apical 4-chamber view in end diastole and end systole. The FAC is then calculated using the formula: (RV end diastolic area – RV end systolic area) / RV end diastolic area x 100%. The two examples above demonstrated the end-systolic and end-diastolic area traced in a normal patient (above left) and a patient with RV dysfunction (above right). (64)

1.5.0 Advanced echocardiographic measures of right ventricular function

Advancements of TTE technology have led to the introduction of speckle-tracking echocardiography (STE) and three-dimensional assessment modalities. These techniques were first introduced to assist with the assessment of LV systolic function and have since been adapted to assist with the evaluation of the RV. (104, 105)

1.5.1 Right ventricular strain and strain rate

Advent of STE introduced angle independent assessment across the entire length of RV myocardial wall. STE uses frame-by-frame tracking of speckle patterns within the myocardium which makes it less affected by reverberation and dropout artefacts compared to traditional measures. (104) The movements of these speckles are then analyzed by dedicated software to determine changes in length of each myocardial segment using the Lagrange strain equation. (64, 106)

Longitudinal strain refers to the shortening of the longitudinal myocardial fibres, and as such is traditionally expressed as a negative value. However, society guidelines now recommend that strain and change in strain be expressed as absolute values. (14, 65) In compliance with the accepted norm, longitudinal strain will henceforth be expressed as absolute values in this thesis unless otherwise specified. (65)

STE derived RV longitudinal strain is thought to be superior to traditional measures of RV longitudinal function and can detect deterioration in RV contractile function before gross systolic impairment manifest. (107, 108) There are two predominant methods of assessing RV longitudinal strain. The first method is by incorporating both the RV free wall and the interventricular septum, which is shared with the LV. This is termed the RV global longitudinal strain (RV-GLS). The second method focuses solely on the RV free wall, termed right ventricular free wall strain (RV-FWS). RV strain has been found to be superior to traditional RV echocardiographic parameters including TAPSE, RVS, RV MPI, and FAC. (97, 98, 109)

RV-GLS reduction in systolic HF is independently association with all cause death (59, 73, 110, 111) as well as combined death, transplant and HF hospitalisation. (71, 112, 113) RV-GLS has been shown to correlate well with RVEF on CMR (113) and RV stroke volume on invasive right heart catheterisation. (67)

RV-FWS is thought by some authors to be a more accurate reflection of RV contractile function since the interventricular septal function is predominantly provided by the LV. (71) RV-FWS has been found to be independently associated with death (33, 65), and with combined death and HF hospitalisation. (71, 109, 114) In a cohort of stable systolic HF patients, Carluccio et al. demonstrated that RV-FWS was superior to RV-GLS in predicting combined outcome of death and HF hospitalisation. In this cohort, RV-FWS remained independently associated with the combined outcome even after correcting for EMPHASIS score and LV systolic function, while RV-GLS was not. (71) Consequently, RV-FWS has emerged just ahead of RV-GLS as the preferred manner of RV strain assessment. (107, 115)

The normal RV-GLS and RV-FWS cutoff values have been defined as 18.2% and 20.0% respectively, based on large population studies by the World Alliance of Societies of Echocardiography. (116) A recent guideline update has adopted a more streamlined normal reference range of >17% for RV-GLS and >20% for RV-FWS. (65) However, these “normal” reference ranges based on the two standard deviations from the mean is thought to be insufficient in systolic HF or HFrEF. (63) Several different cutoff values have been proposed for HFrEF based on the optimal cutoff points on ROC curve analysis. To best discrimination for all-cause death and HF hospitalisation in HFrEF cohorts, cutoff values of ≤14.6%, ≤14.8%, ≤15.4%, ≤19% were identified for RV-GLS (59, 71, 112, 113), and cutoff values of ≤15.3% and ≤19% were identified for RV-FWS. (59, 71, 109)

It should be noted that RV strain measures are affected by heart rate variability in arrhythmias, especially with rapid ventricular rates, where the temporal resolution is reduced. (65) RV strain is also partially load dependent, with increased preload leading to higher strain values and

elevated afterload resulting in a reduction. (99) When compared to other RV functional parameters including three-dimensional echocardiographic parameters, RV strain is less load dependent and even considered relatively load independent by some authors. (117, 118)

Figure 1.8. Right ventricular longitudinal strain

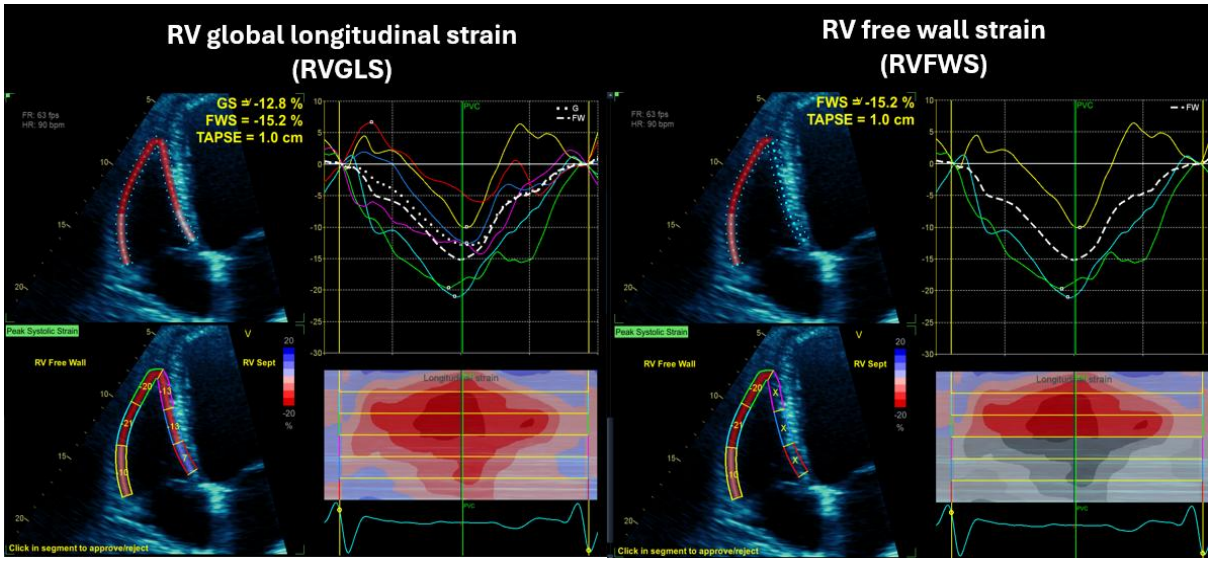

Figure 1.8. Right ventricular global longitudinal strain is assessed by averaging both the septal wall and RV free wall segments (above left). While right ventricular free wall strain assesses the RV free wall in isolation (above right). (14)

Abbreviations. *RV-GLS: right ventricular global longitudinal strain, RV-FWS: right ventricular free wall strain.*

1.5.2 Three-dimensional Right ventricular ejection fraction

Assessment of RV ejection fraction was previously limited to cardiac radionuclide and magnetic resonance imaging modalities. (37, 48) Development of three-dimensional echocardiography with high temporal resolution has allowed for accurate TTE assessment of RV ejection fraction. The use of three-dimensional right ventricular ejection fraction (3D-RVEF) has been proposed to compliment traditional two-dimensional (2D) measures of RV function, with a value of 44.7% defined as the lower limits of normal based on population studies by the World Alliance of Societies of Echocardiography. (119) A rounded off normal reference range of 45% has subsequently been adopted by contemporary guidelines. (14, 65)

The utility of this novel 3D parameter has been applied to several cohorts including the general population, those with HF, valvular heart disease, pulmonary hypertension, B-cell lymphoma, cardiovascular diseases, and those undergoing cardiac surgery. (120-126) The most extensively studied population is that of individuals with pulmonary hypertension, particularly those with pulmonary arterial hypertension. (125-131) Followed by mixed cardiovascular diseases. (120, 132-135) In these two populations, the reduction in 3D-RVEF has been shown to prognosticate various adverse cardiovascular outcomes, including all-cause death, cardiac death, cardiopulmonary death and composite end-points. (123)

Only two studies assessed 3D-RVEF in systolic HF populations. (136, 137) The larger of the two studies by Tolvaj et al. retrospectively included 174 patients with LV systolic impairment who were scheduled for cardiovascular procedures and found a 3D-RVEF of <48.2% to be associated with worse survival. (136) However, a quarter of the mortality was related to the scheduled cardiovascular procedure. The second and smaller study by Vijiiac et al. assessed 50 prospectively recruited patients with dilated NICM in sinus rhythm and found a 3D-RVEF of <43.4% was independently associated with major adverse cardiovascular events. (137)

Outside of these cohorts, one further study examined patients undergoing cardiac surgery. In which preservation of 3D-RVEF at or above 45% is associated with reduced in-hospital mortality and need for LV assist device, independent of EuroSCORE II. (122)

In all these studies, 3D-RVEF was derived from either Philips vendor-specific software (Philips, Andover MA, USA) or TomTec vendor-independent software (TomTec Image Arena Systems, Unterschleissheim, Germany). Interestingly, EchoPAC vendor-specific software (General Electric, Horten, Norway) was not used in any of the studies above. (122, 123, 125, 126)

Of note, the feasibility of 3D-RVEF assessment is currently considered poor. With only 50% of 3D TTE datasets being suitable for 3D-RVEF analysis based on a cohort of patients assessed between 2016 and 2019 by the international collaborative study by the World Alliance of Societies of Echocardiography. (116) This overall low feasibility in clinical practice may explain the scarcity of data examining the role of 3D-RVEF in the literature, particularly in HFrEF.

Figure 1.9. Three-dimensional right ventricular ejection fraction

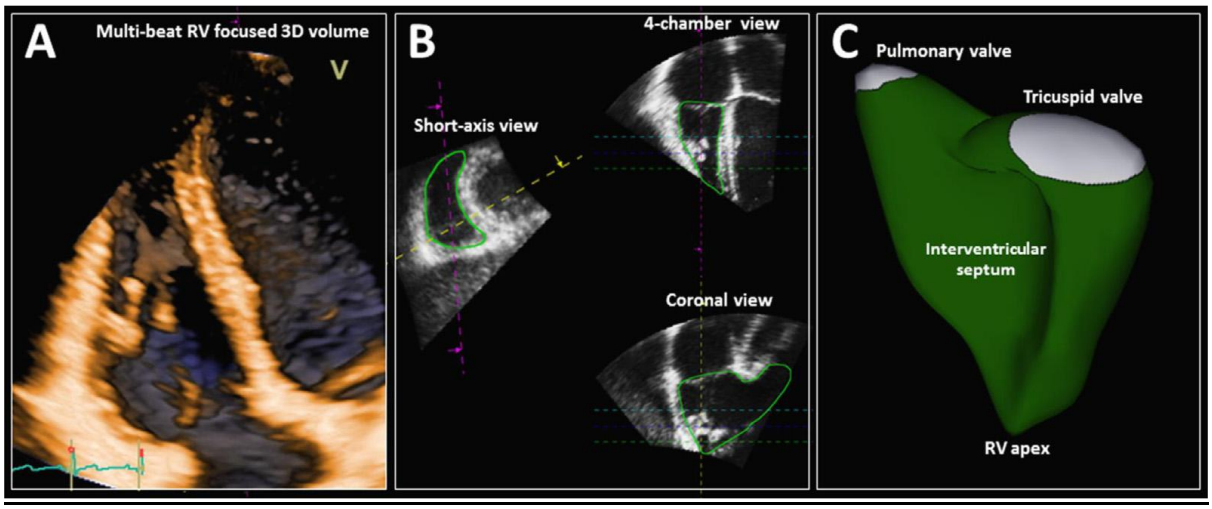

Figure 1.9. A three-dimensional data set is acquired in the RV focused apical view by combining the right ventricular volumes across several beats. The right ventricular endocardium is then semi-automatically identified to generate a three-dimensional model of the right ventricular to enable quantification of right ventricular volumes and ejection fraction. (14)

1.5.3 Right ventricular myocardial work

Myocardial work (MW) is a new concept of assessing myocardial energy expenditure and efficiency through non-invasive assessment of pressure volume loops. MW was initially developed and validated for the left heart and was recently adapted to the RV. (138) This novel parameter accounts for RV afterload and provides a load independent assessment of RV function. An early proof of concept study has demonstrated that one of the MW indices, RV global constructive work, correlated well with RV stroke volume on right heart catheterisation. (138) Currently RV WM technology is not commercially available and has yet to prove itself against clinical outcomes.

1.6.0 Current Knowledge and Short Falls

A review of the literature has found that both traditional and novel TTE parameters of RV systolic function have been shown to be independently associated with clinical endpoints in HFrEF and NICM. The traditional TTE parameters of TAPSE, RVS', and FAC have all demonstrated independent association with death and HF hospitalisation by multiple studies. RV - PA coupling and MPI, on the other hand, have shown mixed results. As for STE parameters, both RV-GLS and RV-FWS have proven their prognostic prowess for adverse cardiovascular outcomes over the traditional parameters in several studies. The newer advanced TTE parameter of 3D-RVEF has only been studied in limited capacity in HFrEF. But it has shown early promise to independently prognosticate major adverse cardiovascular events in small select populations. Finally, the novel concept of RV MW is still experimental at this stage and is only available through proprietary software that is unavailable for widespread commercial use. (138)

In summary, RV systolic function as assessed on TTE have proven to be an integral part of comprehensive cardiac functional assessment in systolic HF. Both traditional markers and advanced markers have shown prognostic utility in systolic HF. However, knowledge gaps still

exist in our understanding of these RV systolic parameters which will be further explored below.

1.6.1 Severity of left ventricular systolic impairment

There is a close correlation between CMR derived LVEF and RV ejection fraction in systolic HF. (57) Therefore, examining the isolated effect of RV dysfunction on clinical outcomes is often confounded by the degree of LV systolic impairment. Current studies in the literature simply select a binary LVEF cutoff and ignore the differential effect different grades of LV systolic dysfunction can impart on RV function. Most studies selected patients either with a LVEF of ≤35% (59, 69, 76, 77, 81, 89, 96, 97, 111, 112, 139, 140), or ≤40% (70-72, 75, 82, 83, 98, 102, 109, 113, 137, 141). Only a small proportion of studies included subjects with LVEF of 45% or less. (86, 110, 142) Interestingly, patients with mild LVEF impairment of 45-49% were not included in any of these cohorts.

Further studies are required to assess the impact of different grades of LV systolic dysfunction on RV systolic dysfunction in HFrEF. Particularly in those with only mild LVEF impairment of 45-49%.

1.6.2 Elevated body mass index and obesity

Elevated body mass index (BMI) and in particular obesity, is a rapidly growing chronic disease in the modern world with approximately 43% of adults being estimated to be overweight across the globe. (143) The adverse impact of elevated BMI and obesity on the development of overall cardiovascular disease is well established, but its specific impact on the RV is less well understood. BMI elevation has been shown to associate with subclinical RV dysfunction in healthy young adults based on tissue Doppler and correspond to worse RV function on invasive right heart catheterisation. (144, 145) Obesity is considered by current TTE guidelines

to be a risk factor for elevated pulmonary pressures. The isolated impact of elevated BMI on RV function without obesity-related comorbidities remains unclear and will require further examination. (65)

1.6.3 Right ventricular pacing

Pacemaker induced cardiomyopathy is a well-established phenomenon where LV systolic dysfunction occurs in the context of RV pacing. (146) It is now recognised that RV pacing and premature ventricular complex burden can lead to RV systolic dysfunction. (147, 148) A recent retrospective study by Boyle et al. further demonstrated that 11% of patients developed new RV systolic dysfunction after exposure to a RV pacing burden of at least 20%. (149) Although it remains unclear whether higher RV pacing burden may have incremental effect on RV systolic function.

Cardiac pacing in the form of permanent pacemaker, automated implantable cardioverter defibrillator, or CRT is commonplace in systolic HF (HF). (27, 150) As such, it is necessary to account for the effect of RV pacing when assessing RV systolic function in a systolic HF cohort.

1.6.4 Atrial fibrillation

Atrial fibrillation (AF) is present in approximately 22% of NICM patients and its presence is associated with increased risk of mortality. (151) AF can contribute to RV dysfunction in HFrEF via several mechanisms including: loss of atrial contraction, increased ventricular rate, irregular cardiac cycle length, and loss of ventricular synchrony. (65, 152) Furthermore, chronic AF can lead to right atrial adverse remodeling and dilatation of the tricuspid annulus which then lead to the development of atrial functional tricuspid regurgitation. (153) Therefore, the presence of AF can confound the assessment of RV function in clinical studies and needs to be accounted for. Most of the studies in the literature included both those with and without

AF, while nine studies circumvented the effect of AF by only including those in sinus rhythm (59, 67, 81, 82, 84, 112-114, 137). None of the studies in the literature examined only patients in AF.

AF commonly coexist with HF and is prevalent in over a quarter of systolic HF patients. (154) Further examining the effect of AF on RV systolic function in the HFrEF population would help bridge an important knowledge gap.

1.6.5 Cardiomyopathy aetiology

The aetiology of cardiomyopathy also plays a major role in determining ventricular function and prognosis. Patients with ischaemic aetiologies are known to have a higher mortality rate and worse overall outcomes compared to those with NICM. (25, 155) Furthermore, incomplete revascularisation of coronary disease is also associated with increased mortality. (156) In comparison to the LV, the RV is relatively well protected from ischaemic injury due to its unique physiology and lower oxygen requirement. (34)

NICM aetiology is associated with a higher prevalence of RV dysfunction. (43-46, 157) Those with ICM exhibit a regional pattern of dysfunction linked to specific coronary artery territories as opposed to the global systolic dysfunction seen in NICM which affects both ventricles. (158)

Studies in the literature examining RV systolic function in HFrEF have recruited from a range of HF aetiologies. Only five studies specified a single aetiology in the inclusion criteria, with two studies only including those with ICM (113, 159), and three studies only including NICM patients (73, 102, 137). The remaining studies were conducted in heterogenous cohorts with a mix of cardiomyopathy aetiologies. (59, 69, 76, 77, 81, 89, 96, 97, 111, 112, 139, 140) (86, 110, 142)

Future studies examining RV systolic function in HFrEF should focus on the NICM population, where there is a high burden of concomitant RV dysfunction and no additional mortality attributed to ischaemic disease, which may confound the observed outcome. (158)

1.6.6 Contemporary heart failure therapy and compensatory status

Implementation of contemporary optimal guideline directed therapy in HFrEF has been reported to improve symptoms and to reduce mortality by over 70%. (160, 161) It would then stand to reason the degree of HF therapy implemented in each study population would play a pivotal role in determining the rate of the adverse cardiovascular outcomes observed. Current HF guidelines recommend initiation and treatment with the “four pillars” of pharmacotherapy in HF with reduced LVEF. (12, 13) Amongst the current literature assessing TTE determinants of RV function in HFrEF, HF pharmacotherapy was not reported at all in ten studies. (67, 77, 85, 103, 110, 113, 114, 136, 162) In the remaining twenty-nine studies, only one study reported angiotensin receptor-neprilysin inhibitor use in which less than 4% of patients were prescribed the agent. (75) None of the studies reported sodium glucose co-transporter 2 inhibitor use as it was only introduced as a therapy for systolic HF in late 2019, which post-dates most of the study periods. (163) On the other hand, angiotensin receptor-neprilysin inhibitors were introduced in 2014, but had delayed adoption as evidenced by CHAMP-HF registry data. (164, 165)

On top of HF therapy, the compensatory status of HF can also influence RV function and was documented in around half of the studies. Thirteen of the studies recruited chronic stable HF patients (57, 59, 69, 71, 86, 88, 98, 109-112, 137, 139), and eight studies included acutely decompensated patients (70, 81, 82, 97, 136, 140, 141, 162). Of note, the duration of HF diagnosis was not well documented in most studies. Just a single study described the duration of HF diagnosis, where only patients with de novo cardiomyopathy were included. (82)

A contemporary study of compensated HFrEF patients should therefore include subjects stabilised on maximally tolerated optimal guideline directed therapy. Otherwise, it would not be an accurate reflection of the real-world chronic HFrEF population.

1.6.7 Right ventricular function as predictors of exercise capacity

RV dysfunction has been linked to reduced exercise capacity in chronic HF alongside other cardiovascular conditions. (166-169) It is believed that RV systolic impairment both impedes venous return and reduces flow into the pulmonary circulation which in turn impairs pulmonary capillary gas exchange. (166) In a HFrEF cohort undergoing cardiac defibrillator implantation, Legris et al. found that of the traditional TTE RV functional parameters, only RV-pulmonary coupling expressed as TAPSE/PASP ratio was independently associated with peak VO2. (170) Of the novel TTE parameters, RV-GLS and 3D-RVEF have both been shown to significantly correlate with peak VO2 in an ICM cohort consisting of 54 patients. (159)

Patients with ICM have been shown to have lower exercise capacity compared to NICM, presumably due to their older age and underlying myocardial ischaemia. (171) Evaluation of exercise capacity in NICM, should therefore be performed separately from those with myocardial ischaemia. However, there are limited studies evaluating the relationship between RV systolic function and exercise capacity in NICM populations.

1.6.8 Normal reference range of right ventricular parameters in heart failure

Most conventional RV echocardiographic parameters have well established standardised cutoff values based on the normal population. (64, 65) However, the application of these cutoffs in systolic HF may not be valid. (14, 107) This is particularly true for advanced parameters such as RV strain as evidenced by the wide range of cutoff values presented across the literature. In all the studies that examined RV strain in systolic HF, they elected not

to institute the normal population cutoff values put forth by prior studies. Instead, these studies determined their own optimal cutoff values based on the discriminatory ability of their receiver operating characteristic curves. (59, 71, 73, 77, 95, 109, 112-114) In regard to predicting death and HF hospitalisation, RV-FWS cutoff values of 15% (114), and 15.3% (71, 109) where identified as the best predictors, while cutoff values of -12.1% (114), -14.6% (71, 109), -14.8% (112), and -15.4% (113) were found for RV-GLS. Similarly, a 3D-RVEF cutoff of 45% was defined based on the normal population, but the utility of this cutoff in a systolic HF cohort has not been well studied. A 3D-RVEF cutoff of <43.4% and <48.2% has been identified to prognosticate adverse cardiovascular events in select systolic HF cohorts. (136, 137)

Further study can help establish a normal reference range for advanced TTE parameters of RV systolic function in NICM, particularly in compensated and stable patients.

1.6.9 Vendor dependency of three-dimensional right ventricular ejection fraction

RV STE and 3D-RVEF measurements are both dependent on the software algorithms employed by their respective vendors. (14) STE including both RV-GLS and RV-FWS have been well studied and verified across a wide range of vendor-independent and vendor-specific softwares in systolic HF. (65) However, the use of 3D-RVEF in HFrEF has only been assessed in using TomTec, a vendor-independent software. Therefore, further studies are required to assess the use of 3D-RVEF using other commercially available software.

1.7.0 Study rationale

HFrEF remains a condition of substantial morbidity and mortality, and improved risk stratification is essential to guide therapeutic decision making and improve clinical outcomes. (172) Emerging evidence suggests that RV systolic dysfunction is not only prevalent in NICM but may also provide independent prognostic value beyond conventional LV parameters. (57)

Nevertheless, current HF guidelines lack specific recommendations for assessing or managing concomitant RV dysfunction in NICM. (12, 13, 26) This represents a critical knowledge gap, particularly given that biventricular involvement may reflect a more advanced or distinct disease phenotype requiring tailored therapeutic strategies. (64)

This doctoral thesis aims to address this gap in knowledge by evaluating the prevalence, severity and clinical correlates of RV systolic dysfunction in NICM. Furthermore, it aims to investigate the prognostic significance of RV dysfunction as measured by echocardiographic parameters including novel techniques including RV strain and 3D-RVEF. By improving the understanding of RV function in NICM, the author hopes this thesis can contribute to the development of more refined risk stratification models and inform future efforts to personalise treatment approaches for patients with biventricular failure distinct from those with isolated LV systolic impairment.

1.8.0 Specific aims and hypotheses

1.8.1 Hypotheses

The following hypotheses will be tested by this thesis

Hypothesis 1: Changes in right ventricular size and function will be present even in early stages of non-ischaemic cardiomyopathy, with increasing prevalence and severity as left ventricular systolic impairment progresses.

Hypothesis 2: Compared to traditional echocardiographic parameters, right ventricular strain is a more sensitive marker of right ventricular dysfunction and possesses stronger prognostic utility in non-ischaemic cardiomyopathy.

Hypothesis 3: Alterations in right ventricular free wall strain will precede changes in right ventricular size and conventional metrics of right ventricular function and will

be influenced by the presence of comorbidities including elevated body mass index, and atrial fibrillation.

Hypothesis 4: Impairment of right ventricular systolic functional indices correlate with reduced exercise capacity in those with stable non-ischaemic cardiomyopathy. (Tested by Specific Aim 3)

Hypothesis 5: Three-dimensional right ventricular ejection fraction captures all three components of right ventricular systolic contraction and would serve as a more specific predictor of adverse cardiovascular outcomes compared to right ventricular free wall strain and other traditional parameters in non-ischaemic cardiomyopathy. (Tested by Specific Aim 3)

Hypothesis 6: Impaired right ventricular free wall strain and three-dimensional right ventricular ejection fraction will have prognostic significance in stable non-ischaemic cardiomyopathy patients and will enhance risk stratification beyond conventional clinical and echocardiographic factors. (Tested by Specific Aim 3)

1.8.2 Specific aims

The above congruent hypotheses will be tested by the following specific aims:

Specific aim 1: To determine the alterations in right ventricular size and function in a retrospective cohort of subjects with non-ischaemic cardiomyopathy across a range of LVEF. (Hypothesis 1 and 2)

Specific aim 2: To ascertain additional clinical and echocardiographic determinants of RV function in subjects with comorbid elevated body mass index; and atrial fibrillation, which are factors commonly associated with non-ischaemic cardiomyopathy. (Hypothesis 3)

Specific aim 3: Evaluate the prognostic value of advanced two-dimensional and three-dimensional RV functional parameters and determine their independent and incremental value over traditional clinical risk factors in patients with stable non-ischaemic cardiomyopathy. (Hypothesis 4, 5, and 6)

1.9.0 References

1. Coronel R, de Groot JR, van Lieshout JJ. Defining heart failure. Cardiovasc Res. 2001;50(3):419-22.
2. Braunwald E. Cardiovascular Medicine at the Turn of the Millennium: Triumphs, Concerns, and Opportunities. New England Journal of Medicine. 1997;337(19):1360-9.
3. Roger VL. Epidemiology of heart failure. Circ Res. 2013;113(6):646-59.
4. Ponikowski P, Anker SD, AlHabib KF, Cowie MR, Force TL, Hu S, et al. Heart failure: preventing disease and death worldwide. ESC Heart Fail. 2014;1(1):4-25.
5. Benjamin EJ, Virani SS, Callaway CW, Chamberlain AM, Chang AR, Cheng S, et al. Heart Disease and Stroke Statistics-2018 Update: A Report From the American Heart Association. Circulation. 2018;137(12):e67-e492.
6. Butler J, Rich J. Epidemiology of Heart Failure and the Discovery of the Cardioprotective Effects of SGLT2 Inhibitors. JACC Heart Fail. 2024;12(6S):S1-S3.
7. Writing Group M, Mozaffarian D, Benjamin EJ, Go AS, Arnett DK, Blaha MJ, et al. Heart Disease and Stroke Statistics-2016 Update: A Report From the American Heart Association. Circulation. 2016;133(4):e38-360.
8. Bleumink GS, Knetsch AM, Sturkenboom MC, Straus SM, Hofman A, Deckers JW, et al. Quantifying the heart failure epidemic: prevalence, incidence rate, lifetime risk and prognosis of heart failure The Rotterdam Study. Eur Heart J. 2004;25(18):1614-9.
9. Hobbs FD, Roalfe AK, Davis RC, Davies MK, Hare R, Midlands Research Practices C. Prognosis of all-cause heart failure and borderline left ventricular systolic dysfunction: 5 year mortality follow-up of the Echocardiographic Heart of England Screening Study (ECHOES). Eur Heart J. 2007;28(9):1128-34.
10. Sahle BW, Owen AJ, Mutowo MP, Krum H, Reid CM. Prevalence of heart failure in Australia: a systematic review. BMC Cardiovasc Disord. 2016;16:32.

11. Parsons RW, Liew D, Neville AM, Audehm RG, Haikerwal D, Piazza P, et al. The epidemiology of heart failure in the general Australian community - study of heart failure in the Australian primary carE setting (SHAPE): methods. BMC Public Health. 2020;20(1):648.
12. McDonagh TA, Metra M, Adamo M, Gardner RS, Baumbach A, Bohm M, et al. 2021 ESC Guidelines for the diagnosis and treatment of acute and chronic heart failure. Eur Heart J. 2021;42(36):3599-726.
13. Authors/Task Force M, McDonagh TA, Metra M, Adamo M, Gardner RS, Baumbach A, et al. 2023 Focused Update of the 2021 ESC Guidelines for the diagnosis and treatment of acute and chronic heart failure: Developed by the task force for the diagnosis and treatment of acute and chronic heart failure of the European Society of Cardiology (ESC) With the special contribution of the Heart Failure Association (HFA) of the ESC. Eur J Heart Fail. 2024;26(1):5-17.
14. Lang RM, Badano LP, Mor-Avi V, Afilalo J, Armstrong A, Ernande L, et al. Recommendations for cardiac chamber quantification by echocardiography in adults: an update from the American Society of Echocardiography and the European Association of Cardiovascular Imaging. J Am Soc Echocardiogr. 2015;28(1):1-39 e14.
15. Ponikowski P, Voors AA, Anker SD, Bueno H, Cleland JGF, Coats AJS, et al. 2016 ESC Guidelines for the diagnosis and treatment of acute and chronic heart failure: The Task Force for the diagnosis and treatment of acute and chronic heart failure of the European Society of Cardiology (ESC)Developed with the special contribution of the Heart Failure Association (HFA) of the ESC. Eur Heart J. 2016;37(27):2129-200.
16. Atherton JJ, Sindone A, De Pasquale CG, Driscoll A, MacDonald PS, Hopper I, et al. National Heart Foundation of Australia and Cardiac Society of Australia and New Zealand: Australian clinical guidelines for the management of heart failure 2018. Med J Aust. 2018;209(8):363-9.

17. Sindone AP, De Pasquale C, Amerena J, Burdeniuk C, Chan A, Coats A, et al. Consensus statement on the current pharmacological prevention and management of heart failure. Med J Aust. 2022;217(4):212-7.
18. Elliott P, Andersson B, Arbustini E, Bilinska Z, Cecchi F, Charron P, et al. Classification of the cardiomyopathies: a position statement from the European Society Of Cardiology Working Group on Myocardial and Pericardial Diseases. Eur Heart J. 2008;29(2):270-6.
19. Maron BJ, Towbin JA, Thiene G, Antzelevitch C, Corrado D, Arnett D, et al. Contemporary definitions and classification of the cardiomyopathies: an American Heart Association Scientific Statement from the Council on Clinical Cardiology, Heart Failure and Transplantation Committee; Quality of Care and Outcomes Research and Functional Genomics and Translational Biology Interdisciplinary Working Groups; and Council on Epidemiology and Prevention. Circulation. 2006;113(14):1807-16.
20. Wang Y, Jia H, Song J. Accurate Classification of Non-ischemic Cardiomyopathy. Curr Cardiol Rep. 2023;25(10):1299-317.
21. Seferovic PM, Polovina MM, Coats AJS. Heart failure in dilated non-ischaemic cardiomyopathy. Eur Heart J Suppl. 2019;21(Suppl M):M40-M3.
22. Kelkar AA, Butler J, Schelbert EB, Greene SJ, Quyyumi AA, Bonow RO, et al. Mechanisms Contributing to the Progression of Ischemic and Nonischemic Dilated Cardiomyopathy: Possible Modulating Effects of Paracrine Activities of Stem Cells. J Am Coll Cardiol. 2015;66(18):2038-47.
23. Goldstein JA. Pathophysiology and management of right heart ischemia. J Am Coll Cardiol. 2002;40(5):841-53.
24. Bello D, Shah DJ, Farah GM, Di Luzio S, Parker M, Johnson MR, et al. Gadolinium cardiovascular magnetic resonance predicts reversible myocardial dysfunction and remodeling in patients with heart failure undergoing beta-blocker therapy. Circulation. 2003;108(16):1945-53.

25. Narins CR, Aktas MK, Chen AY, McNitt S, Ling FS, Younis A, et al. Arrhythmic and Mortality Outcomes Among Ischemic Versus Nonischemic Cardiomyopathy Patients Receiving Primary ICD Therapy. JACC Clin Electrophysiol. 2022;8(1):1-11.
26. Heidenreich PA, Bozkurt B, Aguilar D, Allen LA, Byun JJ, Colvin MM, et al. 2022 AHA/ACC/HFSA Guideline for the Management of Heart Failure: A Report of the American College of Cardiology/American Heart Association Joint Committee on Clinical Practice Guidelines. Circulation. 2022;145(18):e1-e138.
27. Glikson M, Nielsen JC, Kronborg MB, Michowitz Y, Auricchio A, Barbash IM, et al. 2021 ESC Guidelines on cardiac pacing and cardiac resynchronization therapy: Developed by the Task Force on cardiac pacing and cardiac resynchronization therapy of the European Society of Cardiology (ESC) With the special contribution of the European Heart Rhythm Association (EHRA). Rev Esp Cardiol (Engl Ed). 2022;75(5):430.
28. Beggs SAS, Jhund PS, Jackson CE, McMurray JJV, Gardner RS. Non-ischaemic cardiomyopathy, sudden death and implantable defibrillators: a review and meta-analysis. Heart. 2018;104(2):144-50.
29. Kober L, Thune JJ, Nielsen JC, Haarbo J, Videbaek L, Korup E, et al. Defibrillator Implantation in Patients with Nonischemic Systolic Heart Failure. N Engl J Med. 2016;375(13):1221-30.
30. Kagan A. Dynamic responses of the right ventricle following extensive damage by cauterization. Circulation. 1952;5(6):816-23.
31. Fontan F, Baudet E. Surgical repair of tricuspid atresia. Thorax. 1971;26(3):240-8.
32. Sanz J, Sanchez-Quintana D, Bossone E, Bogaard HJ, Naeije R. Anatomy, Function, and Dysfunction of the Right Ventricle: JACC State-of-the-Art Review. J Am Coll Cardiol. 2019;73(12):1463-82.
33. Arrigo M, Huber LC, Winnik S, Mikulicic F, Guidetti F, Frank M, et al. Right Ventricular Failure: Pathophysiology, Diagnosis and Treatment. Card Fail Rev. 2019;5(3):140-6.

34. Hussain K, Mandras SA, Desai S. Right Heart Failure. StatPearls. Treasure Island (FL) ineligible companies. Disclosure: Stacy Mandras declares no relevant financial relationships with ineligible companies. Disclosure: Sapna Desai declares no relevant financial relationships with ineligible companies.2025.

35. Yasuda T, Okada RD, Leinbach RC, Gold HK, Phillips H, McKusick KA, et al. Serial evaluation of right ventricular dysfunction associated with acute inferior myocardial infarction. Am Heart J. 1990;119(4):816-22.

36. Dell'Italia LJ, Lembo NJ, Starling MR, Crawford MH, Simmons RS, Lasher JC, et al. Hemodynamically important right ventricular infarction: follow-up evaluation of right ventricular systolic function at rest and during exercise with radionuclide ventriculography and respiratory gas exchange. Circulation. 1987;75(5):996-1003.

37. Voelkel NF, Quaife RA, Leinwand LA, Barst RJ, McGoon MD, Meldrum DR, et al. Right ventricular function and failure: report of a National Heart, Lung, and Blood Institute working group on cellular and molecular mechanisms of right heart failure. Circulation. 2006;114(17):1883-91.

38. Hahn RT, Lerakis S, Delgado V, Addetia K, Burkhoff D, Muraru D, et al. Multimodality Imaging of Right Heart Function: JACC Scientific Statement. J Am Coll Cardiol. 2023;81(19):1954-73.

39. Lahm T, Douglas IS, Archer SL, Bogaard HJ, Chesler NC, Haddad F, et al. Assessment of Right Ventricular Function in the Research Setting: Knowledge Gaps and Pathways Forward. An Official American Thoracic Society Research Statement. Am J Respir Crit Care Med. 2018;198(4):e15-e43.

40. Manca P, Nuzzi V, Cannata A, Castrichini M, Bromage DI, De Luca A, et al. The right ventricular involvement in dilated cardiomyopathy: prevalence and prognostic implications of the often-neglected child. Heart Fail Rev. 2022;27(5):1795-805.

41. Szabo G, Soos P, Bahrle S, Radovits T, Weigang E, Kekesi V, et al. Adaptation of the right ventricle to an increased afterload in the chronically volume overloaded heart. Ann Thorac Surg. 2006;82(3):989-95.

42. Gomez-Arroyo J, Santos-Martinez LE, Aranda A, Pulido T, Beltran M, Munoz-Castellanos L, et al. Differences in right ventricular remodeling secondary to pressure overload in patients with pulmonary hypertension. Am J Respir Crit Care Med. 2014;189(5):603-6.

43. Pueschner A, Chattranukulchai P, Heitner JF, Shah DJ, Hayes B, Rehwald W, et al. The Prevalence, Correlates, and Impact on Cardiac Mortality of Right Ventricular Dysfunction in Nonischemic Cardiomyopathy. JACC Cardiovasc Imaging. 2017;10(10 Pt B):1225-36.

44. Merlo M, Gobbo M, Stolfo D, Losurdo P, Ramani F, Barbati G, et al. The Prognostic Impact of the Evolution of RV Function in Idiopathic DCM. JACC Cardiovasc Imaging. 2016;9(9):1034-42.

45. La Vecchia L, Zanolla L, Varotto L, Bonanno C, Spadaro GL, Ometto R, et al. Reduced right ventricular ejection fraction as a marker for idiopathic dilated cardiomyopathy compared with ischemic left ventricular dysfunction. Am Heart J. 2001;142(1):181-9.

46. Venner C, Selton-Suty C, Huttin O, Erpelding ML, Aliot E, Juilliere Y. Right ventricular dysfunction in patients with idiopathic dilated cardiomyopathy: Prognostic value and predictive factors. Arch Cardiovasc Dis. 2016;109(4):231-41.

47. Brener MI, Masoumi A, Ng VG, Tello K, Bastos MB, Cornwell WK, 3rd, et al. Invasive Right Ventricular Pressure-Volume Analysis: Basic Principles, Clinical Applications, and Practical Recommendations. Circ Heart Fail. 2022;15(1):e009101.

48. de Groote P, Millaire A, Foucher-Hossein C, Nugue O, Marchandise X, Ducloux G, et al. Right ventricular ejection fraction is an independent predictor of survival in patients with moderate heart failure. J Am Coll Cardiol. 1998;32(4):948-54.

49. Di Salvo TG, Mathier M, Semigran MJ, Dec GW. Preserved right ventricular ejection fraction predicts exercise capacity and survival in advanced heart failure. J Am Coll Cardiol. 1995;25(5):1143-53.

50. Gavazzi A, Berzuini C, Campana C, Inserra C, Ponzetta M, Sebastiani R, et al. Value of right ventricular ejection fraction in predicting short-term prognosis of patients with severe chronic heart failure. J Heart Lung Transplant. 1997;16(7):774-85.

51. Guo YK, Gao HL, Zhang XC, Wang QL, Yang ZG, Ma ES. Accuracy and reproducibility of assessing right ventricular function with 64-section multi-detector row CT: comparison with magnetic resonance imaging. Int J Cardiol. 2010;139(3):254-62.

52. Sugeng L, Mor-Avi V, Weinert L, Niel J, Ebner C, Steringer-Mascherbauer R, et al. Multimodality comparison of quantitative volumetric analysis of the right ventricle. JACC Cardiovasc Imaging. 2010;3(1):10-8.

53. Pickett CA, Cheezum MK, Kassop D, Villines TC, Hulten EA. Accuracy of cardiac CT, radionucleotide and invasive ventriculography, two- and three-dimensional echocardiography, and SPECT for left and right ventricular ejection fraction compared with cardiac MRI: a meta-analysis. Eur Heart J Cardiovasc Imaging. 2015;16(8):848-52.

54. Te Riele A, Tandri H, Sanborn DM, Bluemke DA. Noninvasive Multimodality Imaging in ARVD/C. JACC Cardiovasc Imaging. 2015;8(5):597-611.

55. Hahn RT, Thomas JD, Khalique OK, Cavalcante JL, Praz F, Zoghbi WA. Imaging Assessment of Tricuspid Regurgitation Severity. JACC Cardiovasc Imaging. 2019;12(3):469-90.

56. Sheehan F, Redington A. The right ventricle: anatomy, physiology and clinical imaging. Heart. 2008;94(11):1510-5.

57. Gulati A, Ismail TF, Jabbour A, Alpendurada F, Guha K, Ismail NA, et al. The prevalence and prognostic significance of right ventricular systolic dysfunction in nonischemic dilated cardiomyopathy. Circulation. 2013;128(15):1623-33.

58. Stokes MB, Nerlekar N, Moir S, Teo KS. The evolving role of cardiac magnetic resonance imaging in the assessment of cardiovascular disease. Aust Fam Physician. 2016;45(10):761-4.

59. Houard L, Benaets MB, de Meester de Ravenstein C, Rousseau MF, Ahn SA, Amzulescu MS, et al. Additional Prognostic Value of 2D Right Ventricular Speckle-Tracking Strain for Prediction of Survival in Heart Failure and Reduced Ejection Fraction: A Comparative Study With Cardiac Magnetic Resonance. JACC Cardiovasc Imaging. 2019;12(12):2373-85.

60. Liang K, Baritussio A, Palazzuoli A, Williams M, De Garate E, Harries I, et al. Cardiovascular Magnetic Resonance of Myocardial Fibrosis, Edema, and Infiltrates in Heart Failure. Heart Fail Clin. 2021;17(1):77-84.

61. Rekker LY, Muller SA, Gasperetti A, Bourfiss M, Oerlemans M, Cramer MJ, et al. Diagnostic value of late gadolinium enhancement at cardiovascular magnetic resonance to distinguish arrhythmogenic right ventricular cardiomyopathy from differentials. J Cardiovasc Magn Reson. 2024;26(2):101059.

62. Marwick TH. The role of echocardiography in heart failure. J Nucl Med. 2015;56 Suppl 4:31S-8S.

63. Monitillo F, Di Terlizzi V, Gioia MI, Barone R, Grande D, Parisi G, et al. Right Ventricular Function in Chronic Heart Failure: From the Diagnosis to the Therapeutic Approach. J Cardiovasc Dev Dis. 2020;7(2).

64. Rudski LG, Lai WW, Afilalo J, Hua L, Handschumacher MD, Chandrasekaran K, et al. Guidelines for the echocardiographic assessment of the right heart in adults: a report from the American Society of Echocardiography endorsed by the European Association of Echocardiography, a registered branch of the European Society of Cardiology, and the Canadian Society of Echocardiography. J Am Soc Echocardiogr. 2010;23(7):685-713; quiz 86-8.

65. Mukherjee M, Rudski LG, Addetia K, Afilalo J, D'Alto M, Freed BH, et al. Guidelines for the Echocardiographic Assessment of the Right Heart in Adults and Special Considerations in Pulmonary Hypertension: Recommendations from the American Society of Echocardiography. J Am Soc Echocardiogr. 2025;38(3):141-86.

66. Otto CM. In Practice of Clinical Echocardiography 6th Edition2021.

67. Cameli M, Lisi M, Righini FM, Tsioulpas C, Bernazzali S, Maccherini M, et al. Right ventricular longitudinal strain correlates well with right ventricular stroke work index in patients with advanced heart failure referred for heart transplantation. J Card Fail. 2012;18(3):208-15.

68. Helsen F, Van De Bruaene A, Gabriels C, Claeys M, Troost E, Voros G, et al. Prognostic significance of improvement in right ventricular systolic function during cardiac resynchronization therapy. Acta Cardiol. 2017;72(3):267-75.

69. Leong DP, Hoke U, Delgado V, Auger D, Witkowski T, Thijssen J, et al. Right ventricular function and survival following cardiac resynchronisation therapy. Heart. 2013;99(10):722-8.

70. Badagliacca R, Ghio S, Correale M, Poscia R, Camporotondo R, Ferraretti A, et al. Prognostic significance of the echocardiographic estimate of pulmonary hypertension and of right ventricular dysfunction in acute decompensated heart failure. A pilot study in HFrEF patients. Int J Cardiol. 2018;271:301-5.

71. Carluccio E, Biagioli P, Lauciello R, Zuchi C, Mengoni A, Bardelli G, et al. Superior Prognostic Value of Right Ventricular Free Wall Compared to Global Longitudinal Strain in Patients With Heart Failure. J Am Soc Echocardiogr. 2019;32(7):836-44 e1.

72. Ghio S, Carluccio E, Scardovi AB, Dini FL, Rossi A, Falletta C, et al. Prognostic relevance of Doppler echocardiographic re-assessment in HFrEF patients. Int J Cardiol. 2021;327:111-6.

73. Ishiwata J, Daimon M, Nakanishi K, Sugimoto T, Kawata T, Shinozaki T, et al. Combined evaluation of right ventricular function using echocardiography in non-ischaemic dilated cardiomyopathy. ESC Heart Fail. 2021;8(5):3947-56.

74. Damy T, Kallvikbacka-Bennett A, Goode K, Khaleva O, Lewinter C, Hobkirk J, et al. Prevalence of, associations with, and prognostic value of tricuspid annular plane systolic excursion (TAPSE) among out-patients referred for the evaluation of heart failure. J Card Fail. 2012;18(3):216-25.

75. Shah MA, Soofi MA, Jafary Z, Alhomrani A, Alsmadi F, Wani TA, et al. Echocardiographic parameters associated with recovery in heart failure with reduced ejection fraction. Echocardiography. 2020;37(10):1574-82.

76. Abreu A, Oliveira M, Silva Cunha P, Santa Clara H, Santos V, Portugal G, et al. Predictors of response to cardiac resynchronization therapy: A prospective cohort study. Rev Port Cardiol. 2017;36(6):417-25.

77. Abdelhamid MA, Ghanem MT, Abdelmotaleb AM. Assessment of right ventriclular systolic function prior to cardiac resynchronization therapy: Does it make any difference? Indian Heart J. 2017;69(6):731-5.

78. Wu VC, Takeuchi M. Echocardiographic assessment of right ventricular systolic function. Cardiovasc Diagn Ther. 2018;8(1):70-9.

79. Ueti OM, Camargo EE, Ueti Ade A, de Lima-Filho EC, Nogueira EA. Assessment of right ventricular function with Doppler echocardiographic indices derived from tricuspid annular motion: comparison with radionuclide angiography. Heart. 2002;88(3):244-8.

80. Grover SK, Leong DP, Molaee P, Shirazi M, Chakrabarty A, Penhall A, et al. Validation of echocardiographic indices of right ventriclular systolic function with cardiac magnetic resonance: a comparative study. Journal of Cardiovascular Magnetic Resonance. 2011;2(13):O75.

81. Bistola V, Parissis JT, Paraskevaidis I, Panou F, Nikolaou M, Ikonomidis I, et al. Prognostic value of tissue Doppler right ventricular systolic and diastolic function indexes combined with plasma B-type natriuretic Peptide in patients with advanced heart failure secondary to ischemic or idiopathic dilated cardiomyopathy. Am J Cardiol. 2010;105(2):249-54.

82. Chrysohoou C, Antoniou CK, Kotrogiannis I, Metallinos G, Aggelis A, Andreou I, et al. Role of right ventricular systolic function on long-term outcome in patients with newly diagnosed systolic heart failure. Circ J. 2011;75(9):2176-81.

83. Darahim KE. Right ventricular systolic echocardiographic parameters in chronic systolic heart failure and prognosis. The Egyptian Heart Journal. 2014;66(4):317-25.

84. Meluzin J, Spinarova L, Hude P, Krejci J, Dusek L, Vitovec J, et al. Combined right ventricular systolic and diastolic dysfunction represents a strong determinant of poor prognosis in patients with symptomatic heart failure. Int J Cardiol. 2005;105(2):164-73.

85. Giannini C, Fiorelli F, Colombo A, De Carlo M, Weisz SH, Agricola E, et al. Right ventricular evaluation to improve survival outcome in patients with severe functional mitral regurgitation and advanced heart failure undergoing MitraClip therapy. Int J Cardiol. 2016;223:574-80.

86. de Groote P, Fertin M, Goeminne C, Petyt G, Peyrot S, Foucher-Hossein C, et al. Right ventricular systolic function for risk stratification in patients with stable left ventricular systolic dysfunction: comparison of radionuclide angiography to echoDoppler parameters. Eur Heart J. 2012;33(21):2672-9.

87. Deaconu S, Deaconu A, Scarlatescu A, Petre I, Onciul S, Vijiac A, et al. Right ventricular-arterial coupling - A new perspective for right ventricle evaluation in heart failure patients undergoing cardiac resynchronization therapy. Echocardiography. 2021;38(7):1157-64.

88. Falletta C, Clemenza F, Klersy C, Agnese V, Bellavia D, Di Gesaro G, et al. Additive Value of Biomarkers and Echocardiography to Stratify the Risk of Death in Heart Failure Patients with Reduced Ejection Fraction. Cardiol Res Pract. 2019;2019:1824816.

89. Zaborska B, Smarz K, Makowska E, Czepiel A, Swiatkowski M, Jaxa-Chamiec T, et al. Echocardiographic predictors of exercise intolerance in patients with heart failure with severely reduced ejection fraction. Medicine (Baltimore). 2018;97(28):e11523.

90. Tello K, Dalmer A, Axmann J, Vanderpool R, Ghofrani HA, Naeije R, et al. Reserve of Right Ventricular-Arterial Coupling in the Setting of Chronic Overload. Circ Heart Fail. 2019;12(1):e005512.

91. Guazzi M, Bandera F, Pelissero G, Castelvecchio S, Menicanti L, Ghio S, et al. Tricuspid annular plane systolic excursion and pulmonary arterial systolic pressure

relationship in heart failure: an index of right ventricular contractile function and prognosis. Am J Physiol Heart Circ Physiol. 2013;305(9):H1373-81.

92. Jani VP, Strom JB, Gami A, Beussink-Nelson L, Patel R, Michos ED, et al. Optimal Method for Assessing Right Ventricular to Pulmonary Arterial Coupling in Older Healthy Adults: The Multi-Ethnic Study of Atherosclerosis. Am J Cardiol. 2024;222:11-9.

93. Tei C, Ling LH, Hodge DO, Bailey KR, Oh JK, Rodeheffer RJ, et al. New index of combined systolic and diastolic myocardial performance: a simple and reproducible measure of cardiac function--a study in normals and dilated cardiomyopathy. J Cardiol. 1995;26(6).

94. Tei C, Dujardin KS, Hodge DO, Bailey KR, McGoon MD, Tajik AJ, et al. Doppler echocardiographic index for assessment of global right ventricular function. J Am Soc Echocardiogr. 1996;9(6):838-47.

95. Vonk MC, Sander MH, van den Hoogen FH, van Riel PL, Verheugt FW, van Dijk AP. Right ventricle Tei-index: a tool to increase the accuracy of non-invasive detection of pulmonary arterial hypertension in connective tissue diseases. Eur J Echocardiogr. 2007;8(5):317-21.

96. Field ME, Solomon SD, Lewis EF, Kramer DB, Baughman KL, Stevenson LW, et al. Right ventricular dysfunction and adverse outcome in patients with advanced heart failure. J Card Fail. 2006;12(8):616-20.

97. Verhaert D, Mullens W, Borowski A, Popovic ZB, Curtin RJ, Thomas JD, et al. Right ventricular response to intensive medical therapy in advanced decompensated heart failure. Circ Heart Fail. 2010;3(3):340-6.

98. Vizzardi E, D'Aloia A, Caretta G, Bordonali T, Bonadei I, Rovetta R, et al. Long-term prognostic value of longitudinal strain of right ventricle in patients with moderate heart failure. Hellenic J Cardiol. 2014;55(2):150-5.

99. Mukherjee M, Mathai SC, Jellis C, Freed BH, Yanek LR, Agoglia H, et al. Defining Echocardiographic Degrees of Right Heart Size and Function in Pulmonary Vascular Disease from the PVDOMICS Study. Circ Cardiovasc Imaging. 2024;17(10).

100. Lee JZ, Low SW, Pasha AK, Howe CL, Lee KS, Suryanarayana PG. Comparison of tricuspid annular plane systolic excursion with fractional area change for the evaluation of right ventricular systolic function: a meta-analysis. Open Heart. 2018;5(1):e000667.

101. Schneider M, Binder T. Echocardiographic evaluation of the right heart. Wien Klin Wochenschr. 2018;130(13-14):413-20.

102. Finocchiaro G, Kobayashi Y, Magavern E, Zhou JQ, Ashley E, Sinagra G, et al. Prevalence and prognostic role of right ventricular involvement in stress-induced cardiomyopathy. J Card Fail. 2015;21(5):419-25.

103. Carrion L, Sperotto A, Nazario R, Goldraich LA, Clausell N, Rohde LE, et al. Impaired Right Ventricular Function in Heart Transplant Rejection. Arq Bras Cardiol. 2020;114(4):638-44.

104. Ji M, Wu W, He L, Gao L, Zhang Y, Lin Y, et al. Right Ventricular Longitudinal Strain in Patients with Heart Failure. Diagnostics (Basel). 2022;12(2).

105. Amzulescu MS, De Craene M, Langet H, Pasquet A, Vancraeynest D, Pouleur AC, et al. Myocardial strain imaging: review of general principles, validation, and sources of discrepancies. Eur Heart J Cardiovasc Imaging. 2019;20(6):605-19.

106. Al Saikhan L, Park C, Hardy R, Hughes A. Prognostic implications of left ventricular strain by speckle-tracking echocardiography in population-based studies: a systematic review protocol of the published literature. BMJ Open. 2018;8(7):e023346.

107. Rudski LG, Fine NM. Right Ventricular Function in Heart Failure: The Long and Short of Free Wall Motion Versus Deformation Imaging. Circ Cardiovasc Imaging. 2018;11(1):e007396.

108. Longobardo L, Suma V, Jain R, Carerj S, Zito C, Zwicke DL, et al. Role of Two-Dimensional Speckle-Tracking Echocardiography Strain in the Assessment of Right

Ventricular Systolic Function and Comparison with Conventional Parameters. J Am Soc Echocardiogr. 2017;30(10):937-46 e6.

109. Carluccio E, Biagioli P, Alunni G, Murrone A, Zuchi C, Coiro S, et al. Prognostic Value of Right Ventricular Dysfunction in Heart Failure With Reduced Ejection Fraction: Superiority of Longitudinal Strain Over Tricuspid Annular Plane Systolic Excursion. Circ Cardiovasc Imaging. 2018;11(1):e006894.

110. Lundorff IJ, Sengelov M, Pedersen S, Modin D, Bruun NE, Fritz-Hansen T, et al. Prognostic value of right ventricular echocardiographic measures in patients with heart failure with reduced ejection fraction. J Clin Ultrasound. 2021;49(9):903-13.

111. Sade LE, Ozin B, Atar I, Demir O, Demirtas S, Muderrisoglu H. Right ventricular function is a determinant of long-term survival after cardiac resynchronization therapy. J Am Soc Echocardiogr. 2013;26(7):706-13.

112. Motoki H, Borowski AG, Shrestha K, Hu B, Kusunose K, Troughton RW, et al. Right ventricular global longitudinal strain provides prognostic value incremental to left ventricular ejection fraction in patients with heart failure. J Am Soc Echocardiogr. 2014;27(7):726-32.

113. Park JH, Negishi K, Kwon DH, Popovic ZB, Grimm RA, Marwick TH. Validation of global longitudinal strain and strain rate as reliable markers of right ventricular dysfunction: comparison with cardiac magnetic resonance and outcome. J Cardiovasc Ultrasound. 2014;22(3):113-20.

114. Cameli M, Righini FM, Lisi M, Bennati E, Navarri R, Lunghetti S, et al. Comparison of right versus left ventricular strain analysis as a predictor of outcome in patients with systolic heart failure referred for heart transplantation. Am J Cardiol. 2013;112(11):1778-84.

115. Badano LP, Kolias TJ, Muraru D, Abraham TP, Aurigemma G, Edvardsen T, et al. Standardization of left atrial, right ventricular, and right atrial deformation imaging using two-dimensional speckle tracking echocardiography: a consensus document of the

EACVI/ASE/Industry Task Force to standardize deformation imaging. Eur Heart J Cardiovasc Imaging. 2018;19(6):591-600.

116. Addetia K, Miyoshi T, Citro R, Daimon M, Gutierrez Fajardo P, Kasliwal RR, et al. Two-Dimensional Echocardiographic Right Ventricular Size and Systolic Function Measurements Stratified by Sex, Age, and Ethnicity: Results of the World Alliance of Societies of Echocardiography Study. J Am Soc Echocardiogr. 2021;34(11):1148-57 e1.

117. Randazzo M, Maffessanti F, Kotta A, Grapsa J, Lang RM, Addetia K. Added value of 3D echocardiography in the diagnosis and prognostication of patients with right ventricular dysfunction. Front Cardiovasc Med. 2023;10:1263864.

118. Vijiiac A, Onciul S, Guzu C, Scarlatescu A, Petre I, Zamfir D, et al. Forgotten No More-The Role of Right Ventricular Dysfunction in Heart Failure with Reduced Ejection Fraction: An Echocardiographic Perspective. Diagnostics (Basel). 2021;11(3).

119. Cotella JI, Kovacs A, Addetia K, Fabian A, Asch FM, Lang RM, et al. Three-dimensional echocardiographic evaluation of longitudinal and non-longitudinal components of right ventricular contraction: results from the World Alliance of Societies of Echocardiography study. Eur Heart J Cardiovasc Imaging. 2024;25(2):152-60.

120. Nagata Y, Wu VC, Kado Y, Otani K, Lin FC, Otsuji Y, et al. Prognostic Value of Right Ventricular Ejection Fraction Assessed by Transthoracic 3D Echocardiography. Circ Cardiovasc Imaging. 2017;10(2).

121. Nabeshima Y, Kitano T, Takeuchi M. Prognostic Value of the Three-Dimensional Right Ventricular Ejection Fraction in Patients With Asymptomatic Aortic Stenosis. Front Cardiovasc Med. 2021;8:795016.

122. Posada-Martinez EL, Ivey-Miranda JB, Ortiz-Leon XA, Arias-Godinez JA, Fritche-Salazar JF, Rodriguez-Zanella HG, et al. Association Between Three-Dimensional Right Ventricular Ejection Fraction and In-Hospital Outcomes in Patients Undergoing Cardiac Surgery: A Multicenter Study. J Am Soc Echocardiogr. 2025.

123. Kitano T, Nabeshima Y, Nagata Y, Takeuchi M. Prognostic value of the right ventricular ejection fraction using three-dimensional echocardiography: Systematic review and meta-analysis. PLoS One. 2023;18(7):e0287924.

124. Sayour AA, Tokodi M, Celeng C, Takx RAP, Fabian A, Lakatos BK, et al. Association of Right Ventricular Functional Parameters With Adverse Cardiopulmonary Outcomes: A Meta-analysis. J Am Soc Echocardiogr. 2023;36(6):624-33 e8.

125. Ahmad A, Wang X, Li L, Liu T, Fan FL. Insights from 3D echocardiography: unveiling the prognostic value of RV function in pulmonary hypertension: a systematic review and meta-analysis. Int J Cardiovasc Imaging. 2025;41(2):185-97.

126. de Liyis BG, Suastika LOS, Sutedja JC, Jagannatha GNP, Kosasih AM, Alamsyah AH. Prognostic values of right ventricular echocardiography functional parameters for mortality prediction in precapillary pulmonary hypertension: a systematic review and meta-analysis. Egypt Heart J. 2024;76(1):105.

127. Murata M, Tsugu T, Kawakami T, Kataoka M, Minakata Y, Endo J, et al. Prognostic value of three-dimensional echocardiographic right ventricular ejection fraction in patients with pulmonary arterial hypertension. Oncotarget. 2016;7(52):86781-90.

128. Moceri P, Duchateau N, Baudouy D, Schouver ED, Leroy S, Squara F, et al. Three-dimensional right-ventricular regional deformation and survival in pulmonary hypertension. Eur Heart J Cardiovasc Imaging. 2018;19(4):450-8.

129. Li Y, Guo D, Gong J, Wang J, Huang Q, Yang S, et al. Right Ventricular Function and Its Coupling With Pulmonary Circulation in Precapillary Pulmonary Hypertension: A Three-Dimensional Echocardiographic Study. Front Cardiovasc Med. 2021;8:690606.

130. Li Y, Wang T, Haines P, Li M, Wu W, Liu M, et al. Prognostic Value of Right Ventricular Two-Dimensional and Three-Dimensional Speckle-Tracking Strain in Pulmonary Arterial Hypertension: Superiority of Longitudinal Strain over Circumferential and Radial Strain. J Am Soc Echocardiogr. 2020;33(8):985-94 e1.

131. Li Y, Liang L, Guo D, Yang Y, Gong J, Zhang X, et al. Right Ventricular Function Predicts Adverse Clinical Outcomes in Patients With Chronic Thromboembolic

Pulmonary Hypertension: A Three-Dimensional Echocardiographic Study. Front Med (Lausanne). 2021;8:697396.

132. Surkova E, Kovacs A, Tokodi M, Lakatos BK, Merkely B, Muraru D, et al. Contraction Patterns of the Right Ventricle Associated with Different Degrees of Left Ventricular Systolic Dysfunction. Circ Cardiovasc Imaging. 2021;14(10):e012774.

133. Surkova E, Muraru D, Genovese D, Aruta P, Palermo C, Badano LP. Relative Prognostic Importance of Left and Right Ventricular Ejection Fraction in Patients With Cardiac Diseases. J Am Soc Echocardiogr. 2019;32(11):1407-15 e3.

134. Muraru D, Badano LP, Nagata Y, Surkova E, Nabeshima Y, Genovese D, et al. Development and prognostic validation of partition values to grade right ventricular dysfunction severity using 3D echocardiography. Eur Heart J Cardiovasc Imaging. 2020;21(1):10-21.

135. Kitano T, Kovacs A, Nabeshima Y, Tokodi M, Fabian A, Lakatos BK, et al. Prognostic Value of Right Ventricular Strains Using Novel Three-Dimensional Analytical Software in Patients With Cardiac Disease. Front Cardiovasc Med. 2022;9:837584.

136. Tolvaj M, Tokodi M, Lakatos B, Fábián A, Ujvári A, Bakija F, et al. Added predictive value of right ventricular ejection fraction compared with conventional echocardiographic measurements in patients who underwent diverse cardiovascular procedures. Imaging. 2021;13(2):130-7.

137. Vijiiac A, Onciul S, Guzu C, Verinceanu V, Bataila V, Deaconu S, et al. The prognostic value of right ventricular longitudinal strain and 3D ejection fraction in patients with dilated cardiomyopathy. Int J Cardiovasc Imaging. 2021;37(11):3233-44.

138. Butcher SC, Fortuni F, Montero-Cabezas JM, Abou R, El Mahdiui M, van der Bijl P, et al. Right ventricular myocardial work: proof-of-concept for non-invasive assessment of right ventricular function. Eur Heart J Cardiovasc Imaging. 2021;22(2):142-52.

139. Stolfo D, Tonet E, Merlo M, Barbati G, Gigli M, Pinamonti B, et al. Early right ventricular response to cardiac resynchronization therapy: impact on clinical outcomes. Eur J Heart Fail. 2016;18(2):205-13.

140. Stassen J, van der Bijl P, Galloo X, Hirasawa K, Prihadi EA, Marsan NA, et al. Prognostic Implications of Right Ventricular Free Wall Strain in Recipients of Cardiac Resynchronization Therapy. Am J Cardiol. 2022;171:151-8.

141. Olson J, Samad BA, Alam M. The prognostic significance of right ventricular tissue Doppler parameters in patients with left ventricular systolic heart failure: an observational cohort study. Heart. 2012;98(15):1142-5.

142. Dini FL, Carluccio E, Simioniuc A, Biagioli P, Reboldi G, Galeotti GG, et al. Right ventricular recovery during follow-up is associated with improved survival in patients with chronic heart failure with reduced ejection fraction. Eur J Heart Fail. 2016;18(12):1462-71.

143. Collaborators GBDRF. Global burden of 87 risk factors in 204 countries and territories, 1990-2019: a systematic analysis for the Global Burden of Disease Study 2019. Lancet. 2020;396(10258):1223-49.

144. Sokmen A, Sokmen G, Acar G, Akcay A, Koroglu S, Koleoglu M, et al. The impact of isolated obesity on right ventricular function in young adults. Arq Bras Cardiol. 2013;101(2):160-8.

145. Ma JI, Zern EK, Parekh JK, Owunna N, Jiang N, Wang D, et al. Obesity Modifies Clinical Outcomes of Right Ventricular Dysfunction. Circ Heart Fail. 2023;16(11):e010524.

146. Gavaghan C. Pacemaker Induced Cardiomyopathy: An Overview of Current Literature. Curr Cardiol Rev. 2022;18(3):e010921196020.

147. Naqvi TZ, Chao CJ. Adverse effects of right ventricular pacing on cardiac function: prevalence, prevention and treatment with physiologic pacing. Trends Cardiovasc Med. 2023;33(2):109-22.

148. Berruezo A, Efimova E, Acosta J, Jauregui B. Isolated, premature ventricular complex-induced right ventricular dysfunction mimicking arrhythmogenic right ventricular cardiomyopathy. HeartRhythm Case Rep. 2018;4(6):222-6.

149. Boyle TA, Pothineni NVK, Austin M, Shivamurthy P, Markman T, Guandalini G, et al. Incidence and Predictors of Pacing-Induced Right Ventricular Cardiomyopathy. Circ Arrhythm Electrophysiol. 2024;17(10):e013070.

150. Chung MK, Patton KK, Lau CP, Dal Forno ARJ, Al-Khatib SM, Arora V, et al. 2023 HRS/APHRS/LAHRS guideline on cardiac physiologic pacing for the avoidance and mitigation of heart failure. J Arrhythm. 2023;39(5):681-756.

151. Buckley BJR, Harrison SL, Gupta D, Fazio-Eynullayeva E, Underhill P, Lip GYH. Atrial Fibrillation in Patients With Cardiomyopathy: Prevalence and Clinical Outcomes From Real-World Data. J Am Heart Assoc. 2021;10(23):e021970.

152. Clark DM, Plumb VJ, Epstein AE, Kay GN. Hemodynamic effects of an irregular sequence of ventricular cycle lengths during atrial fibrillation. J Am Coll Cardiol. 1997;30(4):1039-45.

153. Patlolla SH, Schaff HV, Nishimura RA, Stulak JM, Chamberlain AM, Pislaru SV, et al. Incidence and Burden of Tricuspid Regurgitation in Patients With Atrial Fibrillation. J Am Coll Cardiol. 2022;80(24):2289-98.

154. Zafrir B, Lund LH, Laroche C, Ruschitzka F, Crespo-Leiro MG, Coats AJS, et al. Prognostic implications of atrial fibrillation in heart failure with reduced, mid-range, and preserved ejection fraction: a report from 14 964 patients in the European Society of Cardiology Heart Failure Long-Term Registry. Eur Heart J. 2018;39(48):4277-84.

155. Zhang ZH, Meng FQ, Hou XF, Qian ZY, Wang Y, Qiu YH, et al. Clinical characteristics and long-term prognosis of ischemic and non-ischemic cardiomyopathy. Indian Heart J. 2020;72(2):93-100.

156. Yamamoto K, Matsumura-Nakano Y, Shiomi H, Natsuaki M, Morimoto T, Kadota K, et al. Effect of Heart Failure on Long-Term Clinical Outcomes After Percutaneous Coronary Intervention Versus Coronary Artery Bypass Grafting in Patients With Severe Coronary Artery Disease. J Am Heart Assoc. 2021;10(15):e021257.

157. Saraiya S, Agrawal A, C R. Right ventricular dysfunction in ischemic vs nonischemic dilated cardiomyopathy. European Heart Journal - Cardiovascular Imaging. 2025;26.

158. Duncan AM, Francis DP, Gibson DG, Henein MY. Differentiation of ischemic from nonischemic cardiomyopathy during dobutamine stress by left ventricular long-axis function: additional effect of left bundle-branch block. Circulation. 2003;108(10):1214-20.

159. Sljivic A, Pavlovic Kleut M, Bukumiric Z, Celic V. Association between right ventricle two- and three-dimensional echocardiography and exercise capacity in patients with reduced left ventricular ejection fraction. PLoS One. 2018;13(6):e0199439.

160. Heidenreich PA, Bozkurt B, Aguilar D, Allen LA, Byun JJ, Colvin MM, et al. 2022 AHA/ACC/HFSA Guideline for the Management of Heart Failure: A Report of the American College of Cardiology/American Heart Association Joint Committee on Clinical Practice Guidelines. Circulation. 2022;145(18):e895-e1032.

161. Azizi Z, Golbus JR, Spaulding EM, Hwang PH, Ciminelli ALA, Lacar K, et al. Challenge of Optimizing Medical Therapy in Heart Failure: Unlocking the Potential of Digital Health and Patient Engagement. J Am Heart Assoc. 2024;13(2):e030952.

162. Soltani MH, Jamshir M, Taghavi S, Golpira R, Nasiri M, Amin A, et al. Echocardiographic predictors of worsening renal function in acute heart failure: observations from the RASHF registry. ESC Heart Fail. 2018;5(6):1060-8.

163. McMurray JJV, Solomon SD, Inzucchi SE, Kober L, Kosiborod MN, Martinez FA, et al. Dapagliflozin in Patients with Heart Failure and Reduced Ejection Fraction. N Engl J Med. 2019;381(21):1995-2008.

164. McMurray JJ, Packer M, Desai AS, Gong J, Lefkowitz MP, Rizkala AR, et al. Angiotensin-neprilysin inhibition versus enalapril in heart failure. N Engl J Med. 2014;371(11):993-1004.

165. Greene SJ, Butler J, Albert NM, DeVore AD, Sharma PP, Duffy CI, et al. Medical Therapy for Heart Failure With Reduced Ejection Fraction: The CHAMP-HF Registry. J Am Coll Cardiol. 2018;72(4):351-66.

166. Ohara K, Imamura T, Ihori H, Chatani K, Nonomura M, Kameyama T, et al. Association between Right Ventricular Function and Exercise Capacity in Patients with Chronic Heart Failure. J Clin Med. 2022;11(4).

167. Wu XP, Li YD, Wang YD, Zhang M, Zhu WW, Cai QZ, et al. Impaired Right Ventricular Mechanics at Rest and During Exercise Are Associated With Exercise Capacity in Patients With Hypertrophic Cardiomyopathy. J Am Heart Assoc. 2019;8(5):e011269.

168. Kim J, Di Franco A, Seoane T, Srinivasan A, Kampaktsis PN, Geevarghese A, et al. Right Ventricular Dysfunction Impairs Effort Tolerance Independent of Left Ventricular Function Among Patients Undergoing Exercise Stress Myocardial Perfusion Imaging. Circ Cardiovasc Imaging. 2016;9(11).

169. Borlaug BA, Kane GC, Melenovsky V, Olson TP. Abnormal right ventricular-pulmonary artery coupling with exercise in heart failure with preserved ejection fraction. Eur Heart J. 2016;37(43):3293-302.

170. Legris V, Thibault B, Dupuis J, White M, Asgar AW, Fortier A, et al. Right ventricular function and its coupling to pulmonary circulation predicts exercise tolerance in systolic heart failure. ESC Heart Fail. 2022;9(1):450-64.

171. Halle M, Prescott E, Van Craenenbroeck EM, Beckers P, Videm V, Karlsen T, et al. Moderate continuous or high intensity interval exercise in heart failure with reduced ejection fraction: Differences between ischemic and non-ischemic etiology. Am Heart J Plus. 2022;22:100202.

172. Shahim B, Kapelios CJ, Savarese G, Lund LH. Global Public Health Burden of Heart Failure: An Updated Review. Card Fail Rev. 2023;9:e11.

CHAPTER TWO
General methodology

2.0 Abbreviations:

HFrEF = Heart failure with reduced ejection fraction

HF = Heart failure

TTE = Transthoracic echocardiography

6MWT = 6-minute walk test

NICM = Non-ischaemic cardiomyopathy

LVEF = Left ventricular ejection fraction

OSA = Obstructive sleep apnoea

ARNI = Angiotensin receptor neprilysin inhibitor

ACE-I = Angiotensin converting enzyme inhibitor

LV = Left ventricular / left ventricle

LA = Left atria / left atrial

2D = Two-dimensional

RV = Right ventricular / right ventricle

TAPSE = Tricuspid annular plane systolic excursion

RVS' = Tissue Doppler derived peak systolic velocity at the tricuspid annulus

FAC = Fractional area change

STE = Speckle-tracking echocardiography

RV-FWS = Right ventricular free wall strain

RV-GLS = Right ventricular global longitudinal strain

LV-GLS = Left ventricular global longitudinal strain

LASr = Left atrial reservoir strain

3D = Three dimensional

3D-RVEF = Transthoracic echocardiography derived three-dimensional right ventricular ejection fraction

6MWD = 6-minute walk distance

ROC = receiver operating characteristics

2.1.0 Design and methods

The study design and methodology detailed below pertains to the conduct of the prospective sub studies which make up this thesis.

Consecutive patients with heart failure with reduced ejection fraction (HFrEF) were prospectively assessed from outpatient heart failure (HF) clinics in a tertiary hospital in New South Wales, Australia from the period of January 2021 to January 2024. Patients meeting eligibility were invited to participate (section 2.1.1 and 2.1.2). Recruited patients received clinical evaluation with detailed history of coexisting comorbidities, medication history and physical examination. At recruitment, all patients underwent non-invasive blood pressure measurement, oxygen saturation, serum pathology, and electrocardiography. Serum pathology assessed include cell count and differentials, electrolytes, urea, creatinine, calcium, magnesium, phosphate, liver function, thyroid function, lipid profile, glycosylated haemoglobin A1c, iron studies, and N-terminal pro-B-type natriuretic peptide.

All patients received optimised therapy for at least three months prior to concurrent baseline transthoracic echocardiogram (TTE) and submaximal exercise capacity assessment via 6-minute walk test (6MWT). Participants also received symptom evaluation through the New York Heart Association functional classification and Kansas City Cardiomyopathy Questionnaire.

2.1.1 Inclusion criteria

We prospectively recruited consecutive patients between January 2021 to January 2024 with non-ischaemic cardiomyopathy (NICM) who either: attended our outpatient heart failure (HF) service for the management of symptomatic HF; or were admitted for decompensated HF at our tertiary institution (Blacktown Mt-Druitt Hospitals). Patients aged ≥18-years of age with a left ventricular ejection fraction (LVEF) of <50% were included.

We recruited patients with NICM as these patients exhibit a global systolic dysfunction and were more likely to have RV dysfunction as opposed to the regional pattern of ischaemic cardiomyopathy that is linked to specific coronary artery territories.

2.1.2 Exclusion criteria

We excluded those with significant coronary artery disease (defined as ≥70% disease in any of the three main coronary arteries, prior coronary intervention or bypass surgery, evidence of impaired myocardial perfusion or reversible ischemia), significant valvular disease (defined as severe secondary valvular regurgitation, primary valvular abnormalities, previous valve replacement or repair), congenital heart disease, prior cardiac surgery, severe pulmonary hypertension, restrictive or obstructive pulmonary disease requiring hospitalisation, recent pulmonary embolism within 6 months and those with untreated obstructive sleep apnoea (OSA). Furthermore, we also excluded patients with non-cardiac comorbidities which limited their life expectancy to <1 year, and those with inadequate transthoracic echocardiographic image quality for analysis.

2.1.3 Optimised guideline directed heart failure therapy

All included patients were followed up closely at the HF clinic for commencement and optimisation of guideline directed therapy. (1-4) Patients were scheduled for regular reviews in the clinic for rapid initiation and up-titration of their pharmacotherapy, aiming for maximally tolerated doses of the four pillars of HF pharmacotherapy: cardiac specific beta-blockers, angiotensin receptor neprilysin inhibitor (ARNI), sodium-glucose co-transporter 2 inhibitor, and mineralocorticoid receptor antagonists. Those intolerant of ARNI were commenced on an angiotensin converting enzyme inhibitors (ACE-I) or an angiotensin 2 receptor blocker if intolerant of ACE-I. Patients with persistent symptoms and resting sinus rate above 70 beats per minute despite maximally tolerated beta-blocker dosing were prescribed Ivabradine. They

were also commenced on Vericiguat if they exhibit worsening HF symptoms despite optimal therapy based on the VICTORIA trial criteria. (5) Symptomatic patients with reduced iron stores (ferritin <100ug/L; or ferritin100-299ug/L and transferrin saturation <20%) received intravenous ferric carboxymaltose based on AFFIRM-AHF trial criteria and society recommendation. (6, 7) Finally, those meeting criteria also received implantable cardioverter defibrillator, cardiac resynchronisation therapy, direct current cardioversion or pulmonary vein isolation. (8, 9)

2.1.4 Patient follow up

All patients were followed for up to 3 years, with 6-monthly in person or telehealth evaluations in addition to their routine follow-up via the HF service. Adverse cardiovascular outcomes were corroborated from hospital medical records, general practitioner and specialist clinical records. Deaths were corroborated with hospital records and the state registry of birth, marriage and death.

2.2.0 Transthoracic echocardiography

All TTE were performed using commercially available ultrasound systems in accordance with American Society of Echocardiography guideline recommendations. (10-14) The echocardiographic systems used include EPIQ 7c with X5-1 probe (Philips, Andover MA, USA), Vivid E-9 with M5Sc probe and Vivid E-95 with 4Vc probe (General Electric Vingmed, Horton, Norway). The prospective sub studies of this thesis (chapters 6 and 7) exclusively utilised Vivid E-95 systems equipped with 4Vc probes.

2.2.1 Echocardiographic Assessment

In detail, left ventricular (LV) volume and ejection fraction were calculated using modified Simpson's biplane method. Left atrial (LA) volume was measured at end diastole (immediately prior to mitral valve opening) utilising the 2- and 4-chamber views using the biplane method of discs. (10, 12)

Pulse-wave Doppler was performed in the apical 4-chamber view to measure mitral inflow velocities for the assessment of LV filling. These measurements included mitral inflow peak early filling (MVE) and late diastolic filling velocities (MVA), the E/A ratio, deceleration time of early filling velocity, and the isovolumetric relaxation time. Utilising pulse-wave tissue Doppler imaging in the apical views, peak septal and lateral early mitral annular velocities in diastole were obtained (e'). E/e' ratio was subsequently calculated based the ratio of MVE to average e'. (12)

Two-dimensional (2D) parameters of right ventricular (RV) systolic function were assessed by tricuspid annular plane systolic excursion (TAPSE), tissue Doppler derived peak systolic velocity at the tricuspid annulus (RVS'), fractional area change (FAC), and speckle-tracking echocardiography (STE) from the RV-focused apical 4-chamber view. (14, 15)

TAPSE expressed in centimetres, was measured as the systolic displacement of the lateral tricuspid annulus on M-mode with alignment of the cursor across the RV apex and the lateral tricuspid annulus throughout the cardiac cycle. Peak velocity of the lateral tricuspid annulus in systole (RVS') was measured on tissue Doppler imaging placing a 4mm sample volume at the lateral tricuspid annulus with an angle of <20 degrees between the axis of RV free wall contraction and the alignment of the ultrasound probe. RVS' was expressed as centimetres per second. FAC was calculated as the percentage area change between the RV end-diastolic and end-systolic area. The RV areas were measured in the apical RV focused view by tracing the RV endocardial border from the lateral to the medial tricuspid annulus. (14)

For patients in atrial fibrillation or atrial flutter at the time of their study, reported parameters were a mean of measurements from five cardiac cycles. (10) TTE parameters were assessed

by investigators blinded to patient details, baseline characteristics, clinical outcomes and other echocardiographic data.

2.2.2 Speckle-tracking echocardiography

Two-dimensional STE were performed on high frame rate images acquired using dedicated windows. We utilised vendor-independent software for the retrospective sub studies (TomTech Image Arena Systems v2.3, Germany) and vendor-specific software for our prospective sub studies (GE EchoPAC v206, General Electric, Horten, Norway). Longitudinal strain values are expressed as absolute values in line with society recommendations. (10, 14)

LV-global longitudinal strain (LV-GLS) was assessed by tracing the LV endocardium at end-systole and then calculated as the average of the 18-segments obtained across the three standard apical views. The width of the region of interest was adjusted to ensure adequate coverage of the LV wall thickness. The LV endocardium was then tracked throughout the cardiac via automated software.

Left atrial reservoir strain (LASr) was calculated as the average peak strain across 12-segments obtained in the apical 2- and 4-chamber views. The LA endocardium was traced via a semi-automated process in end-systole. The width of the region of interest was adjusted to the smallest thickness to track the LA border. The automated software then tracked the myocardium throughout the cardiac cycle using R to R gating.

RV strain was evaluated by tracing the RV endocardium in the RV-focused apical view. The region of interest was identified via a semi-automated process to include both the RV free wall and the septum. The width was then adjusted to cover the thickness of the RV free wall. The RV endocardium was then tracked via the automated software throughout the cardiac cycle using R to R gating. (16)

We analysed both RV free wall strain (RV-FWS) which was derived from the average peak systolic strain of the three RV free wall segments, and RV global longitudinal strain (RV-GLS)

which was derived from the average of six segments consisting of both the RV free wall and the interventricular septum.

All investigators were blinded to patient details, medical history and clinical status while evaluating STE measures.

2.2.3 Three-dimensional echocardiography

RV full-volume three-dimensional (3D) data sets were obtained in the RV-focused apical four-chamber view over a minimum of 6-cardiac cycles. The acquisition was optimised to include the tricuspid valve, RV apex, the outflow tract and the pulmonary valve. Temporal resolution was also optimised to target at least 20 frames per second. TTE derived 3D-right ventricular ejection fraction (3D-RVEF) was calculated using vendor-specific semi-automated software (GE EchoPAC v206, General Electric, Horten, Norway). Breath holding was employed to minimise stitch artefacts.

The RV landmarks and planes were set manually using the semi-automated software. Which then enabled the construction of an automated 3D model to track the RV volume throughout the cardiac cycle. Further manual adjustment of the RV endocardial border was performed to optimise tracking at all temporal points. End-diastolic and end-systolic timing was assigned based on maximum and minimum RV volumes, respectively.

All investigators were blinded to patient details, medical history and clinical status while evaluating 3D echocardiographic measures.

2.3.0 Exercise capacity testing

We evaluated submaximal exercise capacity via 6MWT which was performed in accordance with published society recommendations. (17) Each participant is asked to walk as far as possible for 6-minutes along our test course.

2.3.1 Test course

Our 6MWTs were performed in a dedicated temperature controlled indoor cardio-pulmonary rehabilitation gymnasium. The course was clearly marked and measured 30 meters in length with additional markings every meter to allow for accurate calculation of partial laps. We ensured that only one participant was using the test course at a time.

2.3.2 Testing protocol

After checking for contraindications to the 6MWT, participants were rested in a chair for at least five minutes during which their oxygen saturation, pulse rate, blood pressure and dyspnoea score was recorded. They were then read the standardised pre-test instructions (Table 2.1). After commencement of the test, the patient is given a standardised encouragement every 60 seconds. If required, a patient can stop to rest in a standing or sitting position of their choosing, during which they are given additional standardised encouragements. (Table 2.2)

A stopwatch was used to calculate the time lapsed from the start of the test, and a lap counter was used to record the number of laps completed. At the end of the test at 6-minutes, the number of laps completed, and the distance walked in the final partial lap was recorded. The total distance walked is then reported as the 6-minute walk distance (6MWD).

All investigators involved in performing the 6MWT was blinded to participant history and echocardiographic findings.

Table 2.1 Standardised 6-minute walk test instructions

Pre-test instructions
The aim of this test is to walk as far as possible for 6 minutes. You will walk along this hallway between the markers, as many times as you can in 6 minutes. I will let you know as each minute goes past, and then at 6 minutes I will ask you to stop where you are. 6 minutes is a long time to walk, so you will be exerting yourself. You are permitted to slow down, to stop, and to rest as necessary, but please resume walking as soon as you are able. Remember that the objective is to walk AS FAR AS POSISBLE for 6 minutes, but don't run or jog. Do you have any questions?

Table 2.2 Standardised encouragements during 6-minute walk test

1 minute You are doing well. You have 5 minutes to go
2 minutes Keep up the good work. You have 4 minutes to go
3 minutes You are doing well. You are halfway.
4 minutes Keep up the good work. You have only 2 minutes left.
5 minutes You are doing well. You have 1 minute to go.
6 minutes Please stop where you are.
Whilst resting Please resume walking whenever you feel able

2.4.0 Statistical Methodology

2.4.1 Statistical analysis

All statistical analysis was performed using the Statistical Package for Social Sciences Software (SPSS Version 22; SPSS Inc., Chicago, IL, USA) unless otherwise specified. All statistical tests were two-tailed, with a p-value <0.05 considered statistically significant.

Continuous variables were presented as mean ± standard deviations. We utilised independent T-test and Mann-Whitney's test for between group comparison for parametric and non-parametric continuous variables respectively. For matched comparisons, paired T-test analysis was employed. For trends between groups, one-way ANOVA was used to identify variables that were significantly different from the group mean. Additionally, Jonckheere-Terpstra test for ordered alternatives was performed to confirm the presence of ordered trends across multiple groups.

Categorical variables were expressed as numbers and percentages. Chi-square or Fisher's exact test were used for investigating the association between the selected categorical variables and the outcome when appropriate.

Receiver operating characteristics (ROC) curves were used to evaluate the predictive strength of RV systolic functional parameters on echocardiography for adverse cardiovascular outcomes and reduced exercise capacity. Z-statistics and Delong's test was performed to compare the strength of the area under the curve of relevant study variables using MedCalc Software (MedCalc software Version 23, Ostend, Belgium). The optimal discriminatory cutoff for the predictor variable was selected using Youden's index method (J-point).

For survival analysis, Log-rank test was used to compare event-free survival between groups and Kaplan-Meier survival analysis was used to estimate the probability of event-free survival over time. Cox proportional hazard model was employed to identify variables independently associated with the primary outcome. Collinearity was assessed using the correlation matrix

of regression coefficients, and coefficients of <-0.7 or >0.7 were considered to represent significant collinearity.

2.4.2 Inter- and intra-observer variability

Quantitation of inter- and intra-observer variability of longitudinal strain and 3D-RVEF was performed in 5% of the population through repeat measurements by a second independent investigator and the original investigator at least one month later. Reproducibility of these measurements were represented by the intra-class correlation coefficient and coefficient of variation.

2.4.3 Sample size and power calculation

With the assumption that the accrual period of recruited patients is over 30-months with a subsequent follow up period of 12 months, using an average event rate of 19.5% from published studies (average rate of 29.5% in high risk group and 9.4% in low risk group), and estimating a 10% drop out rate per year, a sample size of 176-patients (assuming equal distribution across the high and low risk groups) will achieve 90% power at a two-sided p-value of 0.05. (18, 19)

2.5.0 References

1. McDonagh TA, Metra M, Adamo M, Gardner RS, Baumbach A, Bohm M, et al. 2021 ESC Guidelines for the diagnosis and treatment of acute and chronic heart failure: Developed by the Task Force for the diagnosis and treatment of acute and chronic heart failure of the European Society of Cardiology (ESC) With the special contribution of the Heart Failure Association (HFA) of the ESC. Rev Esp Cardiol (Engl Ed). 2022;75(6):523.
2. Authors/Task Force M, McDonagh TA, Metra M, Adamo M, Gardner RS, Baumbach A, et al. 2023 Focused Update of the 2021 ESC Guidelines for the diagnosis and treatment of acute and chronic heart failure: Developed by the task force for the diagnosis and treatment of acute and chronic heart failure of the European Society of Cardiology (ESC) With the special contribution of the Heart Failure Association (HFA) of the ESC. Eur J Heart Fail. 2024;26(1):5-17.
3. Sindone AP, De Pasquale C, Amerena J, Burdeniuk C, Chan A, Coats A, et al. Consensus statement on the current pharmacological prevention and management of heart failure. Med J Aust. 2022;217(4):212-7.
4. Heidenreich PA, Bozkurt B, Aguilar D, Allen LA, Byun JJ, Colvin MM, et al. 2022 AHA/ACC/HFSA Guideline for the Management of Heart Failure: A Report of the American College of Cardiology/American Heart Association Joint Committee on Clinical Practice Guidelines. Circulation. 2022;145(18):e895-e1032.
5. Armstrong PW, Pieske B, Anstrom KJ, Ezekowitz J, Hernandez AF, Butler J, et al. Vericiguat in Patients with Heart Failure and Reduced Ejection Fraction. N Engl J Med. 2020;382(20):1883-93.
6. McDonagh TA, Metra M, Adamo M, Gardner RS, Baumbach A, Bohm M, et al. 2021 ESC Guidelines for the diagnosis and treatment of acute and chronic heart failure. Eur Heart J. 2021;42(36):3599-726.

7. Ponikowski P, Kirwan BA, Anker SD, McDonagh T, Dorobantu M, Drozdz J, et al. Ferric carboxymaltose for iron deficiency at discharge after acute heart failure: a multicentre, double-blind, randomised, controlled trial. Lancet. 2020;396(10266):1895-904.
8. Zeppenfeld K, Tfelt-Hansen J, de Riva M, Winkel BG, Behr ER, Blom NA, et al. 2022 ESC Guidelines for the management of patients with ventricular arrhythmias and the prevention of sudden cardiac death. Eur Heart J. 2022;43(40):3997-4126.
9. Van Gelder IC, Rienstra M, Bunting KV, Casado-Arroyo R, Caso V, Crijns H, et al. 2024 ESC Guidelines for the management of atrial fibrillation developed in collaboration with the European Association for Cardio-Thoracic Surgery (EACTS). Eur Heart J. 2024;45(36):3314-414.
10. Lang RM, Badano LP, Mor-Avi V, Afilalo J, Armstrong A, Ernande L, et al. Recommendations for cardiac chamber quantification by echocardiography in adults: an update from the American Society of Echocardiography and the European Association of Cardiovascular Imaging. J Am Soc Echocardiogr. 2015;28(1):1-39 e14.
11. Badano LP, Kolias TJ, Muraru D, Abraham TP, Aurigemma G, Edvardsen T, et al. Standardization of left atrial, right ventricular, and right atrial deformation imaging using two-dimensional speckle tracking echocardiography: a consensus document of the EACVI/ASE/Industry Task Force to standardize deformation imaging. Eur Heart J Cardiovasc Imaging. 2018;19(6):591-600.
12. Nagueh SF, Smiseth OA, Appleton CP, Byrd BF, 3rd, Dokainish H, Edvardsen T, et al. Recommendations for the Evaluation of Left Ventricular Diastolic Function by Echocardiography: An Update from the American Society of Echocardiography and the European Association of Cardiovascular Imaging. J Am Soc Echocardiogr. 2016;29(4):277-314.
13. Rudski LG, Fine NM. Right Ventricular Function in Heart Failure: The Long and Short of Free Wall Motion Versus Deformation Imaging. Circ Cardiovasc Imaging. 2018;11(1):e007396.

14. Mukherjee M, Rudski LG, Addetia K, Afilalo J, D'Alto M, Freed BH, et al. Guidelines for the Echocardiographic Assessment of the Right Heart in Adults and Special Considerations in Pulmonary Hypertension: Recommendations from the American Society of Echocardiography. J Am Soc Echocardiogr. 2025;38(3):141-86.
15. Rudski LG, Lai WW, Afilalo J, Hua L, Handschumacher MD, Chandrasekaran K, et al. Guidelines for the echocardiographic assessment of the right heart in adults: a report from the American Society of Echocardiography endorsed by the European Association of Echocardiography, a registered branch of the European Society of Cardiology, and the Canadian Society of Echocardiography. J Am Soc Echocardiogr. 2010;23(7):685-713; quiz 86-8.
16. Badano LP, Muraru D, Parati G, Haugaa K, Voigt JU. How to do right ventricular strain. Eur Heart J Cardiovasc Imaging. 2020;21(8):825-7.
17. Holland AE, Spruit MA, Troosters T, Puhan MA, Pepin V, Saey D, et al. An official European Respiratory Society/American Thoracic Society technical standard: field walking tests in chronic respiratory disease. Eur Respir J. 2014;44(6):1428-46.
18. Carluccio E, Biagioli P, Lauciello R, Zuchi C, Mengoni A, Bardelli G, et al. Superior Prognostic Value of Right Ventricular Free Wall Compared to Global Longitudinal Strain in Patients With Heart Failure. J Am Soc Echocardiogr. 2019;32(7):836-44 e1.
19. Carluccio E, Biagioli P, Alunni G, Murrone A, Zuchi C, Coiro S, et al. Prognostic Value of Right Ventricular Dysfunction in Heart Failure With Reduced Ejection Fraction: Superiority of Longitudinal Strain Over Tricuspid Annular Plane Systolic Excursion. Circ Cardiovasc Imaging. 2018;11(1):e006894.

CHAPTER THREE

Degree of left ventricular systolic impairment and its differential impact on right ventricular systolic function

3.0. Abstract

Background: Concomitant right ventricular (RV) systolic dysfunction has been shown to double the mortality in those with systolic heart failure (HF). However, there is limited information on the impact different grades of left ventricular (LV) systolic impairment have on RV systolic function in patients with stable non-ischaemic cardiomyopathy (NICM). We sought to assess the prevalence, degree of impairment and prognostic impact of RV dysfunction in a cohort of patients with NICM across a range of LV systolic impairment.

Methods and Results: Patients from our outpatient HF service with stable NICM and LV ejection fraction <50% were retrospectively assessed. Those with valvular, congenital heart, and significant pulmonary disease were excluded. Two-dimensional transthoracic echocardiographic (TTE) parameters of RV function including RV free wall strain (RV-FWS) were analysed. The 438-patients (60±16.2yrs; 34.8% male; LVEF 35±10%) included were categorised into 3-groups based on LVEF (Group 1: LVEF 41-49%; Group 2: LVEF 31-40%; Group 3: LVEF ≤30%) and were followed up to 36-months for a primary outcome of cardiovascular death and HF hospitalisation. Jonckheere-Terpstra test confirmed a step wise decrease in all RV functional parameters across the 3-groups (all $p<0.01$). Receiver operating characteristics curve analysis identified an optimal RV-FWS cutoff of <14.8% to best discriminate for our primary outcome. Log-rank test confirmed RV-FWS reduction <14.8% was associated with increased incidence of the primary outcome as a function of time ($p<0.001$). Multivariate analysis using a two-stage Cox regression model confirmed RV-FWS<14.8% independently predicts the primary outcome (adjusted HR 2.3, 95% CI: 1.5-3.6, $p<0.001$).

Conclusion: In our cohort of stable NICM patients, deteriorating RV systolic function was observed with worsening grades of LV systolic impairment. RV-FadWS was the only RV parameter which independently prognosticated adverse cardiovascular outcomes. A reduction in RV-FWS to <14.8% was independently associated with a higher incidence of cardiovascular death and HF hospitalisation as a function of time.

Graphical Abstract 3

GRAPHICAL ABSTRACT: There was a stepwise decrease in all right ventricular systolic functional parameters with each grade of worsening left ventricular ejection fraction confirmed on Jonckheere-Terpstra test. Log-rank analysis confirmed that reduction in right ventricular free-wall strain below 14.8% was associated with reduced freedom from cardiovascular death and heart failure hospitalisation as a function of time. Furthermore, this is an independent association after adjusting for clinical and echocardiographic parameters on multivariate Cox-regression analysis.

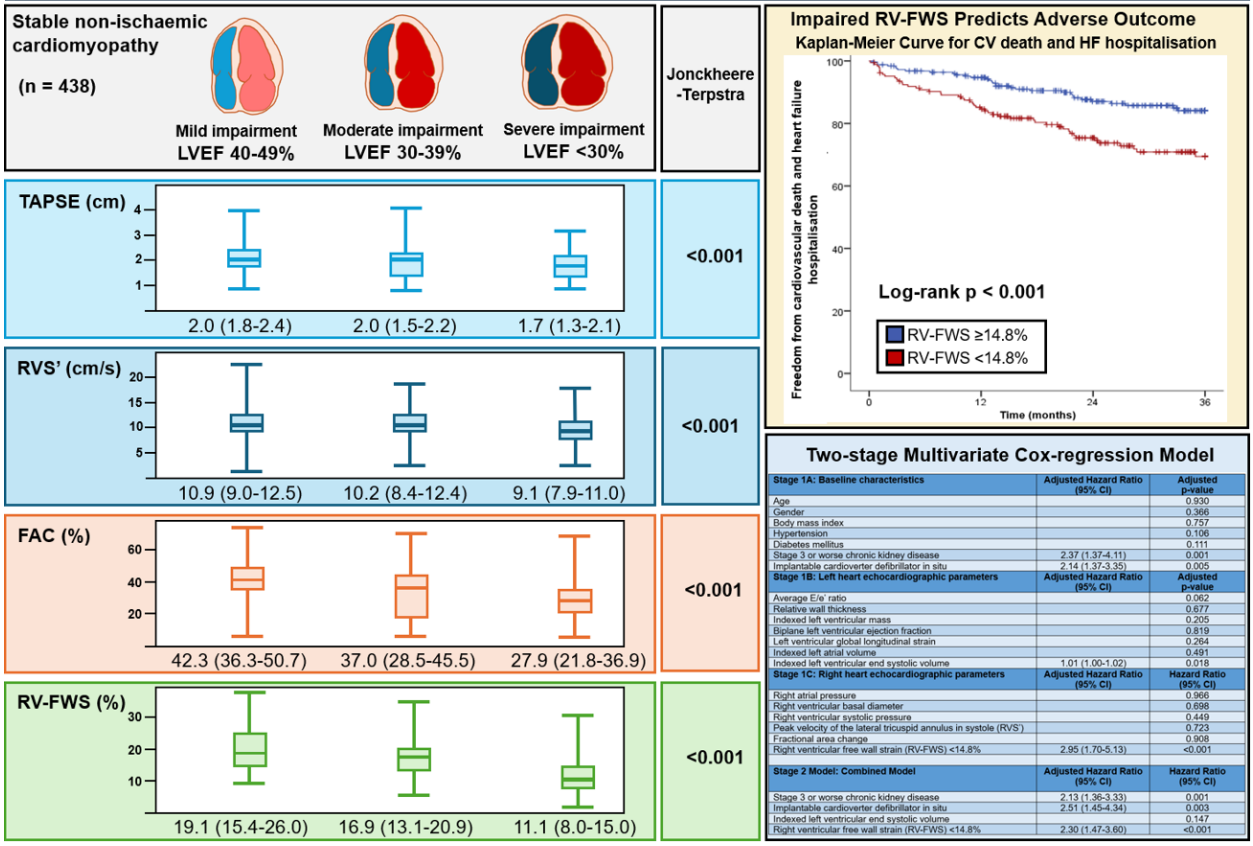

Two-stage Multivariate Cox-regression Model

Stage 1A: Baseline characteristics	Adjusted Hazard Ratio (95% CI)	Adjusted p-value
Age		0.930
Gender		0.366
Body mass index		0.757
Hypertension		0.106
Diabetes mellitus		0.111
Stage 3 or worse chronic kidney disease	2.37 (1.37-4.11)	0.001
Implantable cardioverter defibrillator in situ	2.14 (1.37-3.35)	0.005
Stage 1B: Left heart echocardiographic parameters	**Adjusted Hazard Ratio (95% CI)**	**Adjusted p-value**
Average E/e' ratio		0.062
Relative wall thickness		0.677
Indexed left ventricular mass		0.205
Biplane left ventricular ejection fraction		0.819
Left ventricular global longitudinal strain		0.264
Indexed left atrial volume		0.491
Indexed left ventricular end systolic volume	1.01 (1.00-1.02)	0.018
Stage 1C: Right heart echocardiographic parameters	**Adjusted Hazard Ratio (95% CI)**	**Hazard Ratio (95% CI)**
Right atrial pressure		0.966
Right ventricular basal diameter		0.698
Right ventricular systolic pressure		0.449
Peak velocity of the lateral tricuspid annulus in systole (RVS')		0.723
Fractional area change		0.908
Right ventricular free wall strain (RV-FWS) <14.8%	2.95 (1.70-5.13)	<0.001
Stage 2 Model: Combined Model	**Adjusted Hazard Ratio (95% CI)**	**Hazard Ratio (95% CI)**
Stage 3 or worse chronic kidney disease	2.13 (1.36-3.33)	0.001
Implantable cardioverter defibrillator in situ	2.51 (1.45-4.34)	0.003
Indexed left ventricular end systolic volume		0.147
Right ventricular free wall strain (RV-FWS) <14.8%	2.30 (1.47-3.60)	<0.001

Keywords: Heart failure; Right ventricle; Cardiomyopathy; Echocardiography; Global longitudinal strain

Abbreviations:

RV = right ventricle / right ventricular

HF = heart failure

LV = left ventricle / left ventricular

RVS' = tissue Doppler-derived tricuspid lateral annulus systolic velocity

TAPSE = tricuspid annular plane systolic excursion

RV-FWS = right ventricular free wall strain

TTE = transthoracic echocardiogram

2D = two-dimensional

NICM = non-ischaemic cardiomyopathy

LVEF = left ventricular ejection fraction

LA = left atrial

MV E = mitral inflow peak early filling velocity

STE = speckle-tracking echocardiography

LV-GLS = left ventricular global longitudinal strain

ROC = receiver operating characteristics curve

ICD = implantable cardioverter defibrillator

IVSd = interventricular septa thickness in end diastole

LVIDd = left ventricular internal diameter in end diastole

LVIDs = left ventricular internal diameter in end systole

RA = right atrial

FAC = fractional area change

3.1.0. Introduction

Concurrent right ventricular (RV) dysfunction in heart failure (HF) is linked to worse prognosis in those with left ventricular (LV) systolic impairment. (1, 2) Presence of biventricular systolic impairment has been thought to confer over a two-fold risk of mortality compared to those with isolated LV systolic impairment. (3) The prevalence of RV dysfunction varies and has been estimated to be as low as 20% to upwards of 67% in systolic HF populations. (3-5) However, the prevalence and severity of RV systolic dysfunction across different grades of LV systolic impairment is still unclear. (4, 6, 7)

Longitudinal contraction of the RV free wall is the predominant component that contributes to overall RV systolic contraction. (5) Traditional measures of RV longitudinal function such as tissue Doppler-derived tricuspid lateral annulus systolic velocity (RVS') and tricuspid annular plane systolic excursion (TAPSE) only assess the basal segment of the RV free wall and is limited by angle dependency. RV free wall strain (RV-FWS) has been proposed to be an angle independent measure of longitudinal RV function which has superior prognostication capacity compared to traditional RV parameters on transthoracic echocardiography (TTE) to predict adverse cardiovascular outcomes in systolic HF. (8-10)

3.2.0. Objective and aims

Our study aims to evaluate the prevalence and prognostic significance of traditional and advanced two-dimensional (2D) echocardiographic parameters of RV systolic function in a cohort of patients with compensated non-ischaemic cardiomyopathy (NICM) across different grades of LV systolic impairment.

3.3.0. Materials and methods

3.3.1. Study population

We retrospectively analysed consecutive patients aged ≥18 years with a diagnosis of non-ischaemic cardiomyopathy and a left ventricular ejection fraction (LVEF) of <50% who attended our institution's outpatient heart failure service between January 2017 and December 2020. We included those with stable HF symptoms and underwent an outpatient TTE. A rigorous review of the hospital electronic system and the heart failure service database was performed, and patients with a history of significant coronary artery disease (defined as ≥70% disease in any of the three main coronary arteries, prior coronary artery intervention or grafting, evidence of impaired myocardial perfusion or reversible ischemia), primary valvular disease, valve replacement or repair, congenital heart disease, prior cardiac surgery, severe pulmonary hypertension, restrictive or obstructive pulmonary disease requiring hospitalisation, recent pulmonary embolism within 6 months and those with untreated obstructive sleep apnoea were excluded. Patients with non-cardiac comorbidities which limited their life expectancy to <1 year, those with incomplete medical history or inadequate TTE image quality for strain analysis were also excluded.

Included patients were stratified into three groups i.e. Group 1: mild (LVEF 40-49%), Group 2: moderate (LVEF 30-39%) and Group 3: severe (LVEF <30%) based on severity of LV systolic impairment as defined by LVEF on echocardiography.

The study protocol was approved by the Western Sydney Local Health District Human Research Ethics Committee in compliance with the Declaration of Helsinki.

3.3.2. Follow up and outcomes

Eligible participants were followed up from the date of their index TTE for up to 36-months for the primary composite outcome of cardiovascular death and HF hospitalisation. Outcome data was gathered from the HF service, hospital electronic database, as well as medical records from general practitioners and specialist physicians.

3.3.3. Transthoracic echocardiography

All TTEs were performed using commercially available ultrasound systems in accordance with American Society of Echocardiography guideline recommendations.(6, 11-14) In brief, LV volume and ejection fraction were calculated using modified Simpson's biplane method. Left atrial (LA) volume was measured at end diastole (immediately prior to mitral valve opening) utilising the 2- and 4-chamber views using the biplane method of discs. Pulse-wave Doppler was performed in the apical 4-chamber view to measure mitral inflow velocities for the assessment of LV filling. These measurements included mitral inflow peak early filling (MV E) and late diastolic filling velocities, the E/A ratio, deceleration time of early filling velocity, and the isovolumetric relaxation time. Utilising pulse-wave tissue Doppler imaging in the apical views, mitral annular velocities were obtained, and derived variables included: peak velocity of early (E) and late (A) filling, deceleration time of the E wave velocity and atrial filling fraction. E/e' and lateral e' were subsequently calculated. (13)

Two-dimensional (2D) parameters of RV systolic function were assessed by tricuspid annular plane systolic excursion (TAPSE), tissue Doppler derived peak systolic velocity at the tricuspid annulus (RVS'), fractional area change (FAC), and speckle-tracking echocardiography (STE) from the RV-focused apical 4-chamber view. (6, 11-14)

All reported parameters were a mean of measurements from five cardiac cycles for patients in atrial fibrillation or flutter at the time of the scan. (11)

3.3.4. Speckle-tracking echocardiography

Deformation imaging using STE was performed offline using vendor independent computer software (TomTech Image Arena Systems v2.3, Germany). Measurements were performed by two independent investigators blinded to patient baseline characteristics, outcomes and other echocardiographic data. All STE measurements were expressed as absolute percentages.

LV longitudinal strain (LV-GLS) was assessed by tracing the LV endocardium at end systole. LV-GLS was then calculated as the average of the 18-segments obtained across the three standard apical views. RV strain was evaluated by tracing the RV endocardium in the RV-focused apical view. (13) We analysed RV-FWS which was derived from the average peak systolic strain of the three RV free wall segments.

Quantitation of inter- and intra-observer variability of right ventricular free-wall strain was performed in 5% of the population through repeat measurements by a second independent investigator and the original investigator at least one month later. Reproducibility of these measurements were represented by the intra-class correlation coefficient.

3.3.5. Statistical analysis

All statistical analysis was performed using the Statistical Package for Social Sciences Software (SPSS Version 22; SPSS Inc., Chicago, IL, USA). Continuous variables were presented as mean ± standard deviations. Categorical variables were expressed as numbers and percentages.

We utilised one-way ANOVA analysis to identify TTE parameters that were significantly different from the group mean across the three groups. Jonckheere-Terpstra test for ordered alternatives was then performed for the RV parameters found to be significant on one-way ANOVA to confirm a significant trend across the three LV impairment groups. We further performed independent T-test to compare these RV parameters between adjacent LV systolic impairment subgroups.

To determine the optimal RV-FWS cutoff associated with the primary outcome, we performed Youden index analysis using the receiver operating characteristics (ROC) curve for the combined cohort and the three LV impairment groups. Event rates were estimated by Kaplan-Meier survival analysis for all RV parameters in the combined cohort and each of the three groups. A two-stage multivariate Cox proportional hazard model was then applied to identify

independent predictors of the primary outcome in the combined cohort. All statistical tests were two-tailed, with a p-value <0.05 considered statistically significant.

3.4.0. Results

3.4.1. Participant characteristics

Out of the 1,097 patients with a confirmed diagnosis of systolic HF who attended our HF service during the study period. We excluded 477 patients due to ischaemic heart disease or significant coronary disease, 133 patients due to severe pulmonary hypertension, significant pulmonary disease, primary valvular disease, prior cardiac surgery, or congenital heart disease, and a further 49 were excluded due to inadequate echocardiographic image quality for analysis. A total of 438 patients (40%) met the inclusion criterion and were included in the final analysis. (Figure 3.1)

The cohort was predominantly male (65%) with a mean age of 60.0±16.2 years. Of these, 161 patients (36.8%) were in Group 1 (LVEF 41-49%), 142 patients (32.4%) were in Group 2 (LVEF 31-40%), and 135 patients (30.8%) were in Group 3 (LVEF ≤30%). In terms of comorbidities, 50.0% had hypertension, 30.3% had diabetes mellitus, 31.7% had hyperlipidaemia, 27.5% had stage III or worse chronic kidney disease, 43.0% had atrial fibrillation (AF), 4.9% had atrial flutter, 1.4% had pacemakers, and 13.3% had implantable cardioverter defibrillators (ICD; including cardiac resynchronisation therapy-defibrillator) in situ. By study design, none of the patients had valvular, congenital or ischaemic heart disease. (Table 3.1)

Figure 3.1. Consort diagram

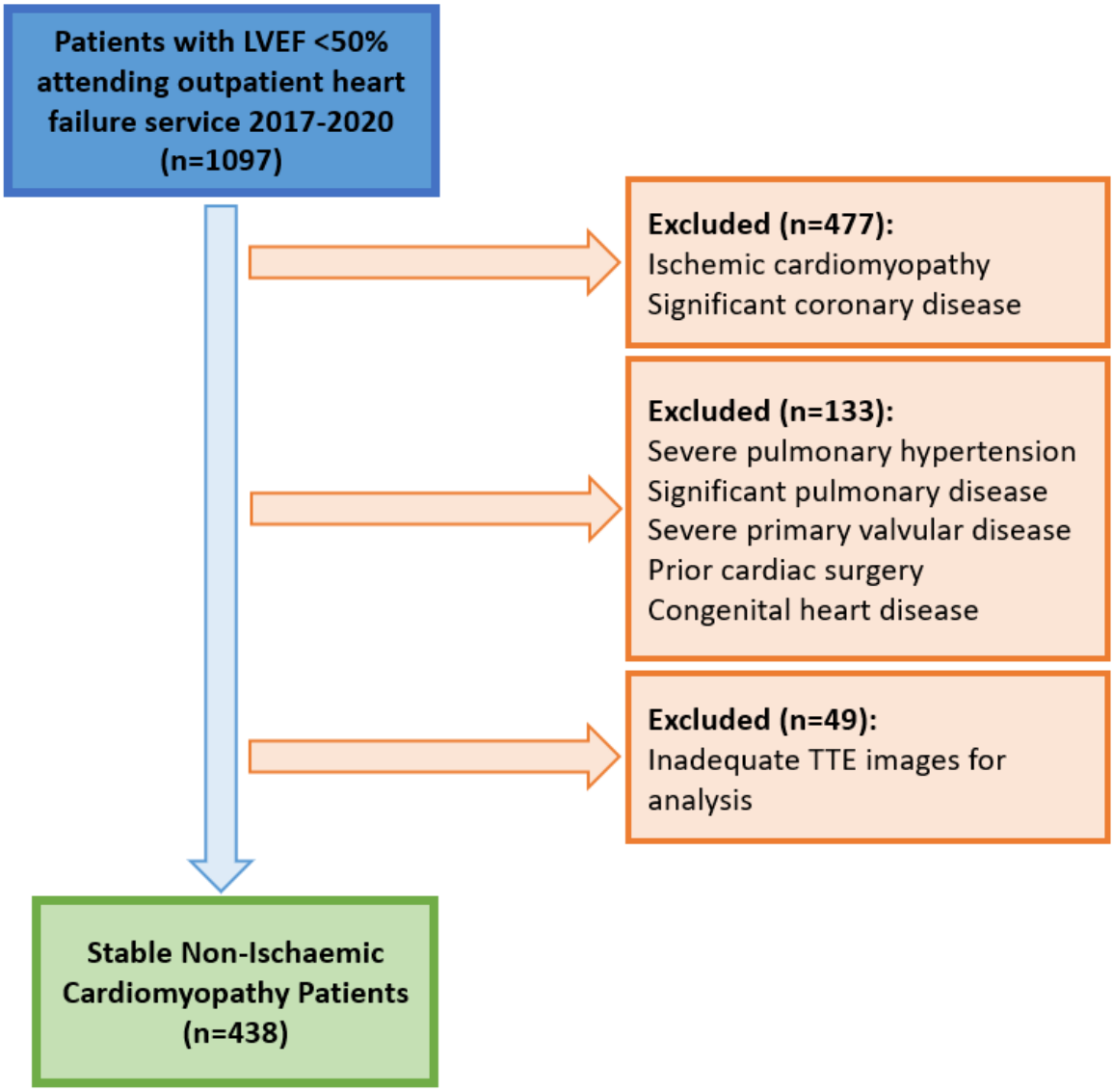

Figure 3.1 A total of 1,097 patients were screened. Of which 477 were excluded for ischaemic cardiomyopathy or significant coronary disease; 133 were excluded for severe pulmonary hypertension, significant pulmonary disease, severe primary valvular disease, prior cardiac surgery, congenital heart disease; and 49 were excluded for inadequate image quality. Four hundred and thirty-eight patients were included in the final analysis.

Tablet 3.1. Baseline characteristics

Baseline Characteristics	Combined Cohort (n=438)	Group 1: Mild LV Impairment (n=161)	Group 2: Moderate LV Impairment (n=142)	Group 3: Severe LV Impairment (n=135)
Sex (% male)	65.1	63.4	61.3	71.1
Age (years)	60.0±16.2	61.8±16.5	63.3±15.3	54.4±15.6
BMI (kg/m^2)	31.6±9.3	30.6±9.1	31.6±8.4	32.8±10.4
Atrial fibrillation (%)	43.0	42.2	43.0	29.9
Atrial flutter (%)	4.9	8.1	4.9	4.5
Pacemaker (%)	1.4	7.5	1.4	3.0
ICD and CRT-D (%)	7.7	6.8	7.7	17.9
CRT-D (%)	5.6	0.6	5.6	2.2
Coronary disease (%)	0	0	0	0
Stroke (%)	7.0	9.3	7.0	1.5
TIA (%)	2.8	1.9	2.8	2.2
Hypertension (%)	50.0	49.1	50.0	43.3
Diabetes mellitus (%)	30.3	26.1	30.3	26.9
Hyperlipidaemia (%)	31.7	30.4	31.7	23.9
eGFR ≤60 (%)	27.5	27.3	27.5	21.5
Asthma (%)	7.8	8.7	7.8	8.2
ILD (%)	0.9	1.2	0.7	0.7
COPD (%)	9.4	11.2	10.6	6.0
OSA (%)	9.2	8.1	9.2	11.9
Prior history of PE (%)	2.8	2.5	2.8	2.2

Table 3.1. Baseline characteristics for the overall cohort and for each grade of left ventricular systolic impairment.

Abbreviations. *BMI: body mass index, ICD: implantable cardioverter defibrillation, CRT-D: cardiac resynchronization therapy and defibrillator, TIA: transient ischaemic attack, eGFR: estimated glomerular filtration rate, ILD: interstitial lung disease, COPD: chronic obstructive pulmonary disease, OSA: obstructive sleep apnoea, PE: pulmonary embolism*

3.4.2. Follow up and outcomes

The primary outcome of combined cardiovascular death and HF hospitalisation occurred in 80 patients (18.3%), of which 22 (5.0%) were attributed to cardiovascular death during a mean follow-up duration of 24.3±11.3 months. Specifically, the primary outcome occurred in 23-patients (14.3%) in group 1, 28-patients (19.7%) in group 2, and 29-patients (21.5%) in group 3. (Table 3.2)

Table 3.2. Patient follow up and outcomes

Outcome	**Total cohort (n=438)**	**Mild LV Systolic Impairment (n=161)**	**Moderate LV Systolic Impairment (n=142)**	**Severe LV Systolic Impairment (n=135)**
Mean follow up duration (months)	24.3±11.3	25.1±11.5	24.3±10.9	23.3±11.5
Combined primary outcome (%)	80 (18.3)	23 (14.3)	28 (19.7)	29 (21.5)
Cardiac death (%)	22 (5.0)	7 (4.3)	6 (4.2)	9 (6.7)
Heart failure hospitalisation (%)	58 (13.3)	16 (10.0)	22 (15.5)	20 (14.8)

Table 3.2. Amongst the 438-patients, a total of 80 patients reached the primary outcome of combined cardiovascular death and heart failure rehospitalisation. Of which 22 were due to cardiovascular death.

Abbreviations. *LV: left ventricular*

3.4.3. Reproducibility analysis

There was good reproducibility of the strain parameters based on the inter- and intra-observer variability. For inter-observer variability, the intra-class correlation coefficient was 0.94 (95% CI 0.87-0.97) for LV-GLS, and 0.96 (95% CI 0.91-0.98) for RV-FWS. For intra-observer variability, the intra-class correlation coefficient was 0.95 (95% CI 0.89-0.99) for LV-GLS, and 0.98 (95% CI 0.97-0.99) for RV-FWS.

3.4.4. Echocardiographic parameters

The mean LVEF across the entire cohort was 35±9.7%. Group specific mean LVEF values were 45±3.2%, 35±3.0%, and 23±4.2% in Groups 1,2 and 3 respectively.

We utilised one-way ANOVA analysis for both left and right heart echocardiographic parameters across the three LV impairment groups to identify which values were significantly different from the group mean. Of the left heart parameters, interventricular septal thickness (IVSd), left ventricular internal diameter in end diastole and end systole (LVIDd and LVIDs), indexed LV mass, LV end diastolic volume, LV end systolic volume, bi-plane LVEF, LV-GLS, MV E velocity, and average E/e' ratio were all significantly different from the group mean on one-way ANOVA (all $P<0.01$). Amongst the right heart parameters, right atrial (RA) area, RVS', TAPSE, fractional area change (FAC), and RV-FWS were significantly different from the group mean on one-way ANOVA (all $p<0.001$). LV posterior wall thickness, indexed LA volume and RV basal diameter were the only parameters that were not significantly different from the group mean ($p=0.521$, $p=0.067$, and $p=0.157$ respective). (Table 3.3)

Table 3.3. Echocardiographic parameters

Transthoracic Echocardiogram	Combined Cohort (n=438)	Group 1: Mild LV Impairment (n=161)	Group 2: Moderate LV Impairment (n=142)	Group 3: Severe LV Impairment (n=135)	One-way ANOVA (p-value)
IVSd (cm)	**1.0±0.3**	**1.1±0.3**	**1.1±0.3**	**1.0±0.2**	**<0.001**
LVIDd (cm)	**5.6±1.0**	**5.0±0.8**	**5.5±0.9**	**6.2±0.9**	**<0.001**
LVIDs (cm)	**4.6±1.1**	**3.8±0.7**	**4.6±0.9**	**5.5±0.9**	**<0.001**
PWd (cm)	1.1±0.3	1.1±0.3	1.1±0.4	1.0±0.2	0.521
Indexed LV mass (g/m^2)	**119.8±39.3**	**108.2±41.2**	**120.9±34.1**	**132.6±38.4**	**<0.001**
Indexed LV EDV (ml/m^2)	**73.0±45.8**	**61.1±59.7**	**69.0±22.2**	**91.4±39.1**	**<0.001**
Indexed LV ESV (ml/m^2)	**48.7±31.5**	**33.7±33.3**	**45.2±15.3**	**70.2±30.1**	**<0.001**
Biplane LVEF (%)	**35.0±9.7**	**45.1±3.2**	**34.8±3.0**	**23.0±4.2**	**<0.001**
LV-GLS (%)	**10.5±3.3**	**13.0±2.8**	**10.3±2.4**	**7.7±2.3**	**<0.001**
MV E velocity (cm/s)	**87.2±39.6**	**80.0±28.3**	**87.0±33.3**	**96.6±53.8**	**0.002**
Average E/e' ratio	**13.8±6.7**	**12.7±6.9**	**13.8±7.2**	**15.1±5.7**	**0.023**
Indexed LA volume (ml/m^2)	48.0±31.7	44.4±44.3	47.5±19.5	52.9±22.2	0.067
Right atrial area (cm^2)	**20.9±8.7**	**19.2±7.6**	**19.6±7.6**	**24.1±10.2**	**<0.001**
RVSP (mmHg)	**35.3±12.8**	**34.1±13.8**	**33.9±12.9**	**38.2±11.0**	**0.015**
RV Base diam. (cm)	4.3±5.3	3.8±0.8	5.0±1.0	4.3±0.8	0.157
TAPSE (cm)	**1.9±0.8**	**2.1±0.5**	**2.0±1.3**	**1.7±0.5**	**0.001**
RVS' (cm/s)	**10.3±3.2**	**10.8±3.7**	**10.6±3.0**	**9.3±2.5**	**0.001**
FAC (%)	**37.2±13.7**	**43.2±12.4**	**37.4±13.0**	**29.8±12.2**	**<0.001**
RV-FWS (%)	**17.0±7.1**	**20.9±6.9**	**17.1±5.5**	**12.3±5.7**	**<0.001**

Table 3.3. Other than posterior wall thickness, indexed left atrial volume and right ventricular basal diameter, all other echocardiographic parameters were significant one-way ANOVA.

Abbreviations. *IVSd: interventricular septal wall thickness in end-diastole, LVIDd: left ventricular internal diameter in end-diastole, LVIDs: left ventricular internal diameter in end-systole, PWd: posterior wall thickness in end-diastole, EDV: end-diastolic volume, ESV: end-systolic volume, LA: left atrial, RVSP: right ventricular systolic pressure, TAPSE: tricuspid annular plane systolic excursion, RVS': tissue Doppler-derived tricuspid lateral annulus systolic velocity, FAC: fractional area change, RV-FWS: right ventricular free wall strain.*

3.4.5. Right ventricular free wall strain cutoff in non-ischaemic cardiomyopathy

As there is no accepted RV-FWS cutoff value in NICM, we sought to identify a new cutoff in our NICM cohort based on its prognostic capacity. (6, 7) We utilised ROC curve analysis and Youden's index method. This identified a RV-FWS cutoff value of <14.8% to exhibit the best performance in discriminating for our primary outcome of cardiovascular death and HF hospitalisation (area under the curve 0.62; sensitivity 60%; specificity 62%).

3.4.6. Prevalence of right ventricular dysfunction across different grades of left ventricular systolic impairment

We assessed the prevalence of RV dysfunction in our overall cohort and in each LV systolic impairment subgroup. This prevalence was lower when using the traditional echocardiographic parameters of RV function using their respective normal reference ranges: i.e. TAPSE ≤1.7 cm; RVS' ≤9.5 cm/s; and FAC ≤35%. Prevalence of RV dysfunction in the overall cohort was lowest with TAPSE at 31.4%, followed by FAC at 44.3% and was highest with RVS' at 45.2%. In detail, the prevalence of RV dysfunction in groups 1, 2 and 3 were respectively: 17.3%, 28.9% and 48.8% based on TAPSE; 34.8%, 43.7% and 59.3% based on RVS'; and were 21.1%, 44.4% and 71.9% based on FAC. (Table 3.4 and Figure 3.2)

RV dysfunction was the most prevalent when using RV-FWS based on a normal reference value of ≥20%. (6, 15) Where 83.6% of the combined cohort, 55.3% of group 1, and 100% in both groups 2 and 3 were found to have reduced RV-FWS. (Table 3.4 and Figure 3.2)

Table 3.4. Prevalence of right ventricular dysfunction on echocardiogram

Transthoracic Echocardiogram	Combined Cohort (n=438)	Group 1: Mild LV Impairment (n=161)	Group 2: Moderate LV Impairment (n=142)	Group 3: Severe LV Impairment (n=135)
TAPSE <1.7cm (n, %)	128 (31.4)	26 (17.3)	41 (28.9)	61 (48.8)
RVS' <9.5cm/s (n, %)	198 (45.2)	56 (34.8)	62 (43.7)	80 (59.3)
FAC <35% (n, %)	194 (44.3)	34 (21.1)	63 (44.4)	97 (71.9)
RV-FWS <20% (n, %)	366 (83.6)	89 (55.3)	142 (100)	135 (100)
RV-FWS <14.8% (n, %)	186 (42.5)	33 (20.5)	53 (37.3)	100 (74.1)

Table 3.4. The table lists the prevalence of right ventricular dysfunction based on each right ventricular echocardiographic functional parameter across the combined cohort and the three left ventricular systolic impairment groups.

Abbreviations. *TAPSE: tricuspid annular plane systolic excursion, RVS': tissue Doppler-derived tricuspid lateral annulus systolic velocity, FAC: fractional area change, RV-FWS: right ventricular free wall strain.*

Figure 3.2. Prevalence of right ventricular dysfunction by echocardiographic parameters across the left ventricular systolic impairment groups.

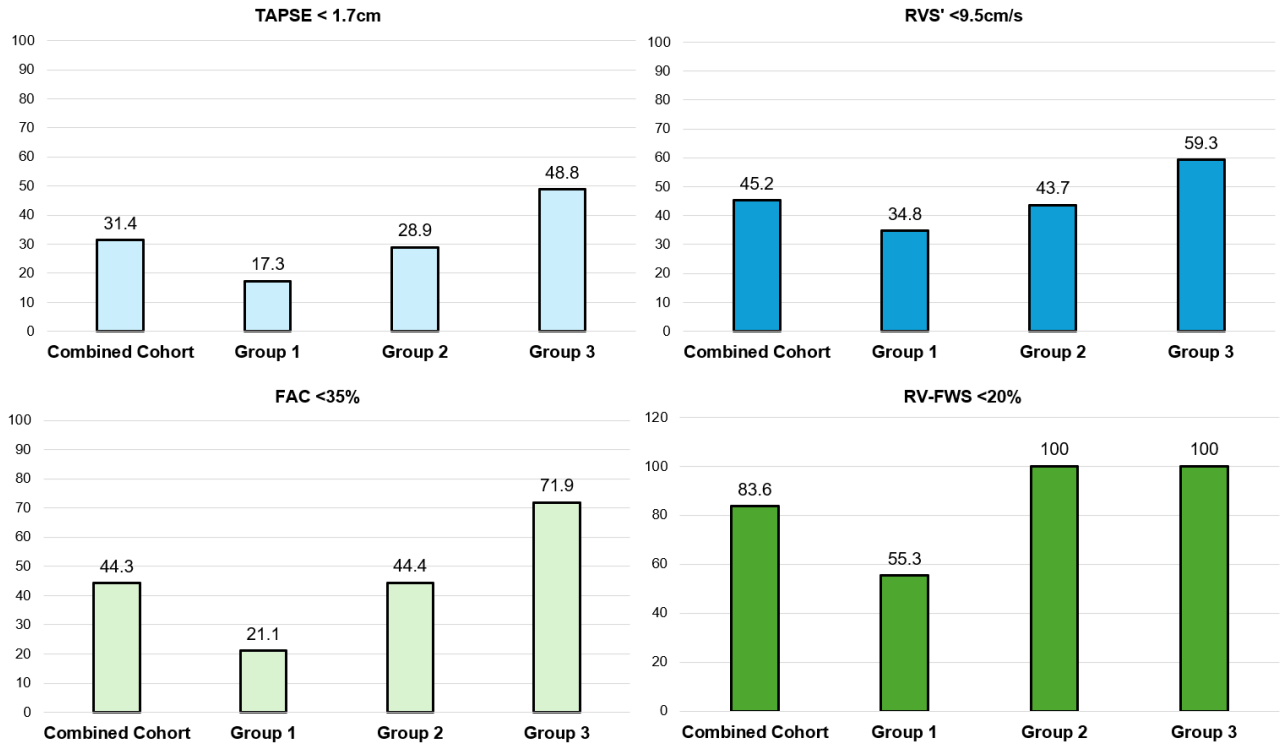

Figure 3.2. A stepwise increase in the prevalence of right ventricular dysfunction is seen with worsening grades of left ventricular systolic impairment. Group 1: LVEF 40-49%; Group 2: LVEF 30-39%; Group 3: LVEF <30%.

Abbreviations. *TAPSE: tricuspid annular plane systolic excursion, RV S': tissue Doppler-derived tricuspid lateral annulus systolic velocity, FAC: fractional area change, RV-FWS: right ventricular free wall strain.*

3.4.7. Right ventricular functional parameters across grades of left ventricular systolic impairment

We performed Jonckheere-Terpstra test to assess for a monotonic trend in RV functional parameters across the three ordered LV systolic impairment subgroups (Group 1: LVEF 40-49%, Group 2: LVEF 30-39%, Group 3 LVEF <30%). The analysis demonstrated a significant stepwise decrease in RV systolic functional parameters across the three groups for all RV functional parameters (all p<0.001). FAC and RV-FWS had the highest Z-values of -10.80 and -8.89 respectively. (Table 3.5)

Specifically, our results confirmed that progressively worsening grades of LV systolic impairment was associated with a corresponding decline in all four echocardiographic parameters of RV systolic function.

We further performed independent T-test to confirm a stepwise decline in these four RV functional parameters between adjacent LV systolic impairment subgroups. A significant decline was observed between the mild and moderate LV systolic impairment groups for TAPSE (2.1±0.5 vs 1.9±0.5cm, p=0.009), FAC (43.2±12.4 vs 37.4±13.0%, p<0.001), and RV-FWS (20.9±6.9 vs 17.1±5.5%, p<0.001), but not for RVS' (10.8±3.7 vs 10.6±3.0cm/s, p=0.702). All four RV parameters significantly dropped between the moderate and severe LV systolic impairment groups (TAPSE: 1.9±0.5cm, p=0.002; RVS': 10.6±3.0 vs 9.3±2.5cm/s, p=0.002; FAC: 37.4±13.0 vs 29.8±12.2%, p<0.001; RV-FWS: 17.1±5.5 vs 12.3±5.7%, p<0.001). (Table 3.6)

A box plot was constructed using the median and interquartile ranges of each RV systolic functional parameter to visually represent their stepwise decline. (Figure 3.3)

Table 3.5. Jonckheere-Terpstra test of right ventricular systolic functional parameters across the left ventricular systolic impairment groups

	TAPSE	RVS'	FAC	RV-FWS
Standard deviation	0.53	3.22	13.69	7.06
Mean Test statistic	27662.5	24587.5	31883.5	31843.1
Standard error	1292.93	1186.01	1440.70	1440.68
Standardised test statistic	-5.73	-4.54	-10.80	-8.89
Significance (2-sided)	<0.001	<0.001	<0.001	<0.001

Table 3.4. Jonckhere-Terpstra test confirms an ordered difference in the median values of these four right ventricular systolic parameters across the left ventricular systolic impairment groups.

Abbreviations. *TAPSE: tricuspid annular plane systolic excursion, RVS': tissue Doppler-derived lateral tricuspid annulus systolic velocity, FAC: fractional area change, RV-FWS: right ventricular free wall strain.*

Table 3.6 Independent T-test between left ventricular systolic impairment groups

	Group 1: Mild LV Impairment (n=161)	Mild vs Moderate Mann-Whitney test (p-value)	**Group 2: Moderate LV Impairment (n=142)**	Moderate vs Severe Mann-Whitney test (p-value)	**Group 3: Severe LV Impairment (n=135)**
TAPSE (cm)	2.1±0.5	0.009	1.9±0.5	0.002	1.7±0.5
RVS' (cm/s)	10.8±3.7	0.146	10.6±3.0	0.002	9.3±2.5
FAC (%)	43.2±12.4	<0.001	37.4±13.0	<0.001	29.8±12.2
RV-FWS (%)	20.9±6.9	<0.001	17.1±5.5	<0.001	12.3±5.7

Table 3.5 Independent T-test between left ventricular systolic impairment groups. There was a significant difference between the mean values for all parameters of RV function measured except for the RVS' value was similar between group 1 and 2.

Abbreviations. *TAPSE: tricuspid annular plane systolic excursion, RV S': tissue Doppler-derived lateral tricuspid annulus systolic velocity, FAC: fractional area change, RV-FWS: right ventricular free wall strain.*

Figure 3.3. Box plot of right ventricular parameters across the left ventricular impairment groups

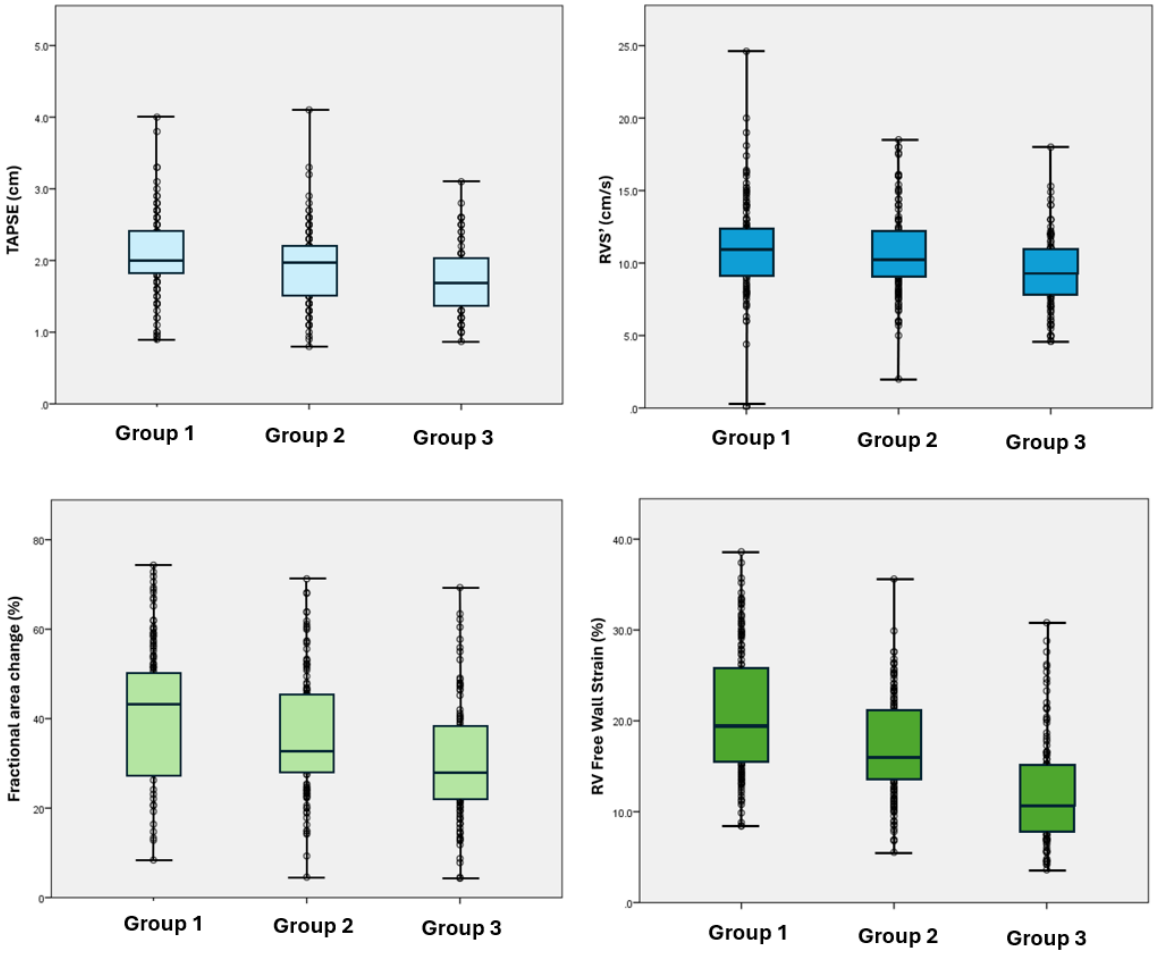

Figure 3.3. Box plot of the right ventricular systolic parameters expressed as median and interquartile range across the three grades of left ventricular systolic impairment. Group 1: LVEF 40-49%; Group 2 LVEF 30-39%; Group 3 LVEF <30%.

Abbreviations. *TAPSE: tricuspid annular plane systolic excursion, RVS': tissue Doppler-derived lateral tricuspid annulus systolic velocity, RV: right ventricular.*

3.4.8. Prognostic value of right ventricular dysfunction on echocardiography

Kaplan-Meier survival analysis was employed to determine the prognostic value of 2D TTE RV functional parameters for predicting our primary outcome of cardiovascular death or HF hospitalisation. Of the traditional RV functional parameters, reduction of FAC, but not TAPSE nor RVS', was associated with the primary outcome as a function of time on log-rank analysis ($p=0.043$, $p=0.996$, and $p=0.295$ respectively). Reduction of RV-FWS to <14.8%, which best predicted the primary outcome in our study, was associated with an increased incidence of cardiovascular death and HF hospitalisation as a function of time on log-rank analysis ($p<0.001$). (Figure 3.4)

We utilised multivariate Cox proportional hazard model to determine which of the clinical characteristics, LV and RV echocardiographic parameters were independent predictors of the primary outcome. To avoid over fitting, we developed a two-stage multivariable Cox proportional hazard model.

In the first stage of the model, we included all relevant clinical variables after consideration for covariates into 3 categories: i.e. clinical characteristics, left heart, and right heart echocardiographic parameters. Age, gender, body mass index (BMI), diabetes mellitus, stage 3 or worse chronic kidney disease (CKD), and the presence of an ICD were included into the clinical characteristics category. For the left heart echocardiographic parameters, we included average E/e' ratio, relative wall thickness, indexed LV mass, LVEF, LV-GLS, indexed LA volume and indexed LV end systolic volume (LVESV). Finally for the right heart parameters, we included right atrial area, RV basal diameter, RV systolic pressure, RVS', FAC, and RV-FWS <14.8%.

Of the clinical characteristics, the presence of CKD and ICD were significantly associated with the primary outcome. Amongst the left and right heart echocardiographic parameters, LVESV and RV-FWS <14.8% were the only two parameters found to be significant in their respective groups. These four covariates were then combined in to the stage 2 model, which confirmed

the presence of an ICD (p=0.003, adjusted HR 95% CI: 2.5, 1.4-4.3), stage III or worse chronic kidney disease (p=0.001, adjusted HR 95% CI: 2.1, 1.4-3.3) and an absolute RV-FWS of <14.8% (p<0.001, adjusted HR 95% CI: 2.3, 1.5-3.6) to be independently associated with the primary outcome of combined cardiac death and HF hospitalisation. (Table 3.7)

Figure 3.4. Cumulative freedom from cardiac death and heart failure hospitalisation in preserved and impaired right ventricular free wall strain in the combined cohort

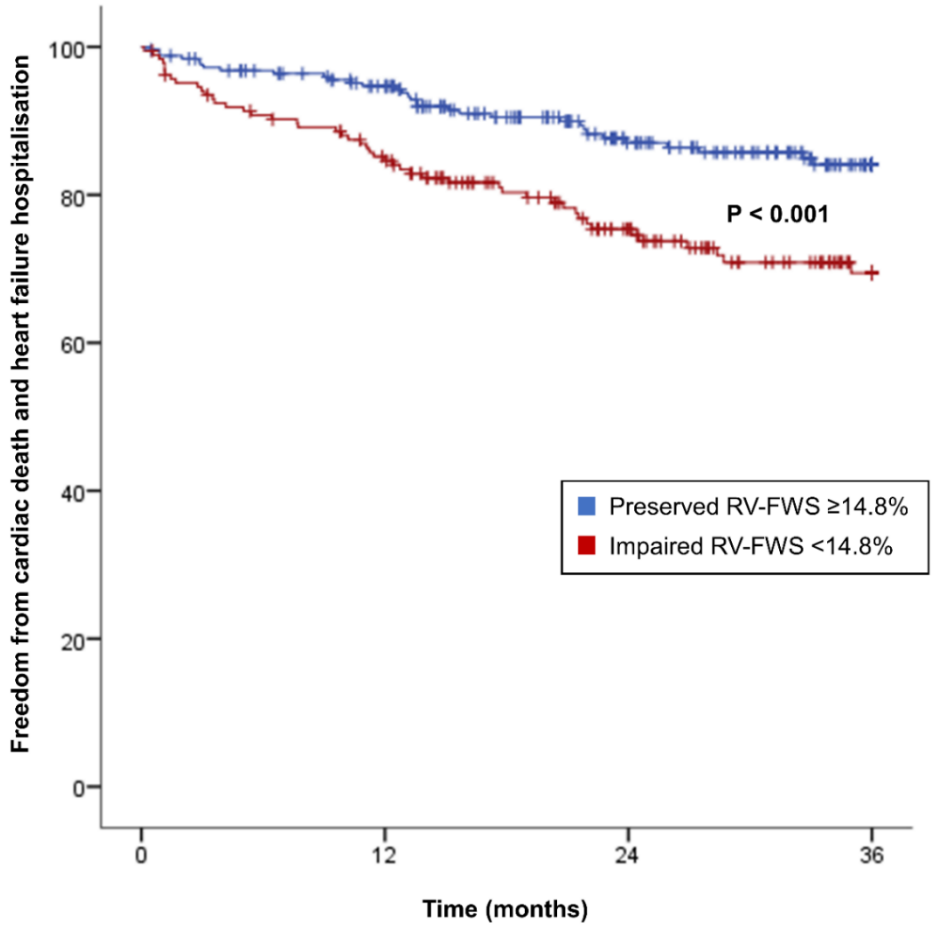

Figure 3.4. Kaplan-Meier survival curve depicting the cumulative freedom from cardiovascular death and heart failure hospitalisation in those with preserved and impaired right ventricular free wall strain.

Abbreviations. *RV-FWS: right ventricular free wall strain.*

Table 3.7. Two-stage Cox proportional hazard model

Stage 1A: Clinical characteristics	**Adjusted Hazard Ratio (95% CI)**	**Adjusted p-value**
Age		0.930
Gender		0.366
Body mass index		0.757
Hypertension		0.106
Diabetes mellitus		0.111
Stage 3 or worse chronic kidney disease	2.37 (1.37-4.11)	0.001
Implantable cardioverter defibrillator	2.14 (1.37-3.35)	0.005
Stage 1B: Left heart TTE parameters	**Adjusted Hazard Ratio (95% CI)**	**Adjusted p-value**
Average E/e' ratio		0.062
Relative wall thickness		0.677
Indexed left ventricular mass		0.205
Left ventricular ejection fraction		0.819
Left ventricular global longitudinal strain		0.264
Indexed left atrial volume		0.491
Indexed left ventricular end systolic volume	1.01 (1.00-1.02)	0.018
Stage 1C: Right heart TTE parameters	**Adjusted Hazard Ratio (95% CI)**	**Adjusted p-value**
Right atrial area		0.966
Right ventricular basal diameter		0.698
Right ventricular systolic pressure		0.449
RVS'		0.723
Fractional area change		0.908
RV-FWS <14.8%	2.95 (1.70-5.13)	<0.001
Stage 2 Model: Combined Model	**Adjusted Hazard Ratio (95% CI)**	**Hazard Ratio (95% CI)**
Stage 3 or worse CKD	2.13 (1.36-3.33)	0.001
ICD or CRT-D in situ	2.51 (1.45-4.34)	0.003
Indexed LVES volume		0.147
RV-FWS <14.8%	2.30 (1.47-3.60)	<0.001

Table 3.6. Mode 1A included the clinical factors, model 1B included the left heart echocardiographic parameters and model 1C included the right heart echocardiographic parameters. Model 2 included all parameters found to be significant in models 1A, 1B, and 1C.

Abbreviations. *RVS': tissue Doppler-derived tricuspid lateral annulus systolic velocity, RV-FWS: right ventricular free wall strain.*

3.5.0. Discussion

The chief findings in our study are threefold: firstly, RV systolic dysfunction does not always accompany LV systolic impairment although the prevalence and severity of RV systolic dysfunction worsened with increasing severity of LV systolic impairment; secondly, the prevalence of RV dysfunction differs based on the 2D echocardiographic parameter used with RV-FWS being the most sensitive marker; finally, the reduction of RV-FWS below a lower threshold of 14.8% best discriminated for and was independently associated with an increased incidence of cardiovascular death and HF hospitalisation in our NICM cohort.

Several previous studies have demonstrated an association between RV-FWS and adverse cardiovascular outcomes in systolic HF. However, these studies have all classified LV systolic function based on a single LVEF cutoff with most studies choosing a value of either 35 or 40%, while only a single study included patients with an LVEF of up to 45%. (7-10, 16-19) Therefore, the impact of different degrees of LV systolic impairment on RV systolic function has not been previously examined.

To our knowledge, our study was the first to demonstrate the stepwise decrease in RV systolic function with each worsening grade of LV systolic impairment; and that RV systolic impairment was independently associated with adverse cardiovascular outcomes in NICM across a wide range of LVEF up to 50%.

3.5.1 Normal right ventricular free wall strain thresholds in non-ischaemic cardiomyopathy

Based on the normal RV reference ranges published by the World Alliance Societies of Echocardiography and the recent joint society guideline, the lowest expected RV-FWS value has been proposed as 20% in the healthy population. (6, 15) A meta-analysis performed by Anastasiou et al. found that the optimal RV-FWS cutoff in HF populations for predicted adverse cardiovascular outcomes varied widely from as low as 8.6% and up to 22% amongst the 24 studies included. (7)

In our cohort, all patients with moderate or severe LV systolic impairment had RV-FWS values below the 20% threshold. Our study identified a lower RV-FWS cutoff of 14.8% across the entire cohort based on its ability to discriminate cardiovascular death and HF hospitalisation. Studies by Carluccio et al. have identified a similar RV-FWS cutoff value of 15.3% in a systolic HF population based on its predictive capacity for adverse cardiovascular outcomes. (8, 9) In contrast, Houard et al. examined a cohort of 'healthier' systolic HF patients without atrial fibrillation or severe chronic kidney disease and presented a higher RV-FWS value of 19% as the optimal threshold. (10)

We believe that a lower RV-FWS threshold such as 14.8% identified in our study, would serve as a more accurate prognostic marker in patients with stable NICM compared to the normal reference range which was derived from healthy populations.

3.5.2 Prevalence of right ventricular dysfunction in non-ischaemic cardiomyopathy

Our results show that the prevalence of right heart dysfunction in NICM may be underestimated when using traditional parameters. Prevalence of RV dysfunction in NICM patients has been reported to be as low as 20% on cardiac magnetic resonance derived RV ejection fraction and up to around two thirds of all systolic HF patients. (3, 5) Amongst our patients, the prevalence of RV dysfunction was higher at 35.8%, 45.2% and 44.3% based on traditional measures of TAPSE, RVS' and FAC respectively. Out of the RV parameters, RV-FWS was the most sensitive marker of RV dysfunction which corresponded with the highest prevalence of RV systolic impairment in the overall cohort and in each LV systolic impairment subgroup. It should be noted that all patients with moderate or severe LV systolic impairment had a RV-FWS value below 20%, which nullifies any discriminatory utility of the normal RV-FWS reference range in these two groups.

Based on our findings, RV-FWS is a more sensitive measure for the detection of RV dysfunction compared to traditional RV functional parameters in stable NICM patients.

3.5.3 Right ventricular functional decline with worsening left ventricular systolic function

HF with reduced ejection fraction has been shown to be associated with RV dysfunction in several previous studies. (4, 7, 20, 21) However, the detrimental effects of increasing grades of LV systolic impairment on RV function is not well understood.

One previous study performed in patients with left heart disease by Surkova et al. found that overall RV ejection fraction remained normal and did not differ significantly between those with normal, mildly reduced or moderately reduced LVEF. Only those with severely reduced LVEF to <30% had significantly lower RV ejection fraction. (22)

Our study was able to demonstrate a significant stepwise decline in all RV functional parameters across the mild, moderate and severe LV systolic impairment groups in a NICM cohort.

3.5.4 Prognostic capacity of right ventricular parameters in non-ischaemic cardiomyopathy

Assessment of RV function is complex due to its anatomy which involves both a longitudinal, radial and anteroposterior component. FAC primarily assesses the radial contraction of the RV and was the only traditional RV parameter found to be associated with our primary outcome on univariate analysis, but this association was not preserved on multivariate analysis. RV-FWS impairment of <14.8%, on the other hand, was associated with our primary outcome as a function of time on univariate analysis and maintained an independent association on multivariate analysis.

RV-FWS is an angle independent measure of longitudinal RV function, which is thought to be the primary contributor to RV systolic function and accounts for approximately 80% of the stroke volume in healthy volunteers. (5) Therefore, amongst 2D measures of RV TTE

parameters, RV-FWS is a superior prognostication tool and can provide additional value to the traditional parameters across the entire spectrum of LV systolic impairment.

3.5.5 Clinical Implications

Our results indicate that RV function declines with worsening LV systolic impairment and that RV-FWS is a sensitive marker in the detection of RV dysfunction with the ability to prognosticate adverse cardiovascular events across a wide range of LV systolic impairment. We have shown that traditional measures of RV systolic function can underestimate the true prevalence of RV dysfunction, whereas RV-FWS can provide a more sensitive assessment. Additionally, a RV-FWS threshold of <14.8% is a strong independent predictor of adverse cardiovascular outcome. The clinical implications of these findings lie in the potential for earlier risk stratification and escalation of HF therapies in NICM to prevent adverse cardiovascular outcomes.

3.5.6 Limitations

The first limitation pertains to our single-centre retrospective cohort study design. Despite being a single centre study, we were still able to accrue a reasonably sized cohort fitting the stringent inclusion and exclusion criterion. The retrospective design would also have limited the standardisation of the HF therapy implemented and the sampling of predictor variables in our study population. However, our study utilised data collected as part of a standardised comprehensive assessment for patients attending our outpatient HF service which implemented optimal guideline directed HF therapy.

The second limitation is the acquisition and analysis of RV-STE. Our study used TTE machines from different vendors and analysed STE using a vendor independent software. This can increase variability compared to vendor-specific software, but our results showed

good intra- and inter observer agreement. Furthermore, RV-STE is not standard clinical practice in most settings and an appropriate RV focused view may not be acquirable in all patients. Thankfully, most patients had adequate visualisation of their RV due to the enhanced imaging quality associated with dilated cardiomyopathies.

Thirdly, assessment of RV function is limited in our study by the constraints of 2D TTE imaging techniques. The RV is a complex three-dimensional (3D) structure and 2D assessments can only assess part of its function. Unfortunately, the feasibility of 3D imaging techniques is poor in this retrospective study.

Finally, our regression model was limited by overfitting and was unable to perform multivariate regression within each LV impairment group. Therefore, the independent association between RV-FWS reduction and our primary outcome can only be confirmed in the overall cohort and not in the individual LVEF impairment subgroups.

3.6.0. Conclusion

In our cohort of stable non-ischaemic cardiomyopathy patients, the prevalence and severity of right ventricular systolic dysfunction, as assessed by two-dimensional echocardiographic parameters, increased progressively with worsening grades of left ventricular systolic impairment. Amongst these right ventricular parameters, a reduction in right ventricular free wall strain below 14.8% independent predicted a higher incidence of cardiovascular death and heart failure hospitalisation.

These findings underscore the prognostic utility of right ventricular free wall strain in identifying patients with biventricular dysfunction who are at elevated risk of adverse cardiovascular outcomes, irrespective of the degree of left ventricular systolic dysfunction.

3.7.0. References

1. Raina A, Meeran T. Right Ventricular Dysfunction and Its Contribution to Morbidity and Mortality in Left Ventricular Heart Failure. Curr Heart Fail Rep. 2018;15(2):94-105.
2. Ghio S, Guazzi M, Scardovi AB, Klersy C, Clemenza F, Carluccio E, et al. Different correlates but similar prognostic implications for right ventricular dysfunction in heart failure patients with reduced or preserved ejection fraction. Eur J Heart Fail. 2017;19(7):873-9.
3. Ghio S, Gavazzi A, Campana C, Inserra C, Klersy C, Sebastiani R, et al. Independent and additive prognostic value of right ventricular systolic function and pulmonary artery pressure in patients with chronic heart failure. J Am Coll Cardiol. 2001;37(1):183-8.
4. Hahn RT, Lerakis S, Delgado V, Addetia K, Burkhoff D, Muraru D, et al. Multimodality Imaging of Right Heart Function: JACC Scientific Statement. J Am Coll Cardiol. 2023;81(19):1954-73.
5. Pueschner A, Chattranukulchai P, Heitner JF, Shah DJ, Hayes B, Rehwald W, et al. The Prevalence, Correlates, and Impact on Cardiac Mortality of Right Ventricular Dysfunction in Nonischemic Cardiomyopathy. JACC Cardiovasc Imaging. 2017;10(10 Pt B):1225-36.
6. Mukherjee M, Rudski LG, Addetia K, Afilalo J, D'Alto M, Freed BH, et al. Guidelines for the Echocardiographic Assessment of the Right Heart in Adults and Special Considerations in Pulmonary Hypertension: Recommendations from the American Society of Echocardiography. J Am Soc Echocardiogr. 2025;38(3):141-86.
7. Anastasiou V, Papazoglou AS, Moysidis DV, Daios S, Tsalikakis D, Giannakoulas G, et al. The prognostic value of right ventricular longitudinal strain in heart failure: a systematic review and meta-analysis. Heart Fail Rev. 2023;28(6):1383-94.
8. Carluccio E, Biagioli P, Lauciello R, Zuchi C, Mengoni A, Bardelli G, et al. Superior Prognostic Value of Right Ventricular Free Wall Compared to Global Longitudinal Strain in Patients With Heart Failure. J Am Soc Echocardiogr. 2019;32(7):836-44 e1.

9. Carluccio E, Biagioli P, Alunni G, Murrone A, Zuchi C, Coiro S, et al. Prognostic Value of Right Ventricular Dysfunction in Heart Failure With Reduced Ejection Fraction: Superiority of Longitudinal Strain Over Tricuspid Annular Plane Systolic Excursion. Circ Cardiovasc Imaging. 2018;11(1):e006894.
10. Houard L, Benaets MB, de Meester de Ravenstein C, Rousseau MF, Ahn SA, Amzulescu MS, et al. Additional Prognostic Value of 2D Right Ventricular Speckle-Tracking Strain for Prediction of Survival in Heart Failure and Reduced Ejection Fraction: A Comparative Study With Cardiac Magnetic Resonance. JACC Cardiovasc Imaging. 2019;12(12):2373-85.
11. Lang RM, Badano LP, Mor-Avi V, Afilalo J, Armstrong A, Ernande L, et al. Recommendations for cardiac chamber quantification by echocardiography in adults: an update from the American Society of Echocardiography and the European Association of Cardiovascular Imaging. J Am Soc Echocardiogr. 2015;28(1):1-39 e14.
12. Badano LP, Kolias TJ, Muraru D, Abraham TP, Aurigemma G, Edvardsen T, et al. Standardization of left atrial, right ventricular, and right atrial deformation imaging using two-dimensional speckle tracking echocardiography: a consensus document of the EACVI/ASE/Industry Task Force to standardize deformation imaging. Eur Heart J Cardiovasc Imaging. 2018;19(6):591-600.
13. Nagueh SF, Smiseth OA, Appleton CP, Byrd BF, 3rd, Dokainish H, Edvardsen T, et al. Recommendations for the Evaluation of Left Ventricular Diastolic Function by Echocardiography: An Update from the American Society of Echocardiography and the European Association of Cardiovascular Imaging. J Am Soc Echocardiogr. 2016;29(4):277-314.
14. Rudski LG, Fine NM. Right Ventricular Function in Heart Failure: The Long and Short of Free Wall Motion Versus Deformation Imaging. Circ Cardiovasc Imaging. 2018;11(1):e007396.
15. Addetia K, Miyoshi T, Citro R, Daimon M, Gutierrez Fajardo P, Kasliwal RR, et al. Two-Dimensional Echocardiographic Right Ventricular Size and Systolic Function

Measurements Stratified by Sex, Age, and Ethnicity: Results of the World Alliance of Societies of Echocardiography Study. J Am Soc Echocardiogr. 2021;34(11):1148-57 e1.

16. Ishiwata J, Daimon M, Nakanishi K, Sugimoto T, Kawata T, Shinozaki T, et al. Combined evaluation of right ventricular function using echocardiography in non-ischaemic dilated cardiomyopathy. ESC Heart Fail. 2021;8(5):3947-56.

17. Lundorff IJ, Sengelov M, Pedersen S, Modin D, Bruun NE, Fritz-Hansen T, et al. Prognostic value of right ventricular echocardiographic measures in patients with heart failure with reduced ejection fraction. J Clin Ultrasound. 2021;49(9):903-13.

18. Sade LE, Ozin B, Atar I, Demir O, Demirtas S, Muderrisoglu H. Right ventricular function is a determinant of long-term survival after cardiac resynchronization therapy. J Am Soc Echocardiogr. 2013;26(7):706-13.

19. Motoki H, Borowski AG, Shrestha K, Hu B, Kusunose K, Troughton RW, et al. Right ventricular global longitudinal strain provides prognostic value incremental to left ventricular ejection fraction in patients with heart failure. J Am Soc Echocardiogr. 2014;27(7):726-32.

20. Edward J, Banchs J, Parker H, Cornwell W. Right ventricular function across the spectrum of health and disease. Heart. 2023;109(5):349-55.

21. Iglesias-Garriz I, Olalla-Gomez C, Garrote C, Lopez-Benito M, Martin J, Alonso D, et al. Contribution of right ventricular dysfunction to heart failure mortality: a meta-analysis. Rev Cardiovasc Med. 2012;13(2-3):e62-9.

22. Surkova E, Kovacs A, Tokodi M, Lakatos BK, Merkely B, Muraru D, et al. Contraction Patterns of the Right Ventricle Associated with Different Degrees of Left Ventricular Systolic Dysfunction. Circ Cardiovasc Imaging. 2021;14(10):e012774.

CHAPTER FOUR

Impact of elevated body mass index on right ventricular systolic function

4.0. Abstract

Background: Obesity has been linked with alterations in hemodynamic, autonomic, and hormonal pathways in the body, leading to a spectrum of cardiovascular changes. We sought to evaluate the effects of obesity on structural and functional changes of the cardiac chambers, particularly the right ventricle, in the absence of cardiac disease and associated risk factors.

Methods: We identified asymptomatic outpatients without any cardiovascular disease or risk factors from our institution's echocardiography database (2017-2020). Patients were stratified by body mass index (BMI; normal: 18.5-25kg/m^2; overweight: 25-30 kg/m^2; class 1 obesity: 30-35 kg/m^2; class 2 obesity: 35-40 kg/m^2; class 3 obesity: >40 kg/m^2). Traditional and advanced echocardiographic parameters of cardiac chamber size and function including left ventricular global longitudinal strain (LV-GLS), left atrial reservoir strain (LASr), and right ventricular free wall strain (RV-FWS) were examined. The optimal cutoff BMI for discriminating LV-GLS (<17.5%), LASr (<23%), and RV-FWS (<23%) impairment was calculated using ROC curves.

Results: 307-patients were assessed (41.5±13.3yrs; 36.5%male; LVEF 61.3±4.8%). No significant differences in indexed chamber volumes or LVEF were appreciated across BMI groups ($p>0.05$ for all). LV-GLS, LASr, and RV-FWS were all significant on one-way ANOVA for differences from the group mean (all $p<0.01$). Jonckheere-Terpstra test confirmed a significant trend of lower absolute LV-GLS, LASr and RV-FWS values across the rising BMI groups. On ROC curve analysis, a BMI value of 29.9 kg/m^2, 35.1 kg/m^2, and 37.3kg/m^2 were associated with LASr (AUC: 0.75), RV-FWS (AUC: 0.72), and LV-GLS (AUC: 0.75) impairment respectively.

Conclusion: Obesity is linked with subclinical reduction of cardiac function in otherwise healthy subjects without cardiovascular risk factors, with reduction of left atrial function occurring at lower BMI, followed by the right and left ventricular function.

Graphical Abstract 4

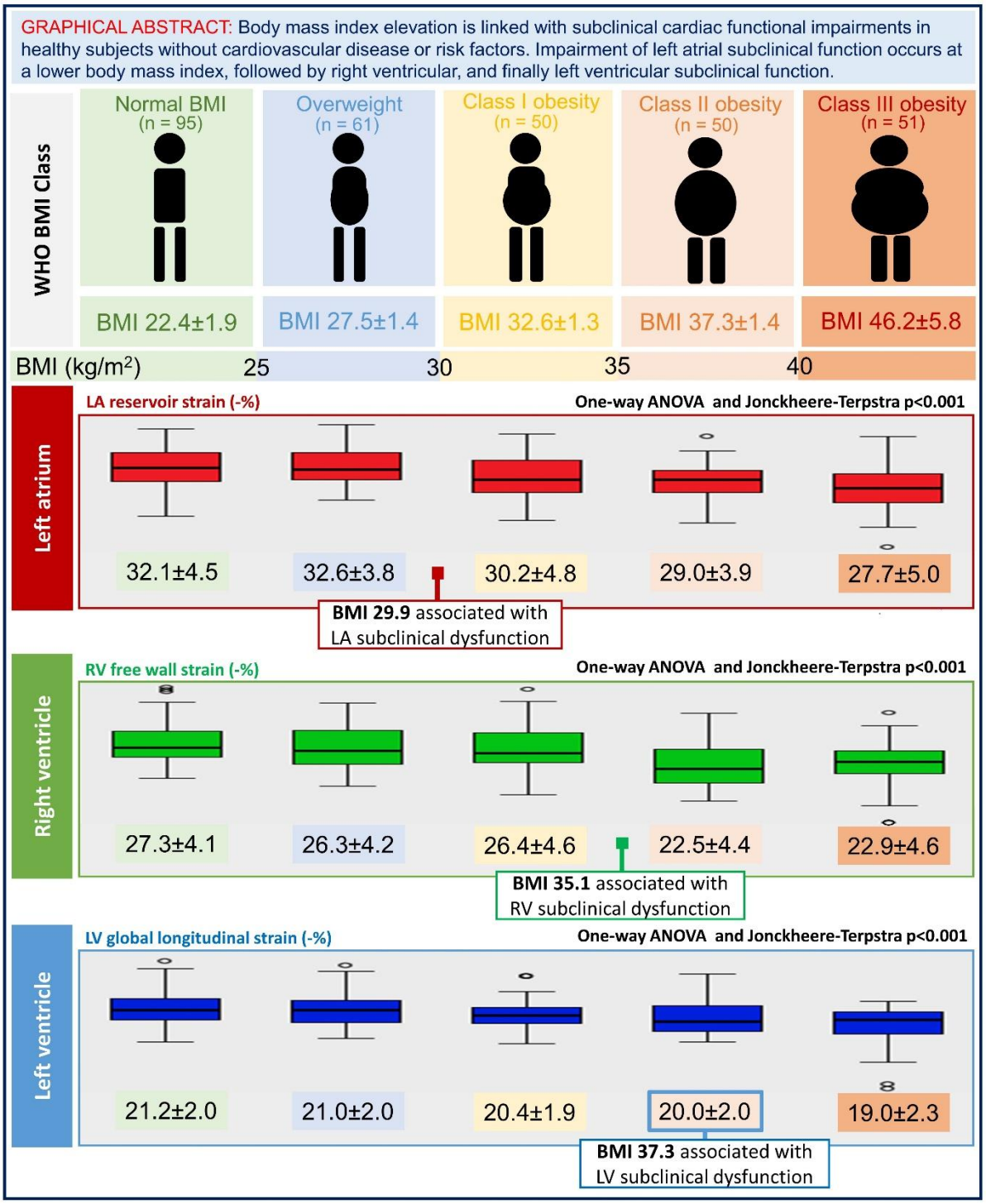

Keywords: Obesity; Echocardiography; Global longitudinal strain; Body mass index; Heart failure

Abbreviations:

LV = Left ventricle

GLS = Global longitudinal strain

LA = Left atrium

RV = Right ventricle

BMI = Body mass index

LV-GLS = Left ventricular global longitudinal strain

LASr = Left atrial reservoir strain

RV-FWS = Right ventricular free wall strain

LVEF = Left ventricular ejection fraction

BSA = Body surface area

ROC = receiver operating characteristics

HbA1c = haemoglobin A1c

FAC = fractional area change

RVS' = tissue Doppler-derived tricuspid lateral annulus systolic velocity

4.1.0 Introduction

Obesity represents a contemporary public health crisis in Western society, affecting 39.6% of adults and 18.5% of children and adolescents in the United States. (1) This sobering statistic is compounded by its health effects, namely an increase in chronic disease, including cardiovascular disease, hypertension, diabetes mellitus, and malignancy. (2) Much of the deleterious health effects of obesity have been attributed to the development of associated cardio-metabolic risk factors, however obesity has been independently associated with a poor prognosis. It has been attributed as the causative aetiology for one in five deaths and carries a significant economic burden, approximating $147 billion in healthcare spending in 2008. (3, 4)

Obesity has been linked to alterations in hemodynamic, autonomic, and hormonal pathways in the body, leading to a spectrum of cardiovascular changes, from subclinical structural cardiac alterations to development of clinical cardiac failure. Much of these changes are caused by alterations in myocardial load dynamics and by coexistent disease states such as hypertension, diabetes mellitus, obstructive sleep apnoea, and ischemic heart disease. (5) Although recent studies have examined the effect of obesity on metabolically healthy patients and found an association with elevated body mass index and subclinical cardiac impairment, there is a paucity of information on cardiac function in obese patients without both cardiac and metabolic risk factors. (6, 7) Patients with obesity without both cardiac and metabolic risk factors are scarce and would serve to illustrate the natural history of the disease process and its effects on the cardiac chambers in isolation.

Current advanced echocardiographic techniques provide a more sensitive method of detecting functional changes. Two-dimensional myocardial deformation indices utilising speckle tracking echocardiography allow for detection of subclinical changes in myocardial function not reflected by conventional measures of cardiac function such as ejection fraction. Its prognostic value has been validated in many populations including coronary disease, cardiomyopathies, chemotherapy cardiotoxicity, cardiac resynchronisation therapy, and in valvular disease. (8)

Previous studies have demonstrated that obesity is associated with impairment in left ventricular (LV) and left atrial (LA) indices including longitudinal strain. (6, 7) However, the impact of obesity on right ventricular (RV) function has not been as well characterised.

4.2.0 Objective and Aims

We aim to evaluate the effects of body mass index (BMI) on structural and functional changes of the LV, LA, and particularly RV in the absence of any cardiac disease and associated risk factors, and to evaluate the stage at which body mass index elevation would begin to affect cardiac structure and function.

4.3.0 Materials and Methods

4.3.1 Study population

We retrospectively identified consecutive asymptomatic adults ≥18 years of age, who attended our institution's outpatient echocardiography service between the 1st of January 2017 to 31st of December 2020 with normal LV systolic and diastolic function. A rigorous inclusion criterion was applied to ensure that only patients with no documented or reported history of any cardiovascular disease or associated risk factors, such as hypertension, diabetes mellitus, hyperlipidaemia, ischemic or structural heart disease, arrhythmias, pulmonary disease, obstructive sleep apnoea, malignancies, and systemic inflammatory or chronic conditions including chronic liver disease were included. We excluded patients who were pregnant, trained athletes, those with a history of excessive alcohol intake (≥8 standard drinks per week) or those who were on cardioactive drug treatment. As these may potentially confound echocardiographic assessments of cardiac structure and function.

A rigorous examination of the hospital electronic medical records, medication history, blood pressure recordings and HbA1c level of each of the included patients was also undertaken to

ensure that there was no recent or remote history of any potential conditions which may potentially confound the echocardiographic parameters and excluded any patient which did not meet inclusion criteria or had incomplete data. Patients with inadequate echocardiographic image quality for analysis were also excluded. (Figure 1)

Eligible patients were grouped based on body mass index (BMI) using the World Health Organisation classification: normal (BMI 18.5 to 24.9 kg/m^2), overweight (BMI 25 to 29.9 kg/m^2), class 1 obesity (BMI 30 to 34.9 kg/m^2), class 2 obesity (BMI 35 to 39.9 kg/m^2) and class 3 obesity (BMI ≥40 kg/m^2).

The study protocol was approved by the Western Sydney Local Health District Human Research Ethics Committee in compliance with the Declaration of Helsinki.

4.3.2 Transthoracic echocardiography

Transthoracic echocardiography was performed using Philips EPIQ (Philips, Andover MA, USA) as well as GE E9 and GE E95 (Boston, Massachusetts, USA) devices in accordance with established clinical practice and measurements in keeping with the American Society of Echocardiography recommendations. (9) In brief, LV volume and ejection fraction were calculated using modified Simpson's biplane method. LA volume was measured at end systole utilizing the 2- and 4-chamber views using the biplane method of discs.

Pulse-wave Doppler was performed in the apical 4-chamber view to measure mitral inflow velocities for the assessment of LV filling. These measurements included mitral inflow peak early filling (E-wave) and late diastolic filling (A-wave) velocities, the E/A ratio, deceleration time of early filling velocity, and the isovolemic relaxation time. Utilising pulse-wave tissue Doppler imaging in the apical views, mitral annular velocities were obtained, and derived variables included: peak velocity of early (E) and late (A) filling, deceleration time of the E wave velocity and atrial filling fraction. E/e' and lateral e' were subsequently calculated.

4.3.3 Speckle-tracking echocardiography

Two-dimensional global longitudinal strain analysis was performed offline using vendor independent computer software (TomTech Image Arena Systems v2.3, Germany). Measurements were performed by two independent investigators blinded to patient demographics, clinical and echocardiographic data. All reported parameters were a mean of measurements from three cardiac cycles.

Briefly, LV longitudinal strain was assessed by tracing the LV endocardium at end systole. LV global longitudinal strain was then calculated as the average of the 18-segments obtained across the three standard apical views. For LA longitudinal strain, the LA endocardium was manually traced in the apical 2- and 4-chamber views at end-systole. LA reservoir strain (LASr) was measured as the peak strain value at the end of the reservoir phase. Right ventricular strain was evaluated by tracing the RV endocardium in the RV-focused apical view at end-systole. We analysed RV free wall strain which was derived from the average peak systolic strain of the 3 RV free wall segments. The automated software tracked the movement of the LV, LA and RV myocardium throughout the cardiac cycle using R to R gating.

Quantitation of inter- and intra-observer variability of longitudinal strain parameters (LV-GLS, LASr and RV-FWS) was performed in 20% of the population through repeat measurements by a second independent investigator and the original investigator at least one month later. Reproducibility of these measurements were represented by the intra-class correlation coefficient and coefficient of variation.

4.3.4 Statistical analysis

All statistical analysis was performed using the Statistical Package for Social Sciences software (SPSS Version 22; SPSS Inc., Chicago, IL, USA). Continuous variables were presented as mean ± standard deviations and compared using Student's unpaired and paired

t-test as appropriate. Categorical variables were expressed as numbers and percentages and compared using Chi-square testing. All tests were 2-tailed with a p value less than 0.05 considered statistically significant. One-way ANOVA was used to assess the associations of all clinical and echocardiographic parameters with BMI class. Post hoc analysis with Tukey-HSD was performed for the advanced echocardiographic parameters found to be significant on one-way ANOVA if assumption of equal variance can be confirmed on Welch test. Jonckheere-Terpstra test for ordered alternatives was performed to confirm the trend of advanced echocardiographic parameters across the rising BMI groups

To evaluate whether the degree of BMI elevation can discriminate cardiac chamber dysfunction and dilatation, we computed receiver operating characteristic (ROC) curves of BMI values against the strain parameters found to be significantly different from the group mean on one-way ANOVA analysis. The optimal cutoff values were selected using Youden index method. Impairment of LV-GLS, LASr, and RV-FWS was defined as <17.5%, <26%, and <23% respectively based on previously published normal values. (10-12)

4.4.0 Results

4.4.1 Participant characteristics

We screened 7,481 echocardiographic studies during the study period, of which 1,477 were individual outpatient studies without metabolic or cardiovascular disease. These studies consisted mainly of hospital staff undergoing health checks, incidental murmurs for investigation and low risk troponin negative chest pains referred for outpatient assessment. From this cohort, we identified 338 healthy individuals who were eligible for inclusion into our study. Of this number, 31 patients were excluded due to inadequate image quality for strain analysis, with 3 patients (3.2%) in the normal, 5 (8.2%) in the overweight, 6 (12%) in the class I obesity, 6 (12%) in the class II obesity, and 11 (21.6%) in the class III obesity groups. (Figure 4.1)

The final 307 included patients were separated into 5 groups based on their BMI: normal (BMI 18.5 to 24.9 kg/m^2, n=95) overweight (BMI 25 to 29.9 kg/m^2, n=61), class 1 obesity (BMI 30 to 34.9 kg/m^2, n=50), class 2 obesity (BMI 35 to 39.9 kg/m^2, n=50) and class 3 obesity (BMI ≥40 kg/m^2, n=51).

The mean age of the entire cohort was 41.5±13.3 years, of which 36.5% were males. Age was not significantly different from the group mean on one-way ANOVA analysis across the BMI groups (p=0.124), but gender was (p=0.002). Class 3 obesity group was predominantly female with only 11.8% male. BMI was significantly different from the group mean on ANOVA by design (p<0.01). (Table 4.1)

There was a significant increase in haemoglobin A1c (HbA1c) level, systolic and diastolic blood pressures across the five groups (p=0.03; <0.01; 0.03 respective), although all blood pressure and HbA1c values remained within the normotensive and non-diabetic range. (Table 4.1)

Figure 4.1. Consort diagram

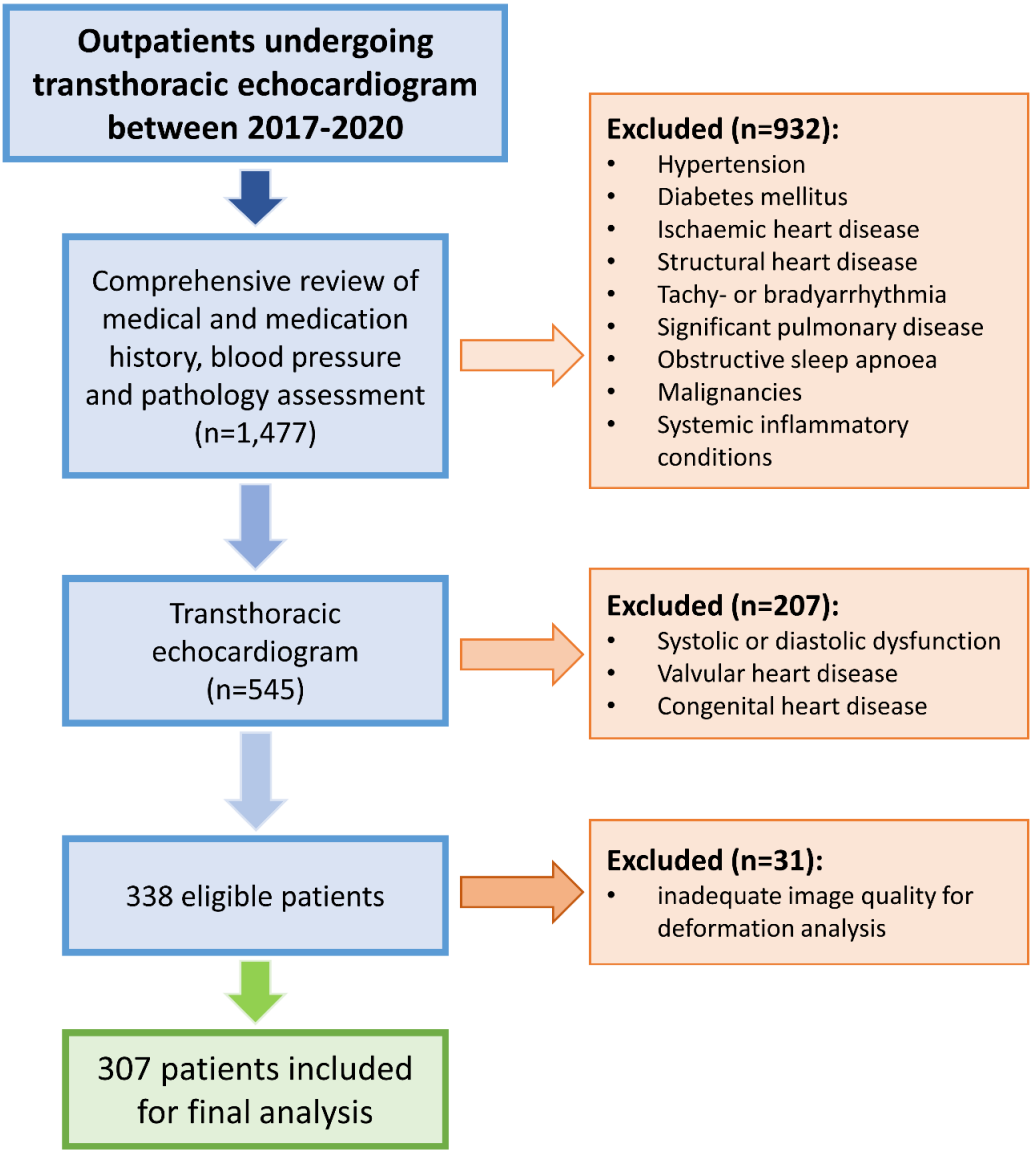

Figure 4.1. 1,477 outpatient transthoracic echocardiogram were performed during the study period. 912 patients were excluded due to cardiovascular disease or risk factors. A further 207 patients were excluded due to structural heart disease including diastolic dysfunction. Finally, 51 patients did not have adequate imaging quality for deformation analysis of all three chambers. 307 patients were included for the final analysis.

Table 4.1 Baseline clinical characteristics across the body mass index groups

Patient baseline characteristics						
	Normal Weight (n=95)	**Over-Weight** (n=61)	**Class 1 Obesity** (n=50)	**Class 2 Obesity** (n=50)	**Class 3 Obesity** (n=51)	One-way ANOVA (p-value)
Age (yrs)	42.2±14.8	41.8±12.4	44.6±13.1	41.2±12.6	37.7±11.5	0.124
Male n (%)	39 (41.1)	27 (44.3)	19 (38)	21 (42)	6 (11.8)	0.002
Height (cm)	167±0.9	167±1.2	166±1.0	167±1.1	166±0.9	0.944
Weight (kg)	62.4±8.0	76.8±9.7	89.8±11.7	104.4±14.6	127.4±23.4	<0.001
BMI (kg/m^2)	22.4±1.9	27.5±1.4	32.6±1.3	37.3±1.48	46.2±5.8	<0.01
HR (bpm)	74.4±13.4	75.6±14.8	72.4±14.4	72.3±10.9	75.6±11.3	0.530
SBP (mmHg)	114.5±12.0	117.2±8.9	118.2±9.7	123.5±12.0	122.9±13.0	<0.001
DBP (mmHg)	72.6±8.9	74.1±9.0	74.9±8.8	76.9±8.8	76.7±10.2	0.030
HbA1c (%)	5.5±0.4	5.4±0.3	5.6±0.4	5.6±0.5	5.7±0.5	0.031

Table 4.1. Illustrates the baseline demographics, anthropometry and haemodynamic readings across the 5 body mass index groups.

Abbreviations. *BMI: body mass index, HR: heart rate (at time of echocardiography), SBP: systolic blood pressure (at time of echocardiography), DBP: diastolic blood pressure (at time of echocardiography), HbA1c: glycated haemoglobin A1c.*

4.4.2 Echocardiographic parameters across body mass index classes

One-way ANOVA analysis was performed on echocardiographic parameters across the five BMI groups. Unsurprisingly, all non-indexed measures of chamber dimension were significant on one-way ANOVA for differences from the group mean. Similarly, LV mass, LV end diastolic volume, LV end systolic volume and LA volume were also significant on allometric indexation using height, height to the power of 1.7 and of 2.7. All echocardiographic measures indexed to body surface area (BSA), on the other hand, were not significant. LV hypertrophy based on BSA indexed LV mass (≥115 g/m^2 for males, ≥95g/m^2 for females) was not significant across the BMI groups on one-way ANOVA analysis for the measure present in 3 (3%) patients in the normal, 1 (2%) patient in the overweight, 4 (8%) patients in the class 1 obesity, 5 (10%) patients in the class 2 obesity, and 4 (8%) in the class 3 obesity groups. (Table 4.2)

In terms of functional parameters, the conventional measure of left ventricular systolic function - left ventricular ejection fraction - was not significant across the BMI groups (p=0.659). Of the diastolic functional parameters, average peak mitral e' velocity (e') and E/e' ratio were the only parameters significant on one-way ANOVA for differences from the group mean. As the BMI rose across the groups, average e' value reduced while the E/e' ratio increased.

The two-dimensional measure of RV systolic function - fractional area change (FAC) - was also significant on one-way ANOVA for differences from the group mean (p=0.001), with the higher BMI groups having lower FAC. Both measures of right ventricular longitudinal function - tricuspid annulus S' velocity (RVS') and tricuspid annular plane systolic excursion - were not significant.

Deformation imaging parameters of LV-GLS, LASr and RV-FWS were all significant from the group mean on one-way ANOVA analysis (all p<0.001). All three of the advanced measures were significantly lower in the higher BMI groups. (Table 4.2)

Table 4.2 Baseline echocardiographic parameters across the body mass index groups

	Normal Weight (n=95)	**Over-Weight** (n=61)	**Class 1 Obesity** (n=50)	**Class 2 Obesity** (n=50)	**Class 3 Obesity** (n=51)	One-way ANOVA (p-value)
Left ventricular parameters						
LVIDd (mm)	43.7±4.9	44.8±5.6	46.0±5.9	47.1±5.1	49.0±5.6	<0.001
LVIDs (mm)	28.5±4.2	28.9±4.3	29.5±4.5	30.2±4.6	31.7±4.5	0.001
IVSd (mm)	8.5±1.4	8.9±1.8	9.4±2.2	9.5±2.0	9.7±1.9	0.001
PWd (mm)	8.5±2.7	8.6±1.7	9.2±3.3	9.4±2.1	10.0±1.9	0.005
RWT	0.39±0.1	0.40±0.1	0.43±0.2	0.41±0.1	0.41±0.1	0.171
LV mass (g)	118.7±28.5	135.7±42.1	155.9±42.0	166.2±49.8	183.0±59.4	<0.001
LV mass / $Ht^{2.7}$ (g/m^2)	29.8±6.5	33.5±7.4	40.0±11.5	41.6±12.0	46.3±11.3	<0.001
LV mass / BSA (g/m^2)	69.7±15.0	71.8±18.9	76.9±20.7	75.4±20.3	75.5±20.2	0.129
LV hypertrophy (n, %)	3 (3%)	1 (2%)	4 (8%)	5 (10%)	4 (8%)	0.254
MV inflow E velocity (m/s)	0.77±0.16	0.76±0.16	0.77±0.15	0.79±0.19	0.81±0.21	0.499
MV inflow A velocity (m/s)	0.59±0.16	0.60±0.16	0.62±0.14	0.61±0.16	0.64±0.16	0.365
E/A	1.4±0.5	1.4±0.5	1.3±0.4	1.4±0.5	1.3±0.5	0.644
Average e' (cm/s)	11.4±2.8	11.2±3.3	10.2±2.4	10.2±2.6	10.1±2.9	0.021
E/e'	7.1±1.9	7.2±2.3	7.8±1.9	8.2±2.4	8.9±5.9	0.013
Biplane LVEF (%)	61.8±5.1	61.0±5.0	61.6±3.5	60.7±4.4	61.0±5.4	0.659
LVED volume (ml)	83.2±24.7	86.1±25.4	94.9±30.0	100.3±29.9	114.1±33.6	<0.001
LVED vol / $Ht^{2.7}$ (ml/m^2)	20.9±5.4	22.0±5.0	24.1±6.5	25.3±7.5	29.1±7.6	<0.001
LVED vol / BSA (ml/m^2)	48.5±13.2	45.3±11.6	46.5±13.1	45.6±13.0	47.2±12.7	0.551
LVES volume (ml)	32.2±11.8	34.8±11.9	36.7±12.7	39.4±13.1	45.2±16.7	<0.001
LVES vol / $Ht^{2.7}$ (ml/m^2)	8.1±2.6	8.6±2.4	9.3±2.8	9.9±3.2	11.5±3.7	<0.001
LVES vol / BSA (ml/m^2)	18.9±6.4	18.3±5.4	18.0±5.6	18.0±5.7	19.2±8.0	0.757
LV-GLS (-%)	21.2±2.0	21.0±2.0	20.4±1.9	20.0±2.0	19.0±2.3	<0.001
Left atrial parameters						
LA volume (ml)	42.1±12.2	45.0±11.0	46.6±13.4	52.8±16.0	54.31±15.6	<0.001
LA volume / $Ht^{2.7}$ (ml/m^2)	11.4±3.4	11.7±3.0	13.1±4.2	15.1±6.5	15.9±4.8	<0.001
LA volume / BSA (ml/m^2)	24.9±7.2	23.9±5.5	22.9±6.4	24.0±6.7	22.8±7.4	0.377
LASr (-%)	32.1±4.5	32.6±3.8	30.2±4.8	29.0±3.9	27.7±5.0	<0.001
Right ventricular parameters						
RV basal dimension (cm)	3.2±0.5	3.2±0.6	3.2±0.5	3.4±0.5	3.5±0.5	0.004
TAPSE (cm)	2.4±0.5	2.4±0.4	2.4±0.5	2.4±0.5	2.4±0.4	0.828
RV S' velocity (m/s)	12.3±2.5	12.1±1.8	12.7±2.6	12.2±2.1	12.6±2.7	0.729
RVSP (mmHg)	18.7±8.3	17.4±7.5	18.3±11.8	20.2±7.8	19.1±10.0	0.711
RV end diastolic area (cm^2)	14.1±3.8	15.0±4.6	14.1±4.3	14.2±3.4	15.5±5.2	0.261
RV end systolic area (cm^2)	7.3±2.1	7.9±2.9	7.6±2.7	7.8±2.2	8.8±3.4	0.023
RV-FAC (%)	48.4±6.9	47.8±6.6	46.3±6.6	45.1±6.4	43.9±7.5	0.001
RV-FWS (-%)	27.3±4.1	26.3±4.2	26.4±4.6	22.5±4.4	22.9±4.6	<0.001

Table 4.2. Between group analysis of the echocardiographic parameters using one-way ANOVA across the body mass index groups.

Abbreviations. *BMI: body mass index, HR: heart rate, SBP: systolic blood pressure, DBP: diastolic blood pressure, bpm: beats per minute, HbA1c: glycated hemoglobin A1c, LVIDd: left ventricular internal diameter end diastole, LVIDs: left ventricular internal diameter end systole, IVSd: interventricular septum thickness end diastole, PWd: posterior wall thickness end diastole, RWT: relative wall thickness, LV: left ventricular, LA: left atrial, MV: mitral valve, LVEF: left ventricular ejection fraction, LVED: left ventricular end diastolic, LVES: left ventricular end systolic, RV: right ventricular, RVSP: right ventricular systolic pressure, RV-FAC: right ventricular fractional area change, LV-GLS: left ventricular global longitudinal strain, LASr: left atrial reservoir strain, RV-FWS: right ventricular free wall strain.*

4.4.3 Subclinical myocardial function across the body mass index classes

On post hoc analysis of the advanced echocardiographic parameters using Tukey HSD, LV-GLS was not significantly different between any adjacent BMI groups, but significantly lower in the class 3 obesity group compared to the class 1 obesity group ($p=0.01$). There was a significant reduction of LASr in the class 1 obesity group compared to the preceding overweight group ($p=0.04$). RV-FWS demonstrated a significant reduction going from class 1 obesity to the adjacent class 2 obesity group ($p<0.01$).

A Jonckheere-Terpstra test for ordered alternatives confirmed that there was a statistically significant trend of lower absolute LV-GLS, LASr and RV-FWS values with higher BMI class (from normal, overweight, class 1, class 2 to class 3 obesity groups; all $P>0.001$). (Figure 4.2)

Figure 4.2. Trends of advanced echocardiographic parameters across the BMI groups on Jonckheere-Terpstra test

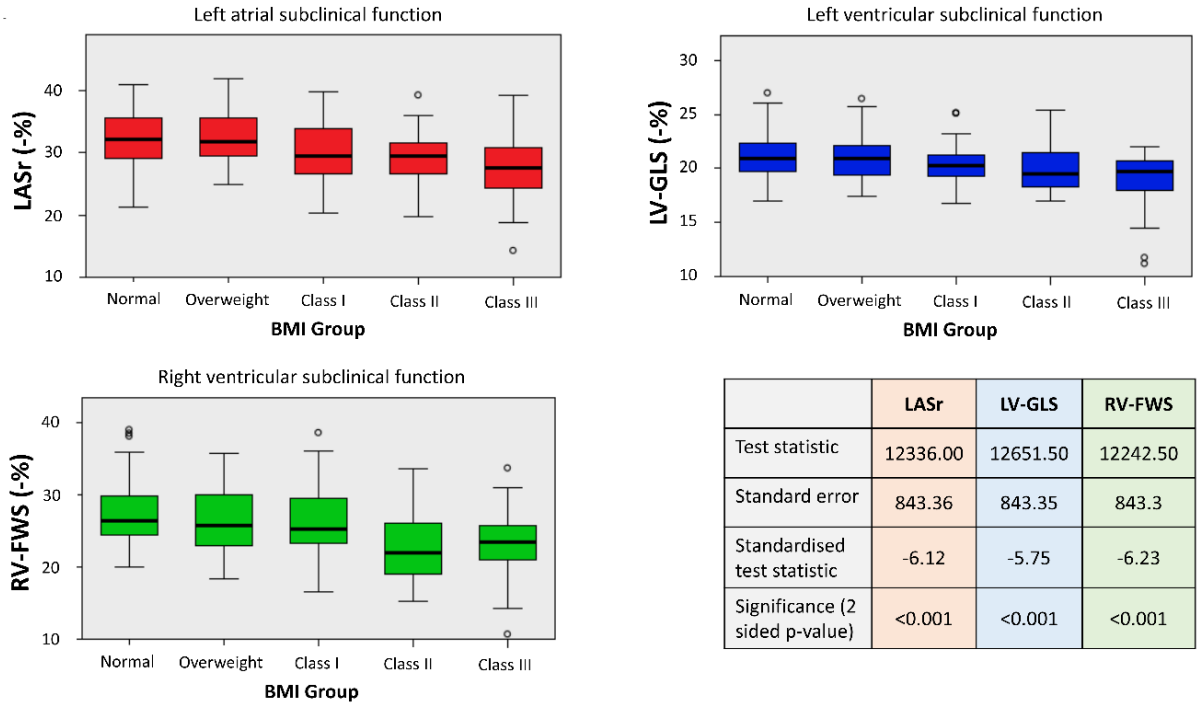

	LASr	LV-GLS	RV-FWS
Test statistic	12336.00	12651.50	12242.50
Standard error	843.36	843.35	843.3
Standardised test statistic	-6.12	-5.75	-6.23
Significance (2 sided p-value)	<0.001	<0.001	<0.001

Figure 4.2. Jonckheere-Terpstra test confirms a significant drop in the absolute strain values of the three measured cardiac chambers across the rising BMI groups. Box plots of the median and interquartile values are displayed for left atrial reservoir strain, left ventricular global longitudinal strain and right ventricular free wall strain.

Abbreviations. *LASr: left atrial reservoir strain, LV-GLS: left ventricular global longitudinal strain, RV-FWS: right ventricular free wall strain.*

4.4.4 Prevalence of subclinical myocardial dysfunction by body mass index class

We tabulated the prevalence of subclinical myocardial dysfunction in each of the BMI groups. An incremental increase in the prevalence of subclinical myocardial dysfunction was seen in all three cardiac chambers as the BMI increased. The overall prevalence of LV-GLS impairment was lowest at 7.3%, ranging from 2.1% to 21.6%. LASr impairment followed with an average prevalence of 16.7%, ranging from 3.2% to 35.3%. RVFWS impairment was the most common at 39.5% across the cohort, ranging from 7.4% to 56.9%.

4.4.5 Predictor of cardiac chamber subclinical dysfunction

We utilised ROC curves to find the optimal BMI cutoff values associated with cardiac chamber subclinical dysfunction.

The optimal BMI cutoff value associated with LASr impairment was the lowest at 29.9 kg/m^2 (sensitivity 86%, specificity 57%). This was followed by RV-FWS which had a BMI cutoff of 35.1 kg/m^2 (sensitivity 58%, specificity 79%). The highest BMI cutoff value was for LV-GLS impairment, at 37.3 kg/m^2 (sensitivity 67%, specificity 79%). (Figure 4.3)

Figure 4.3. Body mass index cutoff values which best discriminate subclinical cardiac chamber dysfunction

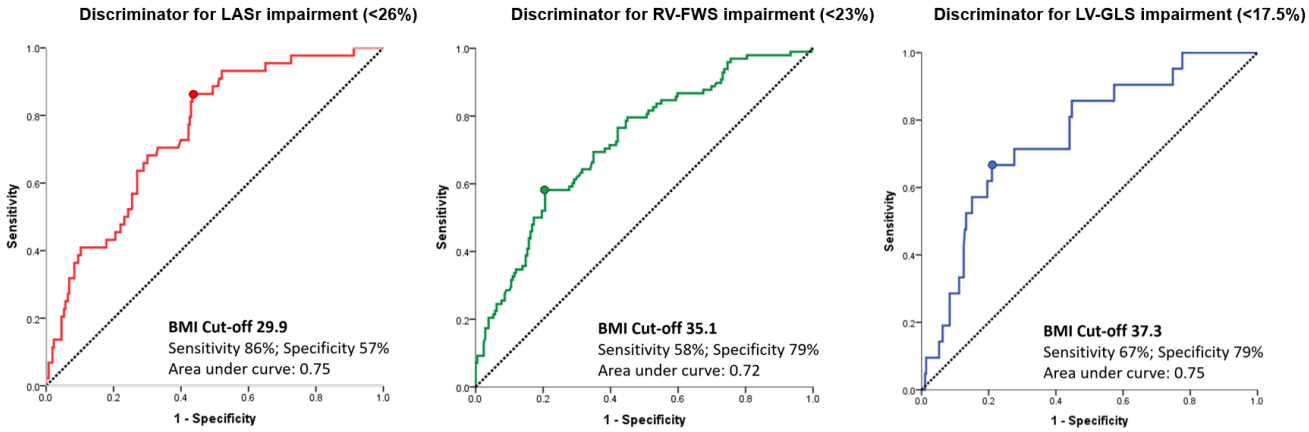

Figure 4.3. Receiver operating characteristic curves found that a BMI of ≥29.9 predicts left atrial reservoir strain impairment (LASr<26%), a BMI of ≥35.1 predicted right ventricular free wall strain impairment (RV-FWS<23%), and a BMI of ≥37.3 predicted left ventricular global longitudinal strain impairment (LV-GLS<17.5%).

Abbreviations. *BMI: Body mass index; LASr: left atrial reservoir strain, LV-GLS: left ventricular global longitudinal strain, RV-FWS: right ventricular free wall strain.*

4.4.6 Single versus multi-chamber subclinical dysfunction

We further sought to identify the best BMI cutoffs for discriminating single versus multi-chamber longitudinal strain impairment utilising ROC curve analysis. Single-chamber strain impairment was defined as longitudinal strain impairment in one or more of the cardiac chambers assessed, while multi-chamber strain impairment refers to strain impairment in at least two cardiac chambers.

A BMI cutoff of 29.2 kg/m^2 was found to be associated with single-chamber impairment with a sensitivity of 78% and specificity of 65%. For multi-chamber impairment, a BMI cutoff of 35.1 kg/m^2 was ideal with a sensitivity of 84% and specificity of 74%. (Figure 4.4)

Figure 4.4. Receiver operating characteristics curve for discriminating single and multi-chamber subclinical dysfunction.

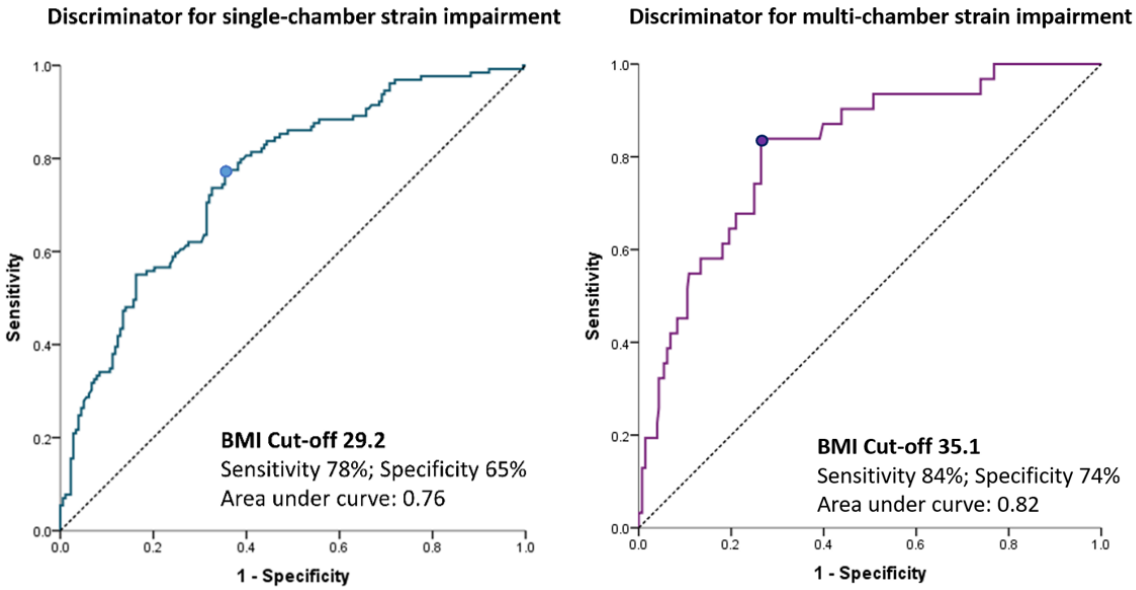

Figure 4.4. Receiver operating characteristic curves demonstrated that single chamber subclinical dysfunction is best discriminated as the BMI approaches obesity (BMI≥29.2), while subclinical dysfunction in two or more cardiac chambers was best discriminated by BMI of ≥35.1 (class II obesity).

Abbreviations. *BMI: Body mass index*

4.4.7 Reproducibility analysis

There was good reproducibility of the strain parameters based on the inter- and intra-observer variability. For inter-observer variability, the intra-class correlation coefficient and the coefficient of variation were 0.90 (95% CI 0.72-0.97) and 3.5% (95% CI 2.9-4.0) for LV-GLS, 0.86 (95% CI 0.75 to 0.92) and 4.8% (95% CI 4.0-5.6) for LASr, 0.95 (95% CI 0.74-0.99) and 4.3% (95% CI 3.6-5.0) for RV-FWS. For intra-observer variability, the intra-class correlation coefficient and the coefficient of variation were 0.93 (95% CI 0.74-0.98) and 2.8% (95% CI 2.4-3.3) for LV-GLS, 0.95 (95% CI 0.81 to 0.99 and 2.9% (95% CI 2.4-3.4) for LASr, 0.97 (95% CI 0.81-0.99) and 2.9% (95% CI 2.5-3.4) for RV-FWS.

4.5.0 Discussion

In this retrospective study of otherwise 'healthy' asymptomatic patients undergoing transthoracic echocardiography, we found an association between increasing BMI and subclinical cardiac dysfunction independent of loading conditions, cardiovascular disease and risk factors. Our findings suggest the degree of BMI elevation is associated with incremental risk of subclinical myocardial dysfunction.

To our knowledge this is the first echocardiographic study that examined subclinical cardiac dysfunction of the LV, LA and RV in the absence of cardiovascular diseases and risk factors. Additionally, the use of stratified BMI groups allowed us to demonstrate the incremental changes with the step wise increase in BMI.

4.5.1 Indexation of cardiac volumes in obesity

Current echocardiographic guidelines recommend indexation of values based on body surface area (BSA). (9) However, accurate adjustment of echocardiographic measurements has been an ongoing challenge in obesity. (13) It is believed that BSA indexation of LV mass and LA volume in obese patients lead to an under recognition of LV hypertrophy and LA dilatation. (14)

Our study showed that non-indexed LV mass, LV and LA volumes are significantly higher with rising BMI groups as expected. After indexing to BSA, these values did not change despite the degree of BMI elevation. These results support the idea that isometric indexation of echocardiographic parameters using BSA may not be as sensitive in detecting structural and functional changes in higher grades of obesity. Allometric indexation using height, height to the power of 1.7 and 2.7 in contrast, may be more suitable to correct for body size in patients with higher BMI. However, allometric indexation can then over- and under-estimate LV mass in shorter and taller patients respectively. (14, 15)

4.5.2 Isolated effect of obesity on subclinical myocardial function

Other similar studies have included cardiac conditions and cardiovascular risk factors which may potentially impact on the echocardiographic measurements obtained,[7,8] which is why we have implemented this stringent selection criteria. Our results have confirmed the effect of BMI on cardiac structure and function in the normotensive 'healthy' obese population.

Due to the strict inclusion criterion, the class 3 obesity cohort in our study was predominantly female with a trend towards younger age. We hypothesise this gender inequality in the highest BMI group is due to age and male gender both being associated with cardiovascular risk factors or disease in extreme obesity, which were subsequently excluded based on our study protocol.

The effects of elevated BMI on cardiac structure and function are hypothesised to arise from several mechanisms. Firstly, increased cardiac work and stroke volume can lead to chamber dilatation and eccentric left ventricular hypertrophy, (16) with associated increases in left ventricular wall stress and myocardial oxygen consumption. (17) Further, insulin resistance, a common complication of elevated BMI, has been shown to be associated with alterations in myocardial substrate metabolism which may lead to contractile dysfunction. (18) Insulin's effects have been proposed to be from its effect on growth stimulation, sodium retention and neuroendocrine mediated pathways. (19) Additionally, elevated adipose tissue can result in increased adipokine production and subsequent systemic inflammation, a possible causative factor in development of myocardial fibrosis and subclinical dysfunction. (20) Undiagnosed obstructive sleep apnoea is a confounding factor in the obese population and may contribute to structural cardiac changes from the combined effect of nocturnal hypertension, cardiac afterload increase, wall stress during apnoeic periods and from upregulation of inflammatory cytokines leading to myocardial fibrosis. (21)

4.5.3 Degree of body mass index elevation affects subclinical myocardial function

Our results have shown that the degree of BMI elevation confers incremental risk of subclinical myocardial dysfunction across the BMI classes.

Left atrial subclinical functional appears to be the most sensitive to BMI elevation. As evidenced by the earlier drop in left atrial strain at just class 1 obesity (BMI ≥30) on post hoc analysis. The optimal cutoff value associated with LASr impairment on ROC curve analysis was similarly early at a BMI of ≥29.9.

As for right ventricular subclinical function, prevalence of RV-FWS impairment rises dramatically from 24% in class 1 obesity group to 56% and 56.9% in class 2 and 3 obesity groups respectively. This aligns with the pronounced drop of RV-FWS at class 2 obesity (BMI ≥35) on post hoc analysis, and the optimal BMI cutoff of ≥35.1 found to associate with RV-FWS impairment on ROC curve analysis.

LV subclinical function, on the other hand, exhibited a gradual decline spread across the entire BMI range on post hoc analysis. The ideal BMI cutoff value associated with LV-GLS impairment on ROC curve analysis was the highest at ≥37.3.

Additionally, we found that a BMI of ≥29.2 and ≥35.1 predicted single chamber and multi chamber subclinical dysfunction respectively. These findings are consistent with the Framingham population-based study where the incidence of heart failure has shown to rise with BMI elevation across the entire BMI range. (22)

4.5.4 Limitations

The main limitation of echocardiographic assessment of the obese population was image quality, particularly in the higher obesity classes. Despite this limitation, we only excluded 10.1% of our cohort due to inadequate image quality for strain analysis. Unsurprisingly, this challenge disproportionately affected the class III obesity group, which had BMI values up to

75kg/m^2. The utility of other modalities such as computed tomography, magnetic resonance and radionuclide imaging would also encounter issues of gantry size restriction and examination table weight limits in extreme obesity.

Another limitation of our study is that this is a single centre study. Despite this, the impact of obesity on subclinical cardiac function within our modest cohort size was evident.

Finally, obesity is a heterogenous condition with a complex array of physiological pathways contributing to cardiac dysfunction. (5) Since the selection our population was focused on apparent cardiovascular health, we did not fully account for all underlying metabolic conditions. Amongst our cohort, we did not perform insulin resistance, fasting lipid profiles, fibroscan and ultrasound investigations to confirm non-alcoholic fatty liver disease. We instead screened HbA1c levels, history of hyperlipidaemia or dyslipidaemia and history of chronic liver disease.

4.6.0 Conclusion

Elevated body mass index can cause subclinical left ventricular, right ventricular and left atrial myocardial dysfunction even in the absence of any cardiovascular disease or risk factors. Furthermore, the degree of body mass index elevation confers incremental risk and prognosticate the presence of subclinical myocardial dysfunction.

4.7.0 References

1. Hales CM, Fryar CD, Carroll MD, Freedman DS, Ogden CL. Trends in Obesity and Severe Obesity Prevalence in US Youth and Adults by Sex and Age, 2007-2008 to 2015-2016. JAMA. 2018;319(16):1723-5.
2. Hubert HB, Feinleib M, McNamara PM, Castelli WP. Obesity as an independent risk factor for cardiovascular disease: a 26-year follow-up of participants in the Framingham Heart Study. Circulation. 1983;67(5):968-77.
3. Masters RK, Reither EN, Powers DA, Yang YC, Burger AE, Link BG. The impact of obesity on US mortality levels: the importance of age and cohort factors in population estimates. Am J Public Health. 2013;103(10):1895-901.
4. Finkelstein EA, Trogdon JG, Cohen JW, Dietz W. Annual medical spending attributable to obesity: payer-and service-specific estimates. Health Aff (Millwood). 2009;28(5):w822-31.
5. Poirier P, Giles TD, Bray GA, Hong Y, Stern JS, Pi-Sunyer FX, et al. Obesity and cardiovascular disease: pathophysiology, evaluation, and effect of weight loss: an update of the 1997 American Heart Association Scientific Statement on Obesity and Heart Disease from the Obesity Committee of the Council on Nutrition, Physical Activity, and Metabolism. Circulation. 2006;113(6):898-918.
6. Lee HJ, Kim HL, Lim WH, Seo JB, Kim SH, Zo JH, et al. Subclinical alterations in left ventricular structure and function according to obesity and metabolic health status. PLoS One. 2019;14(9):e0222118.
7. Wang Y, Liang J, Zheng S, He A, Chen C, Zhao X, et al. Combined associations of obesity and metabolic health with subclinical left ventricular dysfunctions: Danyang study. ESC Heart Fail. 2021;8(4):3058-69.
8. Smiseth OA, Torp H, Opdahl A, Haugaa KH, Urheim S. Myocardial strain imaging: how useful is it in clinical decision making? Eur Heart J. 2016;37(15):1196-207.

9. Mitchell C, Rahko PS, Blauwet LA, Canaday B, Finstuen JA, Foster MC, et al. Guidelines for Performing a Comprehensive Transthoracic Echocardiographic Examination in Adults: Recommendations from the American Society of Echocardiography. J Am Soc Echocardiogr. 2019;32(1):1-64.
10. Sugimoto T, Dulgheru R, Bernard A, Ilardi F, Contu L, Addetia K, et al. Echocardiographic reference ranges for normal left ventricular 2D strain: results from the EACVI NORRE study. Eur Heart J Cardiovasc Imaging. 2017;18(8):833-40.
11. Sugimoto T, Robinet S, Dulgheru R, Bernard A, Ilardi F, Contu L, et al. Echocardiographic reference ranges for normal left atrial function parameters: results from the EACVI NORRE study. Eur Heart J Cardiovasc Imaging. 2018;19(6):630-8.
12. Muraru D, Onciul S, Peluso D, Soriani N, Cucchini U, Aruta P, et al. Sex- and Method-Specific Reference Values for Right Ventricular Strain by 2-Dimensional Speckle-Tracking Echocardiography. Circ Cardiovasc Imaging. 2016;9(2):e003866.
13. Singh M, Sethi A, Mishra AK, Subrayappa NK, Stapleton DD, Pellikka PA. Echocardiographic Imaging Challenges in Obesity: Guideline Recommendations and Limitations of Adjusting to Body Size. J Am Heart Assoc. 2020;9(2):e014609.
14. Marwick TH, Gillebert TC, Aurigemma G, Chirinos J, Derumeaux G, Galderisi M, et al. Recommendations on the Use of Echocardiography in Adult Hypertension: A Report from the European Association of Cardiovascular Imaging (EACVI) and the American Society of Echocardiography (ASE). J Am Soc Echocardiogr. 2015;28(7):727-54.
15. Jeyaprakash P, Moussad A, Pathan S, Sivapathan S, Ellenberger K, Madronio C, et al. A Systematic Review of Scaling Left Atrial Size: Are Alternative Indexation Methods Required for an Increasingly Obese Population? J Am Soc Echocardiogr. 2021;34(10):1067-76 e3.
16. Peterson LR, Waggoner AD, Schechtman KB, Meyer T, Gropler RJ, Barzilai B, et al. Alterations in left ventricular structure and function in young healthy obese women: assessment by echocardiography and tissue Doppler imaging. J Am Coll Cardiol. 2004;43(8):1399-404.

17. Karason K, Sjostrom L, Wallentin I, Peltonen M. Impact of blood pressure and insulin on the relationship between body fat and left ventricular structure. Eur Heart J. 2003;24(16):1500-5.

18. Peterson LR, Herrero P, Schechtman KB, Racette SB, Waggoner AD, Kisrieva-Ware Z, et al. Effect of obesity and insulin resistance on myocardial substrate metabolism and efficiency in young women. Circulation. 2004;109(18):2191-6.

19. Klein LJ, Visser FC. The effect of insulin on the heart : Part 1: Effects on metabolism and function. Neth Heart J. 2010;18(4):197-201.

20. Lelis DF, Freitas DF, Machado AS, Crespo TS, Santos SHS. Angiotensin-(1-7), Adipokines and Inflammation. Metabolism. 2019;95:36-45.

21. Laaban JP, Pascal-Sebaoun S, Bloch E, Orvoen-Frija E, Oppert JM, Huchon G. Left ventricular systolic dysfunction in patients with obstructive sleep apnea syndrome. Chest. 2002;122(4):1133-8.

22. Kenchaiah S, Evans JC, Levy D, Wilson PW, Benjamin EJ, Larson MG, et al. Obesity and the risk of heart failure. N Engl J Med. 2002;347(5):305-13.

CHAPTER FIVE

Immediate impact of successful cardioversion of atrial fibrillation on right ventricular systolic function

5.0 Abstract

Background: Atrial fibrillation (AF) is a common arrhythmia and is highly prevalent in patients with cardiomyopathy. While its detrimental effects on left heart function are well established, the impact of AF – and the restoration of sinus rhythm through direct current cardioversion (DCCV) – on right heart function is less well understood. This study aims to assess the effect of AF on right ventricular (RV) function and the immediate impact of restoring sinus rhythm on RV function.

Methods: We recruited patients undergoing DCCV for non-valvular AF between Jan 2017 to Jan 2018. We excluded those with a history of heart failure, LV systolic impairment, significant valvular disease, or failure to restore sinus rhythm. Transthoracic echocardiogram (TTE) was performed prior to and immediately post restoration of sinus rhythm. RV metrics of systolic function including fractional area change (FAC) and RV free wall strain (RV-FWS) were collected.

Results: Of the 50-patients assessed (64.1±11.0yrs, 60% male), 28% had a history of ischaemic heart disease and 5% had obstructive sleep apnoea. Paired T-test analysis showed upon restoration of sinus rhythm, there was a significant improvement in FAC (pre-DCCV: 37.8±8.9% vs post-DCCV: 40.8±10.2; p=0.02), RV-FWS (pre-DCCV: 16.4±4.9% vs post-DCCV: 21.0±6.8%; p<0.01) and RV-GLS (pre-DCCV: 14.18±4.42% vs post-DCCV: 17.4±4.3%; p<0.01). Based on accepted reference ranges, reduced RV-FWS and RV-GLS values were found in 80% and 82% pre-DCCV, and 50% and 44% post DCCV respectively. Restoration of sinus rhythm was significantly associated with reduced rate of RV systolic dysfunction on Fisher's exact test based on RV-FWS and RV-GLS (both p<0.01).

Conclusion: Reversion of AF back into sinus rhythm was associated with immediate and significant improvements in RV systolic function, which corresponded to a significant reduction in the prevalence of RV systolic impairment based on two-dimensional TTE parameters.

Graphical Abstract 5

GRAPHICAL ABSTRACT: There was a significant increase in TAPSE, RVS', FAC, RV-FWS and RV-GLS values immediately after successful cardioversion of atrial fibrillation back to sinus rhythm. A significant reduction in the prevalence of right ventricular systolic impairment was also seen based on normal reference range for RV-FWS and RV-GLS, but not with TAPSE, RVS' and FAC.

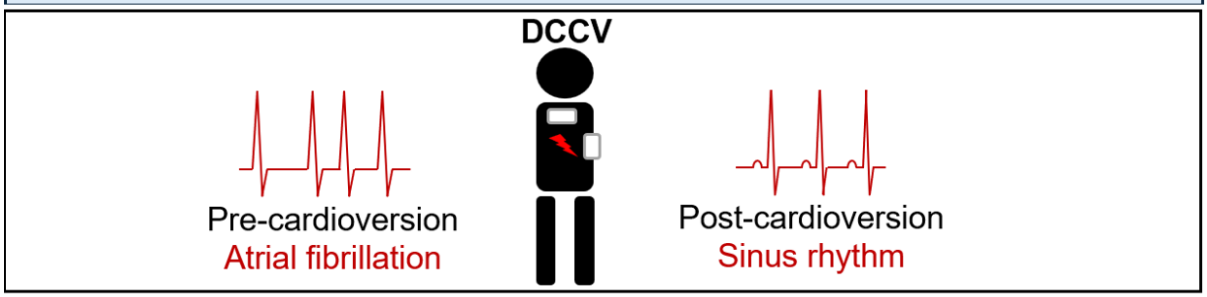

RV Parameter	Mean	Prevalence of impairment	Paired Difference	Mean	Prevalence of impairment	Paired T-test	Fisher's Test
TAPSE (cm)	1.9±0.5	22%	0.2	2.1±0.6	28%	0.001	0.815
RVS' (cm/s)	11.0±3.2	24%	0.4	11.4±3.3	24%	0.003	1.000
FAC (%)	16.4±4.9	40%	3.8	40.8±10.2	26%	0.020	0.202
RV-FWS (%)	16.4±4.9	80%	5.0	21.0±6.8	50%	<0.001	0.003
RV-GLS (%)	14.2±4.4	82%	3.2	17.4±4.3	44%	<0.001	<0.001

Abbreviations. DCCV: direct current cardioversion, *TAPSE: tricuspid annular plane systolic excursion, RVS': peak velocity of the lateral tricuspid annulus in systole, FAC: fractional area change, RV-FWS: right ventricular free wall strain, RV-GLS: right ventricular global longitudinal strain.*

Keywords: Atrial fibrillation; Right ventricle; Echocardiography; Speckle tracking echocardiography; Longitudinal strain; Heart failure

Abbreviations:

AF = atrial fibrillation

HF = heart failure

LV = left ventricular

RV = right ventricular

DCCV = direct current cardioversion

STE = speckle-tracking echocardiography

2D = two-dimensional

TTE = transthoracic echocardiographic

LA = left atrial

TAPSE = tricuspid annular plane systolic excursion

RVS' = peak systolic velocity at the tricuspid annulus

FAC = fractional area change

RV-FWS = right ventricular free wall strain

RV-GLS = right ventricular global longitudinal strain

5.1.0 Introduction

Atrial fibrillation (AF) is the most common arrhythmia and is closely associated with development of left ventricular (LV) systolic dysfunction and clinical heart failure (HF) (1, 2) The persistence of AF is believed to exert deleterious effects on LV performance through a combination of mechanisms including increased filling pressures, neurohumoral activation, electric and structural atrial remodelling, as well as molecular imbalances from irregular LV activation. (1) Restoration of sinus rhythm in patients with HF has been associated with improvements in both LV systolic and diastolic function and reduction in adverse cardiovascular outcomes. (1, 3-8)

While the relationship between AF and left heart dysfunction is well established, growing evidence suggests that AF may also negatively impact right ventricular (RV) function (9, 10) However, the pathophysiological consequences of AF on the RV, as well as the potential reversibility of these effects following the restoration of sinus rhythm, remain incompletely understood. (11)

Direct current cardioversion (DCCV) is a frequently employed therapeutic intervention to restore sinus rhythm in patients with persistent AF. Beyond rhythm control, restoration of sinus rhythm may lead to acute improvements in RV performance. (12-14) Development of advanced imaging modalities such RV longitudinal strain via speckle-tracking echocardiography (STE) have enhanced our ability to characterise RV systolic function with greater sensitivity than traditional echocardiographic parameters, thereby enabling earlier detection of RV dysfunction. (15)

5.2.0 Objectives and Aims

We aim to assess the immediate impact of restoring sinus rhythm on RV systolic function in those with persistent AF, using two-dimensional (2D) echocardiographic parameters.

5.3.0 Materials and Methods

5.3.1 Study population

Patients referred to our echocardiography laboratory for DCCV for non-valvular AF in the period of January 2019 to February 2020 were assessed. As per local treatment protocols, all patients received resting electrocardiogram and comprehensive transthoracic echocardiogram (TTE) prior to and immediately following DCCV. We included adults ≥18 years of age who underwent successful restoration of sinus rhythm. In addition to those with unsuccessful DCCV, we excluded patients with a diagnosis of primary valvular disease, previous cardiac surgery and pre-existing HF and/or LV systolic dysfunction as these conditions can independently affect RV function. Patients with poor quality images limiting assessments of RV function were also excluded.

The study protocol was approved by the Western Sydney Local Health District Human Research Ethics Committee in compliance with the Declaration of Helsinki.

5.3.2 Transthoracic echocardiography

All TTEs were performed using commercially available ultrasound systems in accordance with American Society of Echocardiography guideline recommendations. (16-20) In brief, LV volume and ejection fraction (LVEF) were calculated using modified Simpson's biplane method. Left atrial (LA) volume was measured at end diastole (immediately prior to mitral valve opening) utilising the 2- and 4-chamber views using the biplane method of discs.

We utilised pulse-wave Doppler and tissue Doppler in the apical 4-chamber view to measure early and late peak mitral inflow velocities (MVE and MVA), E/A ratio, septal and lateral mitral annular velocities (septal and lateral e'), with average E/e' being subsequently calculated. (18)

2D parameters of RV systolic function were assessed by tricuspid annular plane systolic excursion (TAPSE), tissue Doppler-derived peak systolic velocity at the tricuspid annulus (RVS'), fractional area change (FAC), and RV strain. (20)

All reported parameters were a mean of measurements from five cardiac cycles whilst in AF at the time of the TTE study. (16)

5.3.3 Speckle-tracking echocardiography

STE of the RV was performed offline using vendor-independent computer software (TomTech Image Arena Systems v2.3, Germany). Measurements were performed by two independent investigators blinded to patient baseline characteristics, outcomes, and other echocardiographic data. All STE measurements were expressed as absolute percentages.

Right ventricular strain was evaluated by tracing the RV endocardium in the RV-focused apical view. We analysed RV free wall strain (RV-FWS), which was derived from the average peak systolic strain of the three RV free wall segments, and RV global longitudinal strain (RV-GLS), which was derived from the average peak systolic strain of six segments consisting of the interventricular septum and the RV free wall. (20)

Quantitation of inter- and intra-observer variability of right ventricular free-wall strain was performed in 5% of the population pre- and 5% of the population post-DCCV through repeat measurements by a second independent investigator and the original investigator at least one month later. Reproducibility of these measurements were represented by the intra-class correlation coefficient.

5.3.4 Statistical analysis

All statistical analysis was performed using the Statistical Package for Social Sciences Software (SPSS Version 22; SPSS Inc., Chicago, IL, USA). Continuous variables were presented as mean ± standard deviations. Categorical variables were expressed as numbers and percentages. All statistical tests were two-tailed, with a p-value <0.05 considered statistically significant.

We performed paired T-test on each 2D RV systolic functional parameters before and after DCCV to assess for significant difference upon restoration of sinus rhythm.

We further utilised Chi-square or Fisher's exact test where appropriate, to investigate the association between restoration of sinus rhythm and prevalence of RV systolic dysfunction, which was defined as ≤1.7cm, ≤9.5cm/s, ≤35%, ≤20.0%, and ≤17% for TAPSE, RVS', FAC, RV-FWS and RV-GLS respectively based on published reference ranges. (20)

5.4.0 Results

5.4.1 Patient characteristics

Of 235-consecutive patients assessed, 50-patients met eligibility and were included for analysis. One hundred and ninety-five patients were excluded: 104-patients did not proceed with DCCV due to intracardiac thrombus or remained in AF, 9-patients had primary valvular disease, 4-patients had previous cardiac surgery, 64-patients had pre-existing HF or LV systolic impairment. A further 5-patients had inadequate TTE imaging quality for analysis and were also excluded. (Figure 5.1)

The mean age of the included cohort was 64.1±11.0 years, 30 (60%) were male, 14 (28%) had ischaemic heart disease, 30 (60%) had hypertension, 14 (28%) had diabetes mellitus, 21 (42%) had hyperlipidaemia, 5 (10%) had obstructive sleep apnoea and 4 (8%) had chronic obstructive pulmonary disease. (Table 5.1)

All patients were in atrial fibrillation prior to DCCV with an average ventricular rate of 91.7±19.8 beats per minute, and in sinus rhythm post DCCV with an average ventricular rate of 68.4±8.2 beats per minute.

5.4.2 Baseline echocardiographic parameters

By design, all patients had normal LV systolic function with an LVEF of ≥50%. The mean indexed LV mass was 106±37 g/m^2. LA dilatation was identified in 56% of patients: 18% had mildly dilated, 10% had moderately dilated and 28% had severely dilated LA. Sixteen-patients (32%) had elevated LV filling pressures at rest with an E/e' ratio of >14. Pulmonary artery systolic pressures were elevated to ≥35mmHg in 10-patients (20%). (Table 5.1)

Figure 5.1. Consort diagram

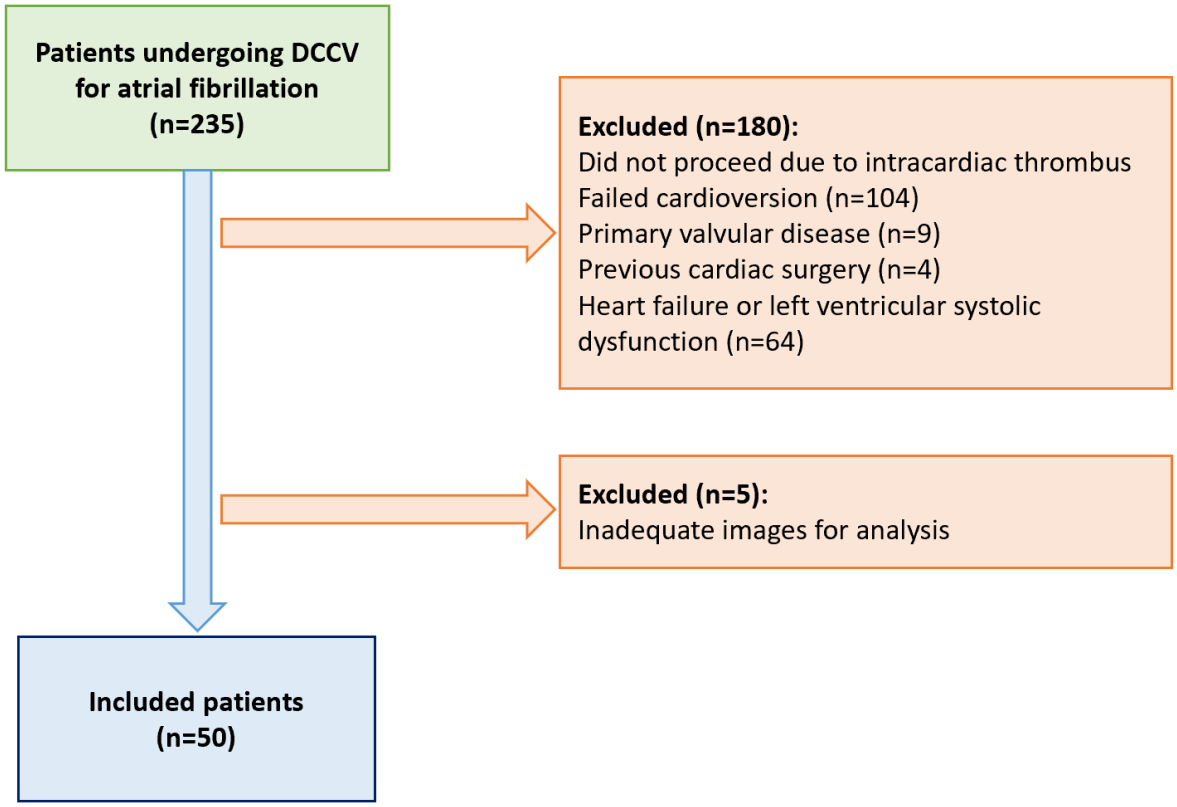

Figure 5.1. Of the 235-patients screened, 104 failed cardioversion or had an intracardiac thrombus identified, and 9 had primary valvular disease, 4 had previous cardiac surgery, 64 had history of heart failure or left ventricular systolic dysfunction. A further 5-patients had inadequate image quality for analysis. Fifty-patients were included in the final analysis.

Abbreviations. *DCCV: direct current cardioversion*

Tablet 5.1. Baseline clinical characteristics and echocardiographic parameters

Baseline Clinical Characteristics	
Age (years)	64.1±11.0
Male gender (n, %)	30 (60)
Resting heart rate (bpm)	91.7±19.8
Ischaemic heart disease (n, %)	14 (28)
Hypertension (n, %)	30 (60)
Diabetes mellitus (n, %)	14 (28)
Hyperlipidaemia (n, %)	21 (42)
Obstructive sleep apnoea (n, %)	5 (10)
Chronic obstructive pulmonary disease (n, %)	4 (8)
Baseline Echocardiographic Parameters	
Interventricular septal wall thickness in end-diastole	1.2±0.2
Left ventricular internal diameter at end-diastole	4.9±0.9
Left ventricular internal diameter at end-systole	3.6±1.1
Posterior wall thickness in end-diastole	1.1±0.2
Relative wall thickness	0.5±0.1
Indexed left ventricular mass (g/m^2)	106±37
Left ventricular ejection fraction (%)	51.5±14.2
Indexed end-diastolic left ventricular volume (ml/m^2)	50.3±19.8
Indexed end-systolic left ventricular volume (ml/m^2)	26.2±17.7
Indexed left atrial volume (ml/m^2)	39.8±12.3
Peak mitral E velocity (m/s)	1.0±0.3
Average E/e’ ratio	12.4±6.6
Pulmonary artery systolic pressure (mmHg)	29.7±8.7
Right ventricular basal diameter (cm)	3.9±0.6
Tricuspid annular plane systolic excursion (cm)	2.1±1.3
Peak velocity of the lateral tricuspid annulus in systole (cm/s)	11.0±3.2
Fractional area change (%)	36.8±8.9
Right ventricular free wall strain (%)	16.4±4.9
Right ventricular global longitudinal strain (%)	14.2±4.4

Tablet 5.1. This table details the baseline clinical characteristics and echocardiographic parameters of the included cohort.

5.4.3 Right ventricular dysfunction in atrial fibrillation

We calculated the prevalence of RV dysfunction based on the published normal reference range for TAPSE (≤1.7cm), RVS' (≤9.5cm/s), FAC (≤35%), RV-FWS (≤20%) and RV-GLS (≤17%). (20)

At baseline and in the presence of AF, 40% of patients had impaired RV function based on the conventional echocardiographic parameter of FAC. Both TAPSE and RVS' were less sensitive, classifying only 22% and 24% of patients as having RV dysfunction respectively. On RV longitudinal strain assessment in contrast, the proportion of patients with RV dysfunction was higher at 80% and 82% based on RV-FWS and RV-GLS respectively, highlighting the increased sensitivity of RV strain assessment in the detection of RV dysfunction. (Table 5.2)

5.4.4 Right ventricular systolic function post cardioversion

Following successful DCCV, there was a significant improvement in RV systolic function irrespective of the echocardiographic measure utilised. On paired t-test of the pre- and post-DCCV echocardiographic values, RV-FWS showed the greatest improvement, increasing from from 16.4±4.9% to 21.0±6.8% (t=-6.1, p<0.001, *d*=-0.87), corresponding with a 30.5% increase. TAPSE exhibited the smallest improvement from 1.9±0.5 to 2.1.1±0.6cm (t=-3.5, p=0.001, *d*=-0.51) corresponding with a 10.5% increase. As for the remaining parameters, RVS' increased from 11.0±3.2 to 11.4±3.3cm/s (t=-3.2, p=0.003, *d*=-0.46); FAC increased from 37.8±8.9 to 40.8±10.2% (t=-2.4, p=0.020, *d*=-0.34); and RV-GLS increased from 14.2±4.4 to 17.4±4.3% (t=-5.2, p<0.001, *d*=-0.73). (Table 5.3)

Table 5.2. Prevalence of right ventricular systolic impairment pre- and post-cardioversion

Prevalence of right ventricular systolic impairment	Pre-DCCV	Post-DCCV	Significance (p-value)
TAPSE ≤1.7 cm (n, %)	11 (22)	14 (28)	0.815
RVS' ≤9.5 cm/s (n, %)	12 (24)	12 (24)	1.000
FAC ≤35% (n, %)	20 (40)	13 (26)	0.202
RV-FWS ≤20% (n, %)	40 (80)	25 (50)	0.003
RV-GLS ≤17% (n, %)	41 (82)	22 (44)	<0.001

Table 5.2. On Fisher's exact test, there was a significant reduction in the prevalence of right ventricular systolic impairment post-direct current cardioversion based on right ventricular free wall strain and right ventricular global longitudinal strain.

Abbreviations. *TAPSE: tricuspid annular plane systolic excursion, RVS': peak velocity of the lateral tricuspid annulus in systole, FAC: fractional area change, RV-FWS: right ventricular free wall strain, RV-GLS: right ventricular global longitudinal strain.*

Table 5.3. Two-dimensional echocardiographic right ventricular functional parameters pre- and post-direct current cardioversion

	Pre-DCCV	Post-DCCV	Paired Difference	Percentage Increase (%)	Paired T-test (p-value)
TAPSE (cm)	1.9±0.5	2.1±0.6	0.2	10.5	0.001
RVS' (cm/s)	11.0±3.2	11.4±3.3	0.4	3.6	0.003
FAC (%)	37.8±8.9	40.8±10.2	3.8	10.1	0.020
RV-FWS (%)	16.4±4.9	21.0±6.8	5.0	30.5	<0.001
RV-GLS (%)	14.2±4.4	17.4±4.3	3.2	22.5	<0.001

Table 5.3. The mean of the right ventricular systolic functional parameters pre- and post- direct current cardioversion. There was a significant increase in all parameters upon restoration of sinus rhythm.

Abbreviations. *TAPSE: tricuspid annular plane systolic excursion, RVS': peak velocity of the lateral tricuspid annulus in systole, FAC: fractional area change, RV-FWS: right ventricular free wall strain, RV-GLS: right ventricular global longitudinal strain.*

5.4.5 Residual prevalence of right ventricular dysfunction post cardioversion

We compared the prevalence of RV dysfunction pre- and post-DCCV using Fisher's exact test. The prevalence of RV dysfunction was similar pre- and post-DCCV for TAPSE (22% to 28%, p=0.815), RVS' (24% to 24%, p=1.000), and FAC (40% to 26%, p=0.202). Significantly less patients had RV dysfunction post-DCCV based on RV-FWS (80% to 50%, p=0.003) and RV-GLS (82% to 44%, p<0.001). (Table 5.2)

Despite improvements of RV systolic function following successful DCCV, 28%, 24%, 26%, 50% and 44% of patients continued to exhibit impaired RV function based on TAPSE, RVS', FAC, RV-FWS, and RV-GLS respectively. Our study unfortunately only examined early RV function recovery and did not assess late recovery of RV function.

5.4.6 Reproducibility analysis

There was good reproducibility of the strain parameters based on the inter- and intra-observer variability. For inter-observer variability, the intra-class correlation coefficient was 0.94 (95% CI 0.87-0.99) for RV-FWS, and 0.96 (95% CI 0.88-0.99) for RV-GLS. For intra-observer variability, the intra-class correlation coefficient was 0.99 (95% CI 0.95-1.00) for RV-FWS, and 0.98 (95% CI 0.93-1.00) for RV-GLS.

5.5.0 Discussion

Our study demonstrated that following successful DCCV of AF, patients had immediate and significant improvement in all RV systolic functional parameters on 2D TTE including STE. This further translates to a lower rate of RV systolic impairment based on RV-FWS and RV-GLS normal reference thresholds.

To our knowledge, no previous study examined the immediate effect of successful DCCV on RV systolic function as measured by STE. One previous study examined the effect of

cardioversion based on TAPSE measurement and another examined both TAPSE and FAC. (14, 21)

5.5.1 Impact of restoring sinus rhythm on right ventricular improvement

AF is believed to reduce overall cardiac output by approximately 20-30% in healthy cohorts and by an even greater amount in those with comorbid cardiac disease. (22) Restoration of sinus rhythm is thought to improve RV longitudinal contraction and interventricular wall function, independent of afterload conditions. (14, 23) A previous study by Alam et al. demonstrated successful DCCV resulted in an immediate improvement in the mean TAPSE value from 1.3cm to 1.7cm. This further rose to 2.5cm one month post-DCCV after resolution of right atrial stunning. (14) A separate study by Yan et al, in an echocardiographic sub study of the GAP-AF pulmonary vein isolation trial, found similar improvements in both TAPSE (1.8cm to 2.0cm) and FAC (38% to 42%) immediately post DCCV. (21, 24) In contrast to our study, these previous studies included all patients with persistent AF, even those with pre-existing structural cardiac disease and known HF.

Our study showed a significant improvement in TAPSE, RVS', FAC, RV-FWS and RV-GLS immediately following successful DCCV of AF in patients without significant structural cardiac disease or HF. Amongst these parameters, the percentage of improvement was highest with RV-FWS at 30.5%, followed by RV-GLS at 22.5%. A lesser improvement was observed with traditional indices of TAPSE, RVS' and FAC at 10.5%, 3.6% and 10.1% respectively. We believe the comparatively greater improvement in RV-FWS and RV-GLS values could be attributed to the higher sensitivity exhibited by STE which tracks the entire length of the RV myocardium. In comparison, TAPSE and RVS' focally assess the movement of the lateral tricuspid annulus relative to the apex during systole, which is affected by atrial stunning. (14) Similarly, FAC predominantly assesses radial function and is also affected by the reduction of RV end-diastolic filling from the loss of right atrial kick. (15) Furthermore, reduction of

conventional RV functional parameters may reflect chronic structural alterations which may not recover as quickly post DCCV.

Based on our findings, we propose that RV-FWS and RV-GLS can more accurately reflect RV functional recovery immediately following DCCV.

5.5.2 Prevalence of right ventricular systolic dysfunction

The previous studies by Alam et al. and Yan et al. alongside our study have all demonstrated improvements in RV systolic parameters following a successful DCCV. (14, 21) However, this does not necessarily indicate recovery of underlying RV systolic dysfunction. For example, the mean TAPSE pre-DCCV in our cohort was assessed at 1.9cm, which is within the normal reference range. (20) Therefore, our study further examined the rates of RV systolic dysfunction pre- and post-DCCV based on published normal reference range for each RV parameter. (20) Prevalence of RV systolic impairment pre-DCCV was the lowest based on TAPSE and RVS', and highest based on RV-FWS and RV-GLS. Interestingly, there was no significant change in the rates of RV systolic impairment post-DCCV based on TAPSE, RVS' and FAC values. Only RV-FWS and RV-GLS was sufficiently sensitive to detect a significant reduction in the rates of RV systolic impairment with successful DCCV. It should be noted that improvements in RV-GLS values would be in part due to improvement of interventricular wall contraction from LV systolic functional improvement.

The superior capacity of RV STE over conventional parameters to detect RV systolic impairment and its recovery is attributed to its higher sensitivity. (20) Hence, we propose that RV-FWS and RV-GLS would be the best parameters to detect the presence of RV systolic impairment in AF and its resolution post successful DCCV.

5.5.3 Clinical impact

While the benefits of AF rhythm control in LV systolic dysfunction are well established, the impact of AF on RV function remains less clear. (1, 3-8, 11) Our study demonstrates that successful DCCV leads to immediate and significant improvements in RV systolic function, even in patients without HF or LV systolic impairment. The superior sensitivity of RV STE underscores its value in detecting subclinical and clinical RV dysfunction in the setting of AF. Routine incorporation of these advanced echocardiographic parameters into clinical practice may improve early detection, enable accurate risk stratification, and facilitate timely intervention. These findings support the consideration of rhythm control strategies as a potential therapeutic approach in managing RV dysfunction, particularly in those with symptomatic or decompensated RV failure.

5.5.4 Limitations

The main limitation of our study was its retrospective design. This would have normally caused significant variations in the timing of the pre- and post-DCCV TTE studies in relations to when the DCCV was performed. However, our centre routinely performs a comprehensive TTE on the morning of planned DCCV and a progress study post successful DCCV as per local protocol.

Secondly, we only assessed the immediate impact of successful DCCV on RV systolic function and could not account for the long-term changes after resolution of atrial stunning. However, our study was still able to show significant RV functional improvements immediately post restoration of sinus rhythm.

Finally, our study was a single-centre endeavour, which limited our sample size. Especially since we only included patients without pre-existing HF or structural cardiac abnormalities. Larger studies would be required to validate our findings and evaluate the long-term implications of RV dysfunction post DCCV.

5.6.0 Conclusion

In our cohort of patients without heart failure or left ventricular systolic dysfunction, successful direct current cardioversion of atrial fibrillation back to sinus rhythm was associated with immediate and significant improvements in right ventricular systolic function and a lower rate of right ventricular systolic dysfunction based on two-dimensional echocardiographic parameters. These findings suggest that rhythm control in atrial fibrillation may represent a viable therapeutic strategy for right ventricular dysfunction, warranting further studies.

5.7.0 References

1. Bergau L, Bengel P, Sciacca V, Fink T, Sohns C, Sommer P. Atrial Fibrillation and Heart Failure. J Clin Med. 2022;11(9).
2. Benjamin EJ, Levy D, Vaziri SM, D'Agostino RB, Belanger AJ, Wolf PA. Independent risk factors for atrial fibrillation in a population-based cohort. The Framingham Heart Study. JAMA. 1994;271(11):840-4.
3. Chen S, Purerfellner H, Meyer C, Acou WJ, Schratter A, Ling Z, et al. Rhythm control for patients with atrial fibrillation complicated with heart failure in the contemporary era of catheter ablation: a stratified pooled analysis of randomized data. Eur Heart J. 2020;41(30):2863-73.
4. Marrouche NF, Brachmann J, Andresen D, Siebels J, Boersma L, Jordaens L, et al. Catheter Ablation for Atrial Fibrillation with Heart Failure. N Engl J Med. 2018;378(5):417-27.
5. Packer DL, Piccini JP, Monahan KH, Al-Khalidi HR, Silverstein AP, Noseworthy PA, et al. Ablation Versus Drug Therapy for Atrial Fibrillation in Heart Failure: Results From the CABANA Trial. Circulation. 2021;143(14):1377-90.
6. Muntinga HJ, van den Berg F, Niemeyer MG, Blanksma PK, van der Wall EE, Crijns HJ. Left ventricular diastolic function after electrical cardioversion of atrial fibrillation. Heart. 2002;87(4):379-80.
7. Raymond RJ, Lee AJ, Messineo FC, Manning WJ, Silverman DI. Cardiac performance early after cardioversion from atrial fibrillation. Am Heart J. 1998;136(3):435-42.
8. O'Neill PG, Puleo PR, Bolli R, Rokey R. Return of atrial mechanical function following electrical conversion of atrial dysrhythmias. Am Heart J. 1990;120(2):353-9.
9. Gorter TM, van Melle JP, Rienstra M, Borlaug BA, Hummel YM, van Gelder IC, et al. Right Heart Dysfunction in Heart Failure With Preserved Ejection Fraction: The Impact of Atrial Fibrillation. J Card Fail. 2018;24(3):177-85.

10. Nishimura S, Izumi C, Yamasaki S, Obayashi Y, Kuroda M, Amano M, et al. Impact of right ventricular function on development of significant tricuspid regurgitation in patients with chronic atrial fibrillation. J Cardiol. 2020;76(5):431-7.
11. Majos E, Dabrowski R, Szwed H. The right ventricle in patients with chronic heart failure and atrial fibrillation. Cardiol J. 2013;20(3):220-6.
12. Van Gelder IC, Rienstra M, Bunting KV, Casado-Arroyo R, Caso V, Crijns H, et al. 2024 ESC Guidelines for the management of atrial fibrillation developed in collaboration with the European Association for Cardio-Thoracic Surgery (EACTS). Eur Heart J. 2024;45(36):3314-414.
13. Joglar JA, Chung MK, Armbruster AL, Benjamin EJ, Chyou JY, Cronin EM, et al. 2023 ACC/AHA/ACCP/HRS Guideline for the Diagnosis and Management of Atrial Fibrillation: A Report of the American College of Cardiology/American Heart Association Joint Committee on Clinical Practice Guidelines. Circulation. 2024;149(1):e1-e156.
14. Alam M, Samad BA, Hedman A, Frick M, Nordlander R. Cardioversion of atrial fibrillation and its effect on right ventricular function as assessed by tricuspid annular motion. Am J Cardiol. 1999;84(10):1256-8, A8.
15. Rudski LG, Lai WW, Afilalo J, Hua L, Handschumacher MD, Chandrasekaran K, et al. Guidelines for the echocardiographic assessment of the right heart in adults: a report from the American Society of Echocardiography endorsed by the European Association of Echocardiography, a registered branch of the European Society of Cardiology, and the Canadian Society of Echocardiography. J Am Soc Echocardiogr. 2010;23(7):685-713; quiz 86-8.
16. Lang RM, Badano LP, Mor-Avi V, Afilalo J, Armstrong A, Ernande L, et al. Recommendations for cardiac chamber quantification by echocardiography in adults: an update from the American Society of Echocardiography and the European Association of Cardiovascular Imaging. J Am Soc Echocardiogr. 2015;28(1):1-39 e14.

17. Badano LP, Kolias TJ, Muraru D, Abraham TP, Aurigemma G, Edvardsen T, et al. Standardization of left atrial, right ventricular, and right atrial deformation imaging using two-dimensional speckle tracking echocardiography: a consensus document of the EACVI/ASE/Industry Task Force to standardize deformation imaging. Eur Heart J Cardiovasc Imaging. 2018;19(6):591-600.
18. Nagueh SF, Smiseth OA, Appleton CP, Byrd BF, 3rd, Dokainish H, Edvardsen T, et al. Recommendations for the Evaluation of Left Ventricular Diastolic Function by Echocardiography: An Update from the American Society of Echocardiography and the European Association of Cardiovascular Imaging. J Am Soc Echocardiogr. 2016;29(4):277-314.
19. Rudski LG, Fine NM. Right Ventricular Function in Heart Failure: The Long and Short of Free Wall Motion Versus Deformation Imaging. Circ Cardiovasc Imaging. 2018;11(1):e007396.
20. Mukherjee M, Rudski LG, Addetia K, Afilalo J, D'Alto M, Freed BH, et al. Guidelines for the Echocardiographic Assessment of the Right Heart in Adults and Special Considerations in Pulmonary Hypertension: Recommendations from the American Society of Echocardiography. J Am Soc Echocardiogr. 2025;38(3):141-86.
21. Yan X, Meyre PB, Aeschbacher S, Bossard M, Zimmermann A, Conen D, et al. Right Heart Structure and Function after Electrical Cardioversion for Atrial Fibrillation. Cardiology. 2023;148(5):402-8.
22. Alpert JS, Petersen P, Godtfredsen J. Atrial fibrillation: natural history, complications, and management. Annu Rev Med. 1988;39:41-52.
23. Melenovsky V, Hwang SJ, Lin G, Redfield MM, Borlaug BA. Right heart dysfunction in heart failure with preserved ejection fraction. Eur Heart J. 2014;35(48):3452-62.
24. Kuck KH, Hoffmann BA, Ernst S, Wegscheider K, Treszl A, Metzner A, et al. Impact of Complete Versus Incomplete Circumferential Lines Around the Pulmonary Veins During Catheter Ablation of Paroxysmal Atrial Fibrillation: Results From the Gap-Atrial

Fibrillation-German Atrial Fibrillation Competence Network 1 Trial. Circ Arrhythm Electrophysiol. 2016;9(1):e003337.

CHAPTER SIX

Right ventricular systolic function independently predicts exercise capacity in patients with non-ischaemic cardiomyopathy

6.0 Abstract

Background: Reduction in exercise capacity (EC) is one of the predominant symptoms in heart failure (HF), where impairment of the left heart function is postulated to be the primary cardiac determinant of EC reduction. The impact of right ventricular (RV) dysfunction on EC is less well understood. Six-minute walk test (6MWT) is a standardised, validated method of assessing submaximal EC. We aim to evaluate the effect of RV systolic impairment on EC based on 6-minute walk distance (6MWD).

Material and methods: We prospectively recruited consecutive ambulant patients with HF secondary to non-ischaemic cardiomyopathy (NICM) and a left ventricular ejection fraction (LVEF) <50%. Participants were optimised on guideline-directed therapy for >3 months in a dedicated HF clinic before concurrent index echocardiography and 6MWT. Conventional and advanced echocardiographic parameters, including left ventricular longitudinal strain, left atrial reservoir strain, RV-free-wall-strain (RV-FWS), and three-dimensional RV ejection fraction, were assessed.

Results: Of 405-patients included (mean age 60.2±16.4 years, 66.9% male, mean LVEF 40.5±10.8%), 144 had reduced 6MWD to <300m. Amongst the RV functional parameters, RV-FWS best discriminated for reduced 6MWD (AUC=0.65) on receiver operating characteristics curve analysis and was not significantly different from left atrial reservoir strain on DeLong's test (p=0.053). After accounting for relevant clinical and echocardiographic parameters, multivariate Logistic regression model confirmed that RV-FWS reduction was independently associated with 6MWD reduction (OR:0.90, 95%CI:0.85-0.94, p<0.001)

Conclusion: Reduction in RV-FWS was associated with 6MWD reduction to <300m in a cohort of stable NICM patients, independent of clinical characteristics and left heart parameters.

Graphical abstract:

GRAPHICAL ABSTRACT: In our cohort of compensated non-ischaemic cardiomyopathy patients, right ventricular free wall strain was the best discriminator for reduced 6-minute walk distance to less than 300 meters on receiver operating characteristics curve amongst the right ventricular echocardiographic parameters. Furthermore, right ventricular free wall strain was independently associated with reduction in 6-minute walk distance to below 300 meters on multivariate regression.

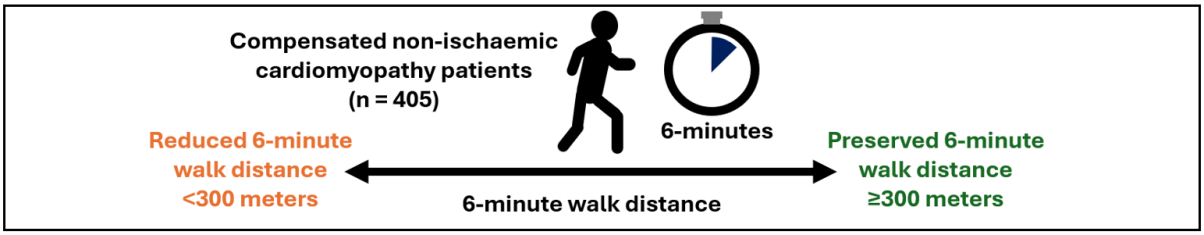

Right ventricular parameters discriminating for 6-minute walk distance <300 meters

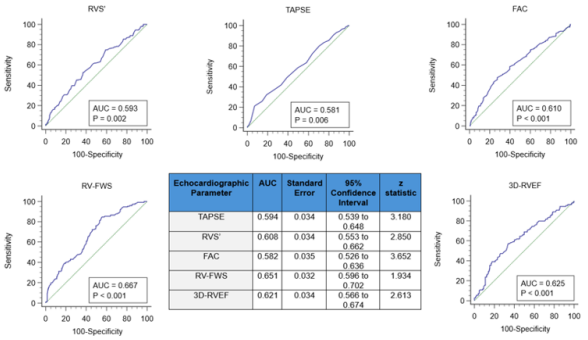

Echocardiographic Parameter	AUC	Standard Error	95% Confidence Interval	z statistic
TAPSE	0.594	0.034	0.539 to 0.648	3.180
RVS'	0.608	0.034	0.553 to 0.662	2.850
FAC	0.582	0.035	0.526 to 0.636	3.652
RV-FWS	0.651	0.032	0.596 to 0.702	1.934
3D-RVEF	0.621	0.034	0.566 to 0.674	2.613

Factors independently associated with 6-minute walk distance <300 meters

Factors independently associated with reduced 6-minute walk distance	Adjusted Hazard Ratio (95% CI)	Adjusted p-value
Height (cm)	0.95 (0.92-0.97)	<0.001
Atrial fibrillation	3.2 (1.77-5.60)	<0.001
Hypertension	2.24 (1.26-4.00)	0.006
Chronic obstructive pulmonary disease	5.2 (2.04-13.05)	0.001
Haemoglobin count (g/L)	0.98 (0.97-0.99)	0.020
PASP (mmHg)	1.04 (1.01-1.06)	0.002
RV-FWS (%)	0.90 (0.85-0.94)	<0.001

Abbreviations. *TAPSE: tricuspid annular plane systolic excursion, RVS': Peak velocity of the lateral tricuspid annulus in systole, FAC: fractional area change, RV-FWS: right ventricular free wall strain, 3D-RVEF: three-dimensional right ventricular ejection fraction, PASP: pulmonary artery systolic pressure.*

Keywords: Heart failure; Right ventricle; Global longitudinal strain; Cardiomyopathy; Exercise capacity; Echocardiography.

Abbreviations:

HF = heart failure

LV = left ventricular

RV = right ventricular

NICM = non-ischaemic cardiomyopathy

TTE = transthoracic echocardiogram

3D-RVEF = three-dimensional right ventricular ejection fraction

6MWT = 6-minute walk test

VO2 = peak oxygen consumption

CPET = cardiopulmonary exercise testing

6MWD = 6-minute walk distance

LVEF = left ventricular ejection fraction

OSA = obstructive sleep apnoea

KCCQ = Kansas City Cardiomyopathy Questionnaire

NYHA = New York Heart Association

AF = atrial fibrillation

LAV = left atrial volume

TAPSE = tricuspid annular plane systolic excursion

RVS' = peak velocity of the lateral tricuspid annulus in systole

FAC = fraction area change

STE = speckle-tracking echocardiography

RV-FWS = right ventricular free wall strain

LV-GLS = left ventricular global longitudinal strain

LASr = left atrial reservoir strain

ROC = receiver operating characteristics

COPD = chronic obstructive pulmonary disease

PASP = pulmonary artery systolic pressure

RA = right atrial

6.1.0 Introduction

Reduction in exertional capacity is a hallmark of heart failure (HF) symptomatology and is a major impediment to quality of life in those with non-ischaemic cardiomyopathy (NICM). The decline in exercise capacity has traditionally been attributed to reduced cardiac reserve from left ventricular (LV) systolic dysfunction. (1, 2) Emerging evidence highlights the contribution of right ventricular (RV) systolic dysfunction and pulmonary arterial coupling to exercise tolerance in HF with preserved ejection fraction and in congestive HF. (3-6) In contrast, the role of RV systolic dysfunction as a determinant of exercise capacity in NICM remains less clearly defined.

Transthoracic echocardiography (TTE) remains the cornerstone of non-invasive assessment for both LV and RV function in NICM. (7) The advent of advanced echocardiographic parameters such as longitudinal strain and three-dimensional RV ejection fraction (3D-RVEF) offer superior sensitivity and specificity in detecting RV systolic dysfunction over traditional measures. (8-10)

The six-minute walk test (6MWT) provides a standardised and validated measure of submaximal exercise capacity, integrating cardiovascular, pulmonary and skeletal muscle performance. (11, 12). Six-minute walk distance (6MWD) not only correlates with peak oxygen consumption (VO2) during cardiopulmonary exercise testing (CPET) but also serves as a strong prognostic marker in systolic HF, with distances below 300 meters consistently found to independently prognosticate adverse cardiovascular outcomes in systolic HF. (11-18)

6.2.0 Objectives and aims

This study aimed to evaluate whether the echocardiographic measures of RV systolic function can discriminate for reduced exercise capacity, as assessed by 6-minute walk distance (6MWD), in patients with stable NICM.

6.3.0 Material and methods

6.3.1 Study population

We prospectively recruited consecutive patients aged ≥18 years with a diagnosis of non-ischaemic cardiomyopathy and a left ventricular ejection fraction (LVEF) of <50% attending our outpatient HF service from January 2021 to January 2024.

We excluded patients who were not independently ambulant, those with a history of significant coronary artery disease (defined as ≥70% disease in any of the three main coronary arteries, prior coronary intervention or bypass surgery, evidence of impaired myocardial perfusion or reversible ischemia on non-invasive testing), primary valvular disease, valve replacement or repair, congenital heart disease, prior cardiac surgery, severe pulmonary hypertension, restrictive or obstructive pulmonary disease requiring hospitalisation, recent pulmonary embolism within 6 months and those with untreated obstructive sleep apnoea (OSA). Patients with incomplete medical history or inadequate TTE image quality for analysis were also excluded.

All patients were followed up through a dedicated HF clinic where optimal guideline-directed therapy was initiated and rapidly up titrated based on current society guidelines. (19-22)

A comprehensive TTE and concurrent exercise capacity assessment including a 6MWT was performed once the patient has been optimised on guideline directed therapy for at least three months. A 6MWD of less than 300 meters was deemed as reduced exercise capacity.

The study protocol complied with the Declaration of Helsinki and was approved by the human research ethics committee of our institution.

6.3.2 Transthoracic echocardiography

All TTEs were performed using a commercially available echocardiogram system (Vivid E-95, 4Vc probe, General Electric Vingmed, Horton, Norway) in accordance with American Society of Echocardiography guideline recommendations. (10, 23-25) Electrocardiogram gated loops of at least five cardiac cycles were acquired for the analysis. For patients in atrial fibrillation (AF) at the time of the study, the reported value was the mean measurement over at least five cardiac cycles.

In brief, LV volume and ejection fraction were calculated using modified Simpson's biplane method. Left atrial volume (LAV) was measured at end diastole (immediately prior to mitral valve opening) utilising the 2- and 4-chamber views using the biplane method of discs. RV parameters were measured using an RV-focused apical 4-chamber view. Tricuspid annulus planar systolic excursion (TAPSE) was measured as the systolic displacement of the lateral tricuspid annulus. Peak velocity of the lateral tricuspid annulus in systole (RVS') was assessed using tissue Doppler imaging at the lateral tricuspid annulus. Fractional area change (FAC) was calculated as the percentage change of RV area between systole and diastole as seen on the apical RV focused view.

6.3.3 Advanced echocardiography assessments

Two-dimensional speckle-tracking echocardiography (STE) and three-dimensional analysis were performed on high frame rate images using a vendor-specific software (GE EchoPAC v206). Measurements were performed by investigators blinded to patient baseline characteristics, exercise capacity and other echocardiographic data.

RV strain was evaluated by tracing the RV endocardium in the RV-focused apical view. We analysed RV free wall strain (RV-FWS), which was derived from the average peak systolic strain of the three RV free wall segments. Similarly, LV-global longitudinal strain (LV-GLS) was assessed by tracing the LV endocardium at end systole and then calculated as the average of the 18-segments obtained across the three standard apical views. Finally, left atrial

reservoir strain (LASr) was derived from the average measure of left atrial (LA) wall deformation throughout diastole across the apical 2- and 4-chamber views.

Right ventricular full-volume three-dimensional data sets were obtained in the RV-focused apical four-chamber view. The acquisition was optimised to include the tricuspid valve, RV apex, the outflow tract and the pulmonary valve. Temporal resolution was optimised with a lower limit of at least 20 frames per second. TTE-derived 3D-RVEF was calculated using semi-automated software (GE EchoPAC v206).

Quantitation of inter- and intra-observer variability of ventricular strain and 3D-RVEF was performed in 5% of the population through repeat measurements by a second independent investigator and the original investigator at least one month later. Reproducibility of these measurements were represented by the intra-class correlation coefficient.

6.3.4 Symptom score and 6-minute walk test

Symptom scores were assessed using the Kansas City Cardiomyopathy Questionnaire (KCCQ), New York Heart Association (NYHA) functional classification and the 6MWT. The 6MWT was performed immediately after the completion of the index TTE by an investigator blinded to the patient's clinical characteristics and TTE parameters.

Performance of the 6MWT is in accordance with published society standards. (26) In brief, our 6MWT was conducted using a 30-meter course on levelled ground in a dedicated cardio-pulmonary rehabilitation gymnasium. The patient was rested in a chair prior to the commencement of the 6MWT and had their oxygen saturation, blood pressure, pulse rate and level of baseline dyspnoea recorded. At the start of the test, patients are given a standardised instruction to "walk for as far as possible in 6 minutes". They were then given standardised encouragements every minute until the 6-minute mark. If the patient stopped during the test, they are given standardised encouragements every 30 seconds. The distance travelled in meters at the end of the 6MWT is recorded as the 6MWD.

6.3.5 Statistical analysis

Unless otherwise specified, all statistical analysis was performed using the Statistical Package for Social Sciences Software (SPSS Version 22; SPSS Inc., Chicago, IL, USA). Continuous variables were presented as mean ± standard deviations. We utilised Mann-Whitney's test for between group comparison given some variables were skewered on parametric testing. Categorical variables were expressed as numbers and percentages. Chi-square or Fisher's exact test were used for investigating the association between the outcomes and selected categorical variables when appropriate. Logistic regression model was employed to identify the factors independently associated with reduction in 6MWD. All tests were 2-sided with a p-value less than 0.05 considered statistically significant.

Receiver operating characteristics (ROC) curve analysis, Z-statistics and Delong's test was performed using MedCalc Software (MedCalc software Version 23, Ostend, Belgium).

6.4.0 Results

6.4.1 Participant characteristics

Four hundred and seventy-one patients were screened, and 405 were included in the final analysis. Sixty-six patients were excluded with 37 excluded due to inability to mobilise independently, 3 excluded due to inadequate TTE image quality for analysis, 4 excluded due to finding of significant coronary disease, 2 excluded due to finding of primary valvular disease, 8 excluded due to significant pulmonary disease or untreated severe obstructive sleep apnoea, and 12 patients declined, were lost to follow up or died before participation in the study. (Figure 1)6

Of the included patients, 271 (66.9%) were male with a mean age of 60.2±16.4 years and LVEF of 40.5±10.8%. All eligible patients were stabilised on optimal guideline directed therapy

with: 394 (97.3%) prescribed a cardiac specific beta-blocker; 379 (93.6%) prescribed an angiotensin converting enzyme inhibitor, angiotensin-II-receptor blocker or combined angiotensin receptor blocker and neprilysin inhibitor (ACEI 6.4%, ARB 7.7%, ARNI 79.5%); 297 (73.3%) prescribed a mineralocorticoid receptor antagonist (MRA); and 243 (60.0%) were prescribed a sodium-glucose cotransporter-2 inhibitor (SGLT2i). Ninety-seven patients had an implanted cardiac device at the time of function capacity assessment. In detail, 23 (5.7%) had a permanent pacemaker with RV pacing, 74 (18.3%) had an implantable cardioverter defibrillator, and 33 (8.1%) had cardiac resynchronisation therapy function active on their device. (Table 1)

6.4.2 Exercise capacity

Amongst the included patients, the mean 6MWD was 333.2±134.7 meters and 152 patients (37.5%) had a reduced 6MWD to less than 300 meters. The mean KCCQ score was 63.3±9.2, and 64 (15.8%) had NYHA functional class of III or IV. (Table 1)

Figure 6.1. Consort Diagram

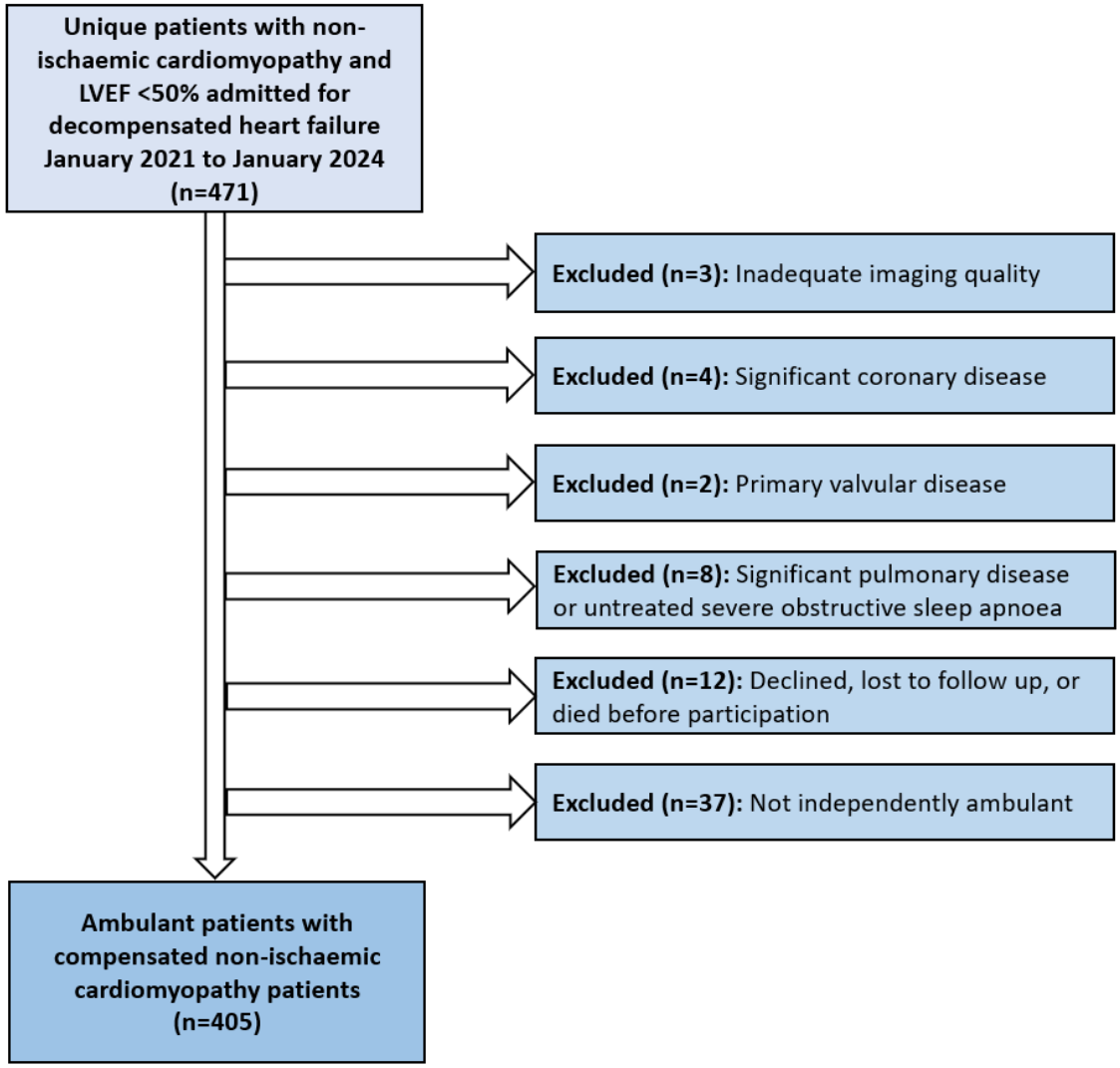

Figure 6.1. Four hundred and seventy-one patients with stable non-ischaemic cardiomyopathy were initially recruited. Three were excluded due to inadequate image quality for analysis, 4 and 2 patients were excluded for subsequent finding of significant obstructive coronary disease and primary valvular disease respectively, 8 for significant pulmonary disease or untreated obstructive sleep apnoea, 12 declined to participate were lost to follow up or died before index assessment. A further 37-patients were excluded as they were unable to ambulant without assistance from an outside party. A total of 405-patients were included for the final analysis.

Table 6.1. Baseline characteristics

Baseline Characteristics (n=405)	
Age (years)	60.2±16.4
Gender (% male)	271 (66.9)
Biplane left ventricular ejection fraction (%)	40.5±10.8
Height (cm)	169.6±10.4
Body mass index (kg/m^2)	31.6±9.6
Haemoglobin count (g/L)	137.5±20.7
Atrial fibrillation (n, %)	168 (41.5)
Permanent pacemaker (n, %)	23 (5.7)
Implantable cardioverter defibrillator (n, %)	74 (18.3)
Cardiac-resynchronisation therapy active (n, %)	23 (5.7)
Stage 4 or worse chronic kidney disease (n, %)	33 (8.1)
Hypertension (n, %)	197 (48.6)
Diabetes mellitus (n, %)	115 (28.4)
Asthma (n, %)	35 (8.6)
Chronic obstructive pulmonary disease (n, %)	43 (10.6)
New York Heart Association class III or IV (n, %)	64 (15.8)
KCCQ score	63.3±9.2
6-minute walk distance (m)	333.2±134.7
Cardio-selective beta-blockers (n, %)	394 (97.3)
Angiotensin converting enzyme inhibitor (n, %)	26 (6.4)
Angiotensin 2 receptor blocker (n, %)	31 (7.7)
Angiotensin receptor and neprilysin inhibitor (n, %)	322 (79.5)
Sodium-glucose transport protein 2 inhibitor (n, %)	297 (73.3)
Mineralocorticoid receptor antagonist (n, %)	243 (60.0)

Table 6.1. The table lists the baseline clinical characteristics and heart failure therapy of included patients.

6.4.3 Correlates of reduced exercise capacity

On Spearman's correlation, 6MWD had a positive correlation with height (r=0.28, p<0.001), haemoglobin count (r=0.28, p<0.001), LVEF (r=0.26, p<0.001), LV-GLS (r=0.30, p<0.001), LASr (r=0.42, p<0.001), TAPSE (r=0.18, p<0.001), FAC (r=0.16, p<0.001), RV-FWS (r=0.25, p<0.001), and 3D-RVEF (r=0.21, p<0.001). Additionally, an inverse correlation was found with age (r=-0.43, p<0.001), E/e' ratio (r=-0.31, p<0.001), indexed LA volume (r=-0.25, p<0.001), pulmonary artery systolic pressure (PASP; r=-0.40, p<0.001), RA area (r=-0.25 p<0.001), and RV basal diameter (r=-0.11, p<0.001). Out of the RV systolic functional parameters, RV-FWS exhibited the closest correlation. Every percentage point rise in RV-FWS corresponded to an additional 5.2 meters walked on 6MWT. (Figure 2)

6.4.4 Predictive capacity of right ventricular function for reduced exercise capacity

ROC curve analysis was employed to determine which of the echocardiographic parameters best predicted reduction in 6MWD to below 300 meters. Of the left heart parameters, LASr had the highest area under the curve (AUC) of all parameters (AUC=0.72, p<0.001), followed by LV-GLS (AUC=0.66, p<0.001), indexed LA volume (AUC=0.64, p<0.001), E/e' ratio (AUC=0.64, p<0.001) and LVEF (AUC=0.63, p<0.001). As for the right heart parameters, PASP exhibited the best performance (AUC=0.72, p<0.001), followed by RV-FWS (AUC =0.67, p<0.001), RA area (AUC=0.65, p<0.001), 3D-RVEF (AUC=0.63, p<0.001), FAC (AUC=0.61, p<0.001), RVS' (AUC=0.59, p=0.002), TAPSE (AUC=0.58, p=0.006), and RV basal diameter (AUC=0.57, p=0.014).

We further performed Delong's test to compare the performance of the RV systolic parameters against that of LASr, which had the highest AUC. TAPSE, RVS', FAC and 3D-RVEF all showed significantly worse performance compared to LASr (p<0.001, p=0.004, p<0.001, p=0.009 respectively). RV-FWS was the only RV systolic parameter not significant different to LASr (p=0.053). (Figure 3)

Figure 6.2. Correlation between right ventricular strain and 6-minute walk distance

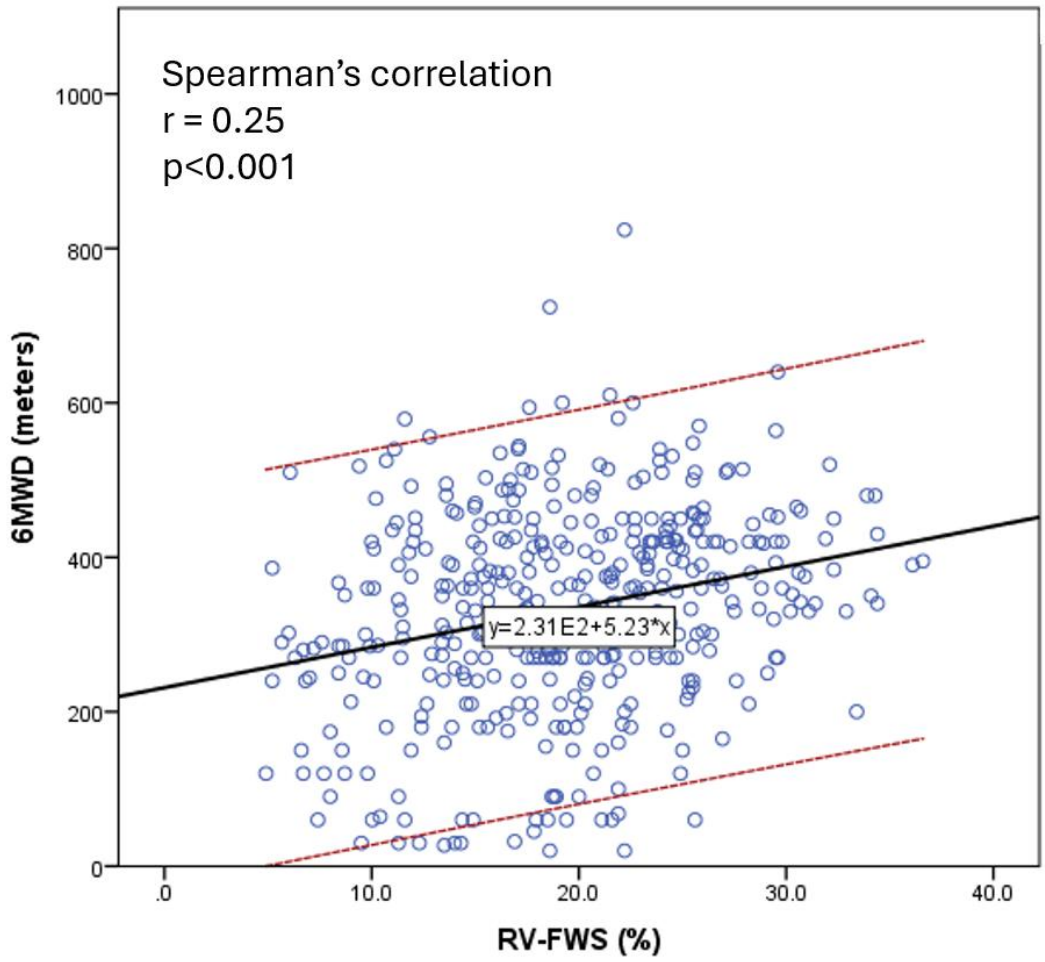

Figure 6.2. Spearman's correlation: Right ventricular free wall strain was associated with 6-minute walk distance. There was a 5.2-meter increase in the distance walked for every percentage increase in strain value.

Abbreviations. *6MWD: 6-minute walk distance, RV-FWS: right ventricular free wall strain*

Table 6.2. Comparison between preserved and reduced 6-minute walk distance groups

	6MWD ≥300m (n=261)	6MWD <300m (n=144)	Significance (p-value)
Male gender (n, %)	**194 (74.8)**	**81 (53.6)**	**<0.001**
Age (years)	**56.6±15.4**	**66.3±16.3**	**<0.001**
Height (cm)	**171.3±9.7**	**166.7±10.9**	**<0.001**
Obesity (n, %)	119 (46.9)	85 (56.3)	0.081
Atrial fibrillation (n, %)	**74 (29.6)**	**94 (62.7)**	**<0.001**
PPM (n, %)	12 (4.8)	11 (7.3)	0.375
ICD (n, %)	40 (15.9)	34 (22.45	0.111
CRT (n, %)	20 (7.9)	13 (8.6)	0.852
Stage 4 or worse CKD (n, %)	15 (5.9)	15 (9.9)	0.169
Hypertension (n, %)	**108 (42.5)**	**89 (58.9)**	**0.001**
Diabetes mellitus (n, %)	70 (27.6)	45 (29.8)	0.650
Asthma (n, %)	25 (9.8)	10 (6.6)	0.361
COPD (n, %)	**19 (7.5)**	**24 (15.9)**	**0.012**
Haemoglobin (g/L)	**140.8±18.2**	**131.9±23.3**	**<0.001**
NT pro-BNP (ng/L)	55552.4±17178.0	4380.8±15400.2	0.587
Biplane LVEF (%)	**42.4±10.1**	**37.4±11.3**	**<0.001**
LV-GLS (%)	**12.3±3.7**	**10.1±3.9**	**<0.001**
E/e' ratio	**11.9±5.6**	**15.1±8.1**	**<0.001**
Indexed LA volume (ml/m^2)	**42.0±24.6**	**48.8±20.0**	**0.002**
LASr (%)	**19.5±9.4**	**12.5±7.6**	**<0.001**
Right atrial area (cm^2)	**17.0±6.9**	**20.3±7.8**	**<0.001**
PASP (mmHg)	**21.3±12.1**	**31.7±13.5**	**<0.001**
RV basal diameter (cm)	**36.2±8.4**	**38.1±10.2**	**0.034**
TAPSE (cm)	**1.9±0.5**	**1.8±0.5**	**0.004**
RVS' (cm/s)	**9.6±2.9**	**8.6±2.8**	**0.002**
Fractional area change (%)	**40.7±11.1**	**36.6±12.0**	**<0.001**
RV-free wall strain (%)	**20.9±6.5**	**17.2±6.1**	**<0.001**
3D-RVEF (%)	**49.2±7.9**	**45.7±8.7**	**0.001**

Table 6.2. Lists and compares the clinical and echocardiographic variables between the those with preserved and reduced 6-minute walk distance. Categorical variables were compared using Chi-square or Fisher exact test. Continuous variables were compared using Mann-Whitney test.

Abbreviations. *PPM: permanent pacemaker, ICD: automated implantable cardioverter defibrillator, CRT: cardiac resynchronisation therapy, CKD: chronic kidney disease, eGFR: estimated glomerular filtration rate, COPD: chronic obstructive pulmonary disease, NYHA:*

New York Heart Association, KCCQ: Kansas City Cardiomyopathy Questionnaire, LVEF: left ventricular ejection fraction, LV-GLS: average left ventricular global longitudinal strain, LA: left atrial, LASr: left atrial reservoir strain, PASP: pulmonary artery systolic pressure, RV: right ventricular, TAPSE: tricuspid annular plane systolic excursion, RVS': peak velocity of the lateral tricuspid annulus in systole, 3D-RVEF: three-dimensional right ventricular ejection fraction.

6.4.5 Determinates of reduced exercise capacity

We performed between group analysis of the clinical characteristics and echocardiographic parameters of those with preserved and reduced 6MWD to below 300 meters.

For the clinical characteristics, the reduced 6MWD group tended to be female (46.4 vs 25.2% female, p<0.001), were shorter (66.3±16.3 vs 56.6±15.4 m, p<0.001), had lower haemoglobin count (131.9±23.3 vs 140.8±18.2, p<0.001), with higher prevalence of AF (62.7 vs 29.6%, p<0.001), hypertension (58.9 vs 42.5%, p=0.001) and chronic obstructive pulmonary disease (COPD; 15.9 vs 7.5%, p=0.012). In terms of echocardiographic parameters, the reduced 6MWD group had higher E/e' ratio (15.1±8.1 vs 11.9±5.6, p<0.001), indexed LA volume (48.8±20.0 vs 42.0±24.6 ml/m^2, p=0.002), right atrial (RA) area (20.3±7.8 vs 17.0±6.9 cm^2, p<0.001), RV basal diameter (38.1±10.2 vs 36.2±8.4 cm, p=0.034), and pulmonary artery systolic pressure (PASP; 31.7±13.5 vs 21.3±12.1 mmHg, p<0.001), but had a lower LVEF (37.4±11.3 vs 42.4±10.1%, p<0.001), LV-GLS (10.1±3.9 vs 12.3±3.7%, p<0.001), LASr (12.5±7.6 vs 19.5±9.4%, p<0.001), TAPSE (1.8±0.5 vs 1.9±0.5, p=0.004), RVS' (8.6±2.8 vs 9.6±2.9 cm/s, p=0.002), FAC (36.6±12.0 vs 40.7±11.1%, p<0.001), RV-FWS (17.2±6.1 vs 20.9±6.5%, p<0.001) and 3D-RVEF (45.7±8.7 vs 49.2±7.9, p=0.001). (Table 2)

Figure 6.3. Receiver operating characteristic curves of right ventricular systolic functional parameters in comparison to left atrial reservoir strain on DeLong's test

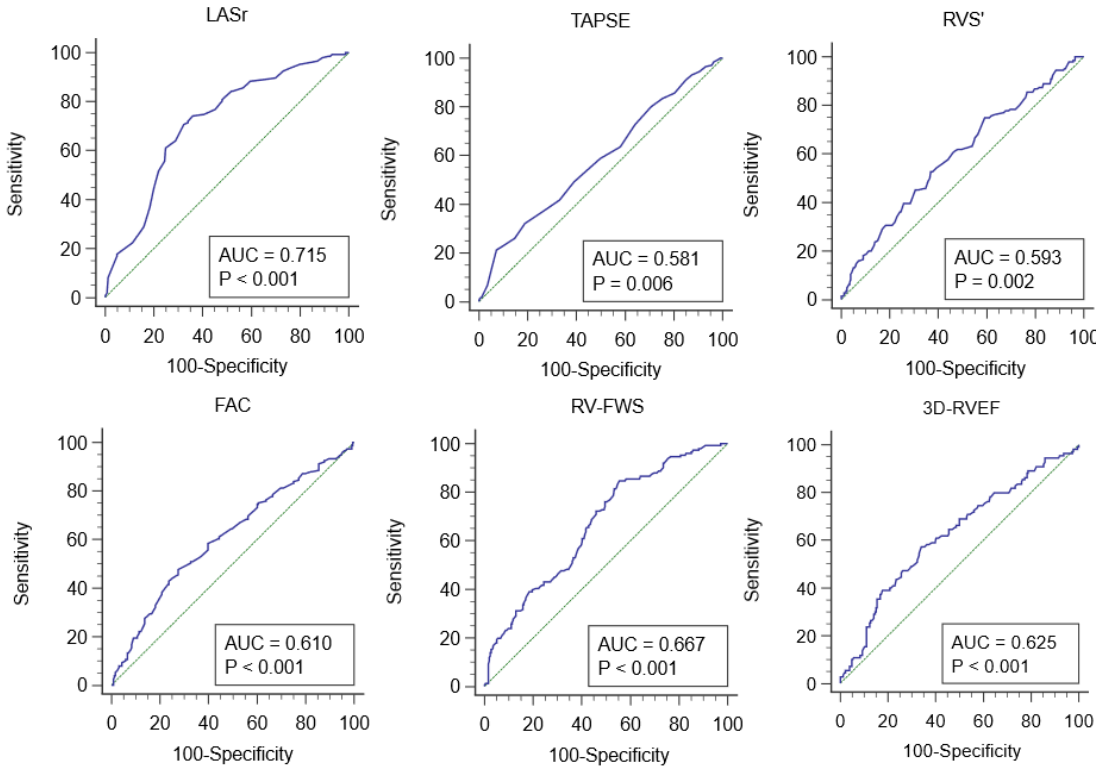

Echocardiographic Parameter	AUC	Standard Error	95% Confidence Interval	z statistic	DeLong's test pairwise comparison to LASr
LASr	0.714	0.030	0.662 to 0.762	N/A	N/A
TAPSE	0.594	0.034	0.539 to 0.648	3.180	p=0.002
RVS'	0.608	0.034	0.553 to 0.662	2.850	p=0.004
FAC	0.582	0.035	0.526 to 0.636	3.652	p=0.001
RV-FWS	0.651	0.032	0.596 to 0.702	1.934	p=0.053
3D-RVEF	0.621	0.034	0.566 to 0.674	2.613	p=0.009

Figure 6.3. Right ventricular free wall strain had the best predictive capacity for reduced 6-minute walk distance to below 300 meters amongst the right ventricular functional parameters and was the only factor not significantly different to left atrial reservoir strain on DeLong's test.

Abbreviations. *LASr: left atrial reservoir strain, TAPSE: tricuspid annular plane systolic excursion, RVS': Peak velocity of the lateral tricuspid annulus in systole, FAC: fractional area change, RV-FWS: right ventricular free wall strain, 3D-RVEF: three-dimensional right ventricular ejection fraction.*

6.4.6 Independent predictors of reduced exercise capacity

Multivariate logistic regression was performed to determine the independent predictors of reduced 6MWD. We included all clinical and echocardiographic variables found to be significant on between group analysis into a two-stage nested model to avoid overfitting.

The clinical variables included into the stage 1A model were gender, age, height, haemoglobin count, presence of AF, hypertension and COPD. The echocardiographic parameters included into the stage 1B model were LVEF, LV-GLS, E/e' ratio, indexed LA volume, LASr, PASP, RA area, RV basal diameter, TAPSE, RVS', FAC, RV-FWS, and 3D-RVEF. Of the stage 1A and 1B models, height, AF, hypertension, COPD, haemoglobin count, LASr, PASP and RV-FWS were found to be significant. These were then combined into the stage 2 model, which confirmed height in centimetres (OR 0.95, 95% CI 0.92-0.97, p<0.001), AF (OR 3.15, 95% CI 1.77-5.60, p<0.001), hypertension (OR 2.24, 95% CI 1.26-3.97, p=0.006), COPD (OR 5.16, 95% CI 2.04-13.05, p=0.001), haemoglobin count (OR 0.98, 95% CI 0.97-1.00 p=0.020), PASP (OR 1.04, 95% CI 1.01-1.06, p=0.001), and RV-FWS (OR 0.90, 95% CI 0.85-0.94, p<0.001) to be independently associated with reduced 6MWD to below 300 meters. (Table 3)

Amongst the RV systolic parameters, only RV-FWS was independently associated with reduction in 6MWD to below 300m. Furthermore, each percentage drop in RV-FWS was independently associated with a 10% increased likelihood of 6MWD reduction to below 300 meters. (Figure 4)

Table 6.3. Two-stage multivariate Cox proportional hazard model

Model 1A: Clinical Factors	**Adjusted Hazard Ratio (95% CI)**	**Adjusted p-value**
Height (cm)	0.96 (0.94-0.99)	<0.001
Atrial fibrillation	4.50 (2.83-7.16)	<0.001
Hypertension	1.68 (1.03-2.65)	0.027
COPD	2.63 (1.28-5.42)	0.009
Haemoglobin count (g/L)	0.98 (0.97-0.99)	0.002
Model 1B: Echocardiographic Parameters	**Adjusted Hazard Ratio (95% CI)**	**Adjusted p-value**
LASr (%)	0.95 (0.91-0.98)	0.008
PASP (mmHg)	1.04 (1.01-1.06)	0.006
RV-FWS (%)	0.95 (0.90-0.99)	0.039
Model 2: Final combined model	**Adjusted Hazard Ratio (95% CI)**	**Adjusted p-value**
Height (cm)	**0.95 (0.92-0.97)**	**<0.001**
Atrial fibrillation	**3.2 (1.77-5.60)**	**<0.001**
Hypertension	**2.24 (1.26-4.00)**	**0.006**
COPD	**5.2 (2.04-13.05)**	**0.001**
Haemoglobin count (g/L)	**0.98 (0.97-0.99)**	**0.020**
PASP (mmHg)	**1.04 (1.01-1.06)**	**0.002**
RV-FWS (%)	**0.90 (0.85-0.94)**	**<0.001**

Table 6.3. A two-stage multivariate Cox proportional hazard model was constructed to avoid over-fitting. Mode 1A included clinical factors: gender, age, height, haemoglobin count, prevalence of obesity, atrial fibrillation, permanent pacemaker, implantable cardioverter-defibrillator, cardiac resynchronisation therapy, hypertension, and chronic obstructive pulmonary disease. Mode 1B included echocardiographic parameters: LVEF, LV-GLS, E/e' ratio, indexed LA volume, LASr, PASP, RA area, RV basal diameter, TAPSE, RVS', FAC, RV-FWS, and 3D-RVEF. Mode 2 combined the variables found to be significant in models 1A and 1B: height, AF, hypertension, COPD, haemoglobin count, LASr, PASP and RV-FWS.

Abbreviations. *COPD: chronic obstructive pulmonary disease, LASr: left atrial reservoir strain, PASP: pulmonary artery systolic pressure, RV-FWS: right ventricular free wall strain.*

6.4.7 Reproducibility analysis

There was excellent reproducibility of RV-FWS and 3D-RVEF measurements based on the inter- and intra-observer variability. For inter-observer variability, the intra-class correlation coefficient was 0.95 (95% CI 0.92-0.97) for RV-FWS, and 0.90 (95% CI 0.78-0.96) for 3D-RVEF. For intra-observer variability, the intra-class correlation coefficient was 0.98 (95% CI 0.97-0.99) for RV-FWS, and 0.95 (95% CI 0.88-0.98) for 3D-RVEF.

6.5.0 Discussion

The primary finding of our study is twofold: firstly, RV-FWS is the best predictor of exercise capacity in NICM patients amongst the RV functional parameters on echocardiography; and secondly RV-FWS is independently associated with reduction in exercise capacity as determined by 6MWT. To our knowledge, this is the first study to establish the independent association between RV systolic dysfunction and reduced exercise capacity in NICM after accounting for clinical characteristics, left heart dysfunction as well as pulmonary pressures .

6.5.1 Right ventricular systolic function as a determinate of exercise capacity

Left heart function has been established to be the main determinate of reduced exercise capacity in HF with LASr being the strongest predictor. (27, 28) In line with current literature, our study found LASr to be the strongest echocardiographic predictor for reduced 6MWD based on ROC curve analysis. Interestingly, multivariate regression analysis did not find LASr to be independently associated with reduced 6MWD. We believe this is due to the high prevalence of AF in our cohort at 41%. Presence of AF is known to cause a sharp drop in observed LASr in a non-linear manner, which is not adjusted for by Logistic regression. Therefore, the presence of AF may have masked the impact of LASr on exercise capacity in our multivariate regression model.

Two previous studies have assessed the relationship between echocardiographic RV functional parameters and exercise capacity. In a cohort of ischaemic cardiomyopathy patients, Slijvic et al. was able to show that RV longitudinal strain and 3D-RVEF correlated with peak VO2 on CPET. (29) In a separate study examining patients referred for CRT, Zaborska et al. showed that RVS' and RV strain is independently associated with peak VO2 after adjusting for age, sex, AF and other two-dimensional RV functional parameters. (30) However, neither study accounted for the impact of pulmonary pressures, or left heart echocardiographic parameters on exercise capacity. In contrast, our study was able to establish that RV systolic function, particularly RV-FWS, maintained an independent association with 6MWD even after adjusting for all relevant clinical and echocardiographic parameters.

6.5.2 Right ventricular longitudinal versus overall contractility

RV-FWS and 3D-RVEF are both advanced echocardiographic measures of RV function that have been shown to be superior predictors of adverse cardiovascular outcomes in cardiomyopathy compared to traditional RV functional parameters. (10, 31-33) RV-FWS predominantly assess the longitudinal component of RV free wall contraction, although being the primary component of overall RV systolic function, it ignores the contribution of radial contraction or anteroposterior shortening. (34) Furthermore, RV-FWS has the advantage of being relatively load independent. (35, 36) In comparison, 3D-RVEF, a more load dependent measure, can simultaneously evaluate all three components of RV contraction and produce an accurate representation of the complex RV geometry and to reflect overall RV volumes systolic function. (10, 35, 36)

It is hypothesised that during exercise, there is incremental rise in afterload secondary to exercise-induced pulmonary hypertension. (6, 37) In a healthy RV, the longitudinal contractile force can be augmented to overcome the increased afterload. (38) Impairment of this RV

contractile reserve in diseased states have been demonstrated to correlate with reduced exercise capacity. (39)

In our study, RV-FWS exhibited superior performance to 3D-RVEF on ROC analysis and was the only RV systolic parameter to be independently associated with 6MWD reduction on multivariate regression. Therefore, the authors theorise that RV-FWS, a relatively load independent measure of RV longitudinal function, provides the best insight into RV contractile reserve, which is a vital factor in determining exercise capacity.

6.5.3 Clinical implications

Reduction in exercise capacity is a key feature of NICM symptomatology, and reduction in 6MWD has been demonstrated to correlate closely with CPET results, poorer quality of life, as well a higher incidence of adverse cardiovascular outcomes. (1, 13, 17, 40) Several studies in HF with preserved ejection fraction have shown the utility of RV systolic function in predicting exercise capacity. (3-6) Exercise capacity in NICM is still thought to be predominantly determined by the left heart and pulmonary function with little attention given to RV systolic function. (1) Our data show that RV systolic function independently contributes to exercise capacity in systolic HF and is a valuable addition to the growing body of knowledge surrounding the role of RV systolic function in NICM. Assessment of RV longitudinal strain can be performed non-invasively via TTE, a part of standard care which is both widely available and easily accessible.

Our findings support the routine assessment of RV systolic function in addition to standard left heart evaluation on echocardiography to better prognosticate exercise capacity in NICM.

6.5.4 Limitations

The main limitation of this study was the choice of 6MWT to assess submaximal exercise capacity as opposed to assessing maximal exercise capacity using graded exercise test or CPET which is the gold standard. 6MWT characterises overall exercise capacity by providing generalised insights into the cardiovascular, pulmonary and musculoskeletal systems as well as providing quality of life information. (1) Further, previous studies suggest that up to a third of HF patients may not be able to perform maximal symptom-limited exercise, which would have skewed patient selection and affected the generalisability of this study. (40, 41) Of course, 6MWT have the added benefit of being easy to administer with less contraindications and little to no risks. (42) In the literature, 6MWT is a well validated tool and a 6MWD of below 300 meters in systolic HF have been shown to predict adverse cardiovascular events and closely correlate with CPET. (1, 13, 17, 40) In a post hoc analysis of the ESCAPE trial, 6MWT but not CPET predicted all-cause mortality and HF rehospitalisation in an acute systolic HF cohort. It was hypothesised by the authors that in significant cardiac dysfunction, the effort required to complete the 6MWT would be at or close to the maximal exercise capacity. (43)

Our second limitation pertains to our study being performed in a single tertiary centre. Despite this we were still able to recruit a sizable cohort. Furthermore, the HF service from which we recruited predominantly receives referrals for patients recently hospitalised with symptomatic or decompensated HF. And as such, most of them have been hospitalised in the year prior to their referral to the service. Therefore, our cohort tended to represent those with newly compensated NICM, as opposed to patients with long-standing stable HF.

Finally, the pathophysiology and mechanics leading to reduced exercise capacity in NICM is complex and multifactorial. This study attempted to account for all biologically plausible clinical and echocardiographic variables that can affect the exercise capacity observed, but there would inevitably be factors that was not tested in our statistical model.

6.6.0 Conclusion

In this cohort of stable non-ischaemic cardiomyopathy patients, right ventricular systolic dysfunction, as assessed by right ventricular free wall strain, was independently associated with reduced 6-minute walk distance to below 300 meters, even after adjusting for clinical covariates and left heart parameters. These findings underscore the pivotal role of right ventricular longitudinal contractile function in determining exercise capacity in non-ischaemic cardiomyopathy and support the concept that right ventricular systolic function may represent a clinically relevant and potentially modifiable therapeutic target in this population.

References

1. Del Buono MG, Arena R, Borlaug BA, Carbone S, Canada JM, Kirkman DL, et al. Exercise Intolerance in Patients With Heart Failure: JACC State-of-the-Art Review. J Am Coll Cardiol. 2019;73(17):2209-25.
2. Chomsky DB, Lang CC, Rayos GH, Shyr Y, Yeoh TK, Pierson RN, 3rd, et al. Hemodynamic exercise testing. A valuable tool in the selection of cardiac transplantation candidates. Circulation. 1996;94(12):3176-83.
3. Lewis GD, Shah RV, Pappagianopolas PP, Systrom DM, Semigran MJ. Determinants of ventilatory efficiency in heart failure: the role of right ventricular performance and pulmonary vascular tone. Circ Heart Fail. 2008;1(4):227-33.
4. Reddy YNV, Olson TP, Obokata M, Melenovsky V, Borlaug BA. Hemodynamic Correlates and Diagnostic Role of Cardiopulmonary Exercise Testing in Heart Failure With Preserved Ejection Fraction. JACC Heart Fail. 2018;6(8):665-75.
5. Ishizaka S, Iwano H, Tsujinaga S, Murayama M, Tsuneta S, Aoyagi H, et al. Determinants of exercise capacity in patients with heart failure without left ventricular hypertrophy. J Cardiol. 2023;81(1):33-41.
6. Ohara K, Imamura T, Ihori H, Chatani K, Nonomura M, Kameyama T, et al. Association between Right Ventricular Function and Exercise Capacity in Patients with Chronic Heart Failure. J Clin Med. 2022;11(4).
7. Marwick TH. The role of echocardiography in heart failure. J Nucl Med. 2015;56 Suppl 4:31S-8S.
8. Monitillo F, Di Terlizzi V, Gioia MI, Barone R, Grande D, Parisi G, et al. Right Ventricular Function in Chronic Heart Failure: From the Diagnosis to the Therapeutic Approach. J Cardiovasc Dev Dis. 2020;7(2).
9. Rudski LG, Lai WW, Afilalo J, Hua L, Handschumacher MD, Chandrasekaran K, et al. Guidelines for the echocardiographic assessment of the right heart in adults: a report from the American Society of Echocardiography endorsed by the European

Association of Echocardiography, a registered branch of the European Society of Cardiology, and the Canadian Society of Echocardiography. J Am Soc Echocardiogr. 2010;23(7):685-713; quiz 86-8.

10. Mukherjee M, Rudski LG, Addetia K, Afilalo J, D'Alto M, Freed BH, et al. Guidelines for the Echocardiographic Assessment of the Right Heart in Adults and Special Considerations in Pulmonary Hypertension: Recommendations from the American Society of Echocardiography. J Am Soc Echocardiogr. 2025;38(3):141-86.
11. Enright PL. The six-minute walk test. Respir Care. 2003;48(8):783-5.
12. Rostagno C, Galanti G, Comeglio M, Boddi V, Olivo G, Gastone Neri Serneri G. Comparison of different methods of functional evaluation in patients with chronic heart failure. Eur J Heart Fail. 2000;2(3):273-80.
13. Roul G, Germain P, Bareiss P. Does the 6-minute walk test predict the prognosis in patients with NYHA class II or III chronic heart failure? Am Heart J. 1998;136(3):449-57.
14. Guazzi M, Dickstein K, Vicenzi M, Arena R. Six-minute walk test and cardiopulmonary exercise testing in patients with chronic heart failure: a comparative analysis on clinical and prognostic insights. Circ Heart Fail. 2009;2(6):549-55.
15. Giannitsi S, Bougiakli M, Bechlioulis A, Kotsia A, Michalis LK, Naka KK. 6-minute walking test: a useful tool in the management of heart failure patients. Ther Adv Cardiovasc Dis. 2019;13:1753944719870084.
16. Zugck C, Kruger C, Durr S, Gerber SH, Haunstetter A, Hornig K, et al. Is the 6-minute walk test a reliable substitute for peak oxygen uptake in patients with dilated cardiomyopathy? Eur Heart J. 2000;21(7):540-9.
17. Bittner V, Weiner DH, Yusuf S, Rogers WJ, McIntyre KM, Bangdiwala SI, et al. Prediction of mortality and morbidity with a 6-minute walk test in patients with left ventricular dysfunction. SOLVD Investigators. JAMA. 1993;270(14):1702-7.
18. Olsson LG, Swedberg K, Clark AL, Witte KK, Cleland JG. Six minute corridor walk test as an outcome measure for the assessment of treatment in randomized, blinded

intervention trials of chronic heart failure: a systematic review. Eur Heart J. 2005;26(8):778-93.

19. Heidenreich PA, Bozkurt B, Aguilar D, Allen LA, Byun JJ, Colvin MM, et al. 2022 AHA/ACC/HFSA Guideline for the Management of Heart Failure: A Report of the American College of Cardiology/American Heart Association Joint Committee on Clinical Practice Guidelines. Circulation. 2022;145(18):e895-e1032.
20. McMurray JJ, Adamopoulos S, Anker SD, Auricchio A, Bohm M, Dickstein K, et al. ESC Guidelines for the diagnosis and treatment of acute and chronic heart failure 2012: The Task Force for the Diagnosis and Treatment of Acute and Chronic Heart Failure 2012 of the European Society of Cardiology. Developed in collaboration with the Heart Failure Association (HFA) of the ESC. Eur Heart J. 2012;33(14):1787-847.
21. Authors/Task Force M, McDonagh TA, Metra M, Adamo M, Gardner RS, Baumbach A, et al. 2023 Focused Update of the 2021 ESC Guidelines for the diagnosis and treatment of acute and chronic heart failure: Developed by the task force for the diagnosis and treatment of acute and chronic heart failure of the European Society of Cardiology (ESC) With the special contribution of the Heart Failure Association (HFA) of the ESC. Eur J Heart Fail. 2024;26(1):5-17.
22. Mebazaa A, Davison B, Chioncel O, Cohen-Solal A, Diaz R, Filippatos G, et al. Safety, tolerability and efficacy of up-titration of guideline-directed medical therapies for acute heart failure (STRONG-HF): a multinational, open-label, randomised, trial. Lancet. 2022;400(10367):1938-52.
23. Lang RM, Badano LP, Mor-Avi V, Afilalo J, Armstrong A, Ernande L, et al. Recommendations for cardiac chamber quantification by echocardiography in adults: an update from the American Society of Echocardiography and the European Association of Cardiovascular Imaging. J Am Soc Echocardiogr. 2015;28(1):1-39 e14.
24. Nagueh SF, Smiseth OA, Appleton CP, Byrd BF, 3rd, Dokainish H, Edvardsen T, et al. Recommendations for the Evaluation of Left Ventricular Diastolic Function by

Echocardiography: An Update from the American Society of Echocardiography and the European Association of Cardiovascular Imaging. J Am Soc Echocardiogr. 2016;29(4):277-314.

25. Badano LP, Kolias TJ, Muraru D, Abraham TP, Aurigemma G, Edvardsen T, et al. Standardization of left atrial, right ventricular, and right atrial deformation imaging using two-dimensional speckle tracking echocardiography: a consensus document of the EACVI/ASE/Industry Task Force to standardize deformation imaging. Eur Heart J Cardiovasc Imaging. 2018;19(6):591-600.
26. Holland AE, Spruit MA, Troosters T, Puhan MA, Pepin V, Saey D, et al. An official European Respiratory Society/American Thoracic Society technical standard: field walking tests in chronic respiratory disease. Eur Respir J. 2014;44(6):1428-46.
27. Maffeis C, Morris DA, Belyavskiy E, Kropf M, Radhakrishnan AK, Zach V, et al. Left atrial function and maximal exercise capacity in heart failure with preserved and mid-range ejection fraction. ESC Heart Fail. 2021;8(1):116-28.
28. Maffeis C, Rossi A, Cannata L, Zocco C, Belyavskiy E, Radhakrishnan AK, et al. Left atrial strain predicts exercise capacity in heart failure independently of left ventricular ejection fraction. ESC Heart Fail. 2022;9(2):842-52.
29. Sljivic A, Pavlovic Kleut M, Bukumiric Z, Celic V. Association between right ventricle two- and three-dimensional echocardiography and exercise capacity in patients with reduced left ventricular ejection fraction. PLoS One. 2018;13(6):e0199439.
30. Zaborska B, Smarz K, Makowska E, Czepiel A, Swiatkowski M, Jaxa-Chamiec T, et al. Echocardiographic predictors of exercise intolerance in patients with heart failure with severely reduced ejection fraction. Medicine (Baltimore). 2018;97(28):e11523.
31. Carluccio E, Biagioli P, Alunni G, Murrone A, Zuchi C, Coiro S, et al. Prognostic Value of Right Ventricular Dysfunction in Heart Failure With Reduced Ejection Fraction: Superiority of Longitudinal Strain Over Tricuspid Annular Plane Systolic Excursion. Circ Cardiovasc Imaging. 2018;11(1):e006894.

32. Carluccio E, Biagioli P, Lauciello R, Zuchi C, Mengoni A, Bardelli G, et al. Superior Prognostic Value of Right Ventricular Free Wall Compared to Global Longitudinal Strain in Patients With Heart Failure. J Am Soc Echocardiogr. 2019;32(7):836-44 e1.
33. Vijiiac A, Onciul S, Guzu C, Verinceanu V, Bataila V, Deaconu S, et al. The prognostic value of right ventricular longitudinal strain and 3D ejection fraction in patients with dilated cardiomyopathy. Int J Cardiovasc Imaging. 2021;37(11):3233-44.
34. Badano LP, Addetia K, Pontone G, Torlasco C, Lang RM, Parati G, et al. Advanced imaging of right ventricular anatomy and function. Heart. 2020;106(19):1469-76.
35. Vijiiac A, Onciul S, Guzu C, Scarlatescu A, Petre I, Zamfir D, et al. Forgotten No More-The Role of Right Ventricular Dysfunction in Heart Failure with Reduced Ejection Fraction: An Echocardiographic Perspective. Diagnostics (Basel). 2021;11(3).
36. Randazzo M, Maffessanti F, Kotta A, Grapsa J, Lang RM, Addetia K. Added value of 3D echocardiography in the diagnosis and prognostication of patients with right ventricular dysfunction. Front Cardiovasc Med. 2023;10:1263864.
37. Gorter TM, van Veldhuisen DJ, Bauersachs J, Borlaug BA, Celutkiene J, Coats AJS, et al. Right heart dysfunction and failure in heart failure with preserved ejection fraction: mechanisms and management. Position statement on behalf of the Heart Failure Association of the European Society of Cardiology. Eur J Heart Fail. 2018;20(1):16-37.
38. Gomez-Arroyo J, Santos-Martinez LE, Aranda A, Pulido T, Beltran M, Munoz-Castellanos L, et al. Differences in right ventricular remodeling secondary to pressure overload in patients with pulmonary hypertension. Am J Respir Crit Care Med. 2014;189(5):603-6.
39. Claeys M, Claessen G, La Gerche A, Petit T, Belge C, Meyns B, et al. Impaired Cardiac Reserve and Abnormal Vascular Load Limit Exercise Capacity in Chronic Thromboembolic Disease. JACC Cardiovasc Imaging. 2019;12(8 Pt 1):1444-56.

40. Rostagno C, Olivo G, Comeglio M, Boddi V, Banchelli M, Galanti G, et al. Prognostic value of 6-minute walk corridor test in patients with mild to moderate heart failure: comparison with other methods of functional evaluation. Eur J Heart Fail. 2003;5(3):247-52.

41. Guyatt GH, Sullivan MJ, Thompson PJ, Fallen EL, Pugsley SO, Taylor DW, et al. The 6-minute walk: a new measure of exercise capacity in patients with chronic heart failure. Can Med Assoc J. 1985;132(8):919-23.

42. Malhotra R, Bakken K, D'Elia E, Lewis GD. Cardiopulmonary Exercise Testing in Heart Failure. JACC Heart Fail. 2016;4(8):607-16.

43. Omar HR, Guglin M. Prognostic value of 6-minute walk test and cardiopulmonary exercise test in acute heart failure (from the ESCAPE trial). Am Heart J Plus. 2021;1:100005.

CHAPTER SEVEN

Three-dimensional right ventricular ejection fraction independently predicts cardiovascular death and heart failure hospitalisation in patients with non-ischaemic cardiomyopathy

7.0 Abstract

Background: Right ventricular (RV) dysfunction is associated with adverse outcomes in cardiomyopathy. Conventional transthoracic echocardiographic (TTE) measures of RV function assess either radial or longitudinal contraction. Three-dimensional RV ejection fraction (3D-RVEF) is an advanced measure incorporating both components. We aimed to evaluate the prognostic value of 3D-RVEF in patients with stable heart failure (HF) secondary to non-ischaemic cardiomyopathy (NICM).

Material and methods: We prospectively recruited consecutive patients with HF secondary to NICM with left ventricular ejection fraction (LVEF) <50%, excluding those with congenital heart disease, primary valvular disease, obstructive coronary disease, severe pulmonary hypertension or severe pulmonary disease. Participants were optimised on guideline-directed-therapy for >3-months in a dedicated HF clinic before index TTE and followed for the primary-outcome of cardiovascular death (CV-death) and HF-related hospitalisation (HFH).

Results: Of the 442-patients included (66.7% men, mean-age 60.7±16.4yrs, mean LVEF 31.8±9.0%), 80 met the primary-outcome during a median follow-up of 23.1-months. 3D-RVEF cutoff of <44.7% best discriminated for the primary outcome on receiver operating characteristics curve analysis using Youden's method (AUC: 0.84, sensitivity 77%, specificity 85%; Figure 1). On log-rank analysis, 3D-RVEF <44.7% was associated with reduced freedom from the primary-outcome as a function of time (p<0.001). In our two-stage multivariable Cox-regression model, 3D-RVEF <44.7% was the only RV functional parameter independently associated with the primary-outcome after adjusting for LV global longitudinal strain, E/e' ratio, left atrial reservoir strain, chronic kidney disease and implantable defibrillator (p<0.001, adjusted-HR: 6.21, 95%CI: 3.26-11.85).

Conclusion: In patients with compensated NICM, 3D-RVEF <44.7% provided best discrimination for and independently conferred a 6.2-fold increased risk of CV-death and HFH. 3D-RVEF may help identify high-risk patients which may benefit from intensification of HF-therapy.

Graphical abstract

GRAPHICAL ABSTRACT: A cohort of 442-patients with compensated non-ischaemic cardiomyopathy underwent baseline transthoracic echocardiography and were followed up for up to 36-months for the primary outcome of cardiovascular death and heart failure hospitalisation. Of the right ventricular echocardiographic parameters, 3D right ventricular ejection fraction of <44.7% best discriminated for the primary outcome on receiver operating characteristics curve analysis. A reduction of 3D right ventricular ejection fraction <44.7% was associated with increased incidence of the primary outcome on Kaplan Meier survival analysis and is independently associated with the primary outcome after adjusting for relevant clinical and echocardiographic variables on multivariate regression.

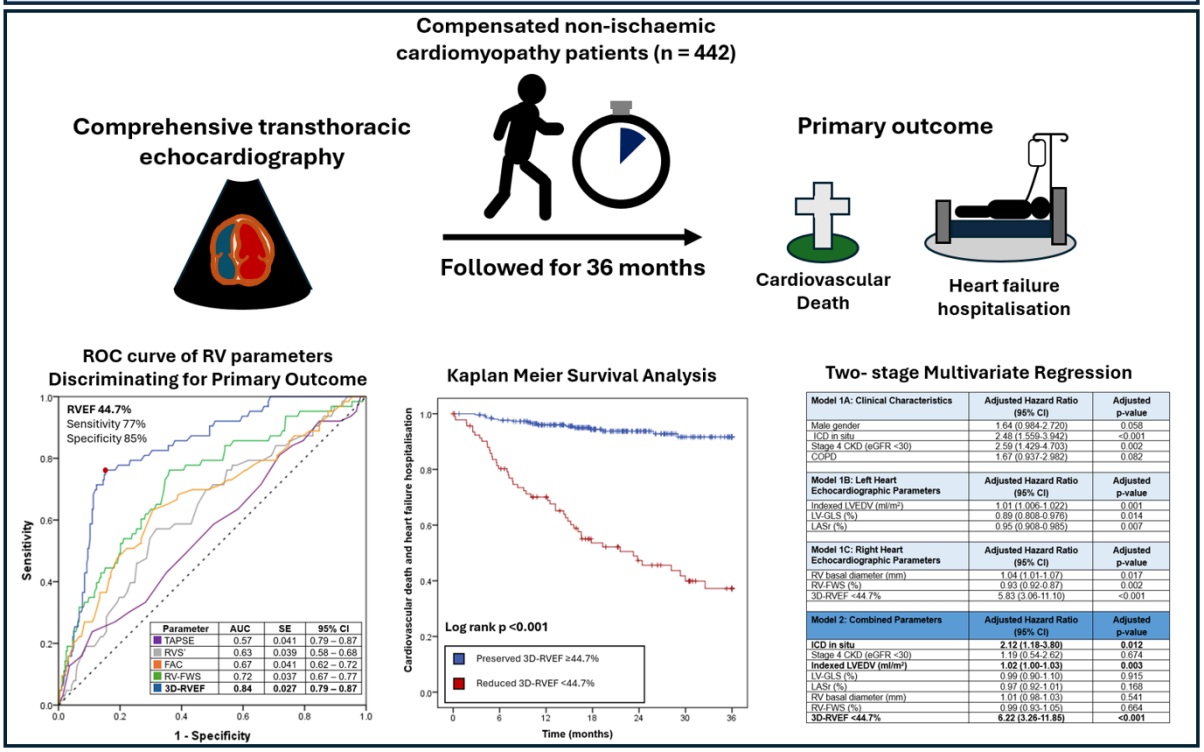

Abbreviations. *ROC: receiver operating characteristics, 3D-RVEF: three-dimensional right ventricular ejection fraction, RV: right ventricular, RV-FWS: right ventricular free wall strain, ICD: implantable cardioverter defibrillator, CKD: chronic kidney disease, COPD: chronic obstructive pulmonary disease, LVEDV: left ventricular end diastolic volume, LV-GLS: left ventricular global longitudinal strain, LASr: left atrial reservoir strain.*

Keywords: Heart failure; Right ventricle; Cardiomyopathy; Echocardiography

Abbreviations:

RV = Right ventricular / right ventricle

CMR-RVEF = Cardiac magnetic resonance imaging derived right ventricular ejection fraction

RVEF = Right ventricular ejection fraction

TTE = Transthoracic echocardiogram

HF = Heart failure

LV = Left ventricular / left ventricle

FAC = Fractional area change

STE = Speckle tracking echocardiogram

3D-RVEF = Three-dimensional right ventricular ejection fraction

NICM = Non-ischaemic cardiomyopathy

OSA = Obstructive sleep apnoea

CV death = Cardiovascular death

HFH = Heart failure hospitalisation

LAV = Left atrial volume

TAPSE = Tricuspid annulus planar systolic excursion

RVS' = Peak velocity of the lateral tricuspid annulus in systole

RV-FWS = Right ventricular free wall strain

LV-GLS = Left ventricular global longitudinal strain

LASr = Left atrial reservoir strain

ICD = Implantable cardioverter defibrillator

CKD = Chronic kidney disease

GGT = Gamma-glutamyl transferase

COPD = Chronic obstructive pulmonary disease

RV-GLS = Right ventricular global longitudinal strain

7.1.0 Introduction

Right ventricular (RV) dysfunction is a well-recognised determinant of adverse cardiovascular outcomes in heart failure (HF) and cardiomyopathies. (1, 2) However, quantifying and defining RV dysfunction remains challenging due to the RV's complex geometry and load dependency. Accurate assessment of RV systolic function requires evaluation of three components of its systolic contraction: radial contraction; longitudinal contraction; and antero-posterior contraction. (3)

Cardiac magnetic resonance imaging-derived RV ejection fraction (CMR-RVEF) can simultaneously assess all three components of RV contraction and is often heralded as the gold-standard for RV functional assessment, yet its widespread use is limited by accessibility, availability and cost. (4, 5) In contrast, transthoracic echocardiography (TTE) remains the most widely used imaging modality in the investigation and management of HF and cardiomyopathies, though no single widely accepted TTE derived parameter has been established as the standard reference for evaluating RV systolic function. (3, 6) Among the conventional TTE RV measures, fractional area change (FAC) primarily reflects radial contraction, while tricuspid annulus planar systolic excursion (TAPSE), peak velocity of the lateral tricuspid annulus in systole (RVS'), and RV free wall strain (RV-FWS) derived from speckle tracking echocardiogram (STE), provides insight into RV longitudinal function. More recently, TTE-derived three-dimensional right ventricular ejection fraction (3D-RVEF) has emerged as a parameter that integrates all three components of RV contraction to offer geometrically accurate assessment of overall RV systolic function. (3)

CMR-RVEF has demonstrated prognostic significance across cardiomyopathy cohorts, including those with non-ischaemic cardiomyopathy (NICM). (7, 8) Similarly, 3D-RVEF has shown similar prognostic value in patients across a wide range of cardiovascular diseases including acute systolic HF. (9, 10) However, since 3D-RVEF is influenced by ventriculo-arterial coupling, it is highly load dependent and may be less reliable in acute or

decompensated HF. (11) Assessing 3D-RVEF in stable, compensated HF may therefore offer more accurate measure of intrinsic RV contractility.

7.2.0 Objectives and aims

Our study aims to evaluate the prognostic value of 3D-RVEF in predicting adverse cardiovascular events in a cohort of patients with compensated NICM.

7.3.0 Material and methods

7.3.1 Study population

We prospectively recruited consecutive patients aged ≥18 years with a diagnosis of NICM, a left ventricular ejection fraction of <50%, and attended our HF service from January 2021 to January 2024.

We excluded patients with a history of significant coronary artery disease (defined as ≥70% diameter stenosis in any of the three main coronary arteries, prior coronary intervention or bypass surgery, evidence of impaired myocardial perfusion or reversible ischemia on non-invasive imaging), primary valvular disease, valve replacement or repair, congenital heart disease, prior cardiac surgery, severe pulmonary hypertension, restrictive or obstructive pulmonary disease requiring hospitalisation, recent pulmonary embolism within 6 months and those with untreated obstructive sleep apnoea (OSA). Patients with non-cardiac comorbidities which limited their life expectancy to <1 year, and those with incomplete medical history or inadequate TTE image quality for analysis were also excluded.

All patients were followed up through a dedicated HF clinic where optimal guideline-directed therapy was rapidly initiated and up-titrated based on guideline recommendation. (12-15)

A comprehensive index TTE was performed once the patient has been optimised on guideline directed therapy for at least three months. (14)

7.3.2 Follow up and outcomes

Eligible participants were followed up to 36-months from the date of their index TTE for the primary composite outcome of cardiovascular death (CV death) and HF hospitalisation (HFH).

7.3.3 Transthoracic echocardiography

All TTEs were performed using commercially available echocardiogram systems (Vivid E-95, 4Vc probe, General Electric Vingmed, Horton, Norway) in accordance with American Society of Echocardiography guideline recommendations. (16-19) Electrocardiogram gated loops of at least five cardiac cycles were acquired for both analyses. For patients in atrial fibrillation at the time of the study, the reported value was the mean measurement over at least five cardiac cycles.

In brief, LV volume and ejection fraction were calculated using modified Simpson's biplane method. Left atrial volume (LAV) was measured at end diastole (immediately prior to mitral valve opening) utilising the 2- and 4-chamber views using the biplane method of discs. RV parameters were measured using a RV-focused apical 4-chamber view. Tricuspid annulus planar systolic excursion (TAPSE) was measured as the systolic displacement of the lateral tricuspid annulus. Peak velocity of the lateral tricuspid annulus in systole (RVS') was assessed using tissue Doppler imaging at the lateral tricuspid annulus.

7.3.4 Advanced Echocardiography Assessments

Two-dimensional speckle-tracking echocardiography (STE) and three-dimensional analysis were performed on high-frame-rate images using a vendor-specific software (GE EchoPAC v206). Measurements were performed by investigators blinded to patient baseline characteristics, outcomes and other echocardiographic data.

RV strain was evaluated by tracing the RV endocardium in the RV-focused apical view. We analysed RV free wall strain (RV-FWS) which was derived from the average peak systolic strain of the three RV free wall segments. Similarly, LV-global longitudinal strain (LV-GLS) was assessed by tracing the LV endocardium at end systole and then calculated as the average of the 18-segments obtained across the three standard apical views. Finally, left atrial reservoir strain (LASr) was the average measure of left atrial (LA) wall deformation throughout diastole across the apical 2- and 4-chamber views.

RV full-volume three-dimensional data sets were obtained in the RV-focused apical four-chamber view. The acquisition was optimised to include the tricuspid valve, RV apex, the outflow tract and the pulmonary valve. Temporal resolution was also optimised to target at least 20 frames per second. TTE derived 3D-RVEF was calculated using semi-automated software (GE EchoPAC v206).

Quantitation of inter- and intra-observer variability of ventricular strain and 3D-RVEF was performed in 5% of the population through repeat measurements by a second independent investigator as well as the original investigator at least one month later. Reproducibility of these measurements were represented by the intra-class correlation coefficient.

7.3.5 Statistical analysis

All statistical analysis was performed using the Statistical Package for Social Sciences Software (SPSS Version 22; SPSS Inc., Chicago, IL, USA). Continuous variables were presented as mean ± standard deviations. We utilised Mann-Whitney's test for between group comparison given some variables were skewered on parametric testing. Categorical variables

were expressed as numbers and percentages. Chi-square or Fisher's exact test were used for investigating the association between the outcomes and selected categorical variables when appropriate. Receiver operating characteristics (ROC) curve analysis, Z-statistics and Delong's test was performed using MedCalc Software (MedCalc software Version 23, Ostend, Belgium). Youden's index method was utilised to identify the optimal cutoff value associated with the primary outcome. Event rates were then estimated by Kaplan-Meier survival analysis. Finally, a multivariate Cox-regression analysis was employed to identify the factors independently associated with the primary outcome. All tests were 2-sided with a p-value less than 0.05 were considered statistically significant.

7.4.0 Results

7.4.1 Participant characteristics

Four hundred and seventy-one patients with non-ischaemic cardiomyopathy referred to the HF service during the study period were screened, of which 442-patients were included in the final analysis. Twenty-nine patients (6%) were excluded with 3 due to inadequate TTE image quality for analysis, 4 due to finding of significant coronary disease, 2 due to finding of primary valvular disease, 8 due to significant pulmonary disease or untreated severe obstructive sleep apnoea, 12 declined, were lost to follow up or died before participation in the study. (Figure 1)

Amongst the included patients, 295 (66.7%) were male with a mean age of 60.67±16.44 years and mean baseline LVEF of 31.8±9.0%. Seventy-one (16.1%) patients had New York Heart Association functional (NYHA) class III or IV symptoms at index TTE.

Three hundred and fifty (78.2%) patients were prescribed three or more pillars of HF therapy. In detail, 425 (96.2%) were prescribed a cardiac-specific beta-blocker; 413 (93.4%) were prescribed an angiotensin converting enzyme inhibitor, angiotensin-II-receptor blocker or combined angiotensin receptor blocker and neprilysin inhibitor (ACEI 7.5%, ARB 7.9%, ARNI

78.1%); 318 (71.9%) were prescribed a mineralocorticoid receptor antagonist (MRA) and 262 (59.3%) were prescribed a sodium-glucose cotransporter-2 inhibitor (SGLT2i). (Table 1)

On index TTE at least 3 months after optimisation of HF therapy, mean LVEF was 40.5±10.8%, indexed LV end diastolic volume (LVEDV) was 66.4±29.1 ml/m^2, indexed LV systolic volume (LVESV) was 41.3±23.8 ml/m^2, LV-GLS was 11.9±4.0%, E/e' ratio was 11.9±4.0, indexed left atrial volume (LAV) was 44.5±22.9ml/m^2, LASr was 16.8±9.3%, tricuspid annular planar systolic excursion (TAPSE) was 1.9±0.5, lateral tricuspid annulus peak systolic velocity (RVS') was 9.3±2.9, fractional area change (FAC) was 39.0±11.5%, RV-FWS was 19.3±6.6%, and 3D-RVEF was 47.9±8.4%. (Table 1)

Figure 7.1. Consort diagram

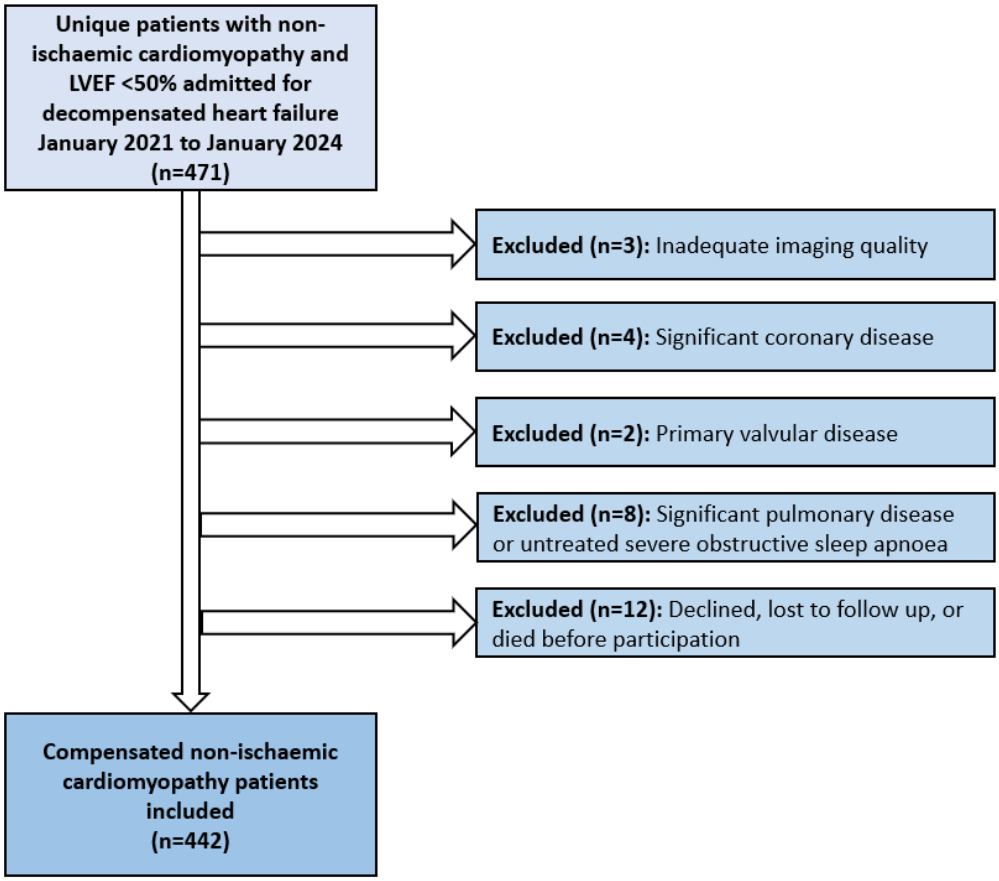

Figure 7.1. Of the 471 patients initially recruited, 3 were excluded due to inadequate echocardiographic imaging quality, 4 due to finding of significant obstructive coronary disease, 2 due to finding of primary valvular dysfunction, 8 due to significant pulmonary disease or untreated severe obstructive sleep apnoea, and 12 declined to participate, were lost to follow up or died before enrolment.

Table 7.1. Participant characteristics

Participant Characteristics (n=442)	
Age (years)	60.67±16.44
Male gender (%)	295 (66.7)
NYHA functional class III or IV	71 (16.1)
Cardiac specific beta-blocker	413 (93.4)
Angiotensin converting enzyme inhibitor (ACE-I)	33 (7.5)
Angiotensin II receptor blocker (ARB)	35 (7.9)
Angiotensin receptor neprilysin inhibitor (ARNI)	345 (78.1)
Mineralocorticoid receptor antagonist (MRA)	318 (71.9)
Sodium-glucose transport protein 2 inhibitor (SGLT2-i)	262 (59.3)
Indexed left ventricular end diastolic volume (ml/m^2)	66.4±29.1
Indexed left ventricular end diastolic volume (ml/m^2)	41.2±23.8
Left ventricular ejection fraction (%)	40.5±10.8
Left ventricular global longitudinal strain (%)	11.9±4.0
E/e' ratio	11.9±4.0
Indexed left atrial volume (ml/m^2)	44.5±22.9
Left atrial reservoir strain (%)	16.8±9.3
Tricuspid annular plane systolic excursion (cm)	1.9±0.5
RVS' (cm/s)	9.3±2.9
Fractional area change (%)	39.0±11.5
Right ventricular free wall strain (%)	19.3±6.6
Three-dimensional right ventricular ejection fraction (%)	47.9±8.4

Table 7.1. Describes the baseline characteristics of the included cohort.

Abbreviations. *NYHA: New York Heart Association, RVS': peak velocity of the lateral tricuspid annulus in systole.*

7.4.2 Patient follow-up

Eighty patients (18.1%) reached the composite primary outcome during a median follow-up duration of 23.1 months (IQR, 15.7-33.9), during which 30 patients (6.8%) died from a cardiovascular cause and 50 patients (11.3%) were hospitalised for decompensated HF.

7.4.3 Right ventricular ejection fraction as a discriminator for the primary outcome

ROC curve was utilised to determine the predictive capacity of all echocardiographic RV functional parameters for the primary outcome. The predictive capacity was greatest using 3D-RVEF with the largest area under the curve (AUC) value of 0.84. On DeLong's test, 3D-RVEF had significantly greater AUC compared to TAPSE (AUC=0.57, $p<0.001$), RVS' (AUC=0.63, $p<0.001$), FAC (AUC=0.67, $p<0.001$), and RV-FWS (AUC=0.72, $p=0.005$). Using Youden's index method, the optimal 3D-RVEF cutoff value for predicting the primary outcome was <44.7% (sensitivity 77%, specificity 85%). (Figure 2)

On log-rank analysis, reduction of 3D-RVEF to <44.7% was associated with reduced freedom from the primary outcome of CV death and HFH as a function of time ($p<0.001$; Figure 3). We further stratified the log-rank analysis based on three LVEF stratum to account for potential confounding from the degree of LV systolic dysfunction (i.e. LVEF <30%, 30-40%, >40%). 3D-RVEF reduction remains associated with a significant increase in the incidence of the primary outcome in all three LVEF stratums ($p<0.001$ for LVEF >40%; $p<0.001$ for LVEF 30-40%; $p=0.002$ for LVEF <30%; Figure 4).

Figure 7.2. Receiver operating characteristics curve for right ventricular parameters as a discriminator for cardiovascular death and heart failure rehospitalisation

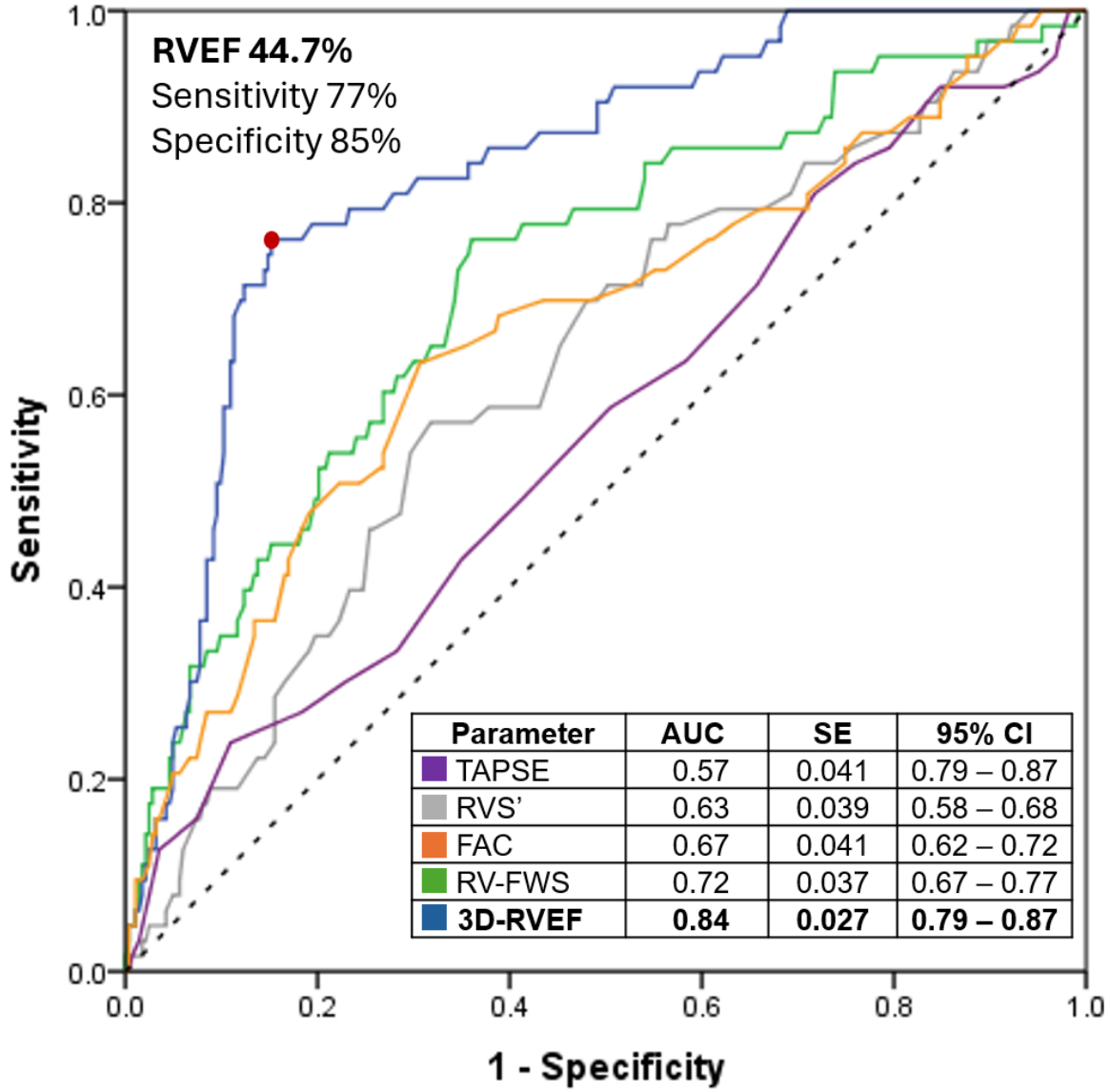

Figure 7.2. Receiver operating characteristics curve analysis of the right ventricular systolic parameters confirm that three-dimensional right ventricular ejection fraction holds the best discriminatory capacity for the primary outcome.

Abbreviations. *AUC: area under the curve, SE: standard error, CI: confidence error, TAPSE: tricuspid annular plane systolic excursion, RVS: peak velocity of the lateral tricuspid annulus in systole, RV-FWS: right ventricular free wall strain, 3D-RVEF: three-dimensional right ventricular ejection fraction.*

Figure 7.3. Kaplan-Meier survival curve of preserved versus reduced three-dimensional right ventricular ejection fraction

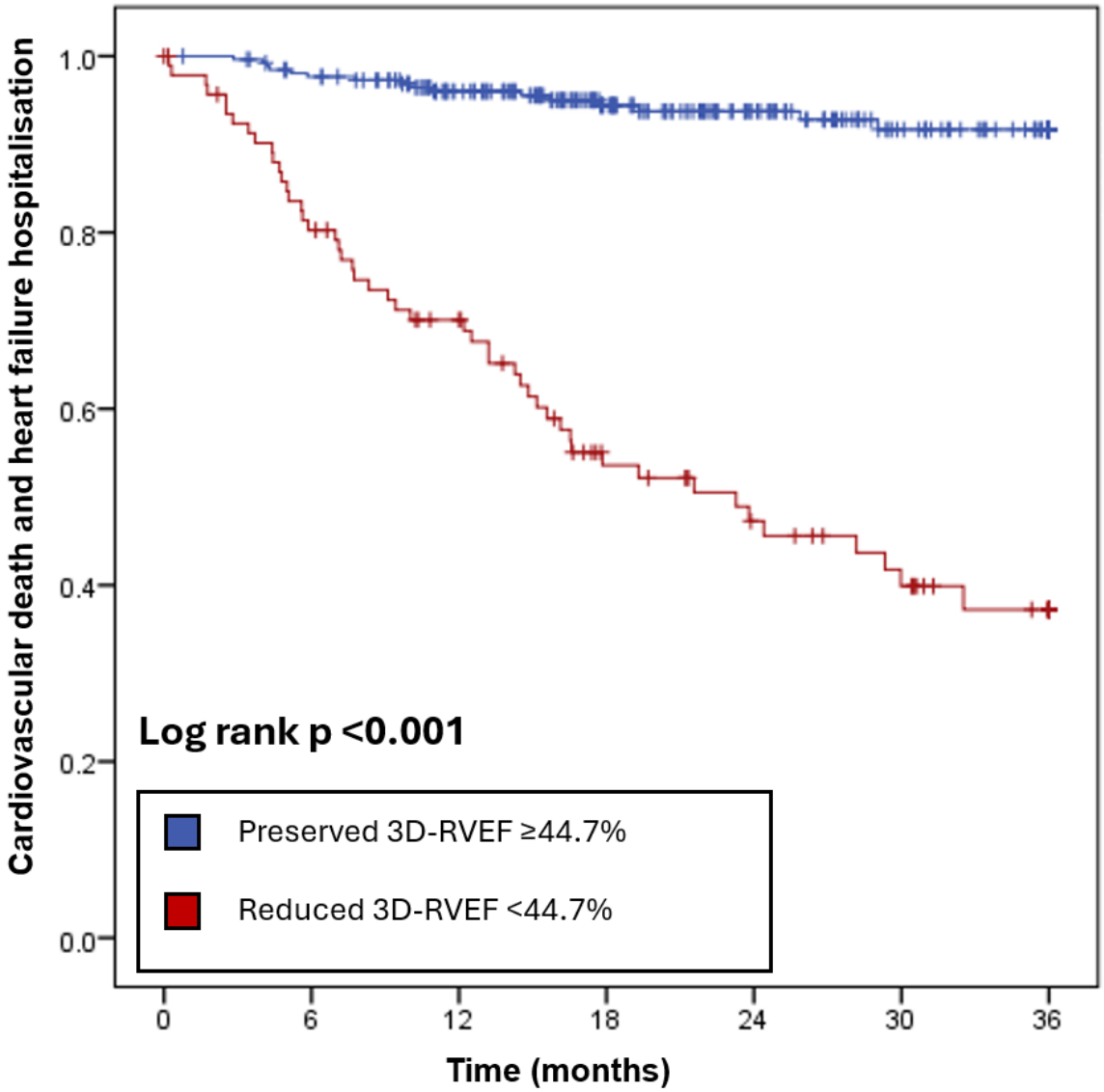

Figure 7.3. Kaplan-Meier survival curve of the combined cohort confirms that preserved three-dimensional right ventricular ejection fraction of 44.7% or higher is associated with a lower prevalence of the primary outcome as a function of time.

Abbreviations. *3D-RVEF: three-dimensional right ventricular ejection fraction*

Figure 7.4. Kaplan-Meier survival curve of preserved versus reduced three-dimensional right ventricular ejection fraction across left ventricular systolic impairment stratum

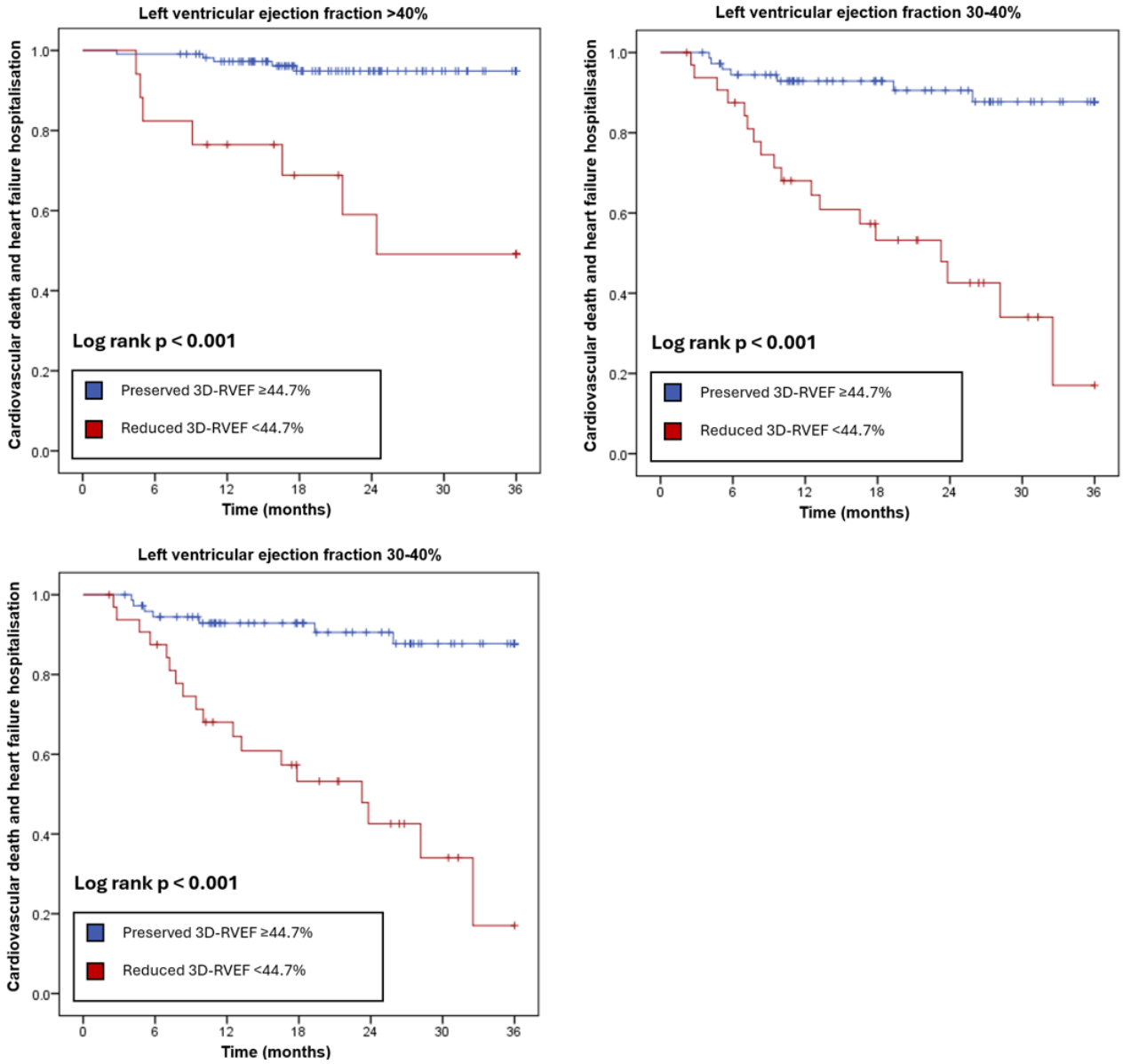

Figure 7.4. Kaplan-Meier survival curves demonstrated preserved three-dimensional right ventricular ejection fraction of 44.7% or higher is associated with lower incidence of the primary outcome as a function of time in each left ventricular systolic impairment subgroup.

Abbreviations. *3D-RVEF: three-dimensional right ventricular ejection fraction*

7.4.4 Univariate predictors of cardiovascular death and heart failure hospitalisation

We conducted a between-group analysis comparing patients who remained free from and those who reached the primary outcome. Categorical variables were analysed using the Chi-square or Fisher's exact test, while continuous variables were assessed using Mann-Whitney's test.

Among the categorical variables, atrial fibrillation (p=0.03), implantable cardioverter defibrillator (ICD) in situ (p<0.01), and stage 4 or worse chronic kidney disease (CKD; p<0.01) were significantly more prevalent in those who reached our primary outcome. (Table 2)

For continuous variables, those who reached the primary outcome tended to have lower haemoglobin count, estimated glomerular filtration rate (eGFR), systolic blood pressure, diastolic blood pressure, LVEF, LV stroke volume, RVS', LV-GLS, LASr, FAC, RV-FWS, and 3D-RVEF (p=0.01 for LV stroke volume, otherwise all p<0.01), but had higher gamma-glutamyl transferase (GGT), indexed LVEDV, indexed LVESV, E/e' ratio, iLAV, RA area, PASP, and RV basal diameter (all p<0.01). (Table 2)

Variables found to be significant on between-group analysis were further examined using univariate Cox regression for continuous and Log-rank test for categorical variables. On univariate Cox regression, eGFR, indexed LVEDV, indexed LVESV, biplane LVEF, E/e' ratio, iLAV, LV-GLS, LASr, RA area, PASP, RV basal diameter, RVS', FAC, RV-FWS and 3D-RVEF were all significantly associated with the primary outcome (all p<0.05). (Table 2) As for the categorical variables, gender, ICD in situ, stage 4 or worse CKD, chronic obstructive pulmonary disease (COPD) and 3D-RVEF <44.7% were all significantly associated with the primary outcome on Log-rank test (all p>0.05). (Table 3)

Table 7.2. Between group analysis

Categorical variables	**Free from CV death & HFH (n=362)**	**CV death or HFH (n=80)**	**p-value**
Gender (male, %)	235 (64.9)	60 (75.0)	0.083
Obesity (n, %)	187 (51.7)	32 (40.0)	0.059
Atrial fibrillation (n, %)	**143 (40.1)**	**43 (53.8)**	**0.025**
Pacemaker (n, %)	19 (5.3)	6 (7.5)	0.429
ICD (n, %)	**50 (13.9)**	**27 (33.8)**	**<0.001**
CRT-D (n, %)	24 (6.7)	10 (12.5)	0.077
CKD eGFR <60 (n, %)	**89 (24.6)**	**33 (41.3)**	**0.003**
CKD eGFR <30 (n, %)	**22 (6.1)**	**13 (16.3)**	**0.002**
Hypertension	172 (47.5)	37 (46.3)	0.838
Diabetes mellitus	102 (28.2)	23 (28.8)	0.918
Hyperlipidaemia	103 (28.5)	17 (21.3)	0.190
Asthma	34 (9.4)	3 (3.8)	0.099
Interstitial lung disease	3 (0.8)	0 (0.0)	1.000
COPD	37 (10.2)	14 (17.5)	0.065
Obstructive sleep apnoea	43 (11.9)	6 (7.5)	0.259
Continuous variables	**Free from CV death & HFH (n=362)**	**CV death or HFH (n=80)**	**p-value**
Age (years)	60.35±16.20	62.30±17.64	0.3228
Body mass index	31.79±9.60	30.69±10.28	0.110
Haemoglobin	**138.77±20.63**	**130.61±17.63**	**<0.001**
eGFR	**71.00±21.26**	**62.30±25.72**	**0.014**
ALT	38.44±41.45	40.04±47.89	0.998
AST	29.68±35.02	30.71±24.66	0.431
GGT	**61.75±88.32**	**78.23±75.64**	**<0.003**
ALP	89.21±43.91	142.86±451.29	0.733
HbA1c	6.76±7.78	6.37±1.76	0.865
Transferrin Saturation	23.25±11.47	22.66±14.62	0.796
Ferritin	293.89±1088.36	252.99±335.12	0.796
Heart rate (bpm)	73.37±14.73	76.41±12.97	0.050
Systolic blood pressure	**126.25±19.74**	**116.68±23.33**	**<0.001**
Diastolic blood pressure	**76.09±11.53**	**71.25±15.73**	**<0.006**
Biplane LVEF (%)	**41.98±10.59**	**33.23±8.52**	**<0.001**
Indexed LVEDV	**62.28±25.26**	**85.48±37.01**	**<0.001**
Indexed LVESV	**37.50±20.59**	**58.43±29.08**	**<0.001**
Stroke volume	**65.14±23.10**	**57.70±20.49**	**0.011**
E/e' ratio	**12.11±5.73**	**17.07±9.06**	**<0.001**
Indexed left atrial volume	**42.19±21.16**	**55.19±27.34**	**<0.001**
Right atrial area	**17.58±7.12**	**21.95±7.61**	**<0.001**
PASP	**23.07±12.90**	**34.35±13.73**	**<0.001**
RV basal diameter	**36.27±8.44**	**40.27±10.52**	**<0.001**
TAPSE	1.87±0.51	1.79±0.54	0.215
RVS'	**9.48±2.97**	**8.34±2.67**	**0.001**
Fractional area change	**40.00±11.15**	**34.29±12.23**	**<0.001**
LV-GLS	**12.14±3.80**	**8.64±3.18**	**<0.001**
Left atrial reservoir strain	**17.97±9.33**	**11.35±6.88**	**<0.001**
RV-FWS	**20.15±6.35**	**15.60±6.20**	**<0.001**
3D-RVEF	**49.69±7.56**	**39.92±7.21**	**<0.001**

Table 7.2. Between group analysis was performed for those who were free from or met the primary outcome.

Abbreviations. *CV: cardiovascular, HFH: heart failure hospitalisation, ICD: implantable cardioverter defibrillator, CKD: chronic kidney disease, eGFR: estimated glomerular filtration rate, COPD: chronic obstructive pulmonary disease, ALT: alanine aminotransferase, AST: aspartate aminotransferase, GGT: gamma-glutamyl transferase, ALP: alkaline phosphatase, HbA1c: glycated haemoglobin A1c, LVEF: left ventricular ejection fraction, LVEDV: left ventricular end diastolic volume, LVESV: left ventricular end systolic volume, PASP: pulmonary artery systolic pressure, RV: right ventricular, TAPSE: tricuspid annular plane systolic excursion, RVS': peak velocity of the lateral tricuspid annulus in systole, LV-GLS: average left ventricular global longitudinal strain, 3D-RVEF: three dimensional right ventricular ejection fraction.*

Table 7.3. Univariate predictors of the primary outcome

Univariate Cox proportional hazard model	Unadjusted HR (95% CI)	Unadjusted p-value
Age	1.006 (0.993-1.020)	0.365
Body mass index	0.986 (0.962-1.010)	0.251
eGFR	**0.986 (0.978-0.995)**	**0.002**
Transferrin saturation	0.998 (0.978-1.019)	0.883
Ferritin	1.000 (1.000-1.000)	0.809
NT-proBNP	1.000 (1.000-1.000)	0.058
Indexed LVEDV	**1.020 (1.015-1.026)**	**<0.001**
Indexed LVESV	**1.026 (1.019-1.033)**	**<0.001**
Biplane LVEF	**0.929 (0.909-0.950)**	**<0.001**
E/e' ratio	**1.063 (1.042-1.084)**	**<0.001**
Indexed left atrial Volume	**1.012 (1.006-1.017)**	**<0.001**
LV-GLS	**0.783 (0.731-0.840)**	**<0.001**
Left atrial reservoir strain	**0.917 (0.889-0.947)**	**<0.001**
Right atrial area	**1.052 (1.030-1.075)**	**<0.001**
PASP	**1.048 (1.030-1.065)**	**<0.001**
Right ventricular basal diameter	**1.047 (1.023-1.072)**	**<0.001**
RVS'	**0.905 (0.841-0.973)**	**0.007**
Fractional area change	**0.962 (0.943-0.981)**	**<0.001**
Right ventricular free wall strain	**0.902 (0.870-0.935)**	**<0.001**
3D-RVEF	**0.905 (0.884-0.926)**	**<0.001**
Kaplan-Meier analysis	**Log-rank (p-value)**	
Gender	**0.044**	
Obesity	**0.037**	
Atrial fibrillation	0.053	
Pacemaker in situ	0.592	
ICD in situ	**<0.001**	
Stage 3 CKD (eGFR <60)	**0.002**	
Stage 4 CKD (eGFR <30)	**0.001**	
Hypertension	0.789	
Type 2 diabetes mellitus	0.859	
Hyperlipidaemia	0.182	
Asthma	0.094	
Interstitial lung disease	0.411	
COPD	**0.047**	
Obstructive sleep apnoea	0.224	
3D-RVEF <44.7	<0.001	

Table 7.3. Univariate analysis was performed for all clinical and echocardiographic parameters found to be significant between those who were free from and those who met the primary outcome.

Abbreviations. *HR: hazard ratio, eGFR: estimated glomerular filtration rate, NT pro-BNP: N-terminal pro B-type natriuetic peptide, LVEDV: left ventricular end diastolic volume, LVESV:*

left ventricular end systolic volume, LVEF: left ventricular ejection fraction, LV-GLS: average left ventricular global longitudinal strain, PASP: pulmonary artery systolic pressure, RVS': peak velocity of the lateral tricuspid annulus in systole, 3D-RVEF: three dimensional right ventricular ejection fraction, ICD: implantable cardioverter defibrillator, COPD: chronic obstructive pulmonary disease.

7.4.5 Independent predictors of cardiovascular death and heart failure hospitalisation

To minimise the risk of overfitting, we employed a two-stage multivariable Cox regression approach. All variables found to be significantly associated with the primary outcome on univariate analysis were included. In the first stage, variables were grouped into three nested models based on three categories: clinical characteristics, left heart echocardiographic parameters, and right heart echocardiographic parameters.

The clinical characteristics model included gender, presence of ICD, stage 4 or worse CKD, and COPD. The left heart echocardiographic parameters model included indexed LVEDV, indexed LVESV, biplane LVEF, E/e' ratio, indexed LAV, LV-GLS, and LASr. Finally, the right heart echocardiographic parameters model included were RA area, PASP, RV basal diameter, RVS', FAC, RV-FWS, and 3D-RVEF <44.7%. (Table 4)

Amongst the three first-stage models, the presence of an ICD (p<0.001; adjusted HR 1.64: 0.98-2.72), stage 4 or worse CKD (p=0.002; adjusted HR 2.59: 1.43-4.70), indexed LVEDV (p=0.001; adjusted HR 1.01:1.01-1.02), LV-GLS (p=0.014; adjusted HR 0.889: 0.81-0.98), LASr (p=0.007; adjusted HR 0.95: 0.91-0.99), RV basal diameter (p=0.017; adjusted HR 1.04: 1.01-1.07), RV-FWS (p=0.002; adjusted HR 0.93: 0.92-0.87), and 3D-RVEF (p<0.001; adjusted HR 5.83: 3.06-11.10) were found to be significant in their respective categories and were entered in to the second-stage model. (Table 4)

Of the covariates in the final combined model, the presence of an ICD (p=0.012; adjusted HR 2.12: 1.18-3.80), indexed LVEDV value (p<0.001; adjusted HR 1.02: 1.00-1.03), and 3D-RVEF below 44.7% (p<0.001; adjusted HR 6.22: 3.26-11.85) were all independently associated with the primary outcome. (Table 4) Importantly, a reduction of 3D-RVEF to below 44.7% was independently associated with a 6.2-fold increased risk (95% CI: 3.3-11.9) of CV death and HFH in our cohort.

7.4.6 Reproducibility analysis

There was excellent reproducibility of RV-FWS and 3D-RVEF measurements based on the inter- and intra-observer variability. For inter-observer variability, the intra-class correlation coefficient was 0.95 (95% CI 0.92-0.97) for RV-FWS, and 0.90 (95% CI 0.78-0.96) for 3D-RVEF. For intra-observer variability, the intra-class correlation coefficient was 0.98 (95% CI 0.97-0.99) for RV-FWS, and 0.95 (95% CI 0.88-0.98) for 3D-RVEF.

Table 7.4. Two-stage Cox proportional hazard model

Model 1A: Clinical Characteristics	**Adjusted Hazard Ratio (95% CI)**	**Adjusted p-value**
Male gender	1.64 (0.984-2.720)	0.058
ICD in situ	2.48 (1.559-3.942)	<0.001
Stage 4 CKD (eGFR <30)	2.59 (1.429-4.703)	0.002
COPD	1.67 (0.937-2.982)	0.082
Model 1B: Left Heart Echocardiographic Parameters	**Adjusted Hazard Ratio (95% CI)**	**Adjusted p-value**
Indexed LVEDV (ml/m^2)	1.01 (1.006-1.022)	0.001
LV-GLS (%)	0.89 (0.808-0.976)	0.014
LASr (%)	0.95 (0.908-0.985)	0.007
Model 1C: Right Heart Echocardiographic Parameters	**Adjusted Hazard Ratio (95% CI)**	**Adjusted p-value**
RV basal diameter (mm)	1.04 (1.01-1.07)	0.017
RV-FWS (%)	0.93 (0.92-0.87)	0.002
3D-RVEF <44.7%	5.83 (3.06-11.10)	<0.001
Model 2: Combined Parameters	**Adjusted Hazard Ratio (95% CI)**	**Adjusted p-value**
ICD in situ	**2.12 (1.18-3.80)**	**0.012**
Stage 4 CKD (eGFR <30)	1.19 (0.54-2.62)	0.674
Indexed LVEDV (ml/m^2)	**1.02 (1.00-1.03)**	**0.003**
LV-GLS (%)	0.99 (0.90-1.10)	0.915
LASr (%)	0.97 (0.92-1.01)	0.168
RV basal diameter (mm)	1.01 (0.98-1.03)	0.541
RV-FWS (%)	0.99 (0.93-1.05)	0.664
3D-RVEF <44.7%	**6.22 (3.26-11.85)**	**<0.001**

Table 7.4. A two-stage multivariate Cox proportional hazard model was constructed. Clinical variables included were male gender, implantable cardioverter defibrillator in situ, stage 4 or worse chronic kidney disease, and chronic obstructive pulmonary disease. Left ventricular echocardiographic parameters included were indexed left ventricular end systolic and end diastolic volumes, biplane left ventricular ejection fraction, E/e' ratio, indexed left atrial volume, left ventricular global longitudinal strain, and left atrial reservoir strain. Right ventricular echocardiographic variables included were right atrial area, pulmonary artery systolic pressure, right ventricular basal diameter, peak velocity if the lateral tricuspid annulus in

systole, fractional area change, right ventricular free wall strain and three-dimensional right ventricular ejection fraction of less than 44.7%.

Abbreviations. *ICD: implantable cardioverter defibrillator, CKD: chronic kidney disease, COPD: chronic obstructive pulmonary disease, LVEDV: left ventricular end diastolic volume, LV-GLS: left ventricular global longitudinal strain, LASr: left atrial reservoir strain, RV: right ventricular, RV-FWS: right ventricular free wall strain, 3D-RVEF: three-dimensional right ventricular ejection fraction.*

7.5.0 Discussion

The main findings of our study are twofold: amongst the RV parameters, 3D-RVEF demonstrated the highest discriminatory capacity for predicting CV death and HFH; and a reduction in 3D-RVEF to below 44.7% independently predicted adverse outcomes, even after adjusting for all relevant clinical and echocardiographic parameters.

7.5.1 Superior Prognostic Capacity of 3D-Right Ventricular Ejection Fraction

RV dysfunction is known to confer a worse prognosis in patients with cardiomyopathy. (1, 2) However, comprehensive assessment of RV systolic function is technically challenging due to its complex anatomy and multi-dimensional motion, comprising of three components. (3)

Conventional indices like RVS' and TAPSE focus on longitudinal motion but are limited by angle dependency. More contemporary studies support the use of STE-derived, angle independent measures such as RV global longitudinal strain (RV-GLS) and RV-FWS. (20, 21) Similarly, FAC, a measure of radial contraction, is limited by its two-dimensional (2D) nature and ignores work contributed by the RV outflow tract. Therefore, isolated 2D measures of RV longitudinal or radial contraction are often inadequate to characterise overall RV systolic function.

Given these limitations, 3D-echocardiographic imaging techniques offer a comprehensive and geometrically accurate evaluation of RV contractile function. (22, 23) Our study demonstrates that 3D-RVEF provides superior discriminatory capacity for adverse cardiovascular outcomes compared to both conventional and advanced 2D echocardiographic measures. Amongst the RV parameters, ROC curve analysis confirms that 3D-RVEF to be the most sensitive and specific predictor of CV death and HFH in this NICM cohort.

7.5.2 Prognostic Capacity of 3D-Right Ventricular Ejection Fraction

While the prognostic value of 3D-RVEF has been established in populations with various cardiovascular diseases including pulmonary arterial hypertension, valvular disease, cardiac transplantation, and HF with preserved ejection fraction, few studies have evaluated its utility in NICM. To our knowledge, our study is the first to assess the prognostic capacity of 3D-RVEF in a large cohort of patients with NICM stabilised on contemporary optimal guideline directed HF therapy regardless of their electrical rhythm.

Only a single study by Vijiiac et al has previously assessed the prognostic utility of 3D-RVEF in NICM, but was limited to 50 patients in sinus rhythm. (24) Viliiac's study had a significantly higher rate of CV death and HFH at 58% over a median follow up of just 16 months. The higher event rate is likely due to the lower mean LVEF of 25% in the study cohort and the presence of severe acute respiratory syndrome coronavirus 2 infection which peaked during their study period (Jan 2019 to June 2021). In contrast, our cohort had a higher mean LVEF of 40.5% and reported an event rate of 18.1% likely reflecting better baseline compensation and widespread use of modern HF therapies. Despite our lower overall event rate, impaired 3D-RVEF to below 44.7% was still associated with an over six-fold increase in the risk of adverse cardiovascular outcomes, emphasising the prognostic impact of RV systolic dysfunction in NICM patients despite being on optimal contemporary therapy.

7.5.3 The Normal Three-Dimensional Right Ventricular Ejection Fraction Threshold

Interestingly, our study identified a 3D-RVEF cutoff of <44.7%, which closely mirrors the <43.4% threshold identified by Vijiiac et al to be independently associated with CV death and HFH. (24) This threshold is also similar to the 45% lower reference range reported in normal populations. (19, 22) In contrast, RV longitudinal strain measures such as RV-GLS and RV-FWS exhibit variable thresholds for prognosticating adverse cardiovascular events across different populations, with lower cutoff values identified in those with worse LV systolic impairment. (19-21, 25) This suggests that, unlike 2D RV strain, 3D-RVEF maintains a more consistent threshold across different cardiac diseases for predicting adverse cardiovascular outcomes.

This consistency could be due to 3D-RVEF being able to incorporate all three components of RV contraction compared to 2D STE techniques in NICM. (3) Nonetheless, 3D-RVEF discriminatory threshold has been shown to be far lower amongst pulmonary hypertension cohorts (reported at 28-45%), which suggests it is afterload dependent. (26)

7.5.4 Other independent predictors of primary outcome

In addition to 3D-RVEF reduction, both larger indexed LVEDV and the presence of an ICD were independently associated with our primary-outcome. Notably, LV systolic functional parameters including LVEF and LV-GLS were not independent prognostic factors.

Persistent LV cavity dilatation in NICM, despite optimal therapy, reflects adverse remodelling without positive reverse remodelling, which has been linked to poorer clinical outcomes. (27) In our cohort, a larger indexed LVEDV likely served as a surrogate marker for this adverse cardiac remodelling and emerged as an independent predictor of the primary-outcome.

According to contemporary guidelines, an ICD is indicated for primary prevention in patients with persistent adverse cardiac remodelling, high myocardial scar burden, severe LV systolic

dysfunction despite optimal treatment, or for secondary prevention following cardiac arrest or life-threatening ventricular arrhythmias. (28, 29) As such, the presence of an ICD in our study likely reflects the cumulative burden of multiple adverse prognostic features, which explain its independent association with the primary outcome.

7.5.5 Limitations

Our study had several limitations. Firstly, our study was a prospective study performed in a single metropolitan centre in Australia. The single centre design may limit the external validity and generalisability of the findings, as patient demographics, referral patterns, TTE protocols and clinical practices may differ to those outside our institution. Although recruitment was restricted by both the single centre setting and stringent inclusion and exclusion criteria, we were nonetheless able to recruit a sizeable cohort, which strengthens the internal validity of our analysis. However, caution is warranted when extrapolating these results to the broader NICM population.

Secondly, although we endeavoured to exclude patients with significant pulmonary disease including untreated OSA from our cohort, we did not perform formal pulmonary function testing and sleep study for all participants. Nevertheless, all patients were screened for OSA using the STOP-Bang and Epworth Sleepiness Scale questionnaires, and those deemed at increased risk of OSA were referred for sleep study assessment and further treatment as part of their HF management. Furthermore, all patients had comprehensive history and assessment including smoking history and chest radiography to screen for underlying pulmonary diseases.

Thirdly, compared to the other three pillars of HF therapy, the use of SGLT2i was relatively low at 59.3%. Most patients in our study were prescribed at least three pillars of HF therapy with nearly all patients being prescribed a cardiac-specific beta-blocker and either an ACEI, ARB or ARNI. The lower prescription rate of SGLT2i was attributed to the delayed listing of

SGLT2i for the treatment of HF on the Australian Pharmaceutical Benefits Scheme (listed for LVEF ≤40% on 1st of January 2022 and for LVEF>40% on 1st of November 2023).

The final limitation pertains to the validity of 3D-RVEF and its feasibility in clinical practice. The vendor dependent 3D-RVEF software and methods used in our study has been well validated and has previously seen good concordance with CMR-RVEF. (10, 30) Furthermore, 3D-RVEF assessment in clinical practice is traditionally thought to require specialised expertise, equipment and post-processing software. (31) The feasibility of 3D-RVEF has been estimated at as low as 50% in an international collaborative study conducted from 2016 to 2019. The challenges to adequate 3D-RVEF acquisition included low frame rate (below 15hz), stitch artefacts, drop out, or incomplete capture of the full RV volume. (22) On the other hand, a meta-analysis of 10 studies examining 3D-RVEF reported good inter-observer reproducibility and a high feasibility of 81-98%. (32) The feasibility of 3D-RVEF in our study was even higher with less than 1% of patients being excluded predominantly due to drop out or difficulty visualising the anterior RV free wall. Our high feasibility was attributed to the favourable acoustic windows provided by dilated cardiac chambers in cardiomyopathy patients.

7.6.0 Conclusion

In our cohort of compensated non-ischaemic cardiomyopathy patients optimised on contemporary guideline directed medical therapy, a three-dimensional right ventricular ejection fraction of <44.7% demonstrated the strongest predictive capacity for adverse cardiovascular outcomes, outperforming other right ventricular parameters on echocardiogram. A reduction in three-dimensional right ventricular ejection fraction below this threshold was independently associated with a 6.2-fold increase in the risk of cardiovascular death and heart failure hospitalisation.

These findings suggest that transthoracic echocardiogram derived three-dimensional right ventricular ejection fraction may serve as an easily accessible and reliable measure of right

ventricular systolic function in patients with compensated non-ischaemic cardiomyopathy. Use of three-dimensional right ventricular ejection fraction may help identify a subgroup of patients at increased risk of adverse cardiovascular outcomes that can be targeted for closer monitoring and intensified therapy.

7.7.0 References

1. Raina A, Meeran T. Right Ventricular Dysfunction and Its Contribution to Morbidity and Mortality in Left Ventricular Heart Failure. Curr Heart Fail Rep. 2018;15(2):94-105.
2. Ghio S, Guazzi M, Scardovi AB, Klersy C, Clemenza F, Carluccio E, et al. Different correlates but similar prognostic implications for right ventricular dysfunction in heart failure patients with reduced or preserved ejection fraction. Eur J Heart Fail. 2017;19(7):873-9.
3. Badano LP, Addetia K, Pontone G, Torlasco C, Lang RM, Parati G, et al. Advanced imaging of right ventricular anatomy and function. Heart. 2020;106(19):1469-76.
4. Heidenreich PA, Bozkurt B, Aguilar D, Allen LA, Byun JJ, Colvin MM, et al. 2022 AHA/ACC/HFSA Guideline for the Management of Heart Failure: A Report of the American College of Cardiology/American Heart Association Joint Committee on Clinical Practice Guidelines. Circulation. 2022;145(18):e1-e138.
5. Sheehan F, Redington A. The right ventricle: anatomy, physiology and clinical imaging. Heart. 2008;94(11):1510-5.
6. Hahn RT, Lerakis S, Delgado V, Addetia K, Burkhoff D, Muraru D, et al. Multimodality Imaging of Right Heart Function: JACC Scientific Statement. J Am Coll Cardiol. 2023;81(19):1954-73.
7. Papanastasiou CA, Bazmpani MA, Kokkinidis DG, Zegkos T, Efthimiadis G, Tsapas A, et al. The prognostic value of right ventricular ejection fraction by cardiovascular magnetic resonance in heart failure: A systematic review and meta-analysis. Int J Cardiol. 2022;368:94-103.
8. Houard L, Benaets MB, de Meester de Ravenstein C, Rousseau MF, Ahn SA, Amzulescu MS, et al. Additional Prognostic Value of 2D Right Ventricular Speckle-Tracking Strain for Prediction of Survival in Heart Failure and Reduced Ejection

Fraction: A Comparative Study With Cardiac Magnetic Resonance. JACC Cardiovasc Imaging. 2019;12(12):2373-85.

9. Kitano T, Nabeshima Y, Nagata Y, Takeuchi M. Prognostic value of the right ventricular ejection fraction using three-dimensional echocardiography: Systematic review and meta-analysis. PLoS One. 2023;18(7):e0287924.

10. Nagata Y, Wu VC, Kado Y, Otani K, Lin FC, Otsuji Y, et al. Prognostic Value of Right Ventricular Ejection Fraction Assessed by Transthoracic 3D Echocardiography. Circ Cardiovasc Imaging. 2017;10(2).

11. Lakatos BK, Rako Z, Szijarto A, da Rocha BRB, Richter MJ, Fabian A, et al. Right ventricular pressure-strain relationship-derived myocardial work reflects contractility: Validation with invasive pressure-volume analysis. J Heart Lung Transplant. 2024;43(7):1183-7.

12. Heidenreich PA, Bozkurt B, Aguilar D, Allen LA, Byun JJ, Colvin MM, et al. 2022 AHA/ACC/HFSA Guideline for the Management of Heart Failure: A Report of the American College of Cardiology/American Heart Association Joint Committee on Clinical Practice Guidelines. Circulation. 2022;145(18):e895-e1032.

13. McMurray JJ, Adamopoulos S, Anker SD, Auricchio A, Bohm M, Dickstein K, et al. ESC Guidelines for the diagnosis and treatment of acute and chronic heart failure 2012: The Task Force for the Diagnosis and Treatment of Acute and Chronic Heart Failure 2012 of the European Society of Cardiology. Developed in collaboration with the Heart Failure Association (HFA) of the ESC. Eur Heart J. 2012;33(14):1787-847.

14. Authors/Task Force M, McDonagh TA, Metra M, Adamo M, Gardner RS, Baumbach A, et al. 2023 Focused Update of the 2021 ESC Guidelines for the diagnosis and treatment of acute and chronic heart failure: Developed by the task force for the diagnosis and treatment of acute and chronic heart failure of the European Society of Cardiology (ESC) With the special contribution of the Heart Failure Association (HFA) of the ESC. Eur J Heart Fail. 2024;26(1):5-17.

15. Mebazaa A, Davison B, Chioncel O, Cohen-Solal A, Diaz R, Filippatos G, et al. Safety, tolerability and efficacy of up-titration of guideline-directed medical therapies for acute heart failure (STRONG-HF): a multinational, open-label, randomised, trial. Lancet. 2022;400(10367):1938-52.
16. Lang RM, Badano LP, Mor-Avi V, Afilalo J, Armstrong A, Ernande L, et al. Recommendations for cardiac chamber quantification by echocardiography in adults: an update from the American Society of Echocardiography and the European Association of Cardiovascular Imaging. J Am Soc Echocardiogr. 2015;28(1):1-39 e14.
17. Nagueh SF, Smiseth OA, Appleton CP, Byrd BF, 3rd, Dokainish H, Edvardsen T, et al. Recommendations for the Evaluation of Left Ventricular Diastolic Function by Echocardiography: An Update from the American Society of Echocardiography and the European Association of Cardiovascular Imaging. J Am Soc Echocardiogr. 2016;29(4):277-314.
18. Badano LP, Kolias TJ, Muraru D, Abraham TP, Aurigemma G, Edvardsen T, et al. Standardization of left atrial, right ventricular, and right atrial deformation imaging using two-dimensional speckle tracking echocardiography: a consensus document of the EACVI/ASE/Industry Task Force to standardize deformation imaging. Eur Heart J Cardiovasc Imaging. 2018;19(6):591-600.
19. Mukherjee M, Rudski LG, Addetia K, Afilalo J, D'Alto M, Freed BH, et al. Guidelines for the Echocardiographic Assessment of the Right Heart in Adults and Special Considerations in Pulmonary Hypertension: Recommendations from the American Society of Echocardiography. J Am Soc Echocardiogr. 2025;38(3):141-86.
20. Carluccio E, Biagioli P, Alunni G, Murrone A, Zuchi C, Coiro S, et al. Prognostic Value of Right Ventricular Dysfunction in Heart Failure With Reduced Ejection Fraction: Superiority of Longitudinal Strain Over Tricuspid Annular Plane Systolic Excursion. Circ Cardiovasc Imaging. 2018;11(1):e006894.

21. Carluccio E, Biagioli P, Lauciello R, Zuchi C, Mengoni A, Bardelli G, et al. Superior Prognostic Value of Right Ventricular Free Wall Compared to Global Longitudinal Strain in Patients With Heart Failure. J Am Soc Echocardiogr. 2019;32(7):836-44 e1.
22. Addetia K, Miyoshi T, Amuthan V, Citro R, Daimon M, Gutierrez Fajardo P, et al. Normal Values of Three-Dimensional Right Ventricular Size and Function Measurements: Results of the World Alliance Societies of Echocardiography Study. J Am Soc Echocardiogr. 2023;36(8):858-66 e1.
23. Cotella JI, Kovacs A, Addetia K, Fabian A, Asch FM, Lang RM, et al. Three-dimensional echocardiographic evaluation of longitudinal and non-longitudinal components of right ventricular contraction: results from the World Alliance of Societies of Echocardiography study. Eur Heart J Cardiovasc Imaging. 2024;25(2):152-60.
24. Vijiiac A, Onciul S, Guzu C, Verinceanu V, Bataila V, Deaconu S, et al. The prognostic value of right ventricular longitudinal strain and 3D ejection fraction in patients with dilated cardiomyopathy. Int J Cardiovasc Imaging. 2021;37(11):3233-44.
25. Ishiwata J, Daimon M, Nakanishi K, Sugimoto T, Kawata T, Shinozaki T, et al. Combined evaluation of right ventricular function using echocardiography in non-ischaemic dilated cardiomyopathy. ESC Heart Fail. 2021;8(5):3947-56.
26. Ahmad A, Wang X, Li L, Liu T, Fan FL. Insights from 3D echocardiography: unveiling the prognostic value of RV function in pulmonary hypertension: a systematic review and meta-analysis. Int J Cardiovasc Imaging. 2025;41(2):185-97.
27. Merlo M, Caiffa T, Gobbo M, Adamo L, Sinagra G. Reverse remodeling in Dilated Cardiomyopathy: Insights and future perspectives. Int J Cardiol Heart Vasc. 2018;18:52-7.
28. Zeppenfeld K, Tfelt-Hansen J, de Riva M, Winkel BG, Behr ER, Blom NA, et al. 2022 ESC Guidelines for the management of patients with ventricular arrhythmias and the prevention of sudden cardiac death. Eur Heart J. 2022;43(40):3997-4126.

29. McDonagh TA, Metra M, Adamo M, Gardner RS, Baumbach A, Bohm M, et al. 2021 ESC Guidelines for the diagnosis and treatment of acute and chronic heart failure. Eur Heart J. 2021;42(36):3599-726.

30. Muraru D, Spadotto V, Cecchetto A, Romeo G, Aruta P, Ermacora D, et al. New speckle-tracking algorithm for right ventricular volume analysis from three-dimensional echocardiographic data sets: validation with cardiac magnetic resonance and comparison with the previous analysis tool. Eur Heart J Cardiovasc Imaging. 2016;17(11):1279-89.

31. Tolvaj M, Kovacs A, Radu N, Cascella A, Muraru D, Lakatos B, et al. Significant Disagreement Between Conventional Parameters and 3D Echocardiography-Derived Ejection Fraction in the Detection of Right Ventricular Systolic Dysfunction and Its Association With Outcomes. J Am Soc Echocardiogr. 2024;37(7):677-86.

32. Sayour AA, Tokodi M, Celeng C, Takx RAP, Fabian A, Lakatos BK, et al. Association of Right Ventricular Functional Parameters With Adverse Cardiopulmonary Outcomes: A Meta-analysis. J Am Soc Echocardiogr. 2023;36(6):624-33 e8.

CHAPTER EIGHT

Summary of findings and concluding remarks

8.0 Abbreviations:

RV = right ventricular

NICM = non-ischaemic cardiomyopathy

LV = left ventricular

RV-FWS = right ventricular free wall strain

HF = heart failure

AF = atrial fibrillation

BMI = body mass index

2D = two-dimensional

3D = three-dimensional

3D-RVEF = three-dimensional right ventricular ejection fraction

HFrEF = heart failure with reduced ejection fraction

8.1.0 Summary of study findings

Our overarching goal in this body of work was to understand the prevalence, determinates and prognostic significance of right ventricular (RV) dysfunction in those with heart failure with reduced ejection fraction (HFrEF). Additionally, we sought to assess the differences between echocardiographic measures of RV function and to evaluate the association of these parameters with exercise capacity and long-term outcomes.

The findings from chapter three revealed that RV systolic dysfunction is highly prevalent in non-ischaemic cardiomyopathy (NICM) and is more common than previously thought. Notably, all patients with moderate or severe left ventricular (LV) systolic impairment exhibited reduced RV free wall strain (RV-FWS). We also showed that the increasing severity of LV systolic impairment corresponded with significant worsening of RV systolic function and prevalence of RV dysfunction. This highlights the strong relationship between worsening LV systolic function and concurrent RV dysfunction. Additionally, among all two-dimensional echocardiographic parameters assessed, RV-FWS emerged as a more sensitive marker of RV dysfunction and had better prognostic utility, outperforming traditional indices in predicting cardiovascular death and heart failure (HF) hospitalisation.

Chapters four and five focused on atrial fibrillation (AF) and obesity respectively, two common comorbidities in NICM and RV dysfunction, and their impact on RV function. (1-4) Our results demonstrated that elevated body mass index (BMI) was associated with subclinical RV dysfunction as evidenced by a drop in RV-FWS even in individuals without cardiovascular disease or risk factors. In a separate cohort with AF in the absence of structural heart disease, restoration of sinus rhythm was associated with immediate improvements in RV functional parameters and a marked reduction in the prevalence of RV dysfunction. These findings underscore the deleterious effect of both obesity and AF on RV function, even in the absence of other overt cardiac pathologies.

Chapters six and seven further explored the prognostic utility of two-dimensional (2D) and three-dimensional (3D) echocardiographic RV functional parameters in a prospective cohort of NICM patients receiving optimal guideline directed therapy. In this cohort, RV-FWS independently predicted reduced performance on 6-minute walk test to below 300 meters, which supports the idea that RV longitudinal contractile reserve plays a pivotal role in exercise capacity. (5) Similarly, 3D RV ejection fraction (3D-RVEF), which integrates all three components of RV contraction, provided the strongest discrimination for adverse cardiovascular outcomes amongst RV parameters, and independently predicted cardiovascular mortality and HF hospitalisation after adjustment for relevant clinical and echocardiographic variables. (6)

Together, our findings highlight the clinical significance of RV dysfunction in NICM and demonstrate the prognostic value of advanced echocardiographic measures such as RV-FWS and 3D-RVEF over traditional indices for both adverse cardiovascular outcomes and exercise capacity. These results support the incorporation of RV echocardiographic assessment into routine evaluation and risk stratification in NICM.

8.2.0 Clinical significance

Despite the observation of worse cardiovascular outcomes amongst those with RV dysfunction, current cardiomyopathy treatment algorithms and guidelines make no distinction between isolated LV systolic dysfunction versus biventricular dysfunction. (7-11) Furthermore, assessment of RV function is not part of routine assessment in NICM, despite its potential to be a potent prognostic tool. (7, 12) Therefore, the findings from this body of work hold significant relevance in bridging the knowledge gaps surrounding the role of RV systolic function in NICM and underscore the prognostic relevance of RV dysfunction. As well as highlighting the limitations of a traditional left heart-centric approach in NICM.

Establishing the prevalence of RV dysfunction in NICM is the logical first step in understanding the role of RV function in NICM. We have demonstrated a close link between worsening LV and RV systolic function in NICM with RV dysfunction being present even in those with mild LV systolic impairment. Our results draw attention to the high prevalence of RV dysfunction even in mild or early cardiomyopathy and support incorporating advanced RV functional measures into routine echocardiographic assessment even in the absence of severe LV systolic impairment or frank HF symptoms.

Secondly, we wished to identify comorbidities in NICM that lead to RV dysfunction. We found elevated BMI and the presence of AF to be associated with reduction in RV systolic function, even without other structural cardiac diseases. These findings suggests that treatment of obesity and rhythm control of AF are modifiable contributors to RV dysfunction in NICM, offering potential new therapeutic strategies.

Finally, understanding the impact of RV dysfunction in NICM is particularly relevant with regards to developing new HF treatment algorithms as well as monitoring responses to treatment. Our findings suggest that RV-FWS has utility in assessing RV contractile reserve and exercise capacity, providing mechanistic insights into the role of RV longitudinal contractile function in the development of HF symptomology and functional capacity. Furthermore, 3D-RVEF as a robust measure of overall RV contractile function, independently predicted adverse cardiovascular outcomes. This indicates that RV systolic function is an integral part of the NICM disease process and can independently contribute to adverse cardiovascular outcomes regardless of left heart function.

Although 2D RV functional echocardiographic parameters have previously been assessed in several cardiomyopathy cohorts, most of these studies evaluated those with HF from mixed aetiologies across a narrow range of LV ejection fractions. Those studies have several limitations, including the inability to simultaneously account for both radial and longitudinal RV function using 2D echocardiographic measures, the extent of contemporary HF therapies prescribed, and the varying degree and extent of coronary revascularisation. Studies looking

at 3D-RVEF, specifically in those with NICM optimised by contemporary HF therapies, are scarce. Filling this gap, our findings enabled a comparison of all 2D and 3D echocardiographic parameters of RV function in a NICM cohort optimised on contemporary HF therapies. The findings from this body of work support the inclusion of advanced RV functional echocardiographic measures in routine practice to enhance risk stratification and monitoring treatment response in patients with NICM.

8.3.0 Future directions

This thesis focused specifically on patients with stable NICM, and as such, our findings cannot be immediately extrapolated to ischaemic cardiomyopathy or those presenting with acute decompensated HF. Future studies are warranted to validate the prognostic significance of RV dysfunction across broader and more heterogenous HF populations, including those with acute decompensated HF, those receiving inotropic therapy, those with de novo versus chronic HF, and across different cardiomyopathy aetiologies.

Several risk prediction models have been developed for HF with reduced ejection fraction (HFrEF), including the CHARM, Seattle HF, CORONA, MECKI and MAGGIC scores. (14-17) All of which rely heavily on LV ejection fraction as a key prognostic component. In contrast, no existing prognostic models incorporate RV functional parameters, leading to a great interest in integrating advanced echocardiographic markers of RV function, such as RV-FWS and 3D-RVEF, into a risk stratification model for NICM.

Another potential direction for future research is serial evaluation and longitudinal tracking of RV function. While improvement in LV systolic function and reverse remodelling process is well documented in the literature, the trajectory of RV recovery remains poorly understood. (18, 19) Verhaert et al. demonstrated that improvements in RV global longitudinal strain were associated with more favourable cardiovascular outcomes in acute decompensated HFrEF. (20) Another serial assessment of RV function was performed by an echocardiography sub-

study of the GISSI trial, which observed an improvement of tricuspid annular plane systolic excursion over a six-month period following acute myocardial infarction. (21) These observations emphasise the need for further longitudinal studies assessing the natural progression and reversibility of RV dysfunction in NICM.

Similarly, the impact of contemporary HF therapies on RV function in NICM remains unexplored. (22) Guideline-directed medical therapy has been shown to promote significant LV reverse remodelling and functional recovery, with improvement rates ranging from 20% to 100% depending on the chronicity and aetiology of the underlying cardiomyopathy process. (22, 23) A retrospective observational study by Merlo et al. has reported promising rates of RV functional recovery in NICM, though this predated the use of advanced echocardiographic techniques and the availability of current HF pharmacotherapies. (24) Further prospective studies are needed to assess whether RV functional recovery, like that of the LV, can be augmented by modern pharmacotherapy. Which in turn, can lead to better cardiovascular outcomes.

Addressing these remaining key knowledge gaps will contribute to a more comprehensive and individualised approach to HF management. One that acknowledges and integrates the prognostic and therapeutic significance of the RV in NICM. In time, this may even lead to new therapies with RV-specific targets.

8.4.0 Concluding remarks

Right ventricular dysfunction is common in non-ischaemic cardiomyopathy. Echocardiographic confirmation of right ventricular dysfunction, based on free wall longitudinal strain and three-dimensional ejection fraction, can independently prognosticate a reduction in exercise capacity as well as adverse cardiovascular outcomes. Evaluation of right ventricular systolic function is therefore vital and should be part of routine assessment in patients with

non-ischaemic cardiomyopathy. Further studies are required to validate the role of RV systolic function as a prognostic marker in this population.

8.5.0 References

1. Buckley BJR, Harrison SL, Gupta D, Fazio-Eynullayeva E, Underhill P, Lip GYH. Atrial Fibrillation in Patients With Cardiomyopathy: Prevalence and Clinical Outcomes From Real-World Data. J Am Heart Assoc. 2021;10(23):e021970.
2. Collaborators GBDRF. Global burden of 87 risk factors in 204 countries and territories, 1990-2019: a systematic analysis for the Global Burden of Disease Study 2019. Lancet. 2020;396(10258):1223-49.
3. Sokmen A, Sokmen G, Acar G, Akcay A, Koroglu S, Koleoglu M, et al. The impact of isolated obesity on right ventricular function in young adults. Arq Bras Cardiol. 2013;101(2):160-8.
4. Ma JI, Zern EK, Parekh JK, Owunna N, Jiang N, Wang D, et al. Obesity Modifies Clinical Outcomes of Right Ventricular Dysfunction. Circ Heart Fail. 2023;16(11):e010524.
5. Claeys M, Claessen G, La Gerche A, Petit T, Belge C, Meyns B, et al. Impaired Cardiac Reserve and Abnormal Vascular Load Limit Exercise Capacity in Chronic Thromboembolic Disease. JACC Cardiovasc Imaging. 2019;12(8 Pt 1):1444-56.
6. Badano LP, Addetia K, Pontone G, Torlasco C, Lang RM, Parati G, et al. Advanced imaging of right ventricular anatomy and function. Heart. 2020;106(19):1469-76.
7. McDonagh TA, Metra M, Adamo M, Gardner RS, Baumbach A, Bohm M, et al. 2021 ESC Guidelines for the diagnosis and treatment of acute and chronic heart failure: Developed by the Task Force for the diagnosis and treatment of acute and chronic heart failure of the European Society of Cardiology (ESC) With the special contribution of the Heart Failure Association (HFA) of the ESC. Rev Esp Cardiol (Engl Ed). 2022;75(6):523.
8. Zeppenfeld K, Tfelt-Hansen J, de Riva M, Winkel BG, Behr ER, Blom NA, et al. 2022 ESC Guidelines for the management of patients with ventricular arrhythmias and the prevention of sudden cardiac death. Eur Heart J. 2022;43(40):3997-4126.

9. Van Gelder IC, Rienstra M, Bunting KV, Casado-Arroyo R, Caso V, Crijns H, et al. 2024 ESC Guidelines for the management of atrial fibrillation developed in collaboration with the European Association for Cardio-Thoracic Surgery (EACTS). Eur Heart J. 2024;45(36):3314-414.
10. Heidenreich PA, Bozkurt B, Aguilar D, Allen LA, Byun JJ, Colvin MM, et al. 2022 AHA/ACC/HFSA Guideline for the Management of Heart Failure: A Report of the American College of Cardiology/American Heart Association Joint Committee on Clinical Practice Guidelines. Circulation. 2022;145(18):e895-e1032.
11. Authors/Task Force M, McDonagh TA, Metra M, Adamo M, Gardner RS, Baumbach A, et al. 2023 Focused Update of the 2021 ESC Guidelines for the diagnosis and treatment of acute and chronic heart failure: Developed by the task force for the diagnosis and treatment of acute and chronic heart failure of the European Society of Cardiology (ESC) With the special contribution of the Heart Failure Association (HFA) of the ESC. Eur J Heart Fail. 2024;26(1):5-17.
12. Gorter TM, van Veldhuisen DJ, Bauersachs J, Borlaug BA, Celutkiene J, Coats AJS, et al. Right heart dysfunction and failure in heart failure with preserved ejection fraction: mechanisms and management. Position statement on behalf of the Heart Failure Association of the European Society of Cardiology. Eur J Heart Fail. 2018;20(1):16-37.
13. Pocock SJ, Ariti CA, McMurray JJ, Maggioni A, Kober L, Squire IB, et al. Predicting survival in heart failure: a risk score based on 39 372 patients from 30 studies. Eur Heart J. 2013;34(19):1404-13.
14. Pocock SJ, Wang D, Pfeffer MA, Yusuf S, McMurray JJ, Swedberg KB, et al. Predictors of mortality and morbidity in patients with chronic heart failure. Eur Heart J. 2006;27(1):65-75.
15. Levy WC, Mozaffarian D, Linker DT, Sutradhar SC, Anker SD, Cropp AB, et al. The Seattle Heart Failure Model: prediction of survival in heart failure. Circulation. 2006;113(11):1424-33.

16. Wedel H, McMurray JJ, Lindberg M, Wikstrand J, Cleland JG, Cornel JH, et al. Predictors of fatal and non-fatal outcomes in the Controlled Rosuvastatin Multinational Trial in Heart Failure (CORONA): incremental value of apolipoprotein A-1, high-sensitivity C-reactive peptide and N-terminal pro B-type natriuretic peptide. Eur J Heart Fail. 2009;11(3):281-91.

17. Agostoni P, Corra U, Cattadori G, Veglia F, La Gioia R, Scardovi AB, et al. Metabolic exercise test data combined with cardiac and kidney indexes, the MECKI score: a multiparametric approach to heart failure prognosis. Int J Cardiol. 2013;167(6):2710-8.

18. Bozkurt B, Coats AJS, Tsutsui H, Abdelhamid CM, Adamopoulos S, Albert N, et al. Universal definition and classification of heart failure: a report of the Heart Failure Society of America, Heart Failure Association of the European Society of Cardiology, Japanese Heart Failure Society and Writing Committee of the Universal Definition of Heart Failure: Endorsed by the Canadian Heart Failure Society, Heart Failure Association of India, Cardiac Society of Australia and New Zealand, and Chinese Heart Failure Association. Eur J Heart Fail. 2021;23(3):352-80.

19. Arrigo M, Huber LC, Winnik S, Mikulicic F, Guidetti F, Frank M, et al. Right Ventricular Failure: Pathophysiology, Diagnosis and Treatment. Card Fail Rev. 2019;5(3):140-6.

20. Verhaert D, Mullens W, Borowski A, Popovic ZB, Curtin RJ, Thomas JD, et al. Right ventricular response to intensive medical therapy in advanced decompensated heart failure. Circ Heart Fail. 2010;3(3):340-6.

21. Popescu BA, Antonini-Canterin F, Temporelli PL, Giannuzzi P, Bosimini E, Gentile F, et al. Right ventricular functional recovery after acute myocardial infarction: relation with left ventricular function and interventricular septum motion. GISSI-3 echo substudy. Heart. 2005;91(4):484-8.

22. Merlo M, Caiffa T, Gobbo M, Adamo L, Sinagra G. Reverse remodeling in Dilated Cardiomyopathy: Insights and future perspectives. Int J Cardiol Heart Vasc. 2018;18:52-7.

23. Goh ZM, Javed W, Shabi M, Klassen JRL, Saunderson CED, Farley J, et al. Early prediction of left ventricular function improvement in patients with new-onset heart failure and presumed non-ischaemic aetiology. Open Heart. 2023;10(2).

24. Merlo M, Gobbo M, Stolfo D, Losurdo P, Ramani F, Barbati G, et al. The Prognostic Impact of the Evolution of RV Function in Idiopathic DCM. JACC Cardiovasc Imaging. 2016;9(9):1034-42.